QoS mechanisms for packet-based mobile networks

Friderikos, Vasilis

Department of Electronic Engineering
Centre for Telecommunications Research
King's College London
University of London
26-29 Drury Lane
London
WC2B 5RL

QoS Mechanisms for Packet Based Mobile Networks

By

Vasilis Friderikos

February 2005

A Thesis submitted to the University of London

For the Degree of Doctor of Philosophy

Abstract

Future heterogeneous mobile networks anticipate supporting IP technology in both the core and wireless access domain, identifying, therefore, a path towards the convergence of fixed IP and mobile networks. All–IP based mobile networks raise a number of acute research issues if they are to support QoS and make efficient utilization of the scarce resources of the wireless interface. In this thesis architectural insights are presented for IP QoS enabled mobile networks together with novel algorithms for providing IP based resource management.

Concerning the core network – which is assumed to support a stateless QoS architecture – the central argument to be defended is that the number of traffic classes should be disassociated with the number of classes on the different wireless access networks. The reasoning behind the proposed core–centric approach together with the benefits are discussed in detail. Additionally, an active queue management (Hop Based Queueing – HBQ) algorithm is proposed that takes into account the number of routers traversed by examining the TTL field of the IPv4 packet (or the Hop Limit field in IPv6). The HBQ mechanism fulfill the aims of performing active queueing management to signal incipient congestion but also provides additional benefits when it operates in the gateway of the mobile network.

Based on the utilization of IP QoS information on the access network the interactions of IP mechanisms with radio link layer mechanisms for CDMA networks are explored. Novel joint power and rate control algorithms are presented that integrate information from the TCP state machine to optimize the performance of TCP traffic over wireless. Also, the different levels of drop-precedence (packet colouring) of the marking functionalities in DiffServ are explored on the link layer to optimize the performance of in-profile (conformant) traffic.

Acknowledgments

It is hard to write appropriate acknowledgments that reflect the assistance and inspiration I was given throughout the years of my research. First and foremost, I would like to thank my advisor, Prof. H. Aghvami, for his guidance and tremendous support throughout my studies and during the completion of this thesis.

Special thank to Mischa Dohler for the infinite interesting blackboard–style discussions we had over the last six years. Another thank you goes out to all of my fellow researchers at CTR for their understanding, support and persistence in pushing me along. Especially (and without order) a big thank you to those one that I have closely work together; Mona Ghasemian, Nikos Georganopoulos, Andrej Mihailovic, Mikio Iwamura, Lin Wang, Thanos Gkelias and Katerina Papadaki. Many thanks to Prof. Ian Groves and Piyush Khengar for the careful proofreading.

Part of the research in the thesis has been supported by Mobile-VCE. Along those same lines, I am grateful for the funding, but more importantly for the privilege of being part of this excellent academic and industrial community.

Maybe the most special thank you goes to my brother Orestis. Well, whatever I write for him falls short. You are the best!

Finally, and above all, I want to thank my parents Athanasios and Sofia, my grandfather, my grandmother and my sister Ermina. Your unconditional love, patience, understanding, joy, happiness and support have made my entire endeavor in life worthwhile. What I owe you is incommensurable.

Contents

List of Tables

List of Figures

Chapter 1

Introduction

Undoubtedly the combination of mobile and Internet technologies/applications would be the next great communication revolution. In this inter-working environment IP technology is envisioned to be the least common denominator between the heterogeneous mobile networks and the Internet. In this chapter a retrospective of both current but also future directions towards 4G Mobile Networks are presented. The discussion on architectural issues span both core and wireless access networks. Under this framework, the major research contributions are presented together with an outline of the thesis.

1.1 Evolution of Wireless Communication Systems

Historically speaking, the reasoning behind the evolution towards the Global System for Mobile Communications (GSM) was mainly twofold. Firstly, and most importantly, European Commission, industry and academia recognized that the utility of analog first generation cellular systems was diminishing by the proliferation of incompatible standards in Europe. Secondly, GSM envisioned to solve the capacity limitation of analog cellular systems by utilizing digital transmission techniques. In that sense, GSM evolved as an extremely successful system that provided higher capacity (hence lower cost services) with international roaming.

GSM was mainly designed as a voice centric communication network with limited data capabilities.

These low data rates of a few Kbps have prevented mobile users from enjoying the full benefits of Internet and World Wide Web services, and this was the main reason for moving beyond 2nd generation systems. Third-generation (3G) mobile cellular systems (UMTS, IMT-2000) have been designed for data rates up to 2 Mbps [1]. Third-generation systems are based on a hierarchical cell structure with suburban macrocells, urban microcells, "hot-spot" picocells and satellite overlay. Seamless coverage, ubiquitous roaming, and operation at vehicular speeds up to 200 km/h can be supported in macrocells and microcells for data rates up to 64Kbps. A richer variety of wireless services, at least for slower-moving platforms, is available with the deployment of 384Kbps data services which will finally bring many of the Internet and Web services to the mobile user. In particular, multimedia services such as MPEG audio and video streaming are expected to unlock new revenue streams for the cellular operators. Even though currently the deployment and adoption of 3G networks in Europe is slow , the telecom landscape is changing at a phenomenal rate with the main driving force a common infrastructure based on IP-technology for both fixed and mobile networks.

Focusing on the mobile arena, technology is moving towards an environment where heterogeneous wireless access techniques (EGPRS, UMTS, WLAN, Bluetooth) will share a common IP-based QoS enabled backbone (the so-called "beyond 3G" or 4G Mobile Networks). This soft migration to IP-based technology will be the enabler for offering a bewildering array of options for future advanced personalized services and applications that will be delivered to any device, independent of user mobility and/or location.

1.2 Outlook toward a future fourth-generation wireless system - 4G

Even though 3G mobile networks are in the early stage of deployment and commercial exploration around the world, attention is currently shifting to what comes next. The research community is therefore focusing in a group of newer technologies for both the core and access network that are, inevitably, being called 4G. In 2001 the Wireless World Research Forum [2] was formed to bring together experts from industry and academia to investigate the future of wireless systems beyond

3G. Work is underway in the WWRF [1] to shape the outlines of a future 4G mobile wireless communication system. As shown in figure 1.1 the general consensus is that mobile communication systems beyond 3G will integrate several types of wireless access systems with a common IP-based backbone network [3]. In that sense 4G will not only be a single new access technology but an integration of current and future wireless access networks in order to realize a ubiquitous mobile computing environment. Wireless access to the IP backbone will be provided by broadband radio LANs, lowcost wireless PANs, new air-interfaces and, of course, by second and third generation cellular systems. The IP backbone network will provide most of the services and applications because of its cost-efficiency and scalability. The envisioned 4G broadband wireless networks will therefore

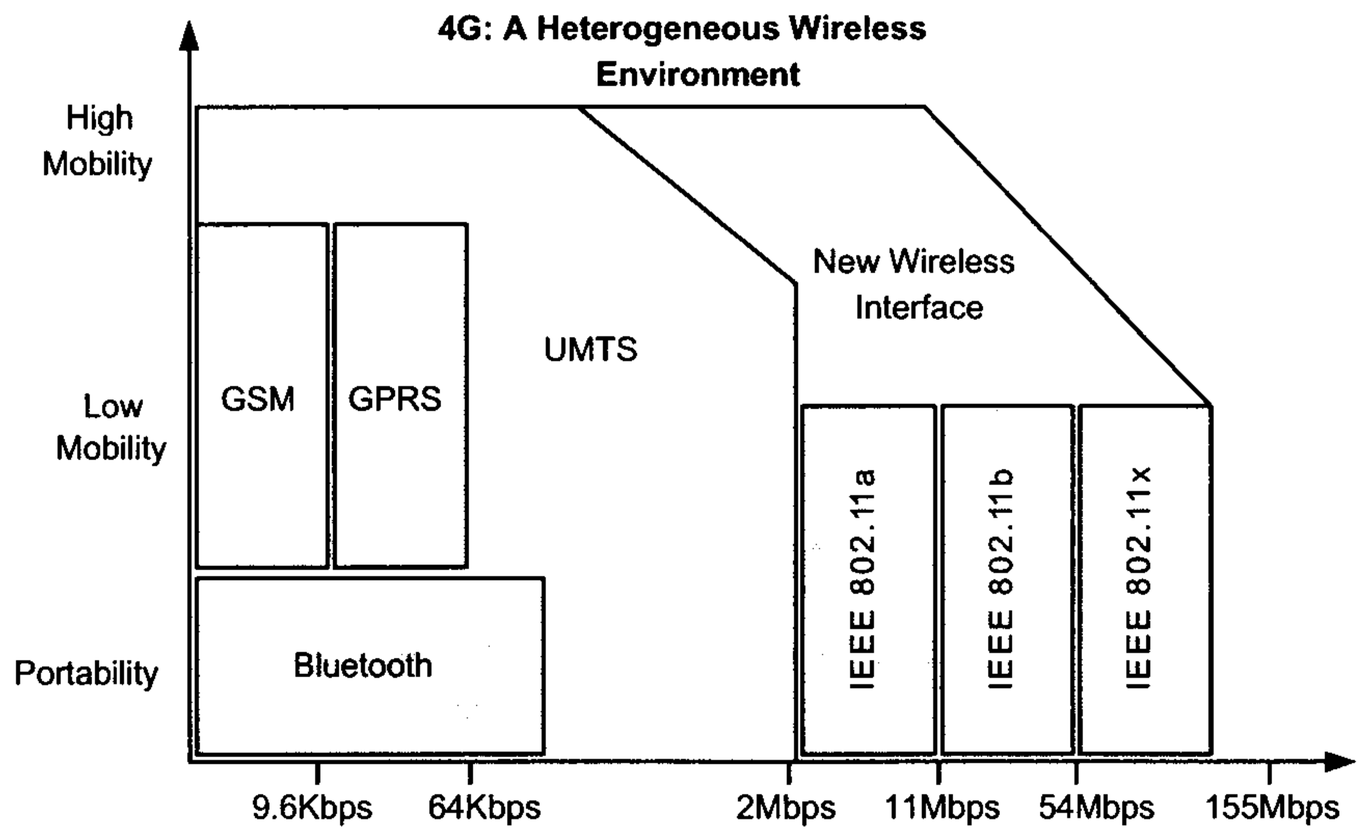

Figure 1.1: The 4^{th} Generation of mobile networks is envisioned to be a co-operative system of heterogeneous wireless technologies.

support "vertical handover" between future access networks and legacy 2G/2.5G and 3G networks. Although there are a large number of architectural unclarities, the research challenges are laying in the area of optimized QoS based IP transmission together with the required protocols that will provide network management, mobility management, and seamless or smooth vertical handovers. Clearly, future 4G wireless systems will also be challenged to provide not only QoS support and dynamic scheduling of bandwidth, but also dynamic link adaptation. It is therefore evident that in

[1] Parallel activities on 4G wireless networks are also developed in China (FuTURE - Future Technologies for Universal Radio Environment, 863-program, `http://www.863.org.cn`), Japan (mITF - Mobile IT Forum, `http://www.mitf.org`), and Korea (NGMC - Next Generation Mobile Communication Forum).

this heterogeneous environment future mobile devices will run multiple concurrent applications and support multiple wireless standards, which translates into the need for multimode and multiband operation. Figure 1.2 shows the evolution of the protocol stack in terms of layering and functionalities.

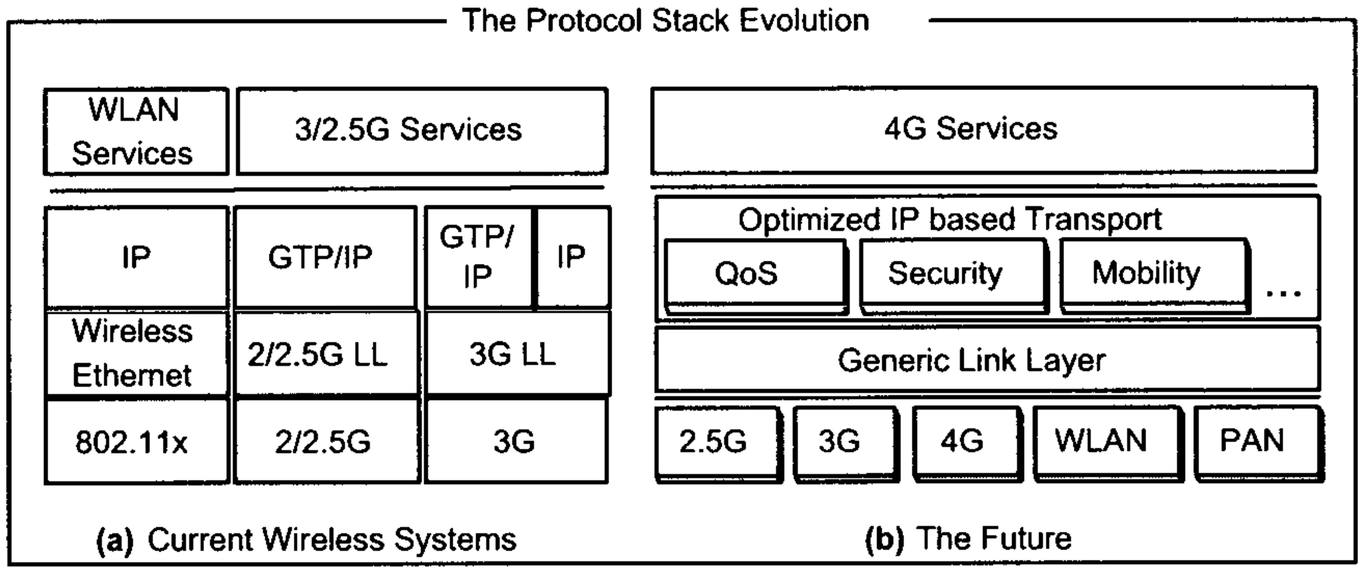

Figure 1.2: The evolution of the protocol stack

As can be seen in figure 1.2(a), currently, different protocol stacks have been defined for different wireless networks. Because there is no homogeneity on the protocol stack, the task of enabling harmonized services and applications among different networks is becoming very difficult. Harmonizing the creation of services and applications is the catalyst for increasing revenues for mobile network operators, but also enhancing the experience perceived by the mobile user. Figure 1.2(b) shows a schematic overview of the protocol stack in a 4G mobile environment. The heterogeneity here lies on the physical layer whereas higher layers are based on pure IP-based global connectivity. In this case a generic link layer is envisioned to provide transparent access to different wireless access technologies, where the selection can be based on the Always Best Connected (ABC) concept [39]. The ABC concept in the 4G environment is mainly about providing transparent connectivity to the mobile user anywhere, anytime, from any network and by using any terminal. This is shown in figure 1.3 where both vertical handovers and session transfers can happen transparently from the end user. In order to provide transparency to the user when using services anywhere at anytime with any terminal, specific mechanism are required in order to make the right decisions depending on the constraints of the mobile user environment. ABC mechanisms will consider, among other things, the QoS requirements of the mobile user services, the terminal characteristics, the network characteristics and the user preferences such as the price of the available networks resources. While

a user may be multi-homed within any network, a set of rules or policies can be specified and stored in the network (e.g. in a policy server). On an access request from the user, these will be triggered and enforced according to the mobile user context and preferences.

In that sense, 4G is envisioned to be user-centric in the sense that the Quality of Service (QoS) experienced by the end user will be the main driving force behind different proposed technical solutions. The user experience is global and holistic, involving and merging all the elements of the network, terminal, service and application. The difficulty lies on the subjective perception of what "Quality" means to different users, which cannot just be directly evaluated by measuring only technical parameters. The user perception is heavily influenced by expectations, previous experiences and expectative about the service; 4G networks will have to consider all the above issues in order to provide services that fulfill user demands [40]. User-oriented network design, in the sense of always-

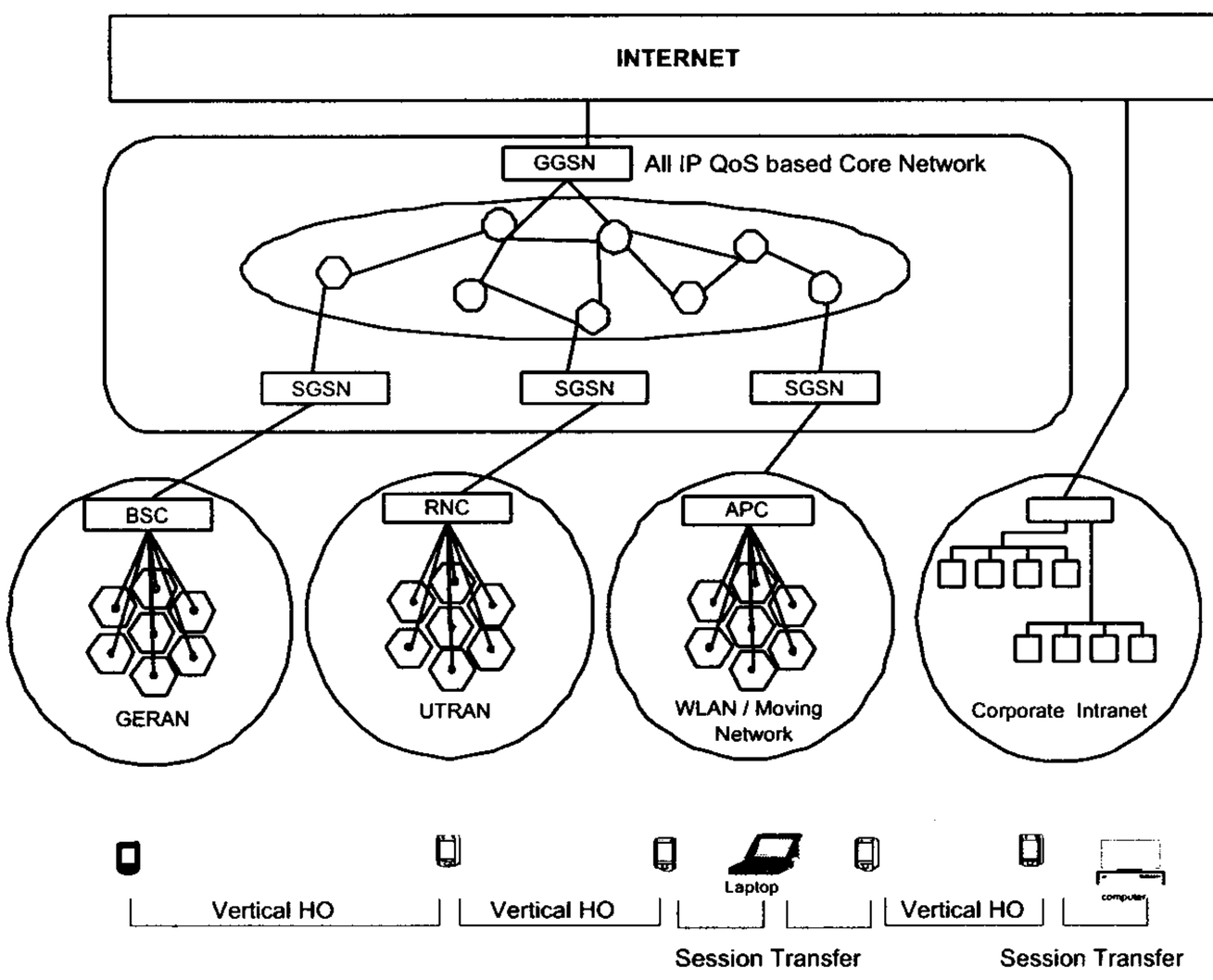

Figure 1.3: An envisioned 4G Network environment.

best-connected, as mentioned before, shift the emphasis on the necessary technological requirements for integrating heterogeneous wireless networks in such way that, on one hand, their singularity can no longer be recognized by the end user, and on the other hand, provide open interfaces which leave its heterogeneous parts visible. This last issue is currently an active research topic but we will not

delve further into it, since it is outside the scope of the thesis.

1.3 Previous Work

1.3.1 Active queueing mechanisms

In today's Internet, packet loss from First Input First Output (FIFO) queues with a drop-tail discard semantic is the primary indication of congestion. These queues are intended to absorb bursty packet arrivals before forwarding them to the outbound link. With drop-tail there is no flexibility on deciding whether or not to drop a packet but it is rather a passive one. Especially, during periods of persistent congestion drop-tail queues have two well known non-desirable phenomena, i.e., lock-out and full queues. The first one occurs due to TCP synchronization effects where packets from some flows always arrive to a full-queue and subsequently dropped. As a consequence of this effect only a small subset of the active flows monopolize resources [4]. The second one is actually self-explained and relates with the problematic situation of actually having routers with full queues during congestion intervals. In that case, routers have no capabilities of absorbing bursty arrivals. In other words, drop-tail queues respond to congestion only after the congestion had actually happened.

These flaws prompted research into a more active schemes for performing queue management (AQM)[4]. The most well known AQM technique is the Random Early Detection (RED) mechanism [27]. In the RED queue the probability of dropping an arriving packet is a function of the average queue occupancy and the number of packets that have arrived since the last packet was dropped. The use of dynamic drop probability of packets ensures that routers would react differently to different level of congestion in the network. In other words, the rational behind active queueing mechanisms is that the probability of dropping a packet should monotonously increase as the average queue-size increases. Even though RED queue effectively deals with flows that are based on TCP, it has been widely recognized that issues related to traffic that is unresponsive to congestion indications should be addressed. Responding to these issues, active queueing management techniques have been developed that use state information in order to ensure fair allocation of resources between flows [6], [7].

It is envisioned that AQM techniques will be an important ingredient of future IP based Mobile network architectures. In a DiffServ environment the role of AQM beyond congestion control is prioritizing packet discard depending on their priority. AF PHB defines differentiated forwarding of packets which can be classified in up to four classes. Packets from different classes are processed in different physical or logical queues, where within each class, there can be up to three drop precedences. In the case of congestion, packets with lower priority are the first to be marked/dropped. Such differentiated discarding inside the router call for sophisticated AQM mechanisms, which can be seen as extensions of RED. RED with In and Out (RIO) [5] can be seen as the extension of the RED queue in order to accommodate preferential dropping in AF PHB. RIO uses two sets of parameters to differentiate the discard of In (in-profile) and Out (out-of-profile) packets. RIO uses the average size of the total queue, formed by both In and Out packets for deciding whether to discard out-of-profile packets. On the contrary, for in-profile packets RIO uses the average size of a virtual queue formed only by In packets. Using the same principle, RIO can be extended to handle three different priorities [2].

1.3.2 TCP over wireless

The TCP state machine has been designed for wireline networks where packet loss was mainly due to congestion on the network (buffer overflow) rather than transmission errors [9], [10]. Wireless transmission, on the other hand, is more vulnerable to packet loss due to fading channels, shadowing and user mobility. These random phenomena are responsible for introducing random packet losses patterns during the session period which are negatively affect TCP performance. The reason is that the TCP state machine interpret these packet losses as a sign of congestion and unnecessarily reduce the congestion window (*cwnd*). In order to alleviate these effects a plethora of different techniques have been proposed over the last few years that aim to increase the performance of TCP protocol over wireless links.

[2]Most commonly, when three level drop priorities are used the drop precedence is indicated with different colors, i.e., *green* for lowest drop precedence, *yellow* for the middle one and *red* for the highest drop precedence

TCP aware Link Layer

The snoop protocol introduces a module, called the snoop agent, at the base station. The agent monitors every packet that passes through the TCP connection in both directions and maintains a cache of TCP segments sent across the link that have not yet been acknowledged by the receiver. A packet loss is detected by the arrival of a small number of duplicate ACKs from the receiver or by a local timeout. The snoop agent retransmits the lost packet if it has it cached and suppresses the duplicate ACKs. Thus, the snoop protocol is a transport-aware link protocol. The main advantage of this approach is that it suppresses duplicate ACKs for TCP segments lost and retransmitted locally, thereby avoiding unnecessary fast retransmissions and congestion control invocations by the sender. Also, the per-connection state maintained by the snoop agent at the base station is soft, and is not essential for correctness.

TCP agnostic Link Layer

A natural first attempt to hide packet losses from higher layers was through Forward Error Correction (FEC) and Automatic-Repeat- Request (ARQ). Sophisticated FEC schemes can indeed reduce the effective BER on the wireless link (at the cost of reduced available bandwidth for the actual payload and increased complexity for encoding/decoding) and decrease the effect of link layer bit-error rates to higher layers [12]. Additionally, the benefits of utilizing ARQ have also been considered in order to hide packet loss from the TCP sender by retransmitting them over the link layer [13]. The above two techniques can also be combined in order to increase system performance [13].

The benefit of utilizing TCP agnostic link layer protocols is that they keep the traditional protocol stack concept, where functionalities are organized into nested level of abstractions and decisions in each layer are performed independently. Therefore different transport protocols can be supported without affecting link layer functionalities. Even though these solutions can increase the performance, TCP can still be negatively affected under bad channel conditions that require multiple retransmissions. The skepticism that have been received by opponents of TCP unaware solutions is that the uncoordinated mechanisms between link layer and transport layer lead to situations where there is a conflict between packet recovery at the link layer and at the transport layer. For example, it is possible that even though a backlogged packet have been successfully transmitted to the mobile

host after several retransmission at the link layer, duplicate ACK's generated during that time can cause a TCP based retransmission (in addition to the link layer retransmission) [15].

The Transport Unaware Link Improvement Protocol (TULIP)[16], [17] provide a reliable service to higher layers and even though the base station does not maintain state information about TCP, it implicitly avoids retransmission due to three duplicate acknowledgements by allowing only in-order delivering of packets. Another solution that have been proposed is through Delayed Duplicate Acknowledgments (DD) [18]. In that case, even though the link layer is unaware of TCP functionalities, the base station delays transmission of the assumed TCP ACKs to the sender (because there are retransmission of packets from the base station to mobile host) by a specific amount of time. The main idea of the protocol is to mimic the Snoop protocol but without the requirement that the link layer have access to the TCP header (thus, DD allows encryption of TCP header).

Alternatives to TCP

TCP Santa Cruz [23] deviate from traditional TCP implementations and propose an alternative congestion control and error recovery strategy. The aim of the protocol is to successfully handle asymmetric links, variable delays, links with random losses and out-of-order packet delivery. Although the simulation results reported in [23] are very promising, actual adoption of the protocol in the Internet is problematic due to the fact that already hundred of millions of computers run more traditional TCP implementations (such as Reno or New Reno).

An alternative solution have been proposed in [19], which is called Indirect-TCP (I-TCP). The main critical idea behind this protocol is to split the connection in two parts; the wireless and the wireline part. In this case there are two different TCP sessions; one between the fixed node and the base station and the other between the mobile node and the base station. One of the main drawbacks of the I-TCP is the problematic behavior of the protocol in the cases of handover [20]. In that case, unacceptable delays introduced for transferring state information from the old to the new base station. From the architectural perspective the drawback of I-TCP is that it breaks the end-to-end principle of the Internet architecture [21]. The same is true also for M-TCP [22] which is again based on splitting the connection in two parts and therefore violating the fundamental end-to-end argument.

Another suggested approach was the Explicit Loss Notification (ELN) scheme [24]. The idea behind the ELN is to inform the sender about the loss of a packet. In that case the sender can differentiate between a loss due network congestion and a random loss due to wireless transmission. In a similar fashion Explicit Bad State Notification (EBSN) scheme [25] send EBSN messages from the base station to the sender whenever the base station is unsuccessful in transmitting a packet over the wireless network.

1.3.3 Power and Rate Control

When the transmitter is supplied with channel conditions, transmission can be adapted in order to efficiently utilize the channel but also to increase the overall system performance. In the general case the transmitter can alter the transmission power and data rate. Adaptive variation of the transmission power has been very early seen as a technique to increase system performance and received attention in late sixties by the work of Hayes , [26]. This was followed by adaptive variation of the data rate (symbol rate) [27], constellation size [28], coding rate [29], [30] or a combination of the above techniques [31]. Doubtlessly, the main goal of these techniques was to increase the average spectral efficiency of the system, which is defined as the average transmitted data rate per unit bandwidth, i.e., R/W $[Bits/s/Hz]$.

For CDMA systems which are interference limited, power control is a core functionality of the system and is responsible to mitigate the so-called *near-far effect* in which mobile nodes with higher received powers (i.e., near to the base station) can overwhelm the communication quality of the mobile nodes with lower received powers (i.e., far away from the base station). In practise, each mobile adjusts its own transmit power to ensure an adequate quality of service (QoS) or signal-to-interference ratio (SIR) at the base station. In that sense, the mobiles transmit power can be either increased or reduced depending on instructions received by the base station (uplink power control).

Centralized power control is often referred to as optimum power control due to the upper performance bounds achieved by the algorithms. In such approaches, a central station controls all the links in a cellular system. The goal of centralized power control research is to develop upper bounds for power control algorithms. The results are used for comparison with the distributed power control algorithms implemented in cellular systems. The classic paper on the topic of centralized power

control was written by Jens Zander in 1992 [32]. The paper investigates optimum transmitter power control for general cellular systems. The algorithms are for the downlink, base station to mobile station, but similar results were later developed for the uplink, mobile to base, in [33]. Contrary to centralized power control, in Distributed Power Control (DPC) each base station is responsible to calculate and update the transmitted powers using information only from the local mobile stations. Thus, power control functionalities are *distributed* to all base stations and a centralized controller is not required. The aim of DPC is to reduce computational complexity and at the same time the total link gain matrix is not required. The required information for distributed power control is SIR values for the mobile hosts attached to the specific base station and the corresponding link gains. The combination of power and rate control algorithms have been extensively discussed in [34], [35], [36]. In [34], two different algoreithms have been proposed, the first one was based on Lagrangian relaxation technique and the second one, was an extension of a fixed rate power control algorithm, which was called selective power control. On the other hand, the basic idea in [35], [36] was to reduce the rate when the transmit power required to achieve a target QoS exceeds a threshold. Also, using a different perspective on resource management, the work of Ji and Huang [37] and Feng et al. [38] was one of the first attempts to study the power control problem from a game-theoretic perspective. Based on Game theory they have developed a power control algorithm that converges to a Nash equilibrium.

1.4 Contributions

In chapter 2 we propose a core centric approach for providing QoS support in heterogeneous wireless access networks. The motivation behind this approach is that the number of different standards and systems is likely to remain high during the continuing evolution of wireless systems. This diversity of access technologies will allow innovative new concepts to be introduced in order to improve spectral efficiency, system performance, power consumption, and functionality of wireless platforms and devices. From this point of view, a single-standard wireless system which integrate or replace all present systems is likely not to happen over the next few years.

Responding to a proliferation of studies on future all IP based mobile networks, a fundamental conceptual distinction from previous work is that we propose a *core-centric* approach in contrast

to an *air-interface centric* approach. A key difference between the wireless access domain and the core network is that bandwidth management and network dimensioning rules on these two domains follows rather different paths, so they can be thought as uncoupled. In that respect, the number of traffic classes in the more restrictive environment of the access domain should not be a priori imposed to the core network. We will argue that there is no viable criterion for such restriction to be possed on the core network and at the heart of our position two main arguments will be discussed in order to back this claim. The first one lies in the fact that future core networks will support multiple wireless access networks. From this perspective it seems plausible that we must ultimately disassociate per-flow or per-class specific functionalities of the core network from the different wireless access networks in order the core network to support a plethora of different wireless access IP QoS techniques. The second one relates to the traffic management related mechanisms of the core network. Utilizing a high number of traffic classes on the core network will mainly posse an increased amount of required signalling on the control plane and a more restrictive network management for resource control in order to guarantee statistical QoS. In the DiffServ domain for example each aggregate traffic class would need certain amount of network resources (link bandwidth and router buffer space) for assuring the statistical QoS requirements. With an increased number of traffic classes the critical issue is that the required slack bandwidth in each traffic class, in order to avoid saturation situations, will be decreased. Therefore a more stringent policy will be required for management of all routers in the domain by the bandwidth broker. This will potentially lead to a laborious and complicated control plane in the core network. The simulations in this chapter have been contacted with the help of A. Abella.

After introducing in chapter 2 an all IP based core and wireless access architecture for mobile networks, in chapter 3 a novel active queueing management technique for the ingress router of the DiffServ domain is presented. With IP technology integrated into future mobile networks a sound assumption would be that these networks can be considered as an integral part of the Internet. Due to the fact that wireless networks can be classified as stub rather than transit networks, from a topological point of view they belong on the periphery (edge) of the Internet, close to the end user. The seminal aspect of the proposed Hop Based Queueing (HBQ) mechanism is that utilize this property of wireless networks, i.e., that they belong on the periphery of the Internet. In HBQ

the packet dropping decision takes also into account the number of traversed routers in the Internet. The legitimate benefit of utilizing this kind of side information is mainly twofold. First, the proposed scheme reduce the probability of packet dropping for those packets that have crossed a large number of routers in the Internet and therefore there is a capacity saving. The second benefit lies on the fact that on the average the Round Trip Time (RTT) in the Internet increases as the number of hops increases and relates with the performance of TCP (which count for almost 90% of all traffic in the Internet). TCP encompass a complex state machine based on additive increase multiplicative decrease (AIMD) congestion control algorithms that reflected on the "sawtooth" like pattern of the congestion window (cwnd). More formally speaking, for connections with large bandwidth-delay products, where the probability of a timeout event is very small, it has been shown that the following, so-called *square root formula*, can model accurately the actual throughput [21] of TCP connections,

$$T = MSS \cdot min\left[\frac{1}{\overline{RTT}}\sqrt{\frac{c}{p}}, \frac{W_{max}}{\overline{RTT}}\right] \tag{1.1}$$

where MSS is the maximum segment size, W_{max} the advertised receiver window size, $\overline{RTT}$ denotes the average RTT of the connection, c is a constant that depends on the flavor of TCP used and the process of inter-loss times [26], finally, p denote the probability of packet loss. As can be seen, the throughput of TCP connections is inversely proportional to the RTT of the connection. The Hop Based Queueing algorithm by utilizing the information from the number of hops, indirectly and on the average, increases the performance of TCP connections with long RTTs.

In chapter 4, an algorithm for resource management in CDMA network is presented which utilizes information from the TCP layer. Contemporary resource management in wireless networks mainly involve lower layer information such as channel condition and/or buffer occupancy. The weakness of such approaches lies on the fact that they are agnostic of the requirements and operation of higher layers. These approaches, as will be discussed in chapter 4, have received several skeptical attacks over the last few years, which are mainly related with performance aspects of TCP over wireless networks.

Based on this avocation, i.e. thinking beyond the constraints imposed only by lower layers on resource control, the proposed power and rate control scheme turns towards utilization of higher layer information. Two critical side information metrics, that heavily affect TCP performance, have been

taken into account i.e., the RTT of the connections and the corresponding cwnd sizes of the TCP flows. A multi-objective optimization problem is formulated which is solved with gradient based techniques because of the availability of the derivatives. In the most general case the whole Pareto frontier can be unfolded, and among all solutions the one with the minimum Euclidean distance from a "utopian" point is selected. Gradient based techniques have superlinear convergence [3], so they posse high complexity and require extensive CPU cycles for real time operation. In order to tackle this problem a greedy algorithm is proposed where the complexity increases linearly with the number of mobile hosts. Even though the proposed greedy algorithm has sub-optimum performance, it has the benefit that can be implemented and used for real time decisions.

In chapter 5 we propose resource management schemes that integrate QoS information from the forwarding plane of the DiffServ architecture in order to optimize packet transmission. By differentiating packet transmission according to the drop-precedence of IP packets significant power gains can be achieved by deterring to compensate deep fades of out-of-profile packets.

Finally, in chapter 6 we present a novel resource management scheme that utilize information from the TCP friendly (TFRC) [44] [29] transport protocol and the type of MPEG-4 frame [8] (i.e, Intra, Predictive or Bidirectional) together with lower layer criteria in order to optimize packet transmission over the wireless link.

1.5 Organization of Thesis

In chapter 2 different candidate IP QoS technologies for both the core and access networks together with their distinctive requirements will be presented. This will followed with analysis of the proposed core-centric architectural approach for all IP based heterogeneous wireless networks. In chapter 3 a novel active queueing mechanism (Hop Based Queueing) is presented that can be utilized in the ingress DiffServ node of the all IP architecture in the core network. We proceed in chapter 4 with the necessary methodological foundations for utilizing IP based information for resource management in CDMA networks. A family of novel objective functions is discussed together with the related

[3] In iterative techniques for solving non-linear optimization problems, the stopping criterion for the solution, $x_1, x_2, \ldots, x_n$, is when the error, $e_k = x_k - x^*$, is sufficient small, i.e. when $\|e_k\| < \epsilon$. The convergence rate is determined by looking at the equation $\|e_{k+1}\| = C\|e_k\|^r$ with $C \geq 0$ in the limit as $k \longrightarrow \infty$. If $r = 1$ we say that the convergence rate is linear. If $1 < r < 2$ the convergence rate is superlinear, and if $r = 2$ the convergence rate is quadratic.

simulation results on system performance. Also, theoretical formulations and implementation details of a greedy algorithm for resource management that is TCP aware are also presented. Chapter 5 discuss a novel resource management scheme that utilize information from the DiffServ forwarding plane. Chapter 6 focus on resource management algorithms for handling TCP-friendly based real-time streaming flows. Finally, chapter 7 concludes and outlines future research directions deemed by this work.

Bibliography

[1] W. Mohr and W. Konhauser, Access Network Evolution Beyond Third Generation Mobile Communications, *IEEE Commun. Mag. 38, No. 12, 122133, December 2000*

[2] Book of Vision 2001, Wireless World Research Forum, v1.0, Paris, France, December 2001; http://www.wireless-world-research.org

[3] Jorge Pereira, European approach to Fourth Generation a personal perspective, *Proc. Fourth Generation Forum, 13-14 May 2002, London, UK*

[4] B. Braden, D. Clark, J. Crowcroft, B. Davie, S. Deering, D. Estrin, S. Floyd, V. Jacobson, G. Minshall, C. Partridge, L. Peterson, K. Ramakrishnan, S. Shenker, J. Wroclawski, L. Zhang, Recommendations on Queue Management and Congestion Avoidance in the Internet, *Request for Comments: 2309, April 1998*

[5] S. Floyd, V. Jacobson, Random Early Detection Gateways for Congestion Control, *IEEE/ACM Transactions on Networking, 1(4):397-413, August 1993*

[6] Dong Lin and Robert Morris, Dynamics of Random Early Detection, *in Proc. ACM SIGCOMM '97*

[7] Farooq M. Anjum, Leandros Tassiulas, Balanced-RED: An Algorithm to Achieve Fairness in the Internet, *in Proc. IEEE Infocom '99, March 1999*

[8] D. Clark, W. Fang, Explicit Allocation of Best-Effort Packet Delivery Service, *IEEE/ACM Transactions on Networking 6 (1998) 362-373*

[9] J. B. Postel, Transmission Control Protocol, *RFC 793, September 1981*

[10] V. Jacobson, R. Braden, and D. Borman, TCP Extensions for High Performance, *RFC 1323, May 1992*

[11] H. Balakrishnan, S. Seshan, and R.H. Katz, Improving Reliable Transport and Handoff Performance in Cellular Wireless Networks, *ACM Wireless Networks, 1(4), December 1995*

[12] D. Eckhardt, P. Steenkiste, Improving Wireless LAN Performance via Adaptive Local Error Control, 6^{th} *IEEE International Conference on Network Protocols (ICNP'98), Austin, October, 1998*

[13] E.Ayanoglou, S. Paul, T. F. Laportaa, K.K. Sabani, R. D. Gitlin, AIRMAIL: A Link-Layer Protocol for Wireless Networks, *ACM/Baltzer Wireless Networks Journal, 1:47-60, February 1995*

[14] A. Chockalingam, M. Zorzi, V. Tralli. Wireless TCP performance with link layer FEC/ARQ *Proc. IEEE ICC'99, 1212-1216, 1999*

[15] H. Balakrishnan, V. Padmanabhan, S. Seshan, and R. Katz, A comparison of mechanisms for improving TCP performance over wireless links, *ACM SIGCOMM, Stanford, CA, August 1996*

[16] C. Parsa and J. J. Garcia-Luna-Aceves, Improving TCP Performance over Wireless Networks at the Link Layer, *Mobile Networks and Applications, 1999*

[17] C. Parsa, J. J. Garcia-Luna-Aceves. TULIP: A link-level protocol for improving TCP over wireless links *Proc. IEEE WCNC'99, 1253-1257, 1999*

[18] N. H. Vaidya, M. Mehta, C. Perkins and G. Montenegro, Delayed Duplicate Acknowledgement: a TCP unaware Approach to Improve Performance of TCP over Wireless, *Journal of Wireless Communications and Mobile Computing, special issue on Reliable Transport Protocols for Mobile Computing, February 2002*

[19] A. Bakre and B. R. Badrinath, I-TCP: Indirect TCP for Mobile Hosts, *Proc. 15th Intl. Conf. Distributed Computing Systems, May 1995*

[20] R. Caceres and L. Iftode, Improving the Performance of Reliable Transport Protocols in Mobile Computing Environments, *IEEE JSAC, vol. 13, no. 5, June 1995*

[21] M. Blumenthal and D. Clark, Rethinking the design of the Internet: The end to end arguments vs. the brave new world, *ACM Transactions on Internet Technology, 1(1):70-109, August 2001*

[22] Brown and S. Singh, M-TCP: TCP for Mobile Cellular Networks, *Computer Communication Review, vol. 27, no. 5, October 1997*

[23] C. Parsa and J.J. Garcia-Luna-Aceves, Improving TCP Congestion Control over Internets with Heterogeneous Transmission Media, *Proc. IEEE ICNP 99, Toronto, October 1999*

[24] H. Balakrishnan and R. Katz, Explicit Loss Notification and Wireless Web Performance, *in Proceedings of GLOBECOM, November 1998*

[25] B. S. Bakshi, N. Vaidya, and D. K. Pradhan, Improving the Performance of TCP over Wireless Networks, *in Proceedings of 17th, International Conference on DCS, pages 365373, July 1997*

[26] J. F. Hayes, Adaptive feedback communications, *IEEE Transactions on Communications, vol. COM-16, pp. 2934, Feb. 1968*

[27] J. K. Cavers, Variable-rate transmission for Rayleigh fading channels, *IEEE Transactions on Communications, vol. COM-20, pp. 1522, Feb. 1972*

[28] W. T.Webb and R. Steele, Variable rate QAM for mobile radio, *IEEE Transactions on Communications, vol. 43, pp. 2223-2230, July 1995*

[29] Alamouti and S. Kallel, Adaptive trellis-coded multiple-phaseshift keying for Rayleigh fading channels, *IEEE Transactions on Communications, vol. 42, pp. 2305-2314, June 1994*

[30] B. Vucetic, An adaptive coding scheme for time-varying channels, *IEEE Transactions on Communications, vol. 39, pp. 653-663, May 1991*

[31] T. Ue, S. Sampei, and N. Morinaga, Symbol rate and modulation level controlled adaptive modulation/TDMA/TDD for personal communication systems, *IEICE Transactions on Communications, vol. E78-B, pp. 1117-1124, Aug. 1995*

[32] Jens Zander, Performance of Optimum Transmitter Power Control in Cellular Radio Systems, *IEEE Transactions On Vehicular Technology, vol. 41, no. 1, pp. 57-62, February 1992*

[33] Jens Zander and Magnus Frodigh, Comment on 'Performance of Optimum Transmitter Power Control in Cellular Radio Systems', *IEEE Transactions On Vehicular Technology, vol. 43, no. 3, pp. 636, August 1994*

[34] S.-L. Kim, Z. Rosberg and J. Zander. Combined Power Control and Transmission Rate Selection in Cellular Networks. In Proc. of VTC Fall, pp. 1653-1657, 1999

[35] S. Kim, Y.H. Lee. Combined Rate and Power Adaptation in DS/CDMA Communications over Nakagami Fading Channels. IEEE Transactions on Communications, vol. 48, no. 1, January 2000

[36] B. Hashem and E. Sousa. A combined power/rate control scheme for data transmission over a DS/CDMA system *In Proc. IEEE VTC, May 1998*

[37] H. Ji and C.-Y. Huang, Non-cooperative uplink power control in cellular radio systems, *Wireless Networks, vol. 4, no. 3, pp. 233240, 1998*

[38] N. Feng, N. B. Mandayam, and D. J. Goodman, Joint power and rate optimization for wireless data services based on utility functions, *in Proc. Conf. Inform. Sci. and Sys. (CISS99), Johns Hopkins University, Baltimore, MD, 1999*

[39] Gustafsson E. and Jonsson A. Always Best Connected *IEEE Wireless Communications February 2003. pp. 49-55*

[40] V. Friderikos, et al., ANWIRE Analysis of User Requirements for Future Heterogeneous Wireless Networks, *International Workshop on Wireless, Mobile and Always Best Connected, Glasgow, April 22, 2003*

[41] Teunis J. Ott, J.H.B. Kemperman, and Matt Mathis, The Stationary Behavior of Ideal TCP Congestion Avoidance, *accesible via ftp://ftp.bellcore.com/pub/tjo/TCPWindow.ps, August 1996.*

[42] Altman, K. Avrachenkov, and C. Barakat, A stochastic model of TCP/IP with stationary random losses, *ACM SIGCOMM, Stockholm, pp.231-242, August 2000.*

[43] Radha, H., van der Schaar, M., Chen, Y., The MPEG-4 fine-grained scalable video coding method for multimedia streaming over IP, *IEEE Transactions on Multimedia 3, pp. 5368, 2001*

[44] M. Handley, S. Floyd, J. Padhye, J. Widmer, TCP Friendly Rate Control (TFRC): Protocol Specification, *IETF, Request for Comments: 3448, January 2003.*

[45] Michael Zink, Carsten Griwodz, Jens Schmitt, and Ralf Steinmetz, Scalable TCP-friendly Video Distribution for Heterogeneous Clients, *SPIE Conference on Multimedia Computing and Networking (MMCN) 2003*

Chapter 2

Core-Centric Approach for QoS Support in Heterogeneous Mobile Networks

As future evolution of mobile networks escalates towards all-IP based solutions, one important issue that influence proposed architectures, is QoS support. Current proposed architectures are mainly based on different ramifications of the Differentiated Services and/or Integrated Services. The least common denominator of these proposals is the *air-interface-centric* approach of mapping traffic classes of the wireless link into Expedited Forwarding (EF) and Assured Forwarding (AF) Per Hop Behaviors (PHB) in the core network. The stance to be defended hereafter is that the number of traffic classes in the core network can be actually seen as an orthogonal choice related to the number of traffic classes in the wireless access network. In essence, this work proposes a *core-centric* approach on the mapping issue, where the impetus is to consider the degree of over-provisioning needed for a best-effort domain or a minimalist DiffServ domain in order to provide the same QoS support with a DiffServ domain with multiple traffic classes. The prerogative of the proposed approach is that the core network can provide QoS support in a multi-technology mobile network without being tight with one specific wireless access network. The air-interface centric approach may lead to

an elaborate management plane because of the increased number of traffic classes that need to be controlled. Therefore, an additional benefit of the proposed approach is that the complexity of the control plane can be reduced. We will not dwell into the dilemma of choosing a specific architecture but rather, provide an insight on the pros and cons of different QoS architectural regimes by a scrupulous comparison of the traffic characteristics between a best-effort and a DiffServ enabled domain. The results indicate that because QoS support includes a synergy of different mechanisms such as routing, traffic engineering and admission control, the forwarding plane should be kept with the minimum required number of traffic classes in order to avoid increased complexity on the control plane.

2.1 Introduction

One critical issue towards all-IP based mobile networks is to support *Quality of Service* to the end-users. The introduction of this key term - *QoS* - has engendered a lively debate over recent years and in the plethora of different architectures that have been proposed, Integrated Services (IntServ) and Differentiated Services (DiffServ) are clearly seen as the most important ones. For all-IP based mobile networks different ramifications of the above mentioned IETF developed standards have been considered. Although there have been major research efforts in order to enchase the Internet architecture with new service models (QoS enabled), the question of whether or not to provide multiple service classes on the Internet have not been thoroughly discussed. Additionally, providing QoS on the Internet beyond being a theoretical debate [1], proved also to be a huge complex task, i.e QoS-enabled applications, different networking layers and network architectures, new network management schemes, but also different business models that need to be introduced.

Traditional IP networks offer users best-effort service. In this best-effort semantic, all packets compete equally for the available network resources. Because of this, best-effort service without adequate bandwidth provisioning cannot provide predictability and reliability in end-to-end packet delivery, which make it unsuitable for real-time or mission-critical business applications. These constraints require the ability from the network to provide Quality of Service (QoS) i.e., to offer service differentiation based on the requirements of users and applications. It was in this confrontation between the introduction of real-time services and the lack of control over a best-effort domain where

different QoS architectures were born and brought an aura of fascination that continued to draw research over the last years. In that respect, QoS mechanisms do not provide more bandwidth but a way of real time managing the bandwidth in order to support the wide range of different application requirements.

While QoS provisioning for fixed networks has already received an enormous research attention, providing QoS for a diverse set of IP applications for future IP-based mobile networks can still be considered in early stages [4]. QoS support in a mobile network introduce some unique features that makes off the shelf solutions for QoS support in stub or transit wireline networks not applicable (at least without some major modifications). The issues of mobility, the scare resources of the air-interface and the interactions with the complex link layers of wireless access technologies make mobile networks a distinctive paradigm. Especially, issues like QoS re-negotiation which is due to handover or variability of channel and network conditions, have been seen as one of the biggest hindrances in the development of QoS architectures in mobile networks. Our main argument is that these difficulties can be bypassed (or, at least waned) with a well over-provisioned core network which is based on best-effort paradigm or on stateless QoS techniques but with the minimum possible number of traffic classes.

The main driving force behind this work is that wireless access technologies for global-area licensed bands (e.g. GSM, GPRS, UMTS) or for hot-spot areas in the unlicensed band (e.g. IEEE 802.11b, HIPERLAN II, Bluetooth) can be relatively more resource constrained compared with wired IP networks. Examining existing proposed QoS architectures, one area of critical sameness, is the *air-interface-centric* mapping between traffic classes on the wireless link and on the core-IP. This approach asserts that the minimum number of traffic classes in the core-IP is constrained by the number of traffic classes in the air-interface. Looking more closely at the mapping issue, we question the tenability of the above approach by proposing a *core-centric* point of view which considers minimization of the number of traffic classes in the core-IP. The prerogative of this approach is that it opens the path for more efficient and scalable network management solutions. The thorny problem with large number of traffic classes in the core-IP is the requirement of a fastidious control plane in the architecture, since controlling each class may require detailed information from all routers in the core network.

We should stress that our intention is neither to provide a solution to all the above problems (which are still very open) nor to compare all possible QoS architectures, but instead to present and highlight critical observations from an extensive set of simulations. More specifically, we investigate traffic characteristics of best-effort and DiffServ enabled domains under different traffic scenarios. The degree of over-provisioning needed for an IP best-effort domain to provide the required QoS to real-time applications that can be achieved by DiffServ is explored, together with other important QoS metrics.

2.2 QoS in pure-IP mobile networks

Recently there have been several different proposed QoS architectures proposed, INSIGNIA [2], BRAIN [3], that have sought to combine mobility with guaranteed QoS. These efforts are based mainly on IETF QoS architectures with extensions for mobility support. IETF proposed two very different QoS architectures, i.e *Integrated Services*(IntServ) and *Differentiated Services* (DiffServ). The IntServ approach provides absolute per flow QoS measures for data rate and delay but requires a substantial amount of per-flow state to be maintained in the routers of the network. DiffServ on the other hand, segregates traffic with different quality-of-service requirements into a small number of quality-of-service classes. The main concept behind the DiffServ paradigm is the dissociation between network operations performed in the core, and those performed at the edges of the network. Ergo, DiffServ provides a framework for highly scalable mechanisms with minimum impact on elements in the core network which carry the cumulative aggregate traffic. In the sequel we present the main building blocks that can be used in the core IP part of the mobile network and describe briefly the pros and cons of each one. Figure 2.1 depicts the solutions discussed in the sequel.

2.2.1 Integrated Services and RSVP

The basic concept of the IntServ-RSVP [5] model is the enhancement of the existing IP router with complex tasks where the aim is to provide a circuit-switched like service in a datagram network, and thus giving the Internet a connection-oriented character. Hence, operations like policing, shaping, admission control and QoS management must be provided by all RSVP routers on a per IP flow

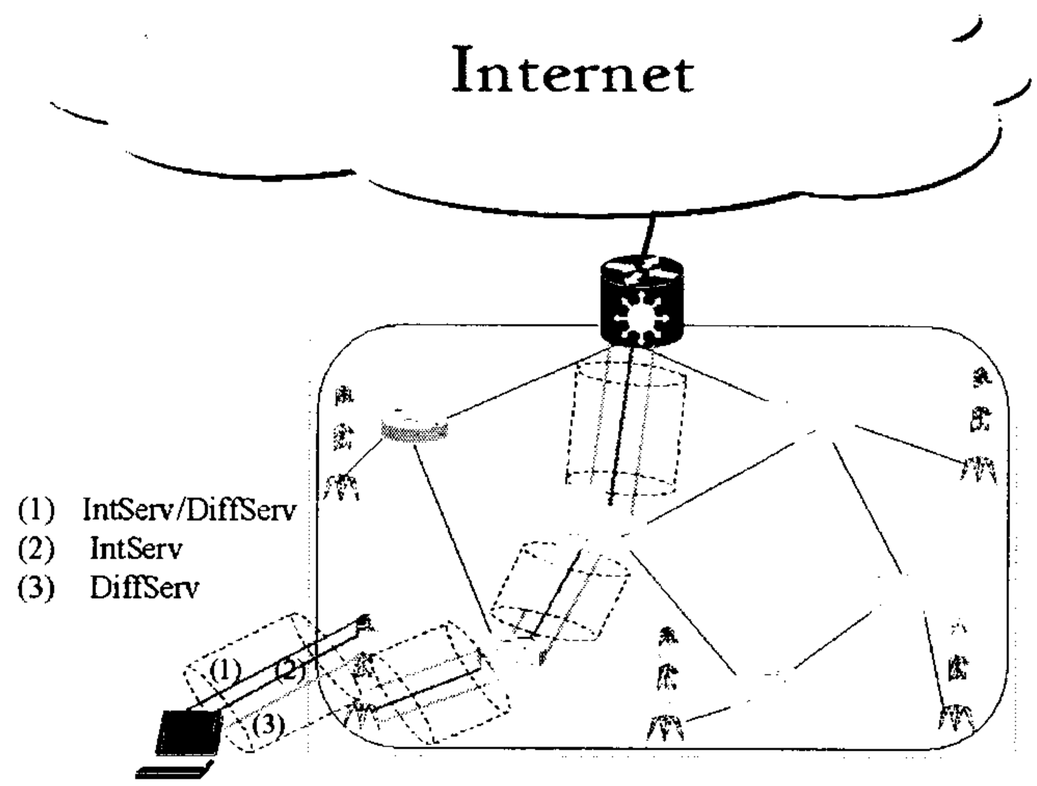

Figure 2.1: Alternative possible QoS techniques for pure-IP Mobile Networks

basis. Therefore, the execution of the above functions for every active IP flow in a core IP router leads to poor performance and to a non-scalable network architecture.

In addition to the well-known shortcomings of scalability, the reservation approach of IntServ, is heavily affected by mobility. According to the original RSVP signaling protocol, the resource reservation path cannot be dynamically adapted along with the movement of a mobile host in time. In other words, whenever a mobile host performs a handoff that incurs a path change, the new path to the mobile host from the correspondent host is discovered by RSVP only after the soft state timers expire in routers. In order to mitigate the above problem, several proposals, [6], [7] consider making advance resource reservations at multiple locations which a mobile host may possibly visit during the session time (the drawback is that many resources can be wasted).

Currently the IETF Seamoby working group is considering solutions to the problem of selecting target access points for the mobile host's handoff. In this case a protocol is required that will allow the discovery of neighboring access points by the mobile host whose capabilities meet its requirements. Thus, a context transfer mechanism, which will allow for exchanging mobile node context information between access routers and gateways, will eliminate the need for explicit advance reservation of resources in all nearby access points. For the above reasons,i.e complexity, scalability,

mobility un-friendliness, the stand alone IntServ/RSVP model may not meet widespread success and acceptance in real implementations.

2.2.2 The DiffServ Architecture

The Differentiated Services (Diffserv) architecture [1] has recently become one of the preferred methods to address QoS issues in IP networks and can be seen as the present heir of a long line of research efforts towards a stateless scalable architecture. This packet marking based approach to IP-QoS is attractive because of its simplicity and ability to scale. An end-to-end differentiated service is obtained by concatenation of per-domain services and Service Level Specifications [1] (SLS) between adjoining domains along the path the traffic crosses from source to destination. Per domain services are realized by traffic conditioning at the edge and simple differentiated forwarding mechanisms at the core of the network. Two of the more popular proposed forwarding mechanisms are Expedited Forwarding (EF) [2] and Assured Forwarding (AF) [3] Per Hop Behavior (PHB). Traffic conditioning includes classification, metering, policing and shaping.

The basic concept of AF-based services is appealing as it proposes simple mark and drop mechanisms to realize IP QoS. The AF approach will provide better than best-effort service by controlling the drop preference of packets at the time of congestion. AF provides an interesting alternative in that it may enable service offerings at reduced cost for audio, video, web and other applications.

The AF PHB draft proposes four classes and three-drop preferences per class. AF is an extension of the RIO scheme [1], which uses a single FIFO queue with two-drop preferences. Most of the current studies of differentiated drop mechanisms are based on the RIO approach. The same issues are applicable to IETF's AF proposal and hereafter we assume a RIO-like framework. The RIO (Random Early Detection with distinction of In-profile and Out-profile packets) mechanism is based on the RED (Random Early Detect) queue and provide differentiated dropping of packets during congestion at the router. In RIO, traffic profiles for end-users are maintained at the edge of the network. When a user's traffic exceeds the contracted target rate, their packets are marked out-of-profile. Otherwise, packets are marked in-profile. The RIO scheme utilizes a single queue. All user

[1]The notions of Service Level Agreement (SLA) and Traffic Conditioning Agreement (TCA) used in the initial DiffServ proposed architecture (RFC 2475), have changed in RFC 3260 to Service Level Specification (SLS) and Traffic Conditioning Specification (TCS) in order to reflect better the technical parameters they represent rather than any pricing or business model

packets are directed to and serviced from the same queue.

Two sets of RED thresholds are maintained, one each for in-profile and out-of-profile. Two separate average buffer occupancy calculations are tracked, one for in-profile packets and one for in-profile plus out-of-profile packets. The possibility of dropping in-profile packets depends only on the buffer occupancy of in-profile packets while the possibility of dropping out-of-profile packets depends on the buffer occupancy of in-profile plus out-of-profile packets. This scheme gives the appearance of two coupled virtual queues within a physical queue. [2]

2.2.3 IntServ over DiffServ

A natural evolution of the DiffServ and IntServ architectures is a new combined model of the two of them [13]. This model inherits the scalability property of the DiffServ architecture and the dynamic network resource allocation feature of the IntServ/RSVP model has been introduced by the Integrated Services over Specific Link Layer (ISSLL) Working group. This model provides per-application resource allocation using IntServ/RSVP and aggregation of flows in the core using Diff-Serv. The main idea is to use IntServ in the stub networks and DiffServ in the backbones (transit). The peripheral routers must understand the two protocols and apply a mapping between IntServ and DiffServ QoS. The ISSLL group has defined a general architecture where IntServ networks sre connected through DiffServ domains, but it does not assume any specific size of these domains. In a mobile network, IntServ can just be implemented at the mobile host site or the access router while the core IP network will be based on DiffServ aggregation. In this case, RSVP reservations can be mapped to DiffServ forwarding classes at the borders of the access network and forwarded according to the regular DiffServ operation. From the RSVP and application point of view, the routed path between the access point and the gateway will be seen as a dedicated line.

2.2.4 Over-Provisioning

In general, an over-provisioned network, i.e a network where the offer is always greater than the demand, can provide low latency, low loss and low jitter. Over-provisioning means that the system will under utilize its resources by operating most of the time in a state that is lower than the available

[2]The policy criteria used can include time of day, source and destination addresses, transport, and/or port numbers. Therefore, any *context* or *traffic content* (including headers or data) can be used to apply policy.

capacity. In other words, traffic differentiation is only useful when congestion occurs in some links on the network. Currently over-provisioning without QoS support is the preferred method used in backbone networks because it is cheaper and simpler to add extra capacity than to switch to complex traffic differentiation techniques. In fact, today's Internet backbone not only has unused capacity but there have been techniques developed to use these spare resources [14].

One important issue that should not be relegated, is the fact that mobile networks will continue to carry huge amount of non-responsive real time traffic (VoIP). Even in the case of high loss rate, where real-time streams will be severely disturbed, sources will keep on sending at the same bit rate, exacerbating the congestion that is causing the loss at the first place. Fortunately, a well over-provisioned best-effort domain would be able to react to congestion when these non-responsive flows of today's Internet will decreased by widely adoption of TCP-friendly rate-based flow control [16], [17] schemes. These schemes involve synergy with the application layer and assume that applications can adapt to network conditions. In future, adaptive applications, i.e applications that can reduce the transmitted data rate in the case of network congestion, will be the norm rather than the exception. This kind of adaption mean that the application will always be able to use in the most efficient way the available resources, and this can be seen as an irrelevant problem from where these resources have been obtained (i.e by reservation or just by a best-effort network).

Finally, mobility patterns and peer-to-peer applications will also heavily affect an uncontrollable over-provisioned best-effort core domain. Multi-technology mobile networks that will be based on the integration of 2.5/3G, WLAN's (HIPERLAN II, IEEE 802.11b, Bluetooth, ZigBee) and ad-hoc networks are expected to produce hot-spot areas with hundreds of Mbps on the edges of the core network. Time and space unpredictability of such hot-spot areas may require not only sufficient over-provisioning but also a sufficient mesh topology to respond to traffic decentralization via alternative route paths.

2.3 Core network centric QoS in multi-technology mobile networks

2.3.1 The control plane of DiffServ - Bandwidth Broker paradigm

Although DiffServ has well defined building blocks for the forwarding path, the control plane of the architecture, the bandwidth broker (BB) [11], [12] as it called, is still in its infancy, especially for mobile networks. The BB is an agent that is configured with service provisioning policies, i.e SLA's between mobile users and network providers. It is responsible for internal and external admission control decisions according to a policy database. Based on such decisions it configures any routers within the domain and is also responsible for negotiating with bandwidth brokers from neighboring domains. In this case, the BB is responsible for allocating different services to users as per their requests and the existing service policy in the network, and for adaptive configuration of network routers with the correct forwarding behavior for the service defined. For doing this it might request detailed information from all routers (through OSPF and SNMP) on one or several paths before admitting a request.

In a mobile network the bandwidth broker should also take into account the mobility of the users, where the agent should be able to negotiate resources not only for admission control but also for the case of handover requests which traditionally have higher priority. The admixture of the scarce resources of the wireless links together with mobility issues may lead to an architecture that encompass subnet bandwidth brokers which are link-layer specific and use an extended parameter set (an augmenting model for example of the IntServ Rspec [3]). It is clear that notwithstanding the plea for an articulated control plane of a DiffServ based mobile networks, there are currently no clear cut solutions and a lot of aspects are actually under investigation.

2.3.2 Reasoning behind the concept of minimalist QoS enabled core network

Having in mind the current primordial state concerning the control plane of the architecture we should stress that future mobile networks are expected to encompass different access technologies

[3] Request SPECification:specify requirements of the flow

with integrated inter-operability capabilities, like reconfigurability and vertical handovers among others. In such scenarios, as depicted in figure 2.2, where multiple access technologies are integrated in a pure IP based network, the last wireless hop can be considered as a transparent bearer. Even without drawing the lines of demarcation between control functionalities in the core and the radio access part of the network, a *core-network centric* perspective has the prerogative of providing QoS to a whole spectrum of radio access technologies. An *air-interface centric* [15] perspective on QoS may result in conflicting requirements for non-static configurable PHBs inside the core network. Worse, this approach pushes detailed information, needed for optimized utilization of the scare resources of the last wireless hop, back to the core network. In the core IP, which consists mainly of wireline and high capacity wireless point-to-point connections, a higher aggregation of traffic classes can be achieved which facilitate management functions.

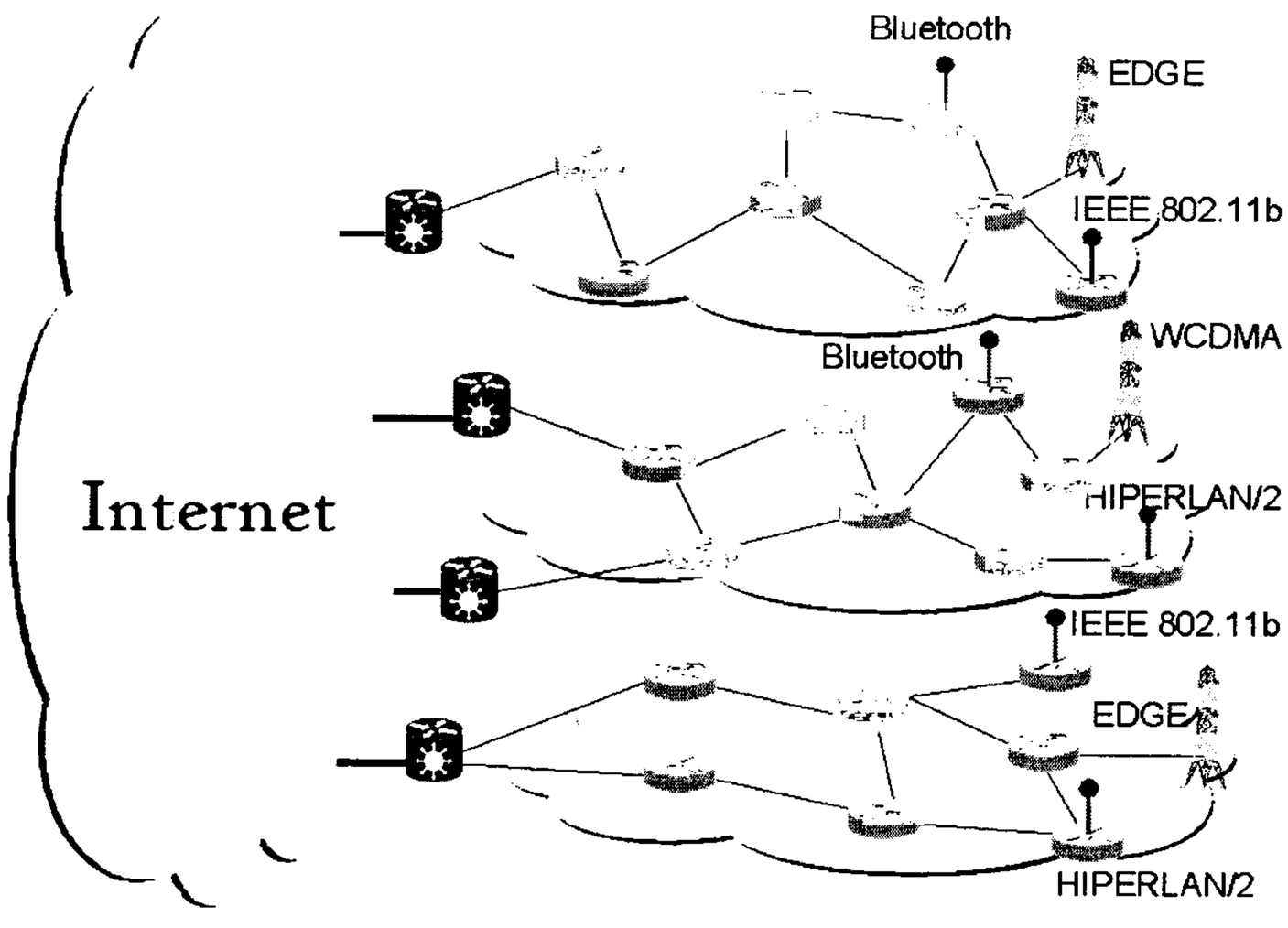

Figure 2.2: Envisioned framework for QoS enabled pure-IP Mobile Networks

In yet another variant, an air-interface centric designed network may lead to a non-minimalist QoS enabled core IP with an elaborate management plane. Figure 2.3 depicts bandwidth utilization versus time in a DiffServ enabled router with different numbers of traffic classes. Both graphs represent one EF class while the upper and lower graph have four and one AF classes respectively.

In adaptive configurable PHBs the bandwidth allocation of each traffic class would be equal to the requested bandwidth plus a tolerance value (cushion) which absorbs traffic fluctuations inside the AF class and depends on observed traffic characteristics. As the number of traffic classes increases the available bandwidth, a_i, per traffic classes decreases, i.e $a > a_i \forall i$. From the bandwidth broker point of view, a smaller cushion interval implies a smaller update interval so that saturation of a specific PHB can be avoided. The overhead in updating the snapshot view of the network from the bandwidth broker yield complexity of $O(kn)$, where k is the update interval and n the number of traffic classes. As the complexity of network management functions increases proportionally with the number of traffic classes, network operators have a vested interest to assess the possibility of using a small number of traffic classes in the core, and question therefore the applicability of complex proposed architectures. In this spirit, the following sections provide some important insights towards the dissociation concept of traffic classes in the air-interface and the core network.

2.4 Simulation Setup

The Network Simulator (ns-2) have been used as the base platform for the simulations. Web generated traffic was based on persistent connections (HTTP/1.1) which produce less aggressive traffic than HTTP/1.0 which opens different TCP connections for each inline object. The different traffic models used are summarized below:

2.4.1 Traffic Models

In all the different simulation scenarios four different applications have been considered, namely, VoIP, WWW, Streaming Video and FTP.

VoIP: Telephone traffic has been modelled as uncompressed voice over IP without silence suppression. Each user produces a Constant-Bit-Rate (CBR) flow of 86.4 Kbps with packets 124 bytes long. The duration of each session is uniformly distributed from 40 to 50 seconds.

Streaming Video: Video traffic is produced by ns-2 according to a trace file. Each record of the file consists of two 32-bit fields. The first contains the time (in microseconds) until the next packet is generated. The second contains the length (in bytes) of the next packet to be

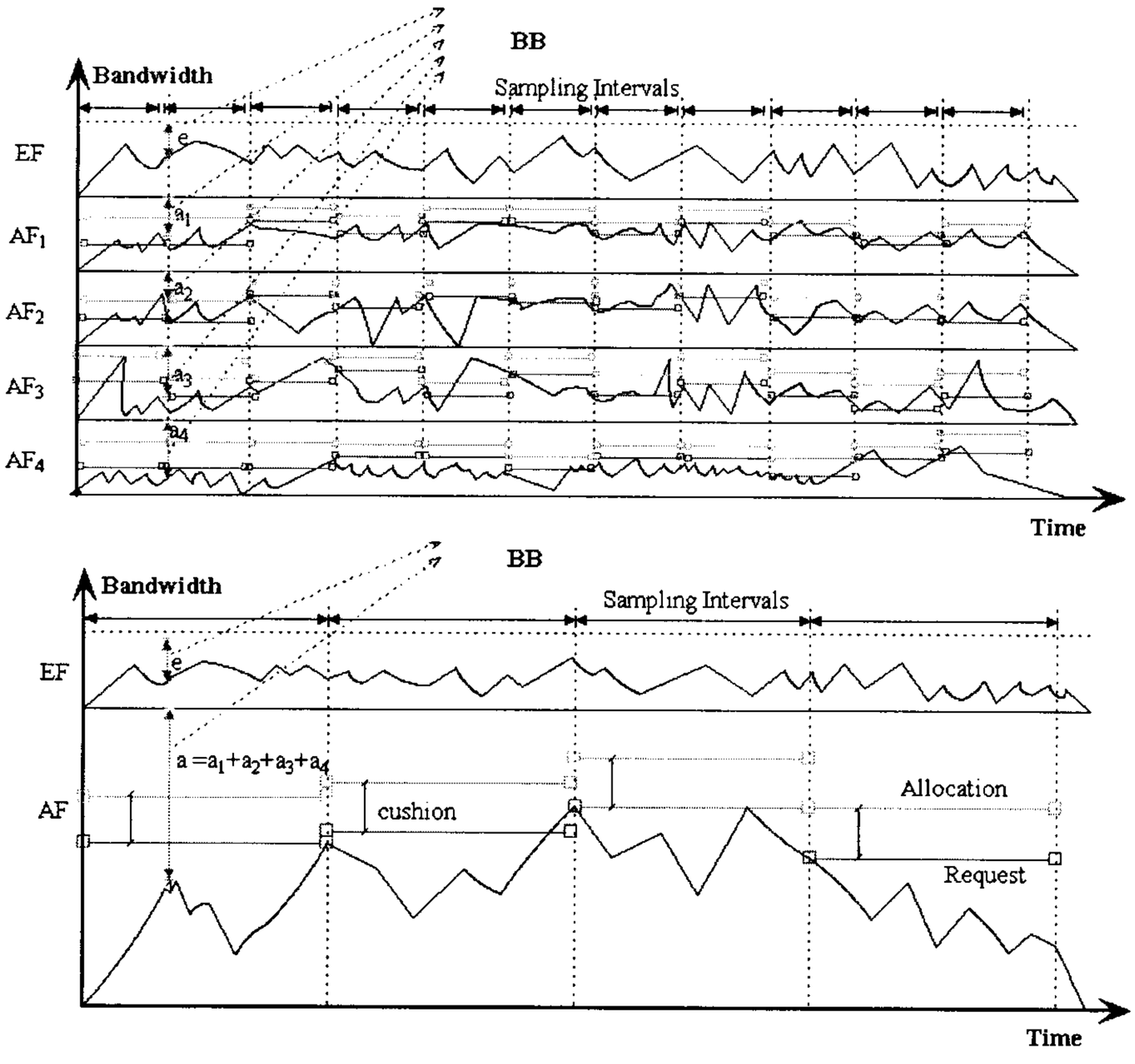

Figure 2.3: Bandwidth Broker related information from a DiffServ enabled router in the case of two (lower) and five (higher) traffic classes

transmitted. This model produces a Variable-Bit-Rate (VBR) flow with a mean throughput of 16 Kbps (with a 92 Kbps peak bit rate) and the average packet size is 429 bytes. The duration of each session is uniformly distributed between 70 and 90 seconds.

HTTP Traffic: To model HTTP traffic, persistent TCP connections have been used to support the HTTP/1.1 protocol. The sizes of web objects (which include the web file and embedded objects) have been generated using heavy-tailed distributions (Pareto) with values according to realistic scenarios. These values are shown in Table 2.1. With the values seen in Table 2.1, the final average size of a web object is 35 Kbytes and the average inter-session time is 20 seconds.

FTP Traffic: FTP users download "heavy" files of uniformly distributed sizes between 200 and

Parameter	*Distrib.*	*Mean*	*Scale*	*Alpha*
Size of Web File	Pareto	5 Kbytes	3 Kbytes	2.5
No. Embedded Obj.	Pareto	1.5 Obj.	1 Obj.	3
Size Embedded Obj.	Pareto	20 Kbytes	15 Kbytes	4
Inter-session Time	Pareto	20 sec.	5 sec.	1.33

Table 2.1: HTTP Pareto distributed parameters.

220 Kbytes. The size of these files can be considered heavy when compared to the size of the web objects used in HTTP.

2.5 Topology

The topology used in all the simulations has a three-layers strict tree structure. There are two main reasons behind this choice. First of all, strict tree topology is widely used for simulations in mobile environments for the evaluation of micro-mobility schemes. Moreover, routing related issues do not influence traffic characteristics (since there is only one possible path between each source and destination pair). We have used the same topology (Figure 2.4) for all the scenarios. This

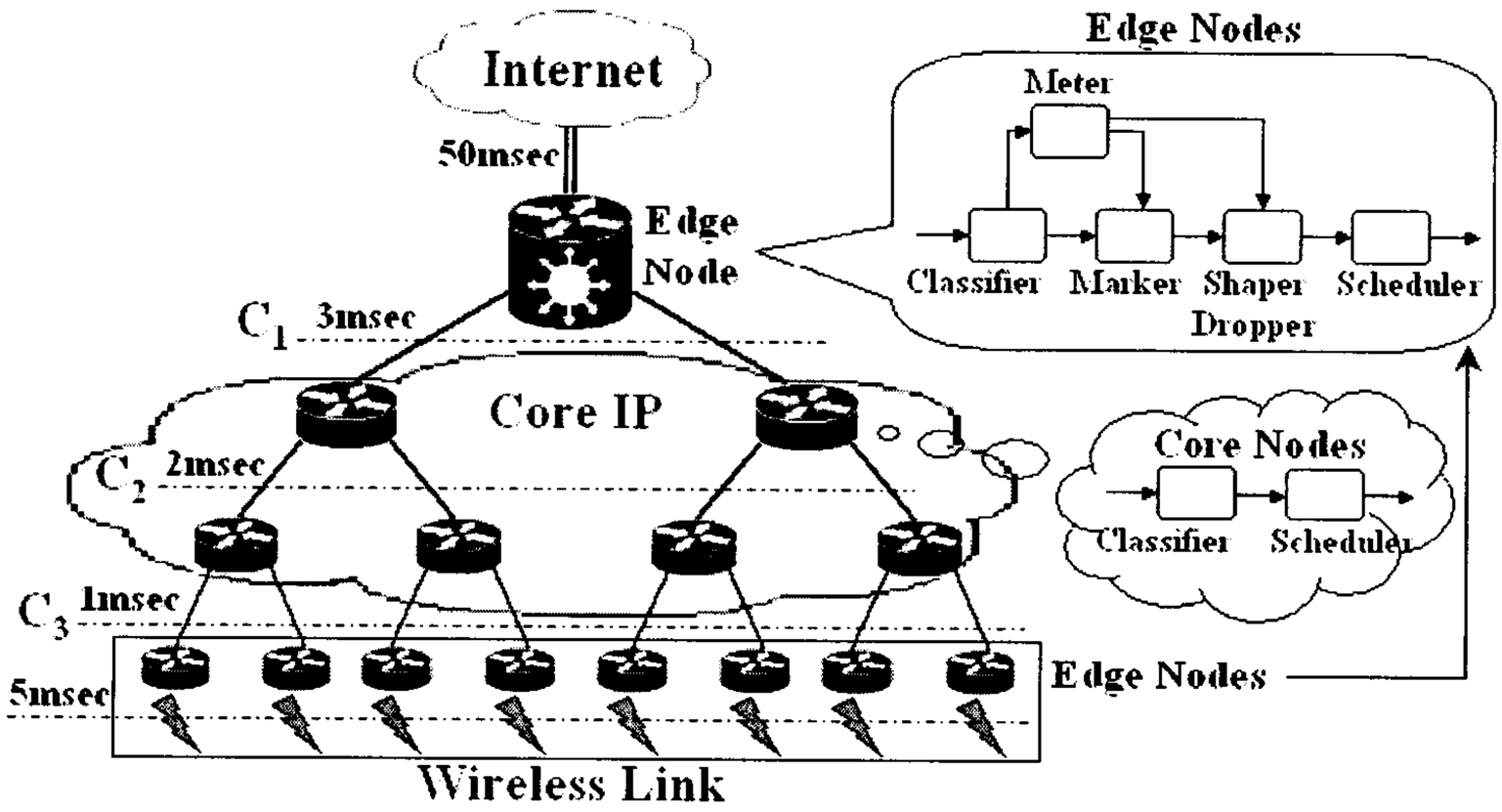

Figure 2.4: Tree topology with Edge and Core nodes schemes.

topology reflects a wireless network. One gateway connects the whole network to the Internet. The core network is consist of routers that interconnect the referred gateway with eight edge nodes (base stations), which are the access points for users to connect to the network (wireless link). Three

levels have been defined in the topology and, within each level, the capacity and propagation delay is equal for all links. These levels are as follows:

Level 1: Links between the gateway and the first row of two routers. The propagation delay is set to 3 milliseconds. Their capacity (C_1) will be changed in different simulations to see its effect on the performance of the traffic.

Level 2: Links between the two rows of routers that compound the core network. Here the propagation delay is 2 milliseconds. The capacity (C_2) is always set to 90% of half the capacity of the higher level C_1 (in order to have a bottleneck link).

Level 3: These are the links that connect the core network with the eight edge routers that are access points for the users. Their propagation delay is 1 millisecond. The capacity (C_3) is 85% of half the capacity of level 2 (C_2).

On both edge sides of this network are servers and clients. As explained before, clients connect to the network via the access points provided by the edge nodes (wireless link). This link has a propagation delay of 5 milliseconds for all the users. On the other side are servers, which connect with clients on the mobile network through the Internet (with a high propagation delay of 30 milliseconds that emulates typical delays experimented across the Internet). The capacities of the last-hop links are 90 Kbps for VoIP, 386 Kbps for streaming video, and 56 Kbps for WWW and FTP. We have used three different sets of capacities in our simulations. As explained above, we will only change C_1 because, when C_1 is set, then C_2 and C_3 are automatically calculated. The values used are shown in Table 2.2.

Capacities	*Set 1*	*Set 2*	*Set 3*
C_1	6 Mbps	10 Mbps	14 Mbps
C_2	2.7 Mbps	4.5 Mbps	6.3 Mbps
C_3	1.1475 Mbps	1.9125 Mbps	2.6775 Mbps

Table 2.2: Different capacities C_1, C_2 and C_3 used in the simulations.

2.6 Scenarios

In all simulations six different scenarios have been considered. Four of them deploy DiffServ and the remaining two are best-effort. In DiffServ scenarios there are two different PHB, EF and AF. In

EF drop-tail is used and in AF the queueing scheme is RIO. In the best-effort case both RED and drop-tail queues have been simulated. The parameters used to configure the different queues are in Table 2.3.

Scenario	*Queue*	min_{th}	max_{th}	max_p
DiffServ	AF In-profile	40	50	0.02
	AF Out-profile	30	40	0.10
	EF Drop-Tail	Queue size = 5 packets		
Best-effort	RED	10	30	0.02
	Drop-Tail	Queue size = 50 packets		

Table 2.3: Queues parameters in DiffServ and Best-effort scenarios.

2.6.1 DiffServ Scenarios

DiffServ scenarios use policing on ingress nodes in order to control the traffic entering the network. We have used a token bucket policer for all the applications, but different Committed Information Rates (CIR) and Committed Burst Sizes (CBS) are allowed in each case, as shown in Table 2.4. There are four different scenarios that deploy DiffServ:

Policing	*VoIP*	*Video*	*HTTP*	*FTP*
Policer	T. Bucket	T. Bucket	T. Bucket	T. Bucket
CIR	90 Kbps	400 Kbps	30 Kbps	20 Kbps
CBS	1 Kbyte	1 Kbyte	20 Kbytes	20 Kbytes

Table 2.4: DiffServ policers and policing parameters.

1. **EF and 3 AF classes (WRR):** In this scenario there are EF PHB and AF PHB. Within AF three classes have been implemented. The EF PHB is reserved only for VoIP traffic (highest priority) and AF PHB is for video, HTTP and FTP (separated one in each class). The scheduling mode is Weighted Round Robin (WRR) whose values are shown in Table 2.5.

2. **EF and 2 AF classes (WRR):** This scenario is equal to 1 but with only two AF classes. In this case, VoIP traffic will still use EF, video will occupy one AF class and the other AF class will be shared by HTTP and FTP. The scheduling mode is also WRR.

3. **EF and 1 AF class (WRR):** In this scenario there are EF and AF with only one class. VoIP will use EF and the other three applications (video, HTTP and FTP) will share the one and only AF class. The scheduling mode is WRR.

4. **EF and 1 AF class (PQ):** This scenario is equal to 3 but instead of using WRR the scheduling mode is Priority Queuing (PQ). PQ gives EF priority over AF by scheduling AF packets only if there are no EF packets waiting to be served.

2.6.2 Best-effort Scenarios

Also best-effort scenarios are simulated in order to compare the results with those obtained in the DiffServ cases. The scheme is very simple; all traffic goes through the same queue. Therefore, no priorities can be given. All applications are treated the same within the network. This is the actual scenario of the current Internet. There are two different scenarios that deploy best-effort.

5. **Best-effort (Drop-Tail):** The queues of the routers in the network are all drop-tail, i.e., any packet will be admitted if there is free space in the queue, or dropped if the queue is full.

6. **Best-effort (RED):** All the routers have a RED queue. The parameters that configure this queue are in Table 2.3.

2.6.3 Traffic Matrices

Nowadays, 90% of the traffic in the Internet is TCP-based. The implications of increased non-responsive traffic on the network performance are not yet known. It is expected that, in the future, all IP mobile networks will continue to carry large volumes of voice traffic. In order to assess the implications of traffic matrices with increased percentage of non-responsive traffic we have implemented three different scenarios in our simulations. The first one, traffic matrix A, has 15% VoIP traffic, then we increase this value to 30% in matrix B, and to 45% in C. We have kept the maximum traffic demand constant for all three traffic matrices. In this case, the number of users per application and their percentage of traffic are detailed in Table 2.5.

2.7 QoS Requirements

The goal of our simulations is to compare the amount of bandwidth needed in different scenarios to satisfy certain QoS parameters. The QoS requirements for VoIP, video and HTTP applications are detailed below, while FTP is treated as background traffic (i.e., no QoS requirement is needed).

	Parameter	*VoIP*	*Video*	*HTTP*	*FTP*
A	**Users**	40	24	680	192
	Users/cell	5	3	85	24
	Traffic %	15%	2.5%	49%	33.5%
	WRR(EF+3AF)	5.93=20%	0.19=3%	3.22=50%	1.00=27%
	WRR(EF+2AF)	1.64=20%	0.05=3%	1.00=77%	
	WRR(EF+1AF)	1.45=20%	1.00=80%		
B	**Users**	80	24	560	160
	Users/cell	10	3	70	20
	Traffic %	30%	2.5%	40%	27.5%
	WRR(EF+3AF)	13.33=35%	0.24=3%	3.40=41%	1.00=21%
	WRR(EF+2AF)	3.56=35%	0.06=3%	1.00=62%	
	WRR(EF+1AF)	3.12=35%	1.00=65%		
C	**Users**	120	24	480	112
	Users/cell	15	3	60	14
	Traffic %	45%	2.5%	34%	18.5%
	WRR(EF+3AF)	33.33=50%	0.42=3%	5.07=35%	1.00=12%
	WRR(EF+2AF)	6.7=50%	0.08=3%	1.00=47%	
	WRR(EF+1AF)	5.8=50%	1.00=50%		

Table 2.5: Users, traffic % and WRR (link bandwidth) for each TM.

VoIP: Three QoS parameters have been discussed in VoIP traffic, packet delay, jitter and drops. Delay mostly affects conversational quality, rather than the voice quality. The packet delay QoS requirement has been chosen according with the values suggested in [18]. In the referred paper, the VoIP quality is measured by the R-factor, which ranges the voice quality from a best case of 100 to a worst of 0.

To calculate the R-factor, the formulas proposed and explained in [18] can be applied (where d is the packet delay, e the percentage of packet drops and $H(x)$ is the heavyside function):

$$R \simeq 94.2 - I_d - I_{ef} \tag{2.1}$$

$$I_d \simeq 0.024\ d + 0.11(d - 177.3)\ H(d - 177.3) \tag{2.2}$$

$$I_{ef}(G.729a) \simeq 11 + 40\ ln(1 + 10\ e) \tag{2.3}$$

The possible VoIP packet delay values explored in the first part of the results are 70, 80, 90 and 100 milliseconds and their R-factor is 72.22, 72, 71.74 and 70.65. Therefore, for all these values, the VoIP quality is considered *medium*. For the rest of the results, the packet delay QoS requirement has been set to 80 milliseconds.

A maximum of 1% packets dropped will be accepted. For the jitter, no QoS thresholds have

been set, but its mean and standard deviation have been used in order to compare the performance of VoIP in the different scenarios. We also measure the frequency of the events where more than three consequent VoIP packets from the same flow are dropped, and we call these events as outages. The outages with length greater than three affect seriously voice quality. Therefore, the percentage of drop packets that occur in bursts of four or more have also been measured.

Streaming Video: This application has been treated similar to VoIP from the QoS perspective. Packet delay, jitter and drops are also the QoS parameters measured. The maximum acceptable value for the delay will be 150 milliseconds (so, we consider streaming video, but not real-time). The percentage of drops must be less than 1%.

HTTP Traffic: The QoS perceived by users requesting HTTP pages has been measured as the average download time for each HTTP page received. This average time has been calculated as the mean of the entire HTTP downloads throughout the simulation. A value of 10 seconds has been set as the maximum download time to satisfy the users QoS requirements.

FTP Traffic: In this case, no QoS requirements have been applied. This is because FTP traffic is considered background traffic and, therefore, its received service will be best-effort.

2.8 Results

The results show the minimum capacity needed to meet the QoS requirements for each scenario and for all the three traffic matrices (Table 2.6). Then, considering every scenario with its calculated minimum QoS capacity, the QoS measurements are discussed in order to compare between different scenarios (Table 2.7).

2.8.1 Key Observations

Over-provisioning: The degree of over-provisioning required for best-effort scenarios, in order to perform as DiffServ and meet all the QoS requirements, varies from 11.0% to 39.6% for traffic matrix A. In traffic matrix B, this over-provisioning is between 15.0% and 35.4%. And for

traffic matrix C, the over-provisioning required is from 24.9% to 36.2%. These values depicted in column labelled "Minimum value of C1" in Table 2.6.

Traffic Matrix: As the percentage of VoIP traffic is increased from 15% to 45%, the bandwidth required to meet the QoS constraints decreases for most of the scenarios (Table 2.6, "Minimum value of C1" column).

AF classes: When deploying DiffServ with EF and AF PHBs, the excess of bandwidth needed when using one AF class only (instead of three) is 24.9% in traffic matrix A, from 12.3% to 16.4% in matrix B and up to 5.0% in C.

RED: Concerning best-effort scenarios, between 1 and 2% less capacity is needed in the RED case than with drop-tail. Although the difference in the simulations is not remarkable, optimization of the RED parameters may end in a considerable improvement.

VoIP: The scenario that gives better performance for VoIP traffic is DiffServ with priority queueing. In this scenario, there are no drops, the jitter mean is zero and its standard deviation is around 0.75 milliseconds. These values can be found in Table 2.7, rows labelled as "DS(EF+AF) PQ".

Best-effort: In the over-provisioned best-effort scenarios, FTP average download time is from 11.3% to 19.2% times smaller than in a DiffServ scenario. Also for HTTP, the average download time is from 19.3% to 35.3% times smaller in best-effort cases.

QoS requirements: The most restrictive QoS requirement in DiffServ scenarios is the VoIP and video drop percentage. On the other hand, best-effort cases are restricted by the VoIP average packet delay (traffic matrix A) and the VoIP percentage of packets dropped (traffic matrices B and C).

2.8.2 Discussion on the Results

One critical aspect revealed by the extended set of simulations was the influence of the traffic matrix on different QoS constraints. As the percentage of VoIP traffic increases, the required bandwidth for a best-effort domain to meet the QoS constraints decreases. This can be explained by the closed loop and packet loss based state machine of TCP protocol which probes for available bandwidth.

The combination of small WWW transactions with this probing mechanism has as a side effect, saturation of the links (i.e introducing queueing delays and packet drops) and thus disruption of VoIP traffic. As the percentage of VoIP traffic increases (which in essence is Poissonian and non-responsive) the available bandwidth left for the erratic traffic characteristics of TCP decreases, which smooths and decreases temporal queueing delays and packet drops.

In the case of best-effort domains, the use of active queueing mechanisms (e.g., RED gateways), instead of simple drop-tail queueing routers, can increase network performance. With RED queues, VoIP and video quality can be increased as they are heavily dependent on bursty packet losses. A critical issue that hindered adoption of this queueing algorithm in the Internet is the fact that there are several degrees of freedom that need to be adjusted in order to achieve optimized performance. Even though a discussion on the optimization methods of these parameters is beyond the scope of the thesis, we should stress that in recent years there has been substantial research effort towards this direction [19], [21].

Simulations results prove the tenability of the proposed concept of a core-centric approach in delivering QoS, as the over-provisioning needed in order to reduce the number of AF classes from three to one has an average, feasible, value of 14% over the different traffic matrices. In case of pure best-effort domains the required factor varied from 11% to 39.6%. These values depend on the most strict QoS parameter which proved to be VoIP delay for the case of best-effort networks. As the constraints for VoIP delay become more strict the required over-provisioning increases non-linearly as depicted in figure 2.5. This result can be explained through traditional teletraffic theory (which provides a lower bound because real aggregate traffic is self-similar) which states that queueing delay decreases exponential with linear increase of the outbound capacity. Reversing this result, we can state that a linear decrease in VoIP delay requires an exponentially increase in the capacity.

2.9 Conclusions

In this chapter we have argued that since different proposed pure-IP based architectures for future mobile networks inevitably lack support of real life tests, should be meticulously examined before being adopted. Even though DiffServ segregates traffic into a small number of QoS classes, the requirement to provide priority for some packets over others may burden routers and weaken the

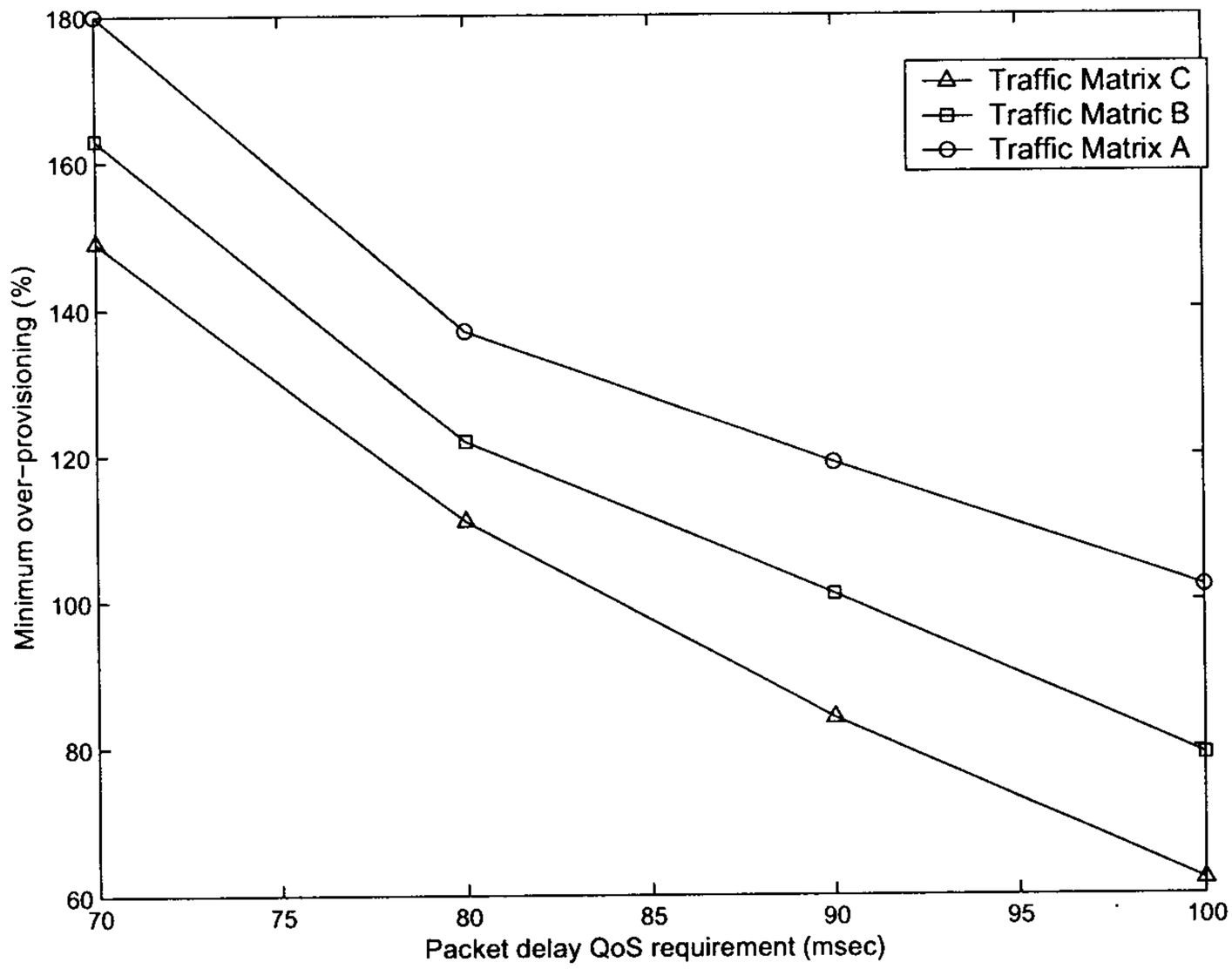

Figure 2.5: Required over-provisioning under different delay constraints

traditional strength of the Internet.

On the other hand, the DiffServ architecture shifts network management complexity to the control plane which is the bandwidth broker. As the number of the EF and AF PHBs increases so does the overhead complexity of managing these classes. Erstwhile proposed architectures map traffic classes of the air-interface onto DiffServ PHBs without taking into account the increased complexity on network management of such decision and, hitherto, without results to justify this choice. From this point of view, we have questioned the need for multiple traffic classes and we have shown that even with one or two AF classes a well provisioned DiffServ enabled core network can provide the requested QoS independent of the number of QoS classes on the wireless link.

With regard to the broader framework sketched above, our results indeed reinforce the question on the applicability of complex architectures and point out that these findings should motivate consideration of the performance by yet more case dependent and extensive studies. Finally, and most apropos, having in mind that the wireless link (last hop) will always be the bottleneck in the network, together with the pragmatic fact of the dubious engineering solutions of QoS enabled

Traffic Matrix A (15% VoIP)	VoIP		Video		HTTP	*Minimum value of C1 (Mbps)*
	Delay < 80 msec (Mbps)	*PER < 1% (Mbps)*	*Delay < 150 msec (Mbps)*	*PER < 1% (Mbps)*	*Download < 10sec (Mbps)*	
DS(EF+3AF) WRR	9.15	**9.85**	< 6	< 6	9.45	**9.85**
DS(EF+2AF) WRR	8.60	**11.75**	< 6	< 6	9.25	**11.75**
DS(EF+AF) PQ	< 6	< 6	9.5	**12.3**	9.35	**12.3**
DS(EF+AF) WRR	8.45	12.05	9.45	**12.3**	9.30	**12.3**
Best-effort DT	**13.75**	13.05	8.5	12.55	9.35	**13.75**
Best-effort RED	**13.65**	13.2	7.25	12.9	9.4	**13.65**

Traffic Matrix B (30% VoIP)	VoIP		Video		HTTP	*Minimum value of C1 (Mbps)*
	Delay < 80 msec (Mbps)	*PER < 1% (Mbps)*	*Delay < 150 msec (Mbps)*	*PER < 1% (Mbps)*	*Download < 10sec (Mbps)*	
DS(EF+3AF) WRR	9.1	**9.75**	< 6	< 6	9.15	**9.75**
DS(EF+2AF) WRR	< 6	**9.85**	< 6	< 6	9.15	**9.85**
DS(EF+AF) PQ	< 6	< 6	9.35	**10.95**	9.25	**10.95**
DS(EF+AF) WRR	< 6	9.8	9.45	**11.35**	9.2	**11.35**
Best-effort DT	**13.2**	**13.2**	7.4	11.7	9.1	**13.2**
Best-effort RED	12.9	**13.05**	< 6	12	9.1	**13.05**

Traffic Matrix C (45% VoIP)	VoIP		Video		HTTP	*Minimum value of C1 (Mbps)*
	Delay < 80 msec (Mbps)	*PER < 1% (Mbps)*	*Delay < 150 msec (Mbps)*	*PER < 1% (Mbps)*	*Download < 10sec (Mbps)*	
DS(EF+3AF) WRR	9.4	**9.95**	< 6	< 6	8.9	**9.95**
DS(EF+2AF) WRR	< 6	**9.8**	< 6	< 6	9.1	**9.8**
DS(EF+AF) PQ	< 6	< 6	9.5	**10.45**	9.2	**10.45**
DS(EF+AF) WRR	< 6	9.85	9.4	**9.95**	9.05	**9.95**
Best-effort DT	12.65	**13.35**	6.6	11.15	8.75	**13.35**
Best-effort RED	12	**13.05**	< 6	11.5	8.85	**13.05**

Table 2.6: Minimum capacity required to meet all the QoS constrains for all scenarios and traffic matrices.

domains, the above results show that an over-provisioned best-effort core IP network is a strong candidate and should not be thoughtlessly taken out of consideration. In the next chapter we will investigate in more detail the active queueing mechanisms of the DiffServ architecture and propose a novel queueing scheme that utilize topological characteristics of the mobile networks.

Traffic Matrix A (15% VoIP)	*C1 (Mbps)*	VoIP					Video			HTTP	FTP
		Average Delay (msec)	*% Packet Drops*	*Jitter mean (msec)*	*Jitter std (msec)*	*% Outages length > 3*	*Average Delay (msec)*	*% Packet Drops*	*% Outages length > 3*	*Download Time (sec)*	*Download Time (sec)*
DS(EF+3AF) WRR	9.85	76	1.0%	0.1	1.24	38.3%	62	0.0%	0.0%	8.05	31.5
DS(EF+2AF) WRR	11.75	69	1.0%	0.09	1.4	74.0%	57	0.0%	0.0%	6.5	34.5
DS(EF+AF) PQ	12.3	66	0.0%	0.0	0.75	0.0%	85	1.0%	0.0%	6.45	36
DS(EF+AF) WRR	12.3	68	0.85%	0.07	0.94	62.6%	86	1.0%	0.0%	6.5	35.3
Best-effort DT	13.75	80	0.3%	0.02	1.91	0.0%	62	0.20%	0.0%	5.95	30.2
Best-effort RED	13.65	80	0.47%	0.04	2.51	20.5%	62	0.34%	0.0%	6.05	31.1

Traffic Matrix B (30% VoIP)	*C1 (Mbps)*	VoIP					Video			HTTP	FTP
		Average Delay (msec)	*% Packet Drops*	*Jitter mean (msec)*	*Jitter std (msec)*	*% Outages length > 3*	*Average Delay (msec)*	*% Packet Drops*	*% Outages length > 3*	*Download Time (sec)*	*Download Time (sec)*
DS(EF+3AF) WRR	9.75	77	1.0%	0.04	1.52	0.0%	65	0.0%	0.0%	7.65	33.2
DS(EF+2AF) WRR	9.85	67.5	1.0%	0.04	0.93	6.0%	57	0.0%	0.0%	7.25	35.6
DS(EF+AF) PQ	10.95	66	0.0%	0.0	0.79	0.0%	93	1.0%	2.2%	6.45	32.6
DS(EF+AF) WRR	11.35	66.5	0.05%	0.0034	1	0.0%	94	1.0%	6.0%	6.4	31.9
Best-effort DT	13.2	80	1.0%	0.034	1.95	9.0%	62	0.34%	0.0%	6	30.3
Best-effort RED	13.05	79	1.0%	0.05	2.21	20.6%	62.5	0.01%	0.0%	6.05	31.5

Traffic Matrix C (45% VoIP)	*C1 (Mbps)*	VoIP					Video			HTTP	FTP
		Average Delay (msec)	*% Packet Drops*	*Jitter mean (msec)*	*Jitter std (msec)*	*% Outages length > 3*	*Average Delay (msec)*	*% Packet Drops*	*% Outages length > 3*	*Download Time (sec)*	*Download Time (sec)*
DS(EF+3AF) WRR	9.95	77.4	1.0%	0.019	1.47	1.8%	65	0.0%	0.0%	6.65	30.8
DS(EF+2AF) WRR	9.8	67.3	1.0%	0.036	0.92	0.0%	58	0.0%	0.0%	7.1	33.6
DS(EF+AF) PQ	10.45	66.5	0.0%	0.0	0.79	0.0%	101	1.0%	0.0%	6.45	32
DS(EF+AF) WRR	9.95	66.9	0.35%	0.013	1.47	0.0%	100	1.0%	0.0%	6.5	31.7
Best-effort DT	13.35	75.9	1.0%	0.027	1.87	0.0%	59	0.23%	0.0%	5.95	30.2
Best-effort RED	13.05	75.8	1.0%	0.043	1.96	6.25%	60	0.4%	0.0%	6	30.4

Table 2.7: QoS measurements in all scenarios for their QoS capacity

Bibliography

[1] D. Clark, Adding Service Discrimination to the Internet, *Proceedings of the 23rd Annual Telecommunications Policy Research Conference (TPRC), Solomons, MD, October 1995.*

[2] Lee et al., INSIGNIA: An IP-based quality of service framework for mobile adhoc networks *Journal of parallel and distributed computing, Vol 60 no 4, pp 374-406, April 2000.*

[3] Broadband Radio Access for IP-based Networks, IST-1999-10050, http://www.ist-brain. org.

[4] Bongkyo Moon and A. H. Aghvami, DiffServ Extensions for QoS Provisioning in IP Mobility Environments , *IEEE Wireless Communications, Volume: 10 Issue: 5 Oct 2003, page(s): 38 - 44*

[5] Wroclawski, J., The Use of RSVP with IETF Integrated Services, *Internet Engineering Task Force, Request for Comments (RFC) 2210, September 1997*

[6] A. Talukdar, B. Badrinath, A. Acrarya, MRSVP: A resource reservation protocol for an integrated services network with mobile hosts, *The Journal of Wireless Networks, vol. 7, no. 1, 2001*

[7] C. Tseng, G. Lee, R. Liu, HMRSVP: A hierarchical mobile RSVP protocol, *International Workshop on Wireless Networks and Mobile Computing (WNMC'01), April 2001*

[8] S. Blake et. al., An Architecture for Differentiated Services, *RFC 2475, Internet Request for Comments, December 1998*

[9] V. Jacobson et. al. An Expedited Forwarding PHB, *RFC 2598, Internet Request for Comments, June 1999*

[10] J. Heinanen et. al. Assured Forwarding PHB Group, *RFC 2597, Internet Request for Comments, June 1999*

[11] 2. K. Nichols, V. Jacobson, and L. Zhang, A Two-bit Differentiated Services Architecture for the Internet, *RFC 2638, Internet Request for Comments, July 1999*

[12] B. Teitelbaum, P. Chimento, Qbone Bandwidth Broker Architecture, *at http://qbone.ctit.utwente.nl/deliverables/1999/d2/bboutline2.html (work in progress)*

[13] Y. Bernet et al. A Framework for Integrated Services Operation over Diffserv Networks, *RFC 2998, Internet Request for Comments, November 2000*

[14] P. Thiran, N. Taft, C. Diot, R. McDonald, H. Zang, A Protection-based Approach to QoS in Packet over Fiber Networks, *Proceedings of the International Workshop on Digital Communications (IWDC), Springer Verlag LCNS, Taormina, Italy, September 2001*

[15] S. Maniatis, E. Nikopoulou, I. Venieris, QoS Issues in the Converged 3G Wireless and Wired Networks, *IEEE Communication Magazine, August 2002*

[16] Sally Floyd, Mark Handley, Jitendra Padhye, and Joerg Widmer, Equation-Based Congestion Control for Unicast Applications, ACM/IEEE SIGCOMM'2000, August 2000

[17] Milan Vojnovic, Jean-Yves Le Boudec, On the Long-Run Behavior of Equation-Based Rate Control, *ACM SIGCOMM 2002, Pittsburgh, August 2002*

[18] R. Cole and J. Rosenbluth, VoIP performance monitoring *Computer Communications Review, ACM SIGCOMM, 31(2):9-24, April 2001*

[19] B. Braden, D. Clark, J. Crowcroft, B. Davie, D. Estrin, S. Floyd, V. Jacobson, G. Minshall, C. Patridge, L. Peterson, K. Ramakrishnan, S. Shenker, J, Wroclawski, L. Zhang, Recommedations on Queue Management and Congestion Avoidance in the Internet, *RFC 2309, April 1998*

[20] M. Christiansen, K. Jeffay, D. Ott, F. Smith, Tuning RED for Web Traffic, *ACM SIGCOMM, August 2000*

Chapter 3

Hop Based Queueing (HBQ): An Active Queue Management Technique

In the previous chapter different QoS architectures for all IP based mobile networks have been examined from the perspective of service differentiation in different aggregate traffic classes. One of the critical components of the architecture is the way that congestion is controlled and the related signalling functionalities for supporting congestion avoidance. In this chapter a novel active queue management technique is proposed, in which the dropping probability depends on the number of wireline/wireless hops traversed by the enqueued packets in the node. The advantages accruing of protecting flows with routes that span over a large number of hops by the proposed Hop Based Queueing (HBQ) algorithm are mainly twofold. Firstly, it decreases the mean excess delay on the network, by assigning higher dropping probability for packets that have traversed less number of intermediate nodes (as will be discussed in more detail in the sequel, in the case of ad hoc networks this technique preserve the scare power resources of the nodes). Secondly, because the vulnerability of the TCP state machine increases with the number of wireless hops, by protecting these TCP flows from buffer overflow due to queueing, the number of timeouts events which have a deleterious effects

on performance due to lengthly recovery through retransmission timeouts, are reduced.

3.1 Introduction

3.1.1 Active Queue Management

The dynamics and stability of the Internet is currently driven by the Transport Control Protocol (TCP) [1], which is a closed loop congestion control protocol. TCP control mechanisms are end-to-end and the state machine of TCP is based on packet loss notification information. Even though these mechanisms are necessary for the stability of the Internet, there has been a general consensus over the last few years that the performance can be further improved if the intermediate routers are also actively participate in managing the congestion in the network. Therefore, the aim of active queueing mechanisms is to facilitate and improve the congestion control in the Internet by working in parallel and in an ancillary fashion to TCP. Before discussing in more detail different schemes we should emphasize that active queue management and scheduling are two different functionalities inside the router; the first one trying to control the size of the queue size and levels of congestion by dropping/marking packets while the primary role of the second one is to prioritize packet transmission and/or bandwidth allocation on the outbound link for the different flows.

The main aim of active queue management techniques is to reduce the average queue length in the routers (by randomly dropping/marking packets before the queue is full) and avoid global synchronization of TCP flows due to drop-tail queueing algorithm. Global synchronization with drop-tail routers happens because in the case of congestion the queues are becoming full and subsequent arriving packets are lost, having as a net result all the TCP flows to reduce their congestion window. Another reason for introducing active queue management techniques is to avoid the 'lock-out' phenomenon of drop-tail queues where a small subset of the flows monopolize queueing occupancy, preventing therefore the other connections to gain a fair allocation of queueing space (the 'lock-out' phenomenon can be seen as a byproduct of global synchronization). Active queue management mechanisms utilize different methods for signalling congestion levels to the end-nodes. The most simple one is to indicate congestion through packet dropping. Another alternative is to signal congestion by utilizing the Explicit Congestion Notification (ECN) addition to IP [20]. In this case,

the routers instead of dropping a packet, set the Congestion Experienced (CE) codepoint in the packet header as an indication of congestion. Networks that are ECN-aware allow a more fair allocation of resources by effectively mitigating lock-out phenomena, as explained before. Also, because ECN can signal congestion information without dropping packets can increase the goodput and the performance of time sensitive applications that are based on closed loop transport protocols [3].

3.1.2 The Queue Management Algorithm "RED"

This section describes the Random Early Detection (RED) algorithm [27], which will be used as a basis for the proposed queueing management scheme. RED calculates the average queue size, using an Exponential Weighted Moving Average (EWMA), which is actually a low-pass filter. The average queue size is compared with two thresholds, a minimum threshold and a maximum threshold. When the average queue size is less than the minimum threshold, no packets are marked/dropped. When the average queue size is greater than the maximum threshold, every arriving packet is marked/dropped. If all source nodes are cooperative, this ensures that the average queue size does not significantly exceed the maximum threshold. When the average queue size is between the minimum and the maximum threshold, each arriving packet is marked/dropped with probability p_a, where p_a is a function of the average queue size (avg). Each time that a packet is marked/dropped, the probability that this packet belongs to a particular connection is roughly proportional to that connection's share of the bandwidth in the router. The general RED algorithm is given in figure 3.1. As it can be seen from the pseudo code of RED queue in figure 3.1, RED utilizes two distinctive algorithms to calculate when to drop packets. The first algorithm controls the average queue size to determine the degree of burstiness that will be allowed in the gateway queue. The second algorithm calculates packet-marking probability to determine how frequently a packet is dropped, given the current level of congestion. The goal is to mark packets at fairly evenly spaced intervals in order to avoid biases, global synchronization, but also to mark packets sufficiently frequently to control the average queue size.

Pseudo Code of RED algorithm

```
Initialization:
      avg ? 0
      count ? - 1
for each packet arrival
      calculate the new average queue size     avg:
            if the queue is nonempty
                  avg ? (1 -wq) avg+wq q
            else
                  m ? f (time-q_time )
                  avg ?  (1 -wq)^m avg
      if minth = avg < maxth
            increment  count
            calculate probability   p_a:
                  p_b ? maxp (avg-minth ) /(maxth-minth )
                  p_a ? pb/ (1-count.pb )
            with probability  pa:
                  mark the arriving packet
                  count ? 0
      else if  maxth = avg
            mark the arriving packet
            count ? 0
      else count ? - 1
when queue becomes empty
      q_time ? time

Saved Variables:
avg: average queue size
q_time : start of the queue idle time
count : packets since last marked packet

Fixed parameters:
wq: queue weight
minth : minimum threshold for queue
maxth : maximum threshold for queue
maxp : maximum value for   p_b

Other:
p_a: current packet-marking probability
q: current queue size
time : current time
f(t): a linear function of the time     t
```

Figure 3.1: RED queueing algorithm

3.2 Motivation Behind the Proposed Scheme

Before describing the proposed active queueing management technique, we present several factors that motivated the investigation of the new active queueing scheme. Hereafter we discuss how global connectivity and wireless links influences the performance of the TCP protocol. We investigate active measurements and discuss performance issues of the TCP protocol in links with random losses. The aim is to highlight the point that due to the size of the Internet (in terms of number of hops and RTT) and radio link impairments on the last hop flows with large number of traversed routers should be protected.

3.2.1 Round trip times and analysis of active measurements

The topological structure of today's Internet spans over the whole globe and there are hundreds of millions users. During the '90s, the Internet was growing at an exponential rate of interconnecting hundreds of thousands of networks and it was doubling in size every ten to twelve months. It is anticipated that the growth of the Internet both in size and traffic volume will continue. In August 2000 the average number of hops in the Internet [1] as reported in [4] was 16.51 with a variance of 14.96. It is interesting to note that the average hop count from 1998 to 2000 has been decreased by one hop. With the integration of mobile networks with the Internet it is anticipated that average hop count will certainly not decreased, if not increased. The variability on the number of hops and network dynamic reflects also on the variability of the round trip times (RTT) in the Internet [5]. In the literature there have been different studies concerned with end-to-end packet delay [7], [8], [9] and end-to-end path characteristics [10]. Even though the correlation of RTT and number of traversed routers in today's Internet is not considered significant (in [6] it has been estimated as 50%), in future it is anticipated that will steadily increase, because QoS will be supported in the networks. Understanding end-to-end packet delay dynamics is crucial since (i) the delay profile affects the QoS of real time applications and (ii) affects the performance of TCP, since RTT variations can lead to unnecessary retransmissions from the sender.

In this study 640 servers in ten countries in Europe and 640 scattered servers in U.S have been used. The servers in each country have been selected as scattered as possible by using geographical information [11]. Active measurements, do not need special hardware arrangement for data collection. Active methods are based on injecting probe packets into the network, like ICMP for example. Main tools that can be used for active probing are ping, traceroute and pathchar. The size of the packets that have been used during all experiments was constant and equal to 64 bytes to avoid artificial RTT variations because of the different transmission times. Each server have been probed for 1 minute with a transmission frequency of 10Hz. The probability density function of the RTT's follows a heavy tail distribution as can be seen in figures 3.2 and 3.3. Outliers of the RTT's highlight the real behavior of the network and are these events that seriously affect the performance of different protocols (especially TCP). In order to investigate these outliers and variations of the

[1] The authors used 210 addresses distributed over 11 European countries, 186 addresses from Asia (distributed in Australia, New Zealand, China, Japan) and 274 addresses from North America.

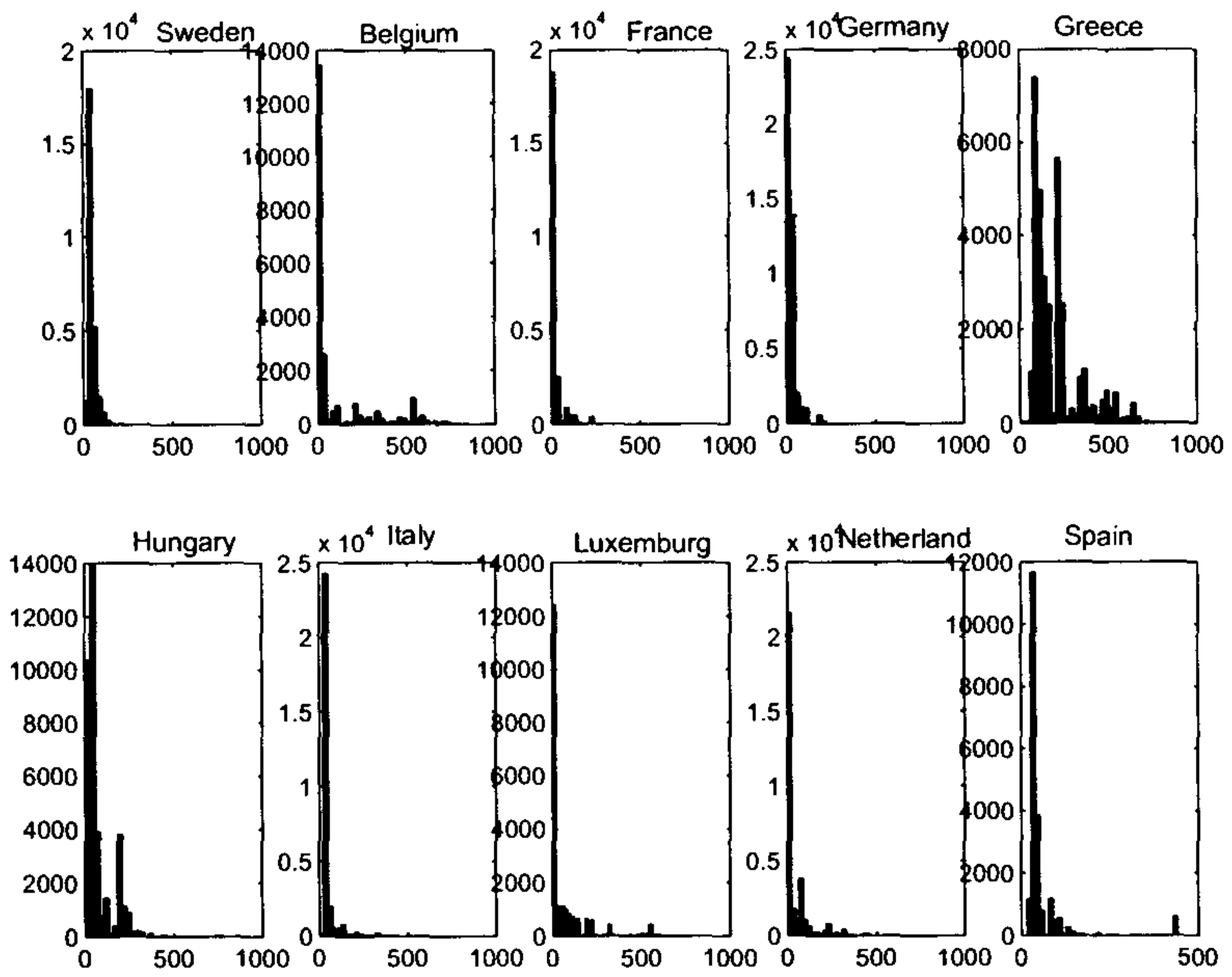

Figure 3.2: Histogram of the RTT from the sample data of Europe

RTT we have used the box-plot representation, which summarizes the actual time series in terms of minimum value, maximum value, 25^{th} percentile, 50^{th} percentile and 75^{th} percentile. Figure 3.4 shows the box-plot representation of the RTT vectors of all the servers probed in the U.S and figure 3.5 zooms in a small subset of these servers that allows a more clear visualization of the Inter-quartile range [2] (IQR). From these graphs two interesting conclusions can be made. The first one is that even though the delay vectors are represented with small IQR amplitude, there is a significant number of outliers in the data. From the statistical point of view, the outliers are defined as values with amplitude greater than $Q_3 + 1.5 \cdot IQR$ (Q_3 represents the 3^{rd} quartile). These are the values which are responsible for the variation of the RTO estimation of the TCP which affect the performance of the protocol in the case of congestion.

Since in TCP the achieved throughput is inversionally proportional to the RTT of the connection, the knowledge of the number of traversed routers contain important information that can be utilized by edge routers in order to differentiate packet dropping. For mobile networks one possible choice for implementing the HBQ scheme can be the ingress router of the core or radio access network. The proposed Hop Based Queueing algorithm utilizes this side information which is available from

[2] IQR represents the range of the middle 50% of the data

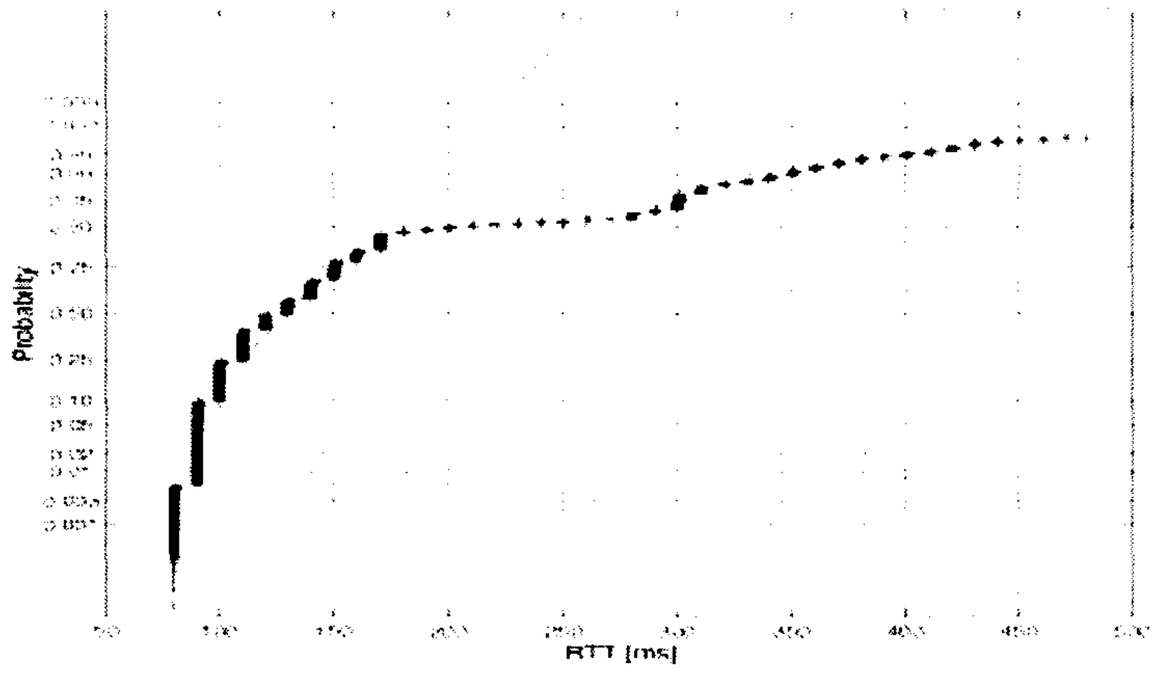

Figure 3.3: Testing for Gaussianity on the RTT distribution

the IP header in order to decide which packets to be dropped/marked. We should also note that the number of hops is an important metric per se, because if we want to consider resource consumption then hop count is becoming more important than the RTT metric.

3.2.2 Effect of random losses on TCP performance

When a TCP connection first begins, the Slow Start (SS) algorithm initializes the congestion window (cwnd) to one segment, which is the maximum segment size (MSS) initialized by the receiver during the connection establishment phase. When acknowledgements are returned by the receiver, the congestion window increases by one segment for each acknowledgement returned before the expiration of the retransmission timer [12]. Therefore, TCP probes for the available bandwidth by exponentially increasing its congestion window per round trip time (RTT). The congestion window is thus increased exponentially either until it equals the receiver's advertised window, or until a loss occurs in the network. If the latter happens, then TCP assumes that there is congestion in the network and therefore reduces the cwnd to half its value and transitions to the more conservative congestion avoidance phase. TCP maintains another variable, the slow start threshold (or ssthresh) in order to determine whether it should be in the slow start or congestion avoidance phase. In a fading channel with correlated packet errors the cwnd will not easily reach the bandwidth delay product and as a result the congestion avoidance phase will be rarely triggered. In the following we

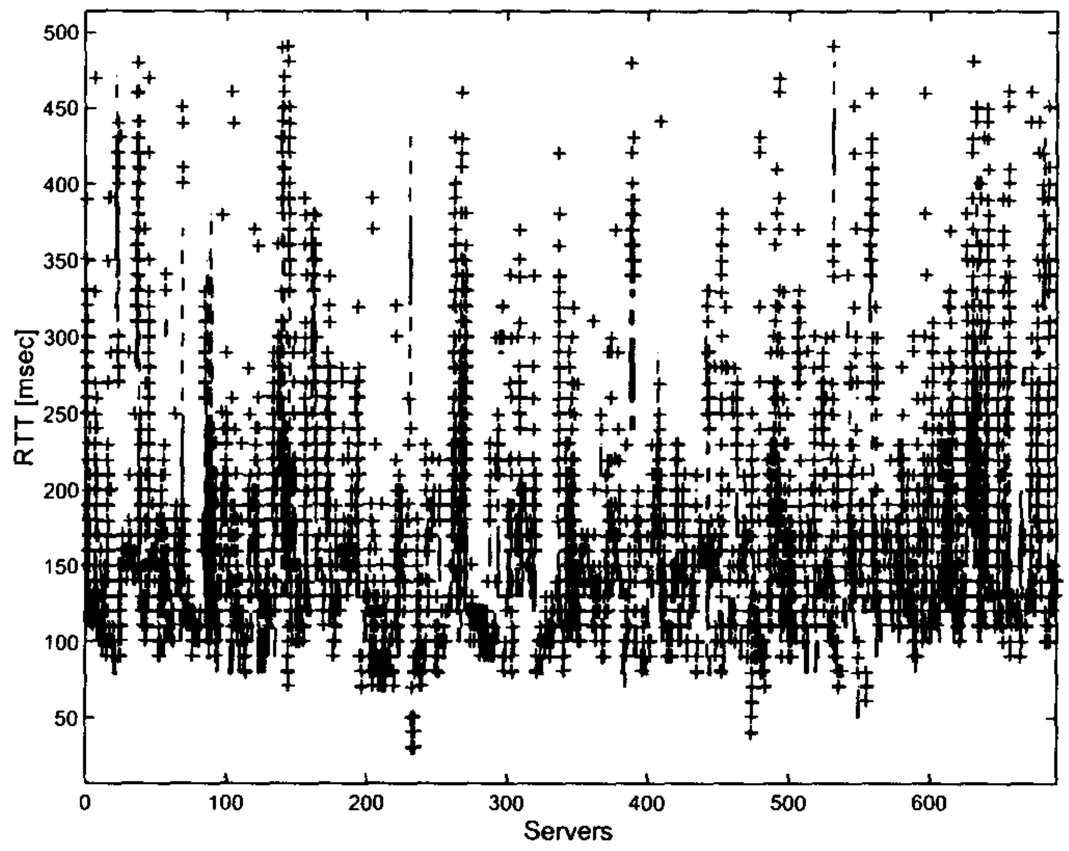

Figure 3.4: Box plot characterization of ping data measurements from 640 servers in U.S

define the channel used in the experiments and explore the evolution of the cwnd.

Channel Model

The fading channel can be modelled as a two states Markov chain as have been shown in [14]. In this case the transition probability matrix will have the following form:

$$C = \begin{pmatrix} P_{GG} & P_{GB} \\ P_{BG} & P_{BB} \end{pmatrix} \tag{3.1}$$

where P_{GB} denotes the conditional probability of a loss at the current time slot given that the previous transmission was successful. The average probability of packet loss P_L depend on the transition probabilities of matrix C which in turn depend on the channel. The transition probabilities depend on the *fading margin* F and the *normalized Doppler bandwidth* $f_D T$, as have been discussed in [14]. Different values of P_L and $f_D T$ produce different fading channels with different degrees of correlation on packet losses. The stationary probabilities for each state will be given from the following equations

$$\pi_G = \frac{P_{BG}}{P_{BG} + P_{GB}}, \pi_B = \frac{P_{GB}}{P_{BG} + P_{GB}}$$

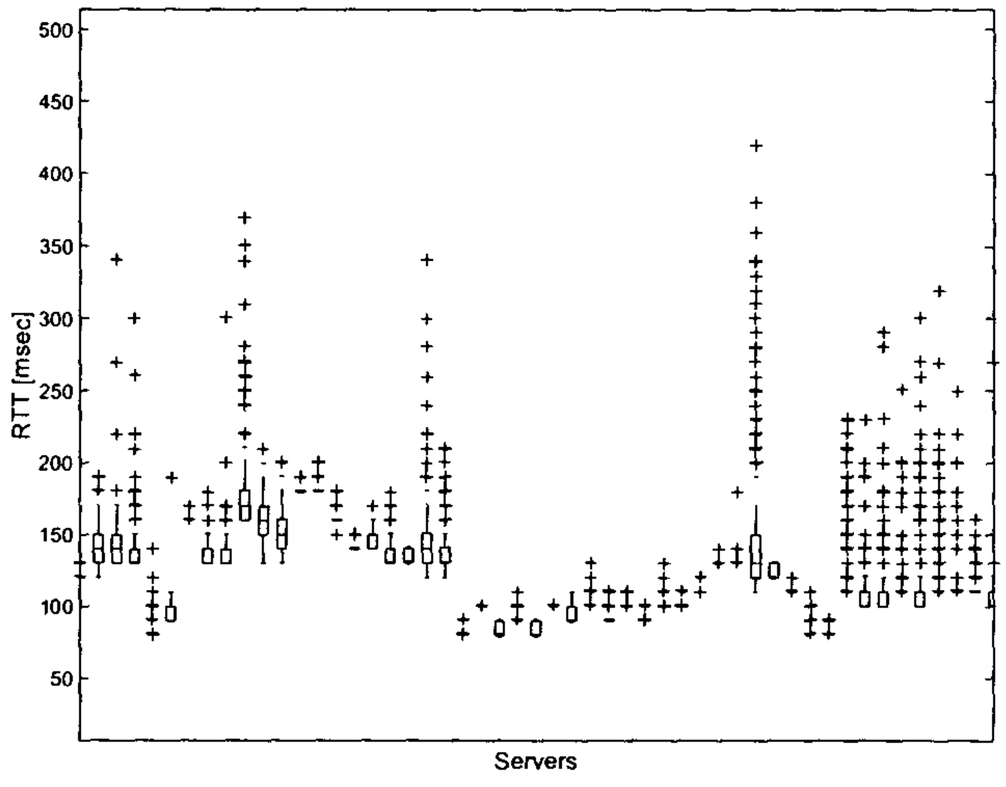

Figure 3.5: Collected ping data from 640 sites in 10 countries in Europe

The average length of burst of erroneous packets will be $(1 - P_{BB})^{-1}$. The case of independent and identical distributed (i.i.d) errors will be a special case of the above model (i.e. a memoryless process), when $P_{BB} = P_{GB} = P_L$. In order to find the n-step ahead transition probabilities we have to consider the spectral representation of C. Assuming that C has two eigenvalues λ_1, λ_2, we can define a matrix Q such that,

$$C = Q \begin{pmatrix} \lambda_1 & 0 \\ 0 & \lambda_2 \end{pmatrix} Q^{-1} \tag{3.2}$$

where the eigenvectors of Q satisfy:

$$Cq_i = \lambda_i q_i, i = 1, 2$$

Therefore,

$$C^n = Q \begin{pmatrix} \lambda_1^n & 0 \\ 0 & \lambda_2^n \end{pmatrix} Q^{-1} \tag{3.3}$$

The effect of the fading channel can be seen in figures 3.6 and 3.7, which shows how the cwnd evolves under different packet error rates. As can be seen in figure 3.7 the cwnd is smaller than five segments, which means that it is not possible for the sender to receive duplicate ACK's and trigger fast retransmit, but has to rely on the performance of the RTO estimation. Therefore, random losses affect seriously the performance of TCP.

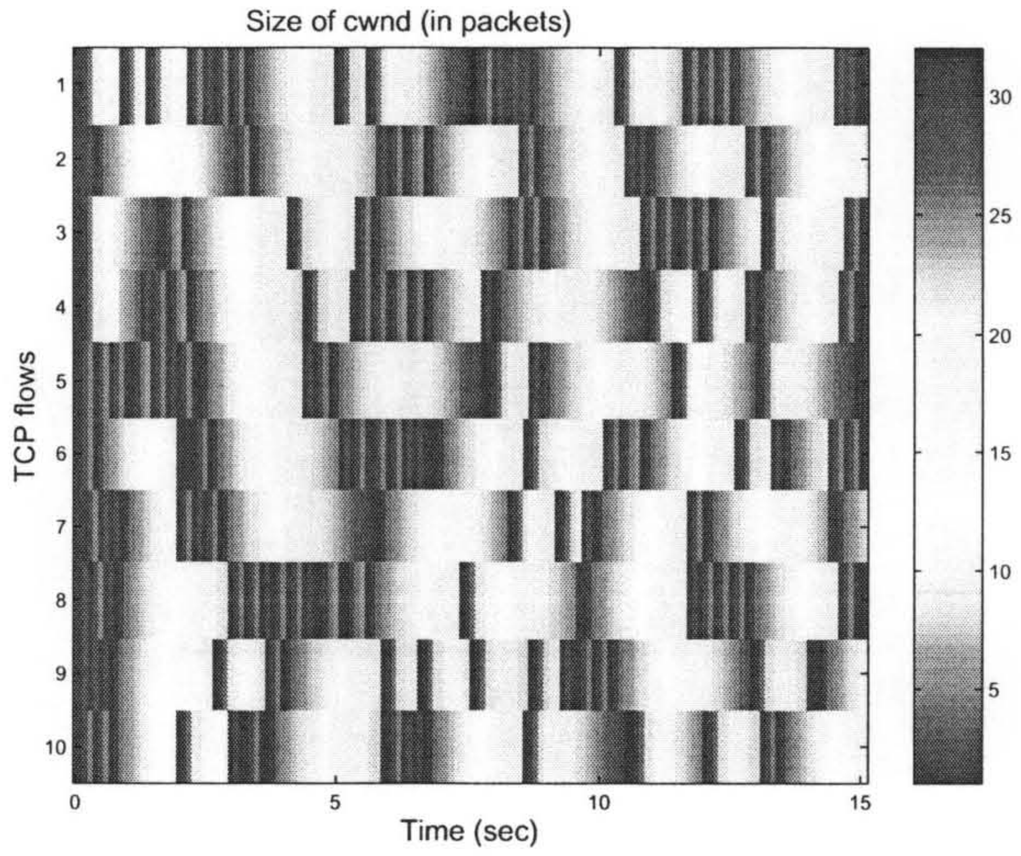

Figure 3.6: Cwnd evolution in a fading channel with 1% packet error rate

3.2.3 HBQ in ad hoc networks

Another scenario where the proposed queueing algorithm can be applied is ad hoc networks. Mobile ad-hoc networks-MANETs are defined as a group of mobile computing devices that communicate among themselves using wireless transmission, without the aid of fixed networking infrastructure and they are based on internal cooperation in order to maintain network connectivity. Ad hoc networks consists of nodes with limited capabilities, in the sense of power and processing speed. As the density of nodes in the network increases, so does the required transmitted traffic, therefore the bottleneck becomes the limited capabilities for packet processing in the nodes. This will have as a net result an increased amount of buffering and eventually packet loss. Due to these limitations energy consumption is of critical importance in such self-organized networks.

We propose an active queue management technique that inherits the functionalities of the RED queue, on how to calculate the probability of marking/dropping a packet, but apply this information in a different manner. In RED queue the above decision applies on the incoming packet, whereas in Hop Based Queueing (HBQ), this decision triggers the creation of a bona fide set of probabilities based on the number of wireline/wireless hops that the packets in the queue have traversed. Therefore, any packet from the queue is eligible to be dropped.

In HBQ the probability of marking/dropping a packet decreases as the arc length (i.e., number of

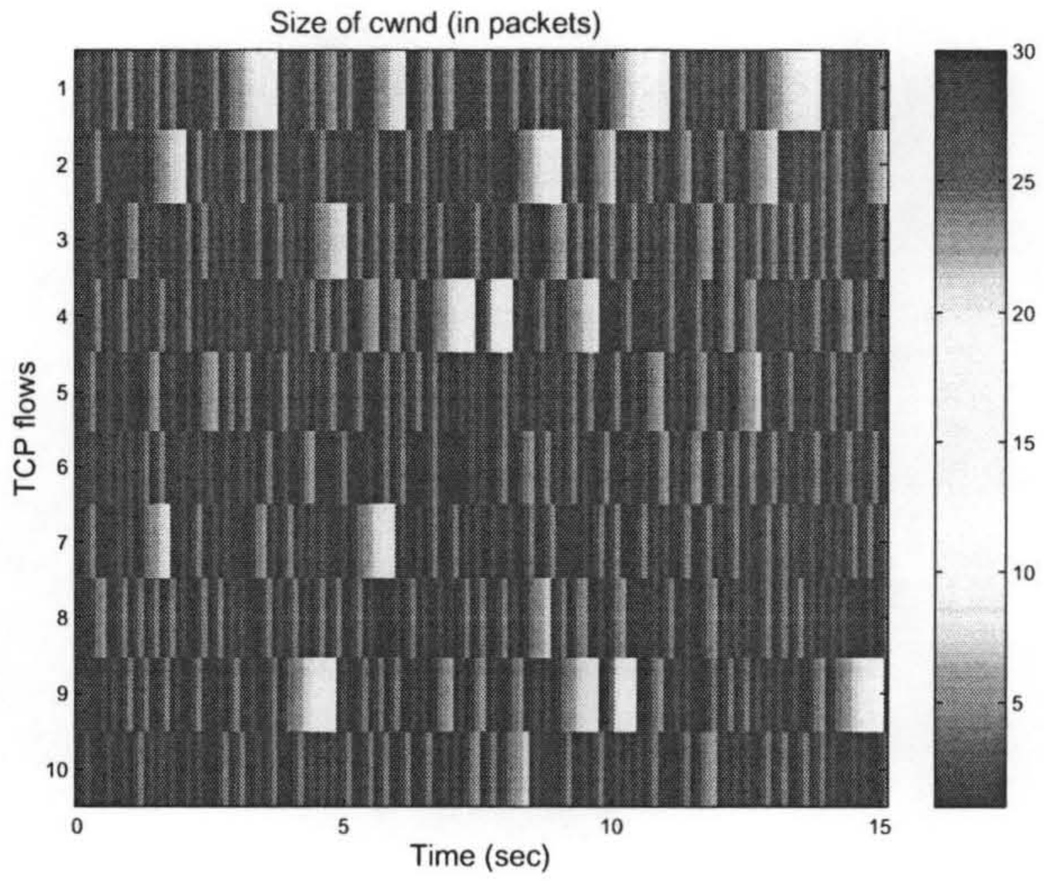

Figure 3.7: Cwnd evolution in a fading channel with 3% packet error rate

traversed routers) of the route increases. This property can also be seen as ancillary to routing because of network dynamics, routes with large arc length have higher probability of becoming obsolete. The first seminal aspect of this high desirable property is that TCP flows with large number of wireless or wireline hops are protected. Protecting these flows is of great importance especially for wireless multi-hop TCP connections. In that case TCP have very small throughput and this is not only because of link impairments but also because of energy consumption, mobility and routing [15]. The second aspect is the reduction of aggregate power consumption in the wireless network and the reduction of average delay in the wireline network. As will be more clearly illustrated in the following sections, if instead of dropping a packet with large number of wireless hops, a packet with a smaller number of hops is selected, then the retransmitted packet will consume less power through the wireless route.

Although there are a plethora of different proposed scheduling techniques for ad hoc networks [16], [17], [18], to the best of authors knowledge there hasn't been any algorithm proposed for active queue management that uses the *number of wireless routers traversed* in order to differentially mark/drop packets from the queue. A relevant queueing mechanisms has been proposed in [19], where information from the link layer is used to adjust the parameters of the queueing algorithm.

3.3 Introspection of HBQ

Hop Based Queueing can be seen as an augmented model of the RED [27] queue, and two different ramifications of the algorithm are considered in the following sections, i.e the *coarse* realization and the *exact* realization. In the coarse realization, a threshold Θ is defined which classify all enqueued packets in two clusters. The impetus behind clustering is that the probability of dropping a packet belonging to the cluster which has a hop count larger than Θ is lower than the probability of dropping a packet with hop count smaller than Θ. In the exact realization of the algorithm each hop count in the queue (which may correspond to more than one packets) have a distinctive dropping probability. In the sequel we examine both realizations of the algorithm after presenting one important result on the advantages of the HBQ scheme over the drop-tail queue.

3.3.1 Theoretical Approach

In the case of the drop tail queue the statistics of the dropped packets, in the sense of the number of hops, follows the same probability density function (pdf) as the actual original pdf, which describes the probability of occurrence of different number of hops in the network. We denote this probability density function as $p(x)$, which is a discrete function with x expressing the number of hops. In order to compare the two approaches we have also to define a discrete function $f(x)$ which express the delay of the packet as a function of the number of hops. One important property of this function is that f_i-$f_{i-1} > 0$, i.e., is strictly positive, since it is a cumulative function of time.

The measure of interest is the mean excess delay (med) that is introduced into the network by these two schemes. By mean excess delay we mean the average time needed by a dropped IP packet to reach again the node. In the case of the drop tail queue the statistics of the incoming traffic will not be altered by the node and the mean excess delay is given by the following expression:

$$med_{TD} = \sum_{i=1}^{M} f_i \cdot p_i \tag{3.4}$$

where M is the maximum number of hops. On the other hand, the mean excess delay introduced by the hop based queueing scheme can be written as:

$$med_{HBQ} = \sum_{i=1}^{\Theta} f_i \cdot p_i + (1-\rho) \sum_{i=\Theta+1}^{M} f_i \cdot p_i + \rho \sum_{i=\Theta+1}^{M} p_i \cdot \sum_{i=1}^{\Theta} f_i \cdot p_i \tag{3.5}$$

where ρ is the probability of dropping packets with hop count less than Θ. In order to prove that the HBQ scheme introduces less mean excess delay than the drop tail queue we have to show that:

$$\sum_{i=\Theta+1}^{M} f_i \cdot p_i - \left[(1-\rho) \sum_{i=\Theta+1}^{M} f_i \cdot p_i + \rho \sum_{i=\Theta+1}^{M} p_i \cdot \sum_{i=1}^{\Theta} f_i \cdot p_i \right] > 0 \tag{3.6}$$

Proposition 3.3.1. *Let's denote by f_i an arbitrary non-decreasing discrete function that represents the accumulated delay and by p_i an arbitrary probability density function describing the number of hops. Then, for the mean excess delay introduced in the network by the two schemes will always hold: $med_{HBQ} \leq med_{DT}$.*

Proof. From equation (3) we have:

$$\sum_{i=\Theta+1}^{M} f_i \cdot p_i - \sum_{i=\Theta+1}^{M} f_i \cdot p_i + \rho \sum_{i=\Theta+1}^{M} f_i \cdot p_i - \rho \sum_{i=\Theta+1}^{M} p_i \cdot \sum_{i=1}^{\Theta} f_i \cdot p_i > 0$$

$$\rho \left[\sum_{i=\Theta+1}^{M} f_i \cdot p_i - \sum_{i=\Theta+1}^{M} p_i \cdot \sum_{i=1}^{\Theta} f_i \cdot p_i \right] > 0$$

$$\sum_{i=\Theta+1}^{M} f_i \cdot p_i - \sum_{i=\Theta+1}^{M} p_i \cdot \sum_{i=1}^{\Theta} f_i \cdot p_i > 0$$

$$\left(f_{\Theta+1} \cdot p_{\Theta+1} + f_{\Theta+2} \cdot p_{\Theta+2} + \cdots + f_M \cdot p_M \right) -$$

$$\left(p_{\Theta+1} \sum_{i=1}^{\Theta} f_i \cdot p_i + \cdots + p_M \sum_{i=1}^{\Theta} f_i \cdot p_i \right) > 0$$

$$p_{\Theta+1} \left[f_{\Theta+1} - \sum_{i=1}^{\Theta} f_i \cdot p_i \right] + \cdots + p_M \left[f_M - \sum_{i=1}^{\Theta} f_i \cdot p_i \right] > 0 \tag{3.7}$$

From (4) it is inferred that in order (3) to be true, we have to show that $\forall$ j $\geq \Theta$:

$$f_j - \sum_{i=1}^{\Theta} f_i \cdot p_i \ > 0 \tag{3.8}$$

By using the conservation law of probabilities we can write equation (5) as follows:

$$\Big[\sum_{i=1}^{M} p_i\Big] \cdot f_j - \sum_{i=1}^{\Theta} f_i \cdot p_i \ =$$

$$(p_1 \cdot f_j + p_1 \cdot f_j + \cdots + p_M \cdot f_j) - (p_1 \cdot f_1 + p_2 \cdot f_2 + p_\Theta \cdot f_\Theta) =$$

$$p_1 \cdot (f_j - f_1) + p_2 \cdot (f_j - f_2) + \cdots + p_\Theta \cdot (f_j - f_\Theta) \tag{3.9}$$

But, as we have mentioned before the discrete function f_i is monotonically increasing because it represents the accumulated delay per hop and so equation (3) is true. □

With the above approach we have proven that in the most general case, where we have arbitrary discrete functions f_i and p_i, the mean excess delay introduced by the HBQ will always be less than the mean excess delay introduced by the drop tail. In order to compare the two schemes and acquire a perception on the differences between them, we can use a log-normal distribution for the number of hops and an approximation with linear increase in delay with the number of hops. We also assume that there are always packets with less number of routers crossed than the hop count of the packet that is considered to be dropped. In this case the continuous time version of equation (3.4) for the mean excess delay introduced by the drop tail queue will be:

$$med_{DT} = \int_0^M (ax + b) \cdot \frac{1}{\sqrt{2\pi}\sigma x} e^{\frac{(lnx - \mu)^2}{2\sigma^2}} dx \tag{3.10}$$

Expanding the above equation, it can be found that for the drop tail this value will be:

$$med_{DT} = \Psi(M) \tag{3.11}$$

where,

$$\Psi(x) = \frac{a \cdot e^{\mu+\sigma^2/2}}{2}\left(Erf\left[\frac{\sigma}{\sqrt{2}}\right] - Erf\left[\frac{\sigma^2 - lnx - \mu}{\sqrt{2}\sigma}\right] + \frac{b}{2}Erf\left[\frac{lnx-\mu}{\sqrt{2}\sigma}\right]\right) \tag{3.12}$$

and,

$$Erf(y) = \frac{2}{\sqrt{\pi}} \cdot \int_0^y e^{-x^2} dx$$

For the case of hop based queueing the continuous time version of equation (2) will have the form:

$$\begin{aligned} med_{HBQ} = &\int_0^{\Theta} (ax+b) \cdot \frac{1}{\sqrt{2\pi}\sigma x} e^{\frac{(lnx-\mu)^2}{2\sigma^2}} dx + \\ &(1-p) \cdot \int_{\Theta}^{M} (ax+b) \cdot \frac{1}{\sqrt{2\pi}\sigma x} e^{\frac{(lnx-\mu)^2}{2\sigma^2}} dx + \\ &p \int_{\Theta}^{M} (ax+b) \frac{1}{\sqrt{2\pi}\sigma x} e^{\frac{(lnx-\mu)^2}{2\sigma^2}} dx \int_0^{\Theta} (ax+b) \frac{1}{\sqrt{2\pi}\sigma x} e^{\frac{(lnx-\mu)^2}{2\sigma^2}} dx \end{aligned} \tag{3.13}$$

After some algebra it can be shown that the mean excess delay introduced by hop based queueing will be given by:

$$\begin{aligned} med_{HBQ} = &\Psi(\Theta) + (1-p)\left[\Psi(M) - \Psi(\Theta)\right] + \\ &p\left[\Psi(M) - \Psi(\Theta)\right]\Psi(\Theta) \end{aligned} \tag{3.14}$$

3.4 Calculation of the dropping probabilities

3.4.1 Exact realization

If a router needs to mark/drop a packet (with corresponding probability p_a), the RED algorithm would apply this decision on the incoming packet, whereas in the case of the HBQ algorithm a packet from the queue will be dropped by using a set of probabilities based on the number of hops and the number of packets per hop. As depicted in figure 3.8 the probability of dropping a packet is a linear function of the number of hops, that decreases as the number of hops increases. By denoting by h_{max} and h_{min} the maximum and minimum number of hops respectively on the network, and by $\lambda_{h_{min}}$ and $\lambda_{h_{max}}$ the corresponding dropping probabilities, the slope of the function will be based on

these parameters. In this case, the un-normalized probability of dropping a packet with h_i number of hops would be given by,

$$\lambda_i = -\frac{\lambda_{h_{max}} - \lambda_{h_{min}}}{h_{min} - h_{max}} \cdot h_i + \lambda_{h_{min}} + \frac{\lambda_{h_{max}} - \lambda_{h_{min}}}{h_{min} - h_{max}} \cdot h_{min} \tag{3.15}$$

To calculate these values, the minimum and maximum probabilities need to be defined, i.e. $\lambda_{h_{min}}$ and $\lambda_{h_{max}}$. Since the sum of these probabilities should be equal to one, we have,

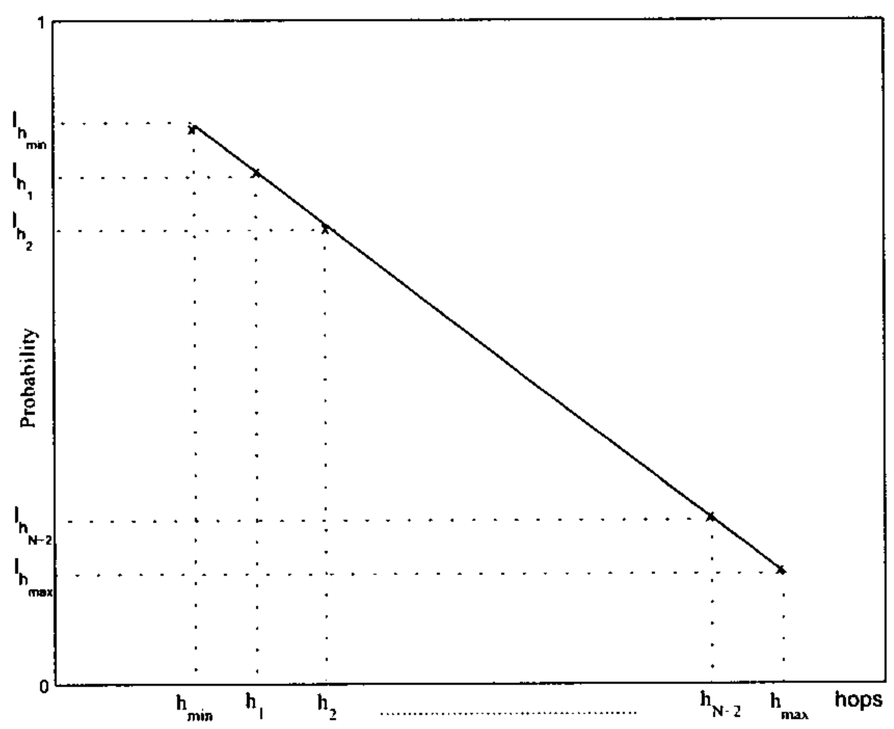

Figure 3.8: Dropping probability λ_{h_i} versus the number of hops

$$\lambda_{h_{max}} + (N-1) \cdot \lambda_{h_{min}} + \sum_{i=1}^{N-2} \left(-\frac{\lambda_{h_{min}} - \lambda_{h_{max}}}{h_{max} - h_{min}} \cdot h_i + h_{max} \cdot \frac{\lambda_{h_{min}} - \lambda_{h_{max}}}{h_{max} - h_{min}} \right) = 1 \tag{3.16}$$

The second equation is based on the relationship between the average transmission rate of TCP flows with the maximum and minimum number of hops in the network. Using a simple deterministic model, the average transmission rate of a TCP flow with average round trip time *rtt* and steady-state packet drop rate p would be given by [22],

$$f(rtt, p) \approx \frac{\sqrt{1.5}}{rtt\sqrt{p}} \tag{3.17}$$

In order to retain in the network the bias in the average transmission rate towards flows with long round trip times, then the following equation should hold,

$$\frac{f_{h_{max}}}{f_{h_{min}}} \approx \frac{rtt_{h_{min}}}{rtt_{h_{max}}} = \frac{g(h_{min})}{g(h_{max})} \tag{3.18}$$

where the rtt can be characterized as a function of the number of hops. If we assume an average queue size in each hop, then the initial packet marking/dropping probability would be,

$$p_b = max_p \cdot \left[\frac{max_{th} - 3min_{th}}{2(max_{th} - min_{th})} \right] \tag{3.19}$$

and the actual dropping probability as given by the RED algorithm would be

$$p_a = \frac{p_b}{1 - E\{count\}p_b} = \frac{2p_b}{1 - p_b} \tag{3.20}$$

The ratio of the average transmission rates for the flows with minimum and maximum number of hops, as defined in equation (3.18), can be written,

$$\frac{g(h_{min}) \cdot \sqrt{h_{min}p_w + \lambda_{h_{min}}}}{g(h_{min}) \cdot \sqrt{h_{min}p_w + \lambda_{h_{min}}}} = \frac{g(h_{min})}{g(h_{max})} \tag{3.21}$$

By solving now, the linear system as defined by equations (3.16) and (3.21), the marking/dropping probabilities for the flows with maximum and minimum number of hops will be,

$$\lambda_{h_{max}} = \frac{1}{N} - \frac{p_w}{p_a}(h_{max} - h_{min}) + \frac{p_w}{p_a}\left(\sum_{i=2}^{N-1} h_i - h_{min} \right) \tag{3.22}$$

$$\lambda_{h_{min}} = \frac{1}{N}\left[1 - \frac{p_w}{p_a}(h_{max} - h_{min}) \right] + \frac{p_w}{p_a}\left(\sum_{i=2}^{N-1} h_i - h_{min} \right) \tag{3.23}$$

The above calculated probabilities and the linear relationship between them assumes equal number of packets for every hop in the router. In order the dropping probabilities to be unbiased for each hop, they need to be normalized with the corresponding number of packets per hop. If we denote by $n_{h_{min}}, n_1, \ldots, n_{N-1}, n_{h_{max}}$ the number of packets for each hop and the percentage of packets per hop by $\nu_{h_{min}}, \nu_1, \ldots, \nu_{N-1}, \nu_{h_{max}}$, where $\nu_i = \frac{n_i}{n}$ with $n = n_{h_{min}} + n_1 + \ldots + n_{N-1} + n_{h_{max}}$, then the

dropping probabilities will be:

$$\pi_{h_{min}} = \lambda_{h_{min}} \cdot \frac{\nu_{h_{min}}}{\pi}, \pi_1 = \lambda_1 \cdot \frac{\nu_1}{\pi}, \ldots, \pi_{h_{max}} = \lambda_{h_{max}} \cdot \frac{\nu_{h_{max}}}{\pi} \tag{3.24}$$

where $\pi = \lambda_{h_{min}} \cdot \nu_{h_{min}} + \lambda_1 \cdot \nu_1 + \ldots + \lambda_{N-2} \cdot \nu_{N-1} + \lambda_{h_{max}} \cdot \nu_{h_{max}}$

Thus, the exact realization of the algorithm includes, at the worst case scenario, N-1 sequential searches in order to drop a packet from the queue. In the next section, we relax this condition, by introducing a threshold and as a result the dropping mechanism will be based on simple binary decisions.

3.4.2 Coarse realization

In this case, a threshold Θ is set on the number of hops, with two different dropping probabilities for packets that have smaller or larger number of hops than the threshold. In the following discussion we will assume a constant value of the threshold, but in actual implementations the threshold can be adaptive depending on the aerage number of hops recorded in the router. The corresponding nomalized dropping probabilities will be given by:

$$\pi_{\Theta_-} = \lambda_{\Theta_-} \frac{\upsilon_{\Theta_-}}{\lambda_{\Theta_-}\upsilon_{\Theta_-} + \lambda_{\Theta_+}\upsilon_{\Theta_+}}, \quad \pi_{\Theta_+} = 1 - \pi_{\Theta_-} \tag{3.25}$$

where λ_{Θ_-} is given by equation (3.23). The following list represent the pseudocode of the HBQ scheme which is based on the RED queue but introduce differentiation of packet treatment depending on the number of hops.

Algorithm 3.4.1: HBQ PSEUDOCODE(based on RED)

comment: RED parameters:p_a, max_{th} and min_{th} are defined in [27]

for every packet received

do
- Calculate average queue size (avg)
- **if** avg $\geq max_{th}$
  - **then**
    - **if** NUMBER OF HOPS $\geq \Theta$
    - DROP PACKET WITH PROBABILITY $1-\rho$
  - **else**
- **if** avg $\geq min_{th}$
  - **then**
    - calculate dropping probability p_a
    - **if** NUMBER OF HOPS $\geq \Theta$
    - DROP PACKET WITH PROBABILITY $1-\rho$
  - **else**
- forward the packet

In the exact realization of the HBQ algorithm the number of hops of the enqueued packets is the sole information that is required in order to calculate the dropping/marking probabilities. On the other hand, in the case of the coarse realization the threshold parameter Θ should be tuned according to the statistics on the number of routers traversed of the incoming traffic. Different scenarios can be distinguished regarding the selection of the threshold value. If the HBQ algorithm is used only on the outgress border gateway of a stub autonomous system (a mobile network falls into this category) then the threshold depends on topological information of the network and can be considered as constant. In the case of ingress traffic the threshold can be updated on regular intervals and set as one standard deviation from the mean number of hops of the packets arriving in the router. If the HBQ algorithm is utilized in different routers within the autonomous system then an autonomous parameterization of the threshold would require an exponential moving average estimation of the number of hops of the incoming traffic.

One critical issue of RED queue consists of tuning the different parameters such as the minimum and maximum threshold and the weight to calculate the average queue size. It has been widely accepted It is difficult to find a set of parameters that offers good performance in all kinds of traffic profiles. Depending on the traffic source behaviour and the set of chosen parameters, RED may start to drop packets too early or too late, nullifying the reasons of why it has been developed. In fact, in [23] Floyd et al. state that the parameterization of the RED queue methods are not

claimed to be optimal or even close to optimal, but they seem to work well in a wide range of traffic scenarios. On the contrary the HBQ is defined solely by the threshold parameter, which is independent on traffic dynamics. Therefore the complexity introduced is the one for updating the threshold using an exponential moving average estimator and the assigned probability of dropping a packet with a specific number of traversed routers. Keeping in mind that the HBQ algorithm does not required state information to be maintained in the router but only the number of traversed routers for each packet in the queue and that the algorithm run only when there should be a packet dropped (therefore does not utilize CPU cycles at all times), the implementation complexity can be considered as reasonable.

3.5 Energy Consumption Analysis

In this section we analyze the performance of the HBQ scheme when it is used in ad hoc networks. As mentioned in the previous sections we are interested in the energy consumption of these networks when there is packet (re)transmission. We adopt the generic model for energy consumption from [24], where the energy spent in transmission is equal to $E_b^T = \varphi_D B D_{i,j}^a + \varphi_T B$ and the energy spent in reception is $E_b^R = \varphi_R B$. With φ_D we denote the energy dissipated per bit per m^2 (taken to be 10^{-10}), φ_T and φ_R is the energy spent by transmission and reception circuit respectively (equal to $50 \cdot 10^{-9}$), B is the number of bits per packet and $D_{i,j}^a$ is the distance between mobile nodes i and j ($a \geq 2$ is a constant denoting the attenuation of the signal). Using this notation, the consumed energy (E_c) for transmitting an IP packet over h wireless hops in an ad hoc network can be defined as follows,

$$E_c = E_b^T + \sum_{i=2}^{h-1}(E_b^R + E_b^T) + E_b^R = \left[\varphi_D B D_{1,2}^a + \varphi_T B\right] + \sum_{i=2}^{h-1}\left[\varphi_D B D_{i,i+1}^a + \varphi_T B\right] + \varphi_R B$$

If we further assume that all mobile nodes are distributed in an equal distance manner, the above expression simplifies to the following:

$$E_c = h(E_b^T + E_b^R) = \underbrace{(h-1)\left[\varphi_D B D_{1,2}^a + \varphi_T B\right]}_{(h-1)\text{transmissions}} + \underbrace{(h-1)[\varphi_R B]}_{(h-1)\text{receptions}} \tag{3.26}$$

From equation 3.26, and assuming a constant packet size, the energy consumption will follow the probability density function of the number of hops in the ad hoc network. We can now examine the energy consumed by the HBQ and drop-tail queue in an ad hoc network with maximum number of wireless hops equal to M.

Proposition 3.5.1. *Let's denote by E_i the accumulated energy consumption for i hops, which is a non-decreasing discrete function, and by e_i the corresponding probability for i wireless hops. Then, the aggregate energy consumption in an ad hoc network that utilize the HBQ scheme is less than the energy consumed by drop-tail queues, i.e.,*

$$E_c^{HBQ} \leq E_c^{DT} \tag{3.27}$$

Proof. The energy consumption by the drop-tail queue, which does not change the statistics of the incoming traffic, will be given by, $E_c^{DT} = \sum_{i=1}^{M} e_i E_i$, while for the HBQ it can be easily shown to be, $E_c^{HBQ} = \sum_{i=1}^{\Theta} e_j E_j + (1-\rho)\sum_{i=\Theta+1}^{M} E_i \cdot e_i + \rho \sum_{i=\Theta+1}^{M} e_i \cdot \sum_{i=1}^{\Theta} E_i \cdot e_i$ In order to prove that the HBQ scheme introduce less aggregate energy consumption than the drop tail queue we have to show that:

$$\sum_{i=\Theta+1}^{M} E_i \cdot e_i - \left\{ (1-\rho) \sum_{i=\Theta+1}^{M} E_i \cdot e_i + \rho \sum_{i=\Theta+1}^{M} e_i \cdot \sum_{i=1}^{\Theta} E_i \cdot e_i \right\} \geq 0 \tag{3.28}$$

$$\sum_{i=\Theta+1}^{M} E_i \cdot e_i - \sum_{i=\Theta+1}^{M} E_i \cdot e_i + \rho \sum_{i=\Theta+1}^{M} E_i \cdot e_i - \rho \sum_{i=\Theta+1}^{M} e_i \cdot \sum_{i=1}^{\Theta} E_i \cdot e_i \geq 0$$

$$\rho\{ \sum_{i=\Theta+1}^{M} E_i \cdot e_i - \sum_{i=\Theta+1}^{M} e_i \cdot \sum_{i=1}^{\Theta} E_i \cdot e_i \} \geq 0$$

$$\sum_{i=\Theta+1}^{M} E_i \cdot e_i - \sum_{i=\Theta+1}^{M} e_i \cdot \sum_{i=1}^{\Theta} E_i \cdot e_i \geq 0$$

$$(E_{\Theta+1} \cdot e_{\Theta+1} + E_{\Theta+2} \cdot e_{\Theta+2} + ... + E_M \cdot e_M) - (e_{\Theta+1} \sum_{i=1}^{\Theta} E_i \cdot e_i + ... + e_M \sum_{i=1}^{\Theta} E_i \cdot e_i) \geq 0$$

$$e_{\Theta+1}\{E_{\Theta+1} - \sum_{i=1}^{\Theta} E_i \cdot e_i\} + ... + e_M\{E_M - \sum_{i=1}^{\Theta} E_i \cdot e_i\} \geq 0 \tag{3.29}$$

From (4) it is inferred that in order (3) to be true, we have to show that $\forall$ j $\geq \Theta$:

$$E_j - \sum_{i=1}^{\Theta} E_i \cdot e_i \ \geq 0 \tag{3.30}$$

By using the conservation law of probabilities we can write equation (5) as follows:

$$\{\sum_{i=1}^{M} e_i\} \cdot E_j - \sum_{i=1}^{\Theta} E_i \cdot e_i \ =$$

$$(e_1 \cdot E_j + e_1 \cdot E_j + ... + e_M \cdot E_j) - (e_1 \cdot E_1 + e_2 \cdot E_2 + e_\Theta \cdot E_\Theta) =$$

$$e_1 \cdot (E_j - E_1) + e_2 \cdot (E_j - E_2) + ... + e_\Theta \cdot (E_j - E_\Theta) \tag{3.31}$$

But E_i is a monotonically increasing discrete function because represents the accumulated energy consumption per hop and so equation 3.28 is true. □

3.6 Numerical Investigations

The coarse realization of the HBQ algorithms can be visualized in figure 3.9 which shows how the threshold Θ clusters the packets into two areas, i.e. above and below the threshold, depending on the number of hops. The difference between HBQ and drop-tail queue in the sense of mean excess delay can be seen in figure 3.10. Clearly, the mean excess delay of the drop tail queue for a specific density function of the number of hops and a linear function of delay will be constant. On the other hand, for the HBQ scheme the performance depends on the selected threshold, Θ, value and the probability, p, of dropping a packet with number of traversed nodes with hops less than Θ. In the limiting case when the threshold Θ is set to the maximum number of hops and independent on the selection of the dropping probability, HBQ will deteriorates to operate as a drop tail queue. Figure 3.10 shows that zero mean excess delay introduced by the HBQ scheme when the threshold is set to be equal to the minimum number of hops and the dropping probability is set to 1. This is of course a theoretical result, which in a real case scenario means that the router has an infinite buffer. It is interesting to note that between these two extreme cases there is a wide range of different thresholds and dropping probabilities values that can be selected that give better performance from the drop

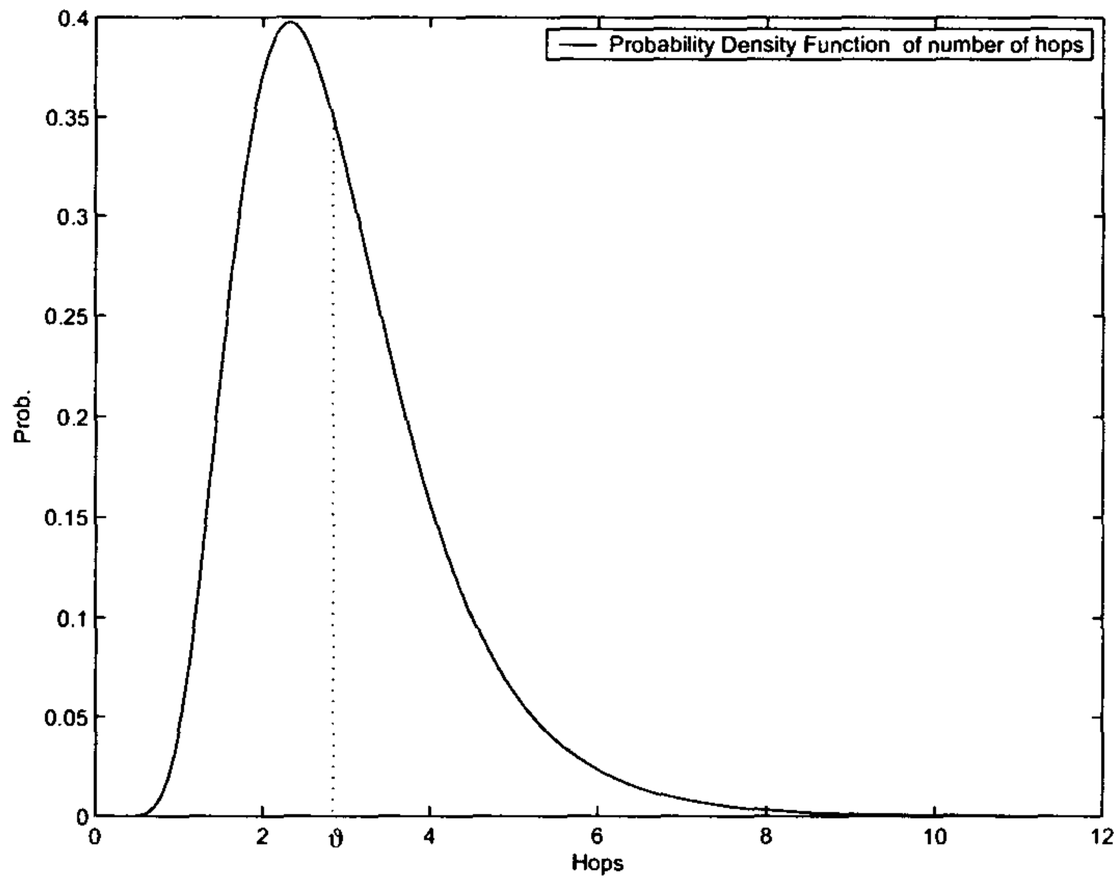

Figure 3.9: The threshold Θ in HBQ differentiate packet treatment depending on the number of hops.

tail queue.

The simulations were performed using the NS-2 platform. The default congestion avoidance algorithm is used, which is the TCP Tahoe. We assume ten different mobile users in total where each one is connected to different remote servers with different number of hops. We analyze the performance by considering that 20% of the users have number of hops greater than the threshold (5) and the other 80% of users are connected two and/or three hops away from the corresponding server. In this case the majority of the users will be below the threshold Θ and the chosen probability of the HBQ algorithms for packets below the threshold chosen to be $p = 0.8$. Figure 3.11 shows the difference in percentage between the sequence numbers for all the users when using the default RED queue and when using the HBQ algorithm. The mean final sequence number for users belonging in the 20% is only 28.5% compared to the mean sequence number for the rest of the users. HBQ increase dramatically (by 40%) the TCP sequence number received (which means the actual data packets that the corresponding mobile users will receive). In order to achieve this increased of the performance by 40%, HBQ will reduce the sequence number received by the rest of the users. As can be seen from figure 3.11, HBQ reduces the sequence number by 8.85% while increasing by 40% the performance of the sensitive users (flows that have large number of hops/RTT). In other words

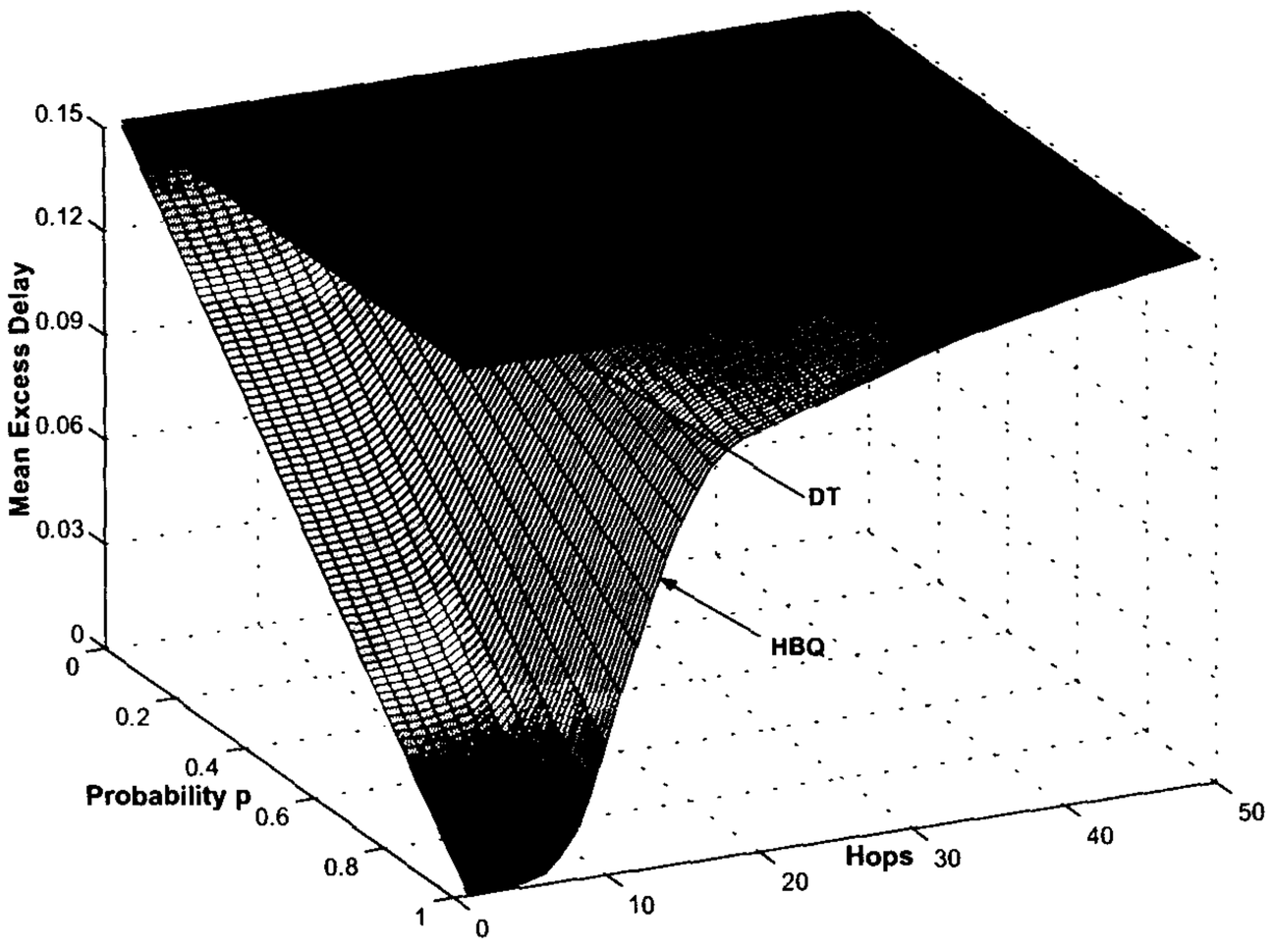

Figure 3.10: Comparison of the mean excess delay introduced by DT and HBQ for log-normal distribution of the number of hops and linear increase of the delay

the throughput variation between the mobile users is decreased by using HBQ. This ratio for the same simulation scenario, i.e., the ratio between the maximum and minimum sequence number in the above simulations are: for Drop tail: 4.35 and for HBQ: 1.54.

3.7 Conclusions

Since future all-IP wireless networks envisioned to support IP technology all the way down to the mobile host, wireless networks will quickly become an integral part of the Internet. The specific characteristics of the last wireless hop together with the round trip time (RTT) variation because of congestion and different number of traversed routers in the Internet, affects the end-to-end TCP/IP traffic characteristics. Increased packet loss due to the wireless channel together with a span of three orders of magnitude in RTT between flows, make optimization of such networks a challenging task. By using active traffic measurements, targeting servers in Europe and USA, we have explored a characteristic sample of wide area RTT's in the Internet and confirmed that RTT's follow a heavy tail distribution with significant outliers. By coupling this observation with the analytical investigations

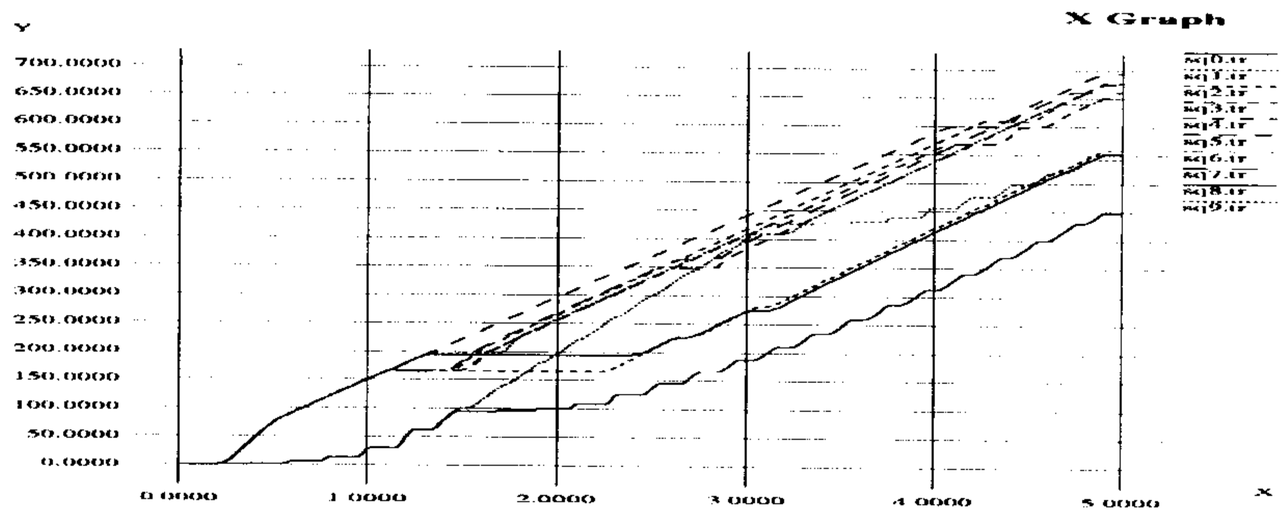

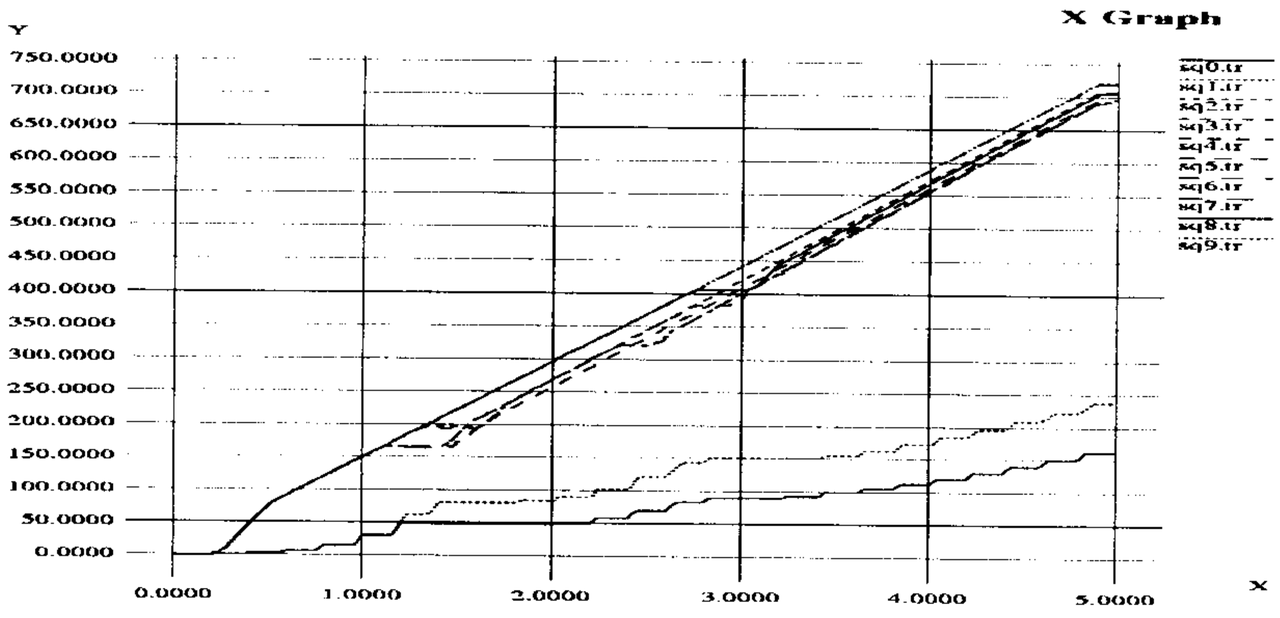

Figure 3.11: Comparison of received packets (in terms of sequence numbers) when using HBQ(up) and Drop-Tail(down) queues.

of how the TCP performance in case of random losses is affected, we have concluded that TCP flows that span over a large number of routers with a wireless last hop can eventually have a very small cwnd size. With small cwnd's, because of bursty channel errors and long RTT's, the state machine of TCP will mainly stay in slow-start phase rather than in congestion avoidance and therefore the performance will deteriorate. From the above discussion it is clear that TCP flows with large RTT and small cwnds can be considered as 'sensitive' flows, that require special treatment.

In that respect, the proposed Hop Based Queueing algorithm explores one critical side information which is the number of hops traversed by the packets currently in the buffer of the node. Packets are

not dropped randomly from the queue, but the logic behind which packet to be dropped is given by a well defined set of probabilities. Decreasing the dropping probability of a packet as the number of wireless/wireline hops traversed increases, has some high desirable properties such as increasing the performance of TCP and decreasing the aggregate delay and power used for packet retransmission. Through theoretical and simulation results these attributes of the proposed queueing mechanisms have been explored.

Based on the above arguments, a more forward looking perspective will be discussed in the next chapters, on how to integrate IP based QoS information and information from the transport layer into resource management functionalities of the access networks.

Bibliography

[1] W. Stevens, TCP Slow Start, Congestion Avoidance, Fast Retransmit, and Fast Recovery Algorithms, *IETF, equest for Comments: 2001, January 1997*

[2] K. Ramakrishnan, S. Floyd, D. Black, The Addition of Explicit Congestion Notification (ECN) to IP, *IETF Request for Comments: 3168, September 2001*

[3] K. Pentikousis and H. Badr, An Evaluation of TCP with Explicit Congestion Notification, *Annals of Telecommunications, 59(1-2), January-February 2004*

[4] F. Begtaevi, P. Van Mieghem, Measurements of the Hopcount in Internet, *Proceedings of Passive and Active Measurement (PAM2001), Amsterdam, The Netherlands, April 23-24, pp. 183-190*

[5] Huffaker, B. Fomenkov, M. Plummer, D. Moore, D. Claffy, K., Distance Metrics in the Internet, *IEEE International Telecommunications Symposium (ITS), 2002*

[6] Katia Obraczka and Fabio Silva, Network Latency Metrics for Server Proximity, *Proceedings of the IEEE Globecom 2000, December 2000*

[7] S. B. Moon, J. Kurose, P. Skelly and D. Towsley, Correlation of packet delay and loss in the Internet,*technical report,Department of Computer Science, University of Massachusetts, USA, Jan., 1998*

[8] J. C. Bolot, Characterizing end-to-end packet delay and loss in the Internet, *Journal of High-Speed Networks, vol.2, pp. 305-323, Dec. 1993*

[9] Vern Paxson, End-toend Internet packet dynamics, *Proceedings of ACM SIGCOMM, pp. 139-152, Sept. 1997*

[10] A. Adams, T. Bu, R. Caceres, N. Duffield, T. Friedman, J. Horowitz, F. L. Presti, S. B. Moon, V. Paxson, D. Towsley, The use of end-to-end multicast measurements for characterizing internal network behavior, *IEEE Communications, May 2000*

[11] http://www.communes.com

[12] W. Richard Stevens, TCP/IP Illustrated, Volume 1: The Protocols, *Addison-Wesley, 1994*

[13] M. Zorzi, R. Rao, The effect of correlated errors on the performance of TCP, *IEEE Communications Letters, vol. 1, pp. 127-129, Sept. 1997*

[14] M. Zorzi, R. R. Rao, and L. B. Milstein, On the accuracy of a first-order Markov Model for data transmission on fading channels, *Proc. IEEE ICUPC'95, pp. 211- 215, November 1995.*

[15] M. Gerla, K. Tang, R. Bagrodia, TCP Performance in Wireless Multi-Hop Networks, *Proceedings of IEEE WMCSA, 1999*

[16] X. Yang, N. Vaidya, Priority Scheduling in Wireless Ad Hoc Networks, *ACM Mobihoc'02, June 2002*

[17] V. Kanodia, C. Li, A. Sabharwal, B. Sadedgi, E. Knightly, Distributed Multi-Hop Scheduling and Medium Access with Delay and Trhoughput Constraints, *Mobicom, August 2001*

[18] M. Barry, A. Campbell, A. Veres, Distributed Control Algorithms for Service Differentiation in Wireless Packet Networks, *IEEE Infocom, April 2001*

[19] Zhenghua Fu, Petros Zerfos, Haiyun Luo, Songwu Lu, Lixia Zhang, Mario Gerla, "The Impact of Multihop Wireless Channel on TCP Throughput and Loss", *in IEEE INFOCOM'03, San Francisco , March 2003.*

[20] K. Ramakrishnan, S. Floyd, A proposal to add explicit ongestion notification (ECN) to IP, *RFC 2481, Jan. 1999*

[21] S. Floyd, V. Jacobson, Random Early Detection Gateways for Congestion Control, *IEEE/ACM Transactions on Networking, 1(4):397-413, August 1993*

[22] T. Lakshman and U. Madhow, The performance of TCP/IP for networks with high bandwidth-delay products and random loss, *IEEE/ACM Transactions on Networking, vol. 5, no. 3, pp. 336-350, 1997.*

[23] Floyd, R. Gummadi, and S. Shenker, Adaptive RED: An algorithm for increasing the robustness of RED, *Technical Report, ACIRI, 2001*

[24] W. R. Heinzelman, A. Chandrakasan, and H. Balakrishnan, Energy efficient communication protocol for wireless microsensor networks, *Proc. Hawaii International Conference on System Sciences, Jan. 2000.*

Chapter 4

TCP-aware Power and Rate Adaptation in CDMA Networks

In this chapter a novel joint power and rate adaptation scheme for DS/CDMA networks is proposed using information from the TCP state machine. The impetus behind this cross layer optimization approach is to satisfy the varying transmission rates of TCP flows which depend on the congestion window (cwnd) and round trip time (RTT). Initially, we define a new family of objective functions that encompass TCP based information. Then, by solving the proposed bi-objective optimization problem using the ε-constraint method, the Pareto frontier is calculated, which gives insight into the trade-off between the desired transmission rate and the corresponding transmitted power. Using a polynomial description of the Pareto frontier the solution with the minimum L_2-norm from a defined utopia point is selected as the optimum trade-off between power consumption and required rate transmission, even though different heuristics can be used. Although the Pareto frontier has been calculated using derivative based optimization techniques, prominent paradimes of knowledge-based techniques can increase the computational efficiency.

Previously proposed schemes allocate resources based on lower layer information, such as channel conditions and link layer buffer occupancy. The novelty and advantage of this cross layer optimization approach is that critical transport layer information is integrated into the design of a power and rate adaptation algorithm for DS/CDMA networks.

4.1 Introduction

The critical catalyst driving architectural designs of beyond 3G mobile/wireless communication systems is the seamless integration of Internet like applications. Today, the majority of Internet like applications such as SMTP, Web-browsing and peer-to-peer are based on TCP, which is the most widely used transport layer protocol over the Internet (TCP makes up about 95% of all Internet traffic). With an increasing popularity of wireless access to the Internet, the interactions of the non-reliable wireless medium with the TCP state machine have posed an altogether new set of challenges for optimum performance. With variable transmission rate, the problem of how to share resources under different optimization criteria had become an important issue.

Since CDMA based systems are interference-limited, power allocation is directly related to spectral efficiency. Especially with power constraints in practical CDMA wireless systems, minimizing power leads to a maximum real-time traffic capacity [14], [12]. With increased volumes of non-real-time data traffic being required to be carried over wireless systems, such as Internet like traffic, the studies in [12], [13] show that rate allocation is one of the efficient approaches to improve data performance in terms of throughput and transmission delay. In more recent studies presented in [14],[15], Jantti et al. have carried out intensive theoretical studies on the optimization of non real time traffic in terms of minimum time span, maximum throughput and minimum power consumption through joint power and rate allocation. Also, in some newly developed MAC protocols that envision to support multi-media traffic over DS-CDMA systems, either rate allocation [15] or power-based rate allocation [16], [17] is deployed to improve non real time data performance in terms of throughput and delay.

The previously mentioned research work clearly demonstrated that throughput maximization is achieved when transmission is based on a hybrid TDMA/CDMA approach. In other words, the throughput maximization problem can be solved when only a subset of the users is allowed to transmit while the rest of the mobile hosts pause transmission. This kind of operation can cause non-desirable interactions with higher layers (i.e, UDP/TCP) because of the delays that can be introduced. These inefficiencies are also mentioned in [18], where the authors propose dynamic power and rate allocation schemes based on measured SIR. They mention that the proposed framework can also be used to evaluate and infer the performance observed by higher layers (e.g., TCP), but

this has been left as future work and the authors do not explicitly discuss interactions with TCP. In [10] the authors propose a multi-objective optimization scheme for power and rate control. In this scheme a weighted error function is introduced with the aim being to keep the transmission power close to the minimum required while at the same time trying to maximize the data rate. Our bi-objective optimization power and rate control scheme differs from the previous mentioned proposals in that previous techniques focus on link layer performance and are *agnostic* of the data rate requirements of higher layers. In this chapter a cross layer optimization apporach is proposed by using information from the TCP layer in terms of required transmission rate, which is the ratio of the current congestion window and RTT of the connection. Using this information a bi-objective optimization problem is formulated where the first objective function depicts the difference between the required rate and the received rate caused by channel conditions and interference, while the second is the total transmitted power. The Pareto frontier of these two conflicting objective functions is calculated using the ε-constraint method and the selected solution is the point with the minimum L_2-norm. As will become clear in later sections, this solution is optimum in the sense of the trade-off between transmitted power and the difference of the actual received rate versus the required data rate. Alternatively, using soft computing techniques, computational complexity and timelining can be decreased by a simultaneous search of multiple points rather than a single point and by using stochastic operators instead of deterministic rules.

The rest of the chapter is organized as follows. In section 4.2, several techniques for cwnd and RTT estimation at the access point are discussed. Section 4.3 contains the analysis of the problem concerning power and rate adaptation and defines new objective functions that utilize TCP information. In section 4.4, the bi-objective optimization algorithm is presented together with the issue of selecting a solution from among the Pareto frontier. Numerical results of the proposed scheme are contained in section 4.7 and finally, the conclusions together with future work end the chapter in section 4.8.

4.2 Cwnd and RTT Estimation at the Access Point

4.2.1 Analysis of TCP

The flow/congestion control algorithms of TCP are designed to probe available bandwidth, through deliberate manipulation of the transmission rate [11]. The instantaneous transmission rate of TCP takes on a familiar sawtooth shape, where it cycles between periods of additive increase separated by multiplicative decrease (AIMD). The maximum number of outstanding packets is controlled by the size of *cwnd* (congestion window) which is in units of bytes but for clarity, in the rest of the chapter the *cwnd* is expressed in units of MSS (Maximum Segment Size). Initially the *cwnd* goes through the slow start phase in which it is increased by one segment every time the sender receives an unduplicated ACK from the receiver. This exponential growth of the *cwnd* is limited by the buffer size of the receiver or sender and by the *ssthresh* value. Initial values of *ssthresh* can be equal to the advertised window while subsequent values are based on recent congestion experience of the connection. When the size of the *cwnd* is equal to *ssthresh*, the TCP state machine enters into the congestion avoidance phase where increments are limited by $1/cwnd$ for every ACK received, resembling a linear increase.

In case of packet loss two distinctive actions can occur. Firstly, if there is a timeout event, the sender will set the value of the *ssthresh* equal to half the number of the current maximum number of unacknowledged packets and the *cwnd* equal to one. Secondly, in order to curtail frequent abrupt shrinkage of the *cwnd* and avoid lengthy timeout events, the TCP state machine includes the fast retransmit/recovery technique. Fast retransmit utilizes the fact that the acknowledgment carries the sequence number of the next expected packet. In the case, where three duplicate ACK's are received, the sender concludes that a packet is lost, retransmits without waiting for a timeout event, reduces *cwnd* to half, and enters the congestion avoidance phase.

Wireless link impairments can raise the packet error probability several orders of magnitude, and as a result frequent decreases of the *cwnd* can be observed. Depending on the fading environment (independent identical distributed (i.i.d) errors or correlated losses) multiple losses inside the *cwnd* will result in retransmissions based on timeout events which will trigger the slow start algorithm. In this case, TCP flows that share the wireless medium will have different instantaneous requirements

for transmission rate depending on the current state of the TCP connection. These transmission rate requirements can be fully revealed by a knowledge of the current size of the *cwnd* and the RTT of the connection. Two different cases can be distinguished; the first is when the TCP state machine is held at the mobile host and the second when the TCP state machine is held at the source host. In the first case, the access point can be aware of the *cwnd* and RTT of the connection by simply triggering the mobile host to piggyback this information to the access point (uplink case), while in the second case the access point should actively or passively infer this information as discussed in the following section (downlink case).

4.2.2 RTT Estimation with emphasis on the downlink

Estimating the RTT of a connection can be carried out using several methods depending on the assumptions of end-to-end information availability at the access point and direction of the traffic. If the sender is the mobile host then all the RTT estimation algorithms are performed locally and so the RTT estimation can be piggybacked to the access point together with other control information. If the mobile host acts as a receiver (i.e sending just ACK's) then the most accurate method for estimating the RTT is by using TCP `timestamp` option. When this option is enabled, TCP sender injects the timestamp in each transmitted segment and the receiver passes this information in the corresponding ACK (for a more detailed discussion we refer the reader in [13]). Thus, timestamps are always sent and echoed in both directions and so an accurate sample of RTT can be reconstructed at the mobile host by modifying the TCP stack and piggybacking this information to the access point.

If the mobile host cannot inform the access point about the estimated RTT or cannot perform RTT estimation using the timestamp option, then the estimation needs to be made actively or passively at the access point. In the first case, the access point has information available on delays on the wireless link and can send an ICMP echo-request to the sender with a timestamp in order to trigger an echo-reply from the sender. The RTT from the access point to the sender can then be calculated then by subtracting the ICMP timestamps (replying cannot be seen as an issue mainly because most hosts currently respond to echo requests). In the second case, coarse RTT estimates

can be performed by passive measurements based on different ramifications of the SYN-ACK or slow-start technique [14]. Using the SYN-ACK technique the RTT can be estimated from the packets exchanged during the three-way handshake period. Alternatively, using the technique based on the slow start phase, the RTT is estimated as the time spacing between the first and second burst. Using the advantage of bidirectional traffic available at the access point, the above two techniques can be used in tandem, increasing the accuracy of RTT estimation.

4.2.3 Cwnd Estimation

The estimation of the cwnd at the AP is based on extracting information from ACK's received from the MH, which triggers a slide in the flow control window at the receiver together with a change of the size of the cwnd. Using the RTT estimations and the ACK's received, the AP can reconstruct the congestion control algorithm and predict the size of the next burst of packets that will arrive back-to-back. This technique has been proposed in [15] in order to estimate bandwidth requirements of the TCP connection. Congestion window prediction mechanisms have also been proposed in [16] and [17] in order to tackle TCP's inherent inefficiency in asymmetric links. Figure 4.1 depicts a general topology where the AP, upon reception of ACK's from the MH, can infer the changes in the TCP state machine of the sender that these ACK's will trigger.

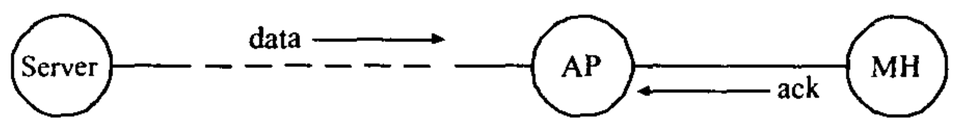

Figure 4.1: Cwnd estimation at the AP in the case of downlink

Using the above topology, figure 4.2 shows how this prediction can infer the change of the cwnd caused by random losses in the wireless link. The phase depicted is the initial slow start where the AP increases the estimated cwnd by one every time an ACK is received (grey arrow), until a random packet loss occurs and the three duplicate ACK's received at the AP imply halving of the cwnd at the receiver. We should also point out that ACK losses in the wireline part, i.e., between AP and the server, can be considered not only as rare events but also the consequences of an ACK loss is minimized by the inherent type of ACK's used by TCP. Since by carrying the sequence number of the next expected byte, TCP ACK's are 'cumulative' in the sense that they convey information on all bytes correctly received at the receiver, so an ACK loss is anticipated by the next correctly

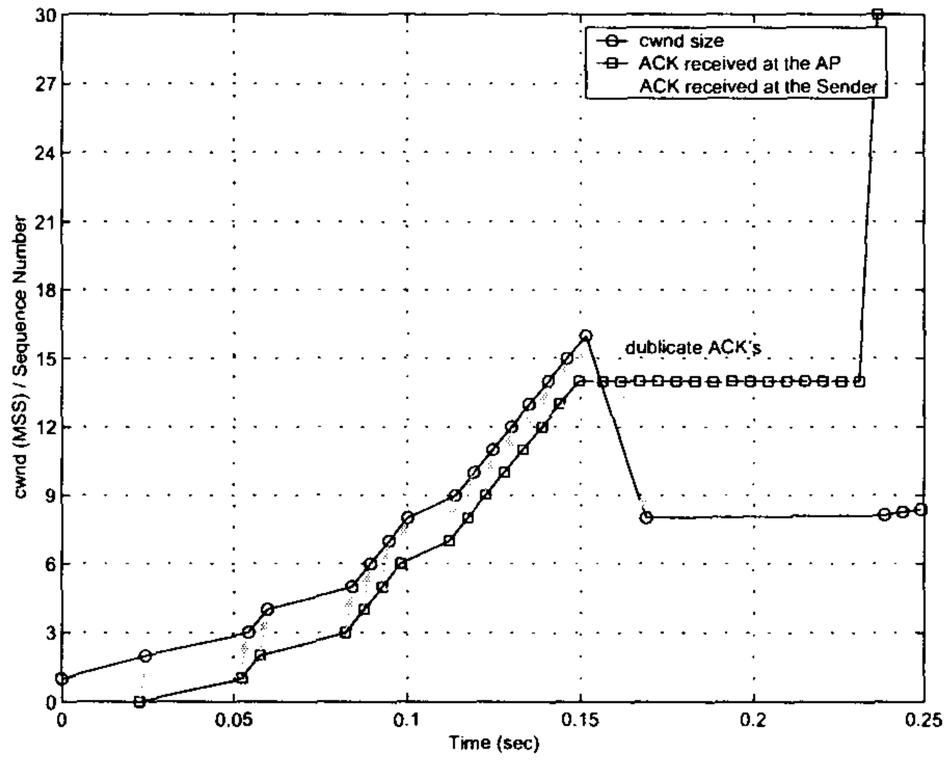

Figure 4.2: Cwnd estimation at the AP based on received ACK's from the MH

received ACK.

4.3 Problem Definition and Analysis

Before describing the integration of the extracted TCP information based on the reasoning developed in the previous section, we first define the general problem of power and rate control in CDMA networks. We consider a single cell in DS/CDMA network with N active TCP flows (this number can also be considered as an admission feasibility policy which is based on user requirements). The chip rate for all users is fixed and the total bandwidth W is shared among all users. Each mobile host i $(1 \leq i \leq N)$ can transmit with power $0 \leq p_i \leq p_{max}$, where p_{max} is the maximum transmission power for each mobile host. A small time interval Δt is considered such that the link gain between each mobile i and the access point is stationary and given by g_i $(1 \leq i \leq N)$. For a given power vector $\mathbf{p} = (p_1, p_2, ..., p_N)^T$ and by making the standard Gaussian approximation for the statistics of the inter-cell and intra-cell interference, the received Signal-to-Interference-Ratio (γ_i) for mobile i, is defined as:

$$\gamma_i(\mathbf{p}) \stackrel{\text{def}}{=} \frac{g_i p_i}{\theta_i \sum_{j \neq i} g_j p_j + \nu}, \quad 1 \leq i \leq N \tag{4.1}$$

where $\nu > 0$ is the lumpsum power of inter-cell interference and the background thermal noise at the mobile host. The orthogonality factor $0 \leq \theta_i \leq 1$, which express multipath effects, can be in

general different for different mobiles and typical values are in the range $[0.1 - 0.6]$ for the downlink and is considered equal to one for the uplink [14]. Using the above definition, we can describe the bit-energy-to-interference-power-spectral-density ratio, E_b/I_0, for mobile host i by

$$\left(\frac{E_b}{I_0}\right) = \frac{W}{r_i} \cdot \gamma_i(\mathbf{p})$$

where r_i is the allocated bit-rate for mobile host i. If we assume a target $(E_b/I_0) = \Gamma$ at the receiver to be constant (which gives a constant bit-error-rate), the constant relationship between rate r_i and γ_i will have the form:

$$\frac{r_i}{\gamma_i} = \frac{W}{\Gamma} \tag{4.2}$$

With a predefined assignment of γ_i targets, the power vector that supports every mobile with the minimum power can be found by solving the linear system of equations in (4.1),

$$p_i^* = \frac{\nu}{1 - \Sigma_{j=1}^{N} \frac{\gamma_j}{1+\gamma_j}} \cdot \frac{\gamma_i}{g_i(1+\gamma_i)} \tag{4.3}$$

From equation (4.3) it is clear that there exists a feasible solution, i.e $\mathbf{p}^* > \mathbf{0}$, without the maximum power limitation, if and only if $\Sigma_j \frac{\gamma_j}{1+\gamma_j} < 1$ [14]. Since transmission power for every mobile host should also be less or equal to p_{max}, the N constraints can be expressed as,

$$\sum_{j=1}^{N} \frac{\gamma_j}{1+\gamma_j} \leq 1 - \frac{\nu}{min_i \left\langle g_i p_{max} \left(\frac{\gamma_i+1}{\gamma_i}\right)\right\rangle} \tag{4.4}$$

4.3.1 Minimum Energy Consumption

The previously derived minimum power vector, i.e equation (4.3), is based on the assumption of arbitrary allocations of γ_i for each mobile host. The optimum feasible allocation of rates (or γ_i) that give a specific throughput (with a maximum aggregate transmission rate $\widetilde{R}$) in the cell will be the

solution of the following joint rate and power control problem of minimizing the sum of powers,

$$\min_{p,\gamma} \quad \sum_{i=1}^{N} p_i$$

$$\text{subject to} \quad \sum_{i=1}^{N} r_i = \widetilde{R} \tag{4.5}$$

$$0 \leq p_i \leq \bar{p}\,, \quad \left(\frac{E_b}{I_0}\right) = \Gamma$$

Using equations (4.2), (4.3) and (4.4) the above problem can be solved in terms of target γ_i as follows (with a maximum aggregate γ_i defined as $\widetilde{\gamma}$),

$$\min_{\gamma} \quad \frac{\nu}{1 - \Sigma_j \frac{\gamma_i}{1+\gamma_i}} \cdot \sum_{i=1}^{N} \frac{\gamma_i}{g_i(1+\gamma_i)}$$

$$\text{subject to} \quad \sum_{i=1}^{N} \gamma_i = \widetilde{\gamma} \tag{4.6}$$

$$\sum_{j=1}^{N} \frac{\gamma_i}{1+\gamma_i} \leq 1 - \frac{\nu}{min_i \left\langle g_i p_{max} \left(\frac{\gamma_i+1}{\gamma_i}\right)\right\rangle}$$

$$\left(\frac{E_b}{I_0}\right) = \Gamma$$

4.3.2 Defining a new Family of Objective Functions

In this section we introduce a new family of objective functions that utilize TCP based information in the sense of RTT and size of the *cwnd* (in segments). The metric of interest is the difference between the required transmission rate of TCP ($R_i^{req.}$) and the actual rate allocation, which is based on channel conditions and interference. We have to emphasize that a further feature of this objective function is that it also reduces RTT variations by tracking the TCP rate. Under this

general framework, the optimization problem can be formulated as follows,

$$\min_p \quad \sum_{i=1}^{N} \left| \frac{1}{RTT_i} \int_0^{RTT_i} [r_i(t) P_s(\Gamma)]\, dt - R_i^{req} \right|$$

$$\text{subject to} \quad 0 \leq p_i \leq \overline{p} \tag{4.7}$$

$$\sum_{i=1}^{N} r_i \leq R_{max}, \quad \left(\frac{E_b}{I_0}\right) = \Gamma$$

where $R_i^{req} = \dfrac{cwnd_i MSS}{RTT_i}$ and $P_s(\Gamma)$ express the probability that a packet is correctly received. Given that the packet size is L bits and the error correction capability of the error correcting code is c, then the probability that a packet is received successfully, under the assumption that the errors in the packet occur independently, would be:

$$P_s(\Gamma) = \sum_{j=0}^{c} \binom{L}{j} P_b^j (1 - P_b)^{L-j}, \tag{4.8}$$

Based on the standard Gaussian approximation, the average bit error probability of the CDMA channel would be given by,

$$P_b = Q\left(\sqrt{\frac{2E_b}{N_0}}\right) \tag{4.9}$$

In a real case scenario the optimization problem can be written in discrete form, where the discrete interval is based on the slot duration Δt,

$$\min_p \quad \sum_{i=1}^{N} \left| r_i(\Delta t) P_s(\Gamma) - \frac{R_i^{req} RTT_i}{m_i} \right|$$

$$\text{subject to} \quad 0 \leq p_i \leq \overline{p} \tag{4.10}$$

$$\sum_{i=1}^{N} r_i \leq R_{max}, \quad \left(\frac{E_b}{I_0}\right) = \Gamma$$

or, by using vector notation,

$$\min_p \quad \frac{WP_s(\Gamma)}{\Gamma} \sum_{i=1}^{N} \left| \frac{\mathbf{e}_i^T \mathbf{p} + \mathbf{d}_i^T I}{\mathbf{f}_i^T \mathbf{p} + \mathbf{h}_i^T \mathbf{I}} \right|$$

$$\text{subject to} \quad 0 \leq p_i \leq \bar{p} \tag{4.11}$$

$$\sum_{i=1}^{N} \frac{g_i p_i}{\Sigma_{j \neq i} g_j p_j + \nu} \leq \Gamma, \quad \left(\frac{E_b}{I_0}\right) = \Gamma$$

where $\mathbf{e}_i^T = [-\dot{c}_i g_1 \; -\dot{c}_i g_2 \cdots g_i \; -\dot{c}_i g_N]$, $\mathbf{d}_i = [0 \cdots -\dot{c}_i \nu \cdots 0]$, $\mathbf{f}_i = [g_1 \cdots 0 \cdots g_N]$, $\mathbf{h}_i = \nu$, with $\dot{c}_i = \frac{R_i^{req} RTT_i}{m_i} \frac{\Gamma}{WP_s(\Gamma)}$, and m_i express the number of slot transmissions in a round trip time interval.

Using (4.2), (4.3) and (4.4) we can also interpret the above optimization problem in terms of SIR target assignment as follows,

$$\min_{\gamma_i} \quad \frac{WP_s(\Gamma)}{\Gamma} \sum_i \left| \frac{\Phi_i}{\sum_j \Phi_j + \nu} - \dot{c}_i \right|$$

$$\text{subject to} \quad \sum_j \frac{\gamma_i}{1+\gamma_i} \leq 1 - \frac{\nu}{min_i \left\langle g_i p_{max} \left(\frac{\gamma_i + 1}{\gamma_i} \right) \right\rangle} \tag{4.12}$$

$$\sum_{i=1}^{N} \gamma_i = \bar{\gamma}, \quad \left(\frac{E_b}{I_0}\right) = \Gamma$$

where $\Phi_i = \dfrac{\nu}{1 - \sum_j \gamma_j/(1-\gamma_j)} \cdot \dfrac{\gamma_i}{1+\gamma_i}$

Proposition 4.3.1. *Assume that* $cwnd_1 \geq cwnd_2 \geq \ldots \geq cwnd_N$ *and* $RTT_1 \leq RTT_2 \leq \ldots \leq RTT_N$. *If there is a feasible set of* γ_i *that satisfy* $\sum_{i=1}^{N} r_i = \widetilde{R}$ *and equation (4.4), then the objective function is minimized when* $\gamma_1^* \geq \gamma_2^* \geq \ldots \geq \gamma_N^*$.

Proof. The objective function of the minimization problem defined in (4.7) can be written as

$$\min \frac{W}{\Gamma} P_s(\Gamma) \sum_i |\gamma_i - a_i| \tag{4.13}$$

where $a_i = \frac{\Gamma}{WP_s(\Gamma)} \cdot \frac{R_i^{req}}{m_i}$ with $R_i^{req} = \frac{cwnd_i MSS}{RTT_i}$ and $m_i = \frac{RTT_i}{\Delta t}$. The values of a_i's are inversely proportional to RTT's and linearly proportional to the size of $cwnd$'s, under the above assumptions on cwnd values and RTT's the following will hold,

$$a_1 \geq a_2 \geq \ldots \geq a_N$$

If with $\boldsymbol{\gamma} = (\gamma_1^*, \gamma_2^*, ..., \gamma_N^*)$ we denote an optimal assignment, then $\forall i, j$ with $i > j$ an assignment with $\hat{\gamma}_i < \hat{\gamma}_j$ would not be optimal because $abs(\hat{\gamma}_i - a_i) + abs(\hat{\gamma}_j - a_j) > abs(\gamma_i^* - a_i) + abs(\gamma_j^* - a_j)$ with $\gamma_i^* \geq \gamma_j^*$. Thus, in order that the objective function 4.13 be minimized, an optimal assignment must have $\gamma_1^* \geq \gamma_2^* \geq \ldots \geq \gamma_N^*$. □

Remark If we further assume that $g_1 \geq g_2 \geq \ldots \geq g_N$, then the above assigned vector $\boldsymbol{\gamma}$ leads also to a minimum transmission power solution (for a proof see [19]). We should stress that the above result represents only one of the possible solutions, because the assumption that has been made regarding the inequalities of the RTT and $cwnd$ is just one from all the possible combinations. As it will become more clear in the sequel, a generalized insight into the problem will be given by considering a multiple objective minimization problem that takes into account 4.7 and the total transmitted power. In this case, the exact trade off between transmission power and required instantaneous rates from TCP will be unfolded by the calculated Pareto front solutions.

4.4 Power and Rate Allocation as a Bi-objective Optimization Problem

Minimum power allocation and satisfaction of the transmission rate required by TCP can be seen as two conflicting objectives. In such multiobjective optimization problem (MOP) there is no longer a single optimal solution but rather a set of possible uncountable equivalent solutions. MOP's with conflicting objective functions give rise to this set of optimal solutions because there is no one that can be considered better than any other with respect to all objective functions. These optimal solutions are called *Pareto solutions*. MOP's require specialized optimization techniques because the objective functions may have different constraints and are in general conflicting. Before discussing

different techniques for solving MOP's, we will first introduce some key definitions in order to ensure consistency.

4.4.1 Pareto Notation

In the following we define the principles of Pareto dominance, Pareto optimality and Pareto front.

Definition. *(**Pareto Dominance**) A variable vector* $\boldsymbol{u} = (u_1, u_2, ..., u_m)$ *is said to dominate* $\boldsymbol{v} = (v_1, v_2, ..., v_m)$ *(denoted by* $\boldsymbol{u} \preceq \boldsymbol{v}$*) if and only if* $\forall\, i \in \{1, ..., n\} : \; f(\boldsymbol{u}) \leq f(\boldsymbol{v}) \;\wedge\; \exists\, j \in \{1, ..., n\} : f(\boldsymbol{u}) < f(\boldsymbol{v})$

Definition. *(**Pareto Optimality**) A solution* $\boldsymbol{p} \in \Omega$ *is said to be Pareto optimal with respect to* Ω *if and only if* $\boldsymbol{p}$ *is non-dominated regarding the whole parameter space* Ω.

Finally, we should also stress the difference between a non-dominated set and a Pareto optimal set. The non-dominated set is defined solely in the context of the sample search space, i.e $\Phi \subseteq \Omega$, that the algorithm under consideration uses. In this specific sample space Φ, solutions that are not dominated by any other solution in the sample space are the non-dominated solutions. The difference is that a Pareto optimal set is a non-dominated set when the sample is the entire search space Ω. The set of objective vectors $\boldsymbol{f}(\boldsymbol{p})$, corresponding to a set of non-dominated parameter vectors in Φ is called the *Pareto optimal front* or *Pareto front.*

4.4.2 Calculating Pareto front solutions

By unfolding the global non-dominated points that form of the Pareto frontier will give a clear idea about the trade-off between the objectives. Optimization methods can generally be divided into gradient (derivative) and non-gradient (non-derivative) methods. There are a large number of non-gradient methods such as genetic algorithms [20], simulated annealing [21] and Tabu search [22] among others. In this study gradient based methods are considered since partial derivatives of the objective functions are accessible. The most classical technique for solving MOP's is by aggregating, with different weights, all the objectives into one overall objective function [34]. The Pareto frontier will be unfolded by repeatedly changing the weighting vector. The disadvantage of the weighted sum method of finding Pareto optimal solutions is that it cannot be used in MOP's that have a

non-convex Pareto optimal frontier. Additionally, there is no guide on how to choose the weighting to ensure an even spread of the Pareto front [24]. In order to remedy the above difficulty the ε-perturbation method is considered. In this method one of the objective functions from the original multiobjective optimization problem is selected to be the single objective function, while the other ones are included as constraints of the single optimization problem. Therefore, the ε-perturbation method transforms the a MOP problem, into the following single objective optimization problem,

$$\begin{aligned} \text{minimize} \quad & f_i(p_1, p_2, ..., p_m) \\ \text{subject to} \quad & g_i(\boldsymbol{p}) \leq 0, \quad i = 1, .., r \\ & f_j(p_1, p_2, ..., p_m) - \varepsilon_j \leq 0, \quad \forall j \neq i \end{aligned} \tag{4.14}$$

The solution of the optimization problem described in 4.14 yields a single point of the Pareto frontier. By varying ε_j over a specific interval of interest, the entire Pareto frontier can be unfolded. Once the Pareto frontier has been generated, a single solution should be selected. The issues of selecting such a solution and defining the corresponding interval of ε_j are discussed in the next section.

4.4.3 Selection from among the Pareto frontier

The critical distinction between the problem of generating the Pareto frontier and the selection of a single point belonging to that set, is that the first problem is objective while the second is subjective. There are numerous methods to manipulate multiple Pareto solutions in a decision-based approach [25]. In this work the most widely adopted method is used which is based on L_ξ norms [26]. The impetus behind this technique is to minimize the distance from the Pareto set to an ideal solution, which is called the utopia point, according to the following formula,

$$\text{minimize} \left[\sum_i (f_i(\boldsymbol{p}) - f_i^*)^\xi \right]^{\frac{1}{\xi}} \tag{4.15}$$

In the following we utilize the L_2 norm ($\xi = 2$) in order to select the optimal compromise solution. Figure 4.3 shows the objective functional space in the case of a bi-objective optimization problem together with the Pareto frontier. The individual optimum for each function is also depicted,

pointing out that optimal performance on any one function implies sub-optimal performance on the other. Whatever solution is chosen it must be a member of the Pareto set since all other solutions give sub-optimal performance in both functions simultaneously. The *utopia point* can be seen as the theoretical optimal performance solution that can be achieved. In this case, the solution is the one from the Pareto frontier which is geometrically closest to the utopia point. The figure shows how the L_2 norm determines the *optimal compromise solution.*

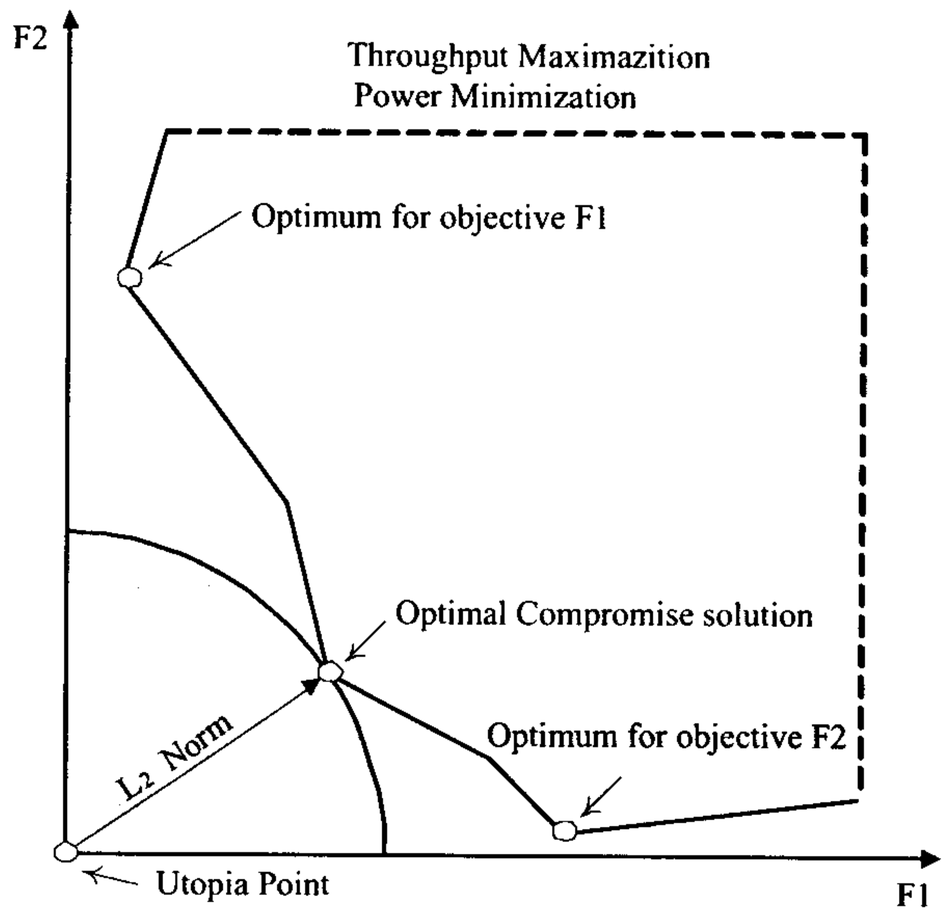

Figure 4.3: Conceptualization of the methodology of selecting a solution from the Pareto front using the L_2 Norm

Let us assume that the y-axis represents the difference between the allocated rate and the required rate from TCP (objective function 4.13) while the x-axis represents the total transmitted power from the mobile users. Then, in the ideal case where the required rates can be accommodated, the ordinate of the utopia point would be equal to zero while the abscissa would be equal to the minimum possible transmitted power by the mobile host, i.e power allocation in the form of a Greedy Rate Packing algorithm for example [19]. The situation where this scenario may occur was discussed in section 6.4.1. The two different grey areas in figure 4.3 depict different resource management strategies. The vertical one represents a solution area where the aim is to minimize the transmitted power, while the horizontal grey area represents power and rate allocation from a throughput maximization point of view.

Under this framework the bi-objective optimization problem that will be numerically solved using the ε-perturbation method can be written as follows,

$$\begin{aligned} \min_p \quad & \frac{WP_s(\Gamma)}{\Gamma} \sum_{i=1}^{N} \left| \frac{\mathbf{e}_i^T \mathbf{p} + \mathbf{d}_i^T I}{\mathbf{f}_i^T \mathbf{p} + \mathbf{h}_i^T \mathbf{I}} \right| \\ \text{subject to} \quad & \sum_{i=1}^{N} p_i - \varepsilon \leq 0 \\ & 0 \leq p_i \leq \overline{p} \\ & \sum_{i=1}^{N} \frac{g_i p_i}{\Sigma_{j \neq i} g_j p_j + \nu} \leq \Gamma, \quad \left(\frac{E_b}{I_0}\right) = \Gamma \end{aligned} \tag{4.16}$$

In the above formulation, the difference between the received transmission rate from the mobile host and the required rate from the TCP layer is used as the single objective function (in relation to figure 4.3, the difference between the actual transmission rate and the required rate from TCP would represent the y-axis). The second objective function, which is the total sum of transmission powers, is used as a constraint with variable ε.

Single objective optimization techniques, i.e power minimization or throughput maximization, do not allow trade off decisions between conflicting objectives, because of non-access of the Pareto frontier. The proposed bi-objective optimization approach, that uses information from the TCP state machine, i.e. being cognizant of required transmission rate, allows us to draw the lines of demarcation for the trade off between transmitted power and rate allocation by exploring the Pareto frontier.

4.5 A Proposed Greedy Algorithm

In this section a greedy algorithm is presented that solves the above optimization problem. In general, solving non-linear constraint optimization problems with iterative techniques has the drawback of heavy computation complexity and convergence rate. From this point of view, gradient based numerical methods with accessibility on the partial derivatives of the objective function (such as the

Augmented Lagrangian method for example) have rather a theoretical approach to finding optimum solutions rather than being candidates for real implementation. The greedy algorithm discussed in

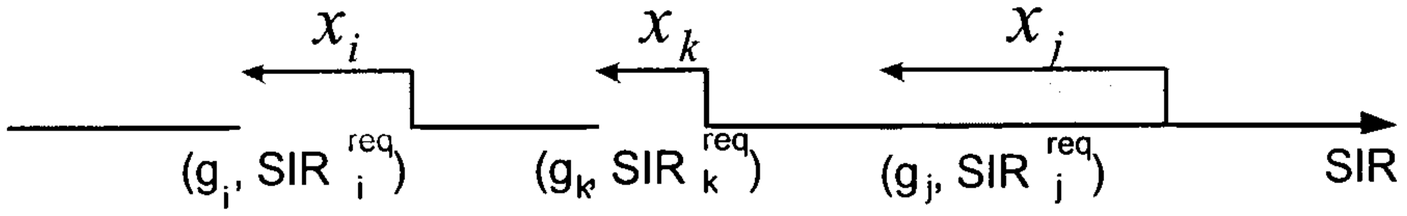

Figure 4.4: Allocation of SIR's (γ) based on the reduction vector $\mathbf{x}$

the sequel, even though it provides suboptimum solutions has the advantage of linear, i.e. $O(N)$, computational complexity. The algorithm is based on the introduced reduction vector $\mathbf{x}$, which allocates SIR values to different TCP flows based on channel conditions and the required rate as graphically shown in figure 4.4. In this case the reduction vector $\mathbf{x}$ will specify the distance between the final allocated SIR and the one required ($SIR^{req\cdot}$), based on channel conditions. In the sequel and before defining the greedy algorithm, auxiliary information which gives insight into the allocation problem is discussed.

Proposition 4.5.1. *Let us assume that*

$$g_1\left\{(\gamma_1^{req}-\psi)^2-\omega(\gamma_1^{req}-\psi)\right\}\geq g_2\left\{\gamma_2^{req}-\psi)^2-\omega(\gamma_2^{req}-\psi)\right\}\geq\ldots \tag{4.17}$$
$$\ldots\geq g_N\left\{\gamma_N^{req}-\psi)^2-\omega(\gamma_N^{req}-\psi)\right\}$$

Then, under a feasible target assignment, the total transmitted power is minimized by assigning the reduction vector $\mathbf{x}$ *such that,* $x_1\leq x_2\leq\ldots\leq x_N$

Proof. Among the feasible reassignments, let us assume there exists an assignment that minimizes the objective function but does not satisfy,

$$x_1\leq x_2\leq\ldots\leq x_N$$

We can find at least one pair of a and b ($1\leq a\leq b\leq N$) such that $x_a>x_b$ ($x_a=x_b+\omega$, with

$\omega \epsilon \mathbb{R}_+$), and compare this assumed optimal assignment as follows,

$$\frac{\gamma_a^{req} - x_a}{g_a(1+\gamma_a^{req} - x_a)} + \frac{\gamma_b^{req} - x_b}{g_b(1+\gamma_b^{req} - x_b)} - \frac{\gamma_a^{req} - x_b}{g_a(1+\gamma_a^{req} - x_b)} -$$

$$- \frac{\gamma_b^{req} - x_a}{g_b(1+\gamma_b^{req} - x_a)} = \frac{\omega(\gamma_a^{req} - x_b)}{g_a(1+\gamma_a^{req} - x_b - \omega)(1+\gamma_a^{req} - x_b)} -$$

$$- \frac{\omega(\gamma_b^{req} - x_b)}{g_b(1+\gamma_b^{req} - x_b - \omega)(1+\gamma_b^{req} - x_b)} + \frac{\omega}{g_b(1+\gamma_b^{req} - x_b - \omega)} -$$

$$- \frac{\omega}{g_a(1+\gamma_a^{req} - x_b - \omega)} = \frac{\omega}{g_b(1+\gamma_b^{req} - x_b - \omega)(1+\gamma_b^{req} - x_b)} -$$

$$- \frac{\omega}{g_a(1+\gamma_a^{req} - x_b - \omega)(1+\gamma_a^{req} - x_b)} =$$

$$\frac{\omega}{g_b\left\{(\gamma_b^{req} - \psi)^2 - \omega(\gamma_b^{req} - \psi)\right\}} - \frac{\omega}{g_a\left\{(\gamma_a^{req} - \psi)^2 - \omega(\gamma_a^{req} - \psi)\right\}} \geq 0$$

with $\psi = x_b - 1$

□

Proposition 4.5.2. *Among the feasible target assignments that result in throughput $R^* = K_1 \cdot \gamma^*$ and having minimum aggregate distance from the required TCP rates, the one from TCP-aware Rate Packing requires the minimum transmission power.*

Proof. Based on proposition (4.5.1) the optimum allocation of reduction factors will be $x_1^* \leq x_2^* \leq \ldots \leq x_N^*$. Assume a new feasible target allocation (where $1 \leq a < b \leq N$):

$$(\hat{x_1}, \hat{x_2}, \ldots, \hat{x_N}) = (x_1^*, \ldots, x_a^* + \Delta, \ldots, x_b^* - \Delta, \ldots, x_N^*)$$

The new reduction vector $\hat{\mathbf{x}}$ will give the same throughput with the reduction vector $\mathbf{x}^*$,independently of where the Δ-shift operates. We have to show that the reduction vector $\hat{\mathbf{x}}$ (i.e., the Δ-shift reduction vector $\mathbf{x}^*$) requires more power than the one given by the TCP-aware power and rate allocation. This will be done by comparing the assumed optimal assignment,

$$\frac{\gamma_a^{req} - \hat{x_a}}{g_a(1+\gamma_a^{req} - \hat{x_a})} + \frac{\gamma_b^{req} - \hat{x_b}}{g_b(1+\gamma_b^{req} - \hat{x_b})} \tag{4.18}$$

with the one given by TCP-aware RP,

$$\frac{\gamma_a^{req} - x_a^*}{g_a(1 + \gamma_a^{req} - x_a^*)} + \frac{\gamma_b^{req} - x_b^*}{g_b(1 + \gamma_b^{req} - x_b^*)} \tag{4.19}$$

Therefore, (4.18)-(4.19) will have the form (in the sequel we assume $x_i^* = x_i$)

$$\left[\frac{\gamma_a^{req} - x_a^* - \Delta}{g_a(1 + \gamma_a^{req} - x_a^* - \Delta)} + \frac{\gamma_b^{req} - x_b^* + \Delta}{g_b(1 + \gamma_b^{req} - x_b^* + \Delta)}\right] -$$

$$\left[\frac{\gamma_a^{req} - x_a^*}{g_a(1 + \gamma_a^{req} - x_a^*)} + \frac{\gamma_b^{req} - x_b^*}{g_b(1 + \gamma_b^{req} - x_b^*)}\right] =$$

$$\left[\frac{\gamma_a^{req} - x_a^*}{g_a(1 + \gamma_a^{req} - x_a^* - \Delta)} - \frac{\gamma_a^{req} - x_a^*}{g_a(1 + \gamma_a^{req} - x_a^*)}\right] +$$

$$\left[\frac{\gamma_b^{req} - x_b^*}{g_b(1 + \gamma_b^{req} - x_b^* + \Delta)} - \frac{\gamma_b^{req} - x_b^*}{g_b(1 + \gamma_b^{req} - x_b^*)}\right] +$$

$$\Delta \cdot \left[\frac{1}{g_b(1 + \gamma_b^{req} - x_b^* + \Delta)} - \frac{1}{g_a(1 + \gamma_a^{req} - x_a^* - \Delta)}\right] =$$

$$\frac{\Delta}{g_b(1 + \gamma_b^{req} - x_b^* + \Delta)(1 + \gamma_b^{req} - x_b^*)} -$$

$$\frac{\Delta}{g_a(1 + \gamma_a^{req} - x_a^* - \Delta)(1 + \gamma_a^{req} - x_a^*)} \geq 0$$

because from proposition (4.5.1),

$$g_a(1 + \gamma_a^{req} - x_a^* - \Delta)(1 + \gamma_a^{req} - x_a^*) \geq g_b(1 + \gamma_b^{req} - x_b^* + \Delta)(1 + \gamma_b^{req} - x_b^*)$$

when $0 \leq \Delta \leq \frac{x_b^* + x_a^*}{2}$

□

Based on the above results the greedy algorithm for the uplink will have the form:

Algorithm 4.5.1: GREEDY ALLOCATION(a)

comment: Initialization

for $i \leftarrow 1$ **to** N

$$\textbf{do} \begin{cases} \gamma_i \leftarrow 0 \\ x_i \leftarrow 0 \\ \gamma_i^{req.} \leftarrow \dfrac{cwnd_i MSS}{RTT_i} \cdot \dfrac{W}{\Gamma} \\ \textbf{comment:} \text{ Sort based on } \gamma_i^{req.} \text{ and } g_i \text{ using (4.17)} \end{cases}$$

comment: Main

$i \leftarrow 1$

$$\textbf{while } \left(\sum_{j=1}^{i} \frac{\gamma_j}{1+\gamma_j} \leq 1 \right) \&(i \leq N)$$

$$\textbf{do} \begin{cases} x_i = a_i \cdot \gamma^{min} \\ \textbf{if } \gamma_i^{req} > x_1 \\ \quad \textbf{then} \begin{cases} \gamma_i = \gamma_i^{req} - x_i \\ i \leftarrow i+1 \end{cases} \\ \quad \textbf{else} \begin{cases} \gamma_i = \gamma_i^{req} \\ i \leftarrow i+1 \end{cases} \end{cases}$$

final

4.6 Relaxation of the bit-energy-to-interference-density ratio

The previous discussion was based on the assumption of a constant E_b/N_o, so that the ratio between SIR's and rates was constant. In this section we relax that condition and seek to adaptively allocate $\varphi_i = (E_b/N_o)_i$ to different flows based on the state of the TCP flows. Even though, eliminating

timeout events in an error prone environment is not possible, rather the algorithm seeks to minimize/avoid retransmission time outs (RTO) events caused by the lack of sufficient duplicate ACK's by allocating more resources to *sensitive* flows. In that respect, the resource allocation strategy will also be a function of the size of the cwnd of different flows. To consider one supporting example, assume two TCP flows with $cwnd_1 = 3$, $cwnd_2 = 10$ and $RTT_1 = RTT_2 = 5$msec that share a constant aggregate $\tilde{\gamma}$ allocation ($\gamma_1 + \gamma_2 = \tilde{\gamma}$). In the traditional approach the SIR budget would be equally distributed among the TCP flows, in other words, $\gamma_1 = \gamma_2 = \tilde{\gamma}/2$. Assuming a non fading additive white Gaussian noise channel and equal TCP segment sizes, this allocation will result both in the same bit error rate and probability of successful packet transmission performance between the two flows. In this case, even though the performance as seen from the link layer perspective is identical, the consequences on the transport layer are dramatically different. A packet in error for the first flow will automatically mean retransmission through a retransmission time out (RTO) event (because of the lack of sufficient duplicate ACKs) which means that a delay of 500msec will be introduced (most TCP implementations set RTO in multiples of 100, 200 or 500msec in order to avoid spurious timeouts). On the other hand, a single packet in error on the second flow will be restored inside one RTT interval, i.e. 5 msec, as there are sufficient duplicate packets. An non-uniform allocation of SIR, i.e $\gamma_1 = \tilde{\gamma}/2 + \Delta, \gamma_2 = \tilde{\gamma}/2 - \Delta$ which can protect the first flow will result in 100 times overall increased performance of the system.

Let $Q(cwnd, p)$ represent the probability of timeout event which is a function of the cwnd size and packet error rate. In [27], it has been shown that this probability is given by:

$$Q(cwnd, p) = \frac{(1-(1-p)^3)(1+(1-p)^3(1-(1-p)^{cwnd-3}))}{1-(1-p)^{cwnd}} \tag{4.20}$$

The packet error rate can be written as a function of the E_b/N_o, as shown in equation (4.9), so in general the probability of a time-out event will be a non-linear function of the size of the cwnd and the E_b/N_o. The probability $Q(\cdot)$: $\mathbb{R}_+ \rightarrow [0, 1]$ is a differentiable, monotonously decreasing function of the φ_i's ($\partial Q_i/\partial \varphi_i < 0$) that depends on factors such as modulation/demodulation technique, interleaving depth and channel coding scheme. In that case, if we assume that $cwnd_1 \leq cwnd_2 \leq \ldots \leq cwnd_N$ then $Q(cwnd_1, \varphi) \geq Q(cwnd_2, \varphi) \geq \ldots \geq Q(cwnd_n, \varphi)$. It can also be shown that

(using L'Hopital's rule):

$$\lim_{\varphi \to \infty} Q(cwnd, \varphi) = \frac{3}{cwnd}, \quad \lim_{\varphi \to 0} Q(cwnd, \varphi) = 1$$

From the above results it is easy to show that [1]

$$\left| \frac{\partial Q(cwnd_i, \varphi)}{\partial \varphi} \right| \leq \left| \frac{\partial Q(cwnd_j, \varphi)}{\partial \varphi} \right|, \forall i, j \text{ with } cwnd_i \leq cwnd_j \tag{4.21}$$

In the sequel we prove that a non-uniform allocation of bit-energy-to-interference-density ratio results in a decreased aggregate probability of a time-out event of the TCP flows compared with a uniform, constant allocation of E_b/N_os.

Proposition 4.6.1. *Let us assume that* $cwnd_1 \leq cwnd_2 \leq \ldots \leq cwnd_N$. *Among the feasible assignments, and under the constraint of* $\sum_i \varphi_i = N \cdot \varphi_0$, *there is a non-uniform allocation of* $\varphi_i's$ *that results in reduced aggregate probability of time-out events compared with a uniform allocation* $\varphi_0 : \forall\, \varphi_0 \,\epsilon\, [0, \infty)$

Proof. Among the feasible reassignments, we can find at least one pair of i and j such that $1 \leq i \leq j \leq N$ and allocated E_b/N_os, $\varphi_i \geq \varphi_0 \geq \varphi_j$. We will define $\varphi_i = \varphi_0 + \Delta\varphi$ and $\varphi_j = \varphi_0 - \Delta\varphi$ where $\Delta \,\epsilon\, \mathbb{R}_+$ Now, we will compare the aggregate probability of time-out event in the case of constant and non-uniform allocation,

$$[Q(cwnd_i, \varphi_0) + Q(cwnd_j, \varphi_0)] - [Q(cwnd_i, \varphi_i) + Q(cwnd_j, \varphi_j)] =$$

$$[Q(cwnd_i, \varphi_0) - Q(cwnd_i, \varphi_i)] + [Q(cwnd_j, \varphi_0) - Q(cwnd_j, \varphi_j)] =$$

$$\left[\frac{Q(cwnd_j, \varphi_0) - Q(cwnd_j, \varphi_0 - \Delta\varphi)}{\Delta\varphi}\right] -$$

$$\left[\frac{Q(cwnd_i, \varphi_0 + \Delta\varphi) - Q(cwnd_i, \varphi)}{\Delta\varphi_0}\right]$$

[1] This follows from the fact the function $Q(.)$ is monotonously decreasing and

a. $\left| \frac{\partial Q(cwnd_1, \varphi)}{\partial \varphi} |^{0+} \right| \leq \left| \frac{\partial Q(cwnd_2, \varphi)}{\partial \varphi} |^{0+} \right| \leq \ldots \leq \left| \frac{\partial Q(cwnd_N, \varphi)}{\partial \varphi} |^{0+} \right|$

b. $\left| \frac{\partial Q(cwnd_1, \varphi)}{\partial \varphi} |^{\infty} \right| = \left| \frac{\partial Q(cwnd_2, \varphi)}{\partial \varphi} |^{\infty} \right| = \ldots = \left| \frac{\partial Q(cwnd_N, \varphi)}{\partial \varphi} |^{\infty} \right| = 0$

If we substitute $\omega = \varphi_0 - \Delta\varphi$ and take the limit as $\Delta\varphi$ goes to zero we have,

$$\lim_{\Delta\varphi \to 0} \left[\frac{Q(cwnd_j, \omega + \Delta\varphi) - Q(cwnd_j, \omega)}{\Delta\varphi} \right] -$$

$$\lim_{\Delta\varphi \to 0} \left[\frac{Q(cwnd_i, \varphi_0 + \Delta\varphi) - Q(cwnd_i, \varphi_0)}{\Delta\varphi} \right]$$

Taking the absolute value on the above substraction, we finally have,

$$\left| \frac{\partial Q_j}{\partial \varphi}|^{\omega} - \frac{\partial Q_i}{\partial \varphi}|^{\varphi_0} \right| \geq 0$$

because

$$\left| \frac{\partial Q_j}{\partial \varphi}|^{\omega} \right| \geq \left| \frac{\partial Q_j}{\partial \varphi}|^{\varphi_0} \right| \geq \left| \frac{\partial Q_i}{\partial \varphi}|^{\varphi_0} \right|$$

which follows from equation (4.21) □

Even though the above result shows that a non-uniform allocation of E_b/N_os can increase the system performance, it does not depict the way that such an allocation should be performed. In the sequel we discuss an optimum means of allocation that minimizes the aggregate probability of time-out events.

4.6.1 Polynomial Approximation and Calculation of E_b/N_0

The proposed non uniform allocation of E_b/N_o values is based on the minimization of the aggregate probability of time out events as given by equation (4.20). In order to avoid complex non-linear optimization procedures, the probability of time out events has been modelled using a second degree polynomial inside a specific interval of interest. This leads us to the very well known problem of quadratic optimization. In figure 4.5 the residual error is depicted, within a realistic packet error rate of up to 20%, when a second degree polynomial is used to approximate function 4.20.

Using a second degree polynomial with coefficients a_2^i, a_1^i, a_0^i the corresponding optimization

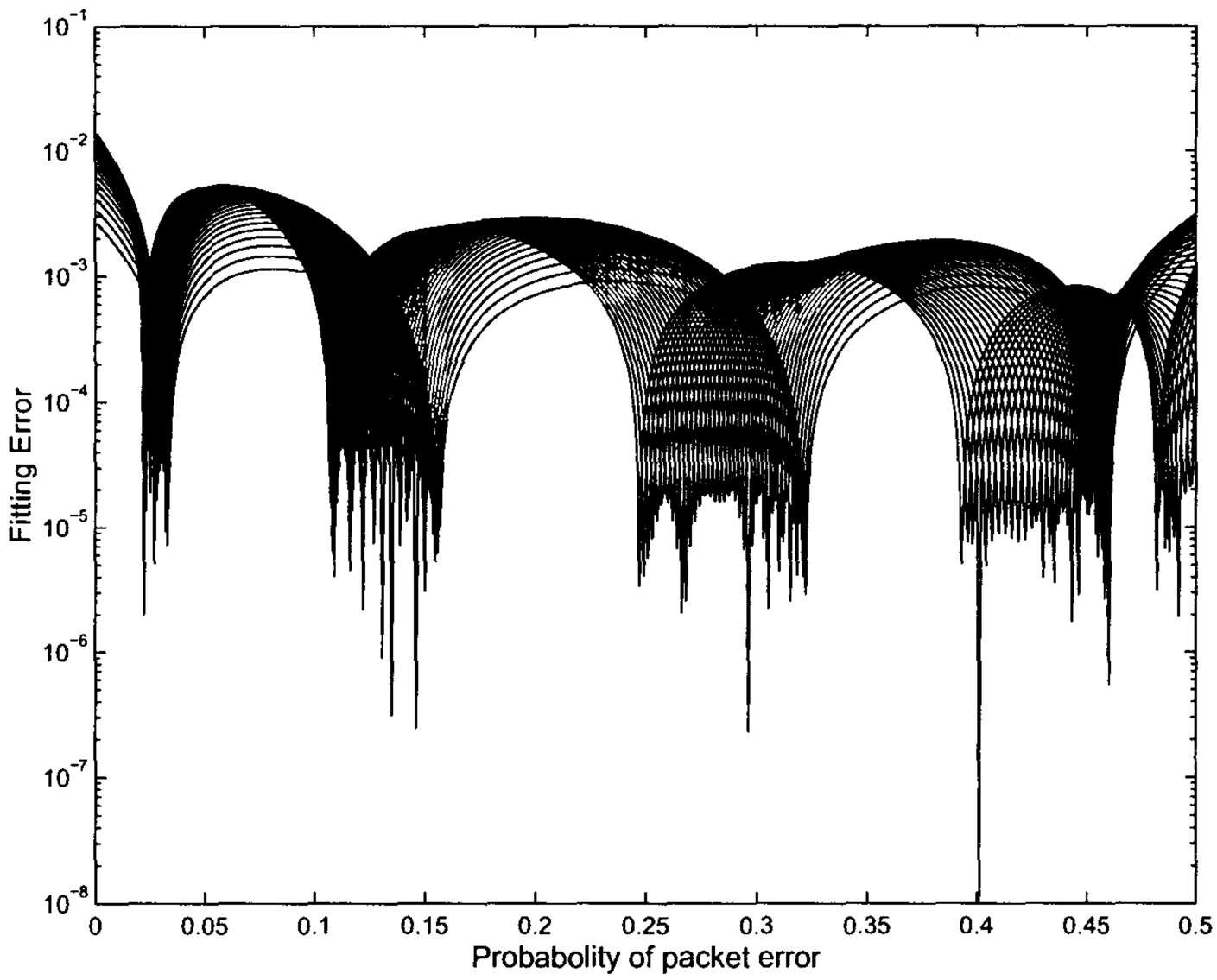

Figure 4.5: The fitting error of approximating function (4.20) with a second degree polynomial

problem in this case will have the form:

$$\begin{aligned} \min \quad & c^T\varphi + \tfrac{1}{2}\varphi^T P\varphi \\ \text{s.t} \quad & A\varphi = b, \\ & \varphi \geq 0 \end{aligned} \tag{4.22}$$

$$\begin{aligned} \nabla_\varphi L(\varphi,\beta) &= c + P\varphi + A^T\beta \\ \nabla_\beta L(\varphi,\beta) &= A\varphi - b = 0 \end{aligned} \tag{4.23}$$

The optimal solution (in matrix form) is obtained by:

$$\begin{pmatrix} \varphi^* \\ \beta^* \end{pmatrix} = \begin{pmatrix} P & A^T \\ A & 0 \end{pmatrix}^{-1} \begin{pmatrix} -c \\ b \end{pmatrix} \tag{4.24}$$

where

$$P = \begin{bmatrix} \frac{1}{2}a_2^1 & 0 & \dots & 0 & 0 \\ 0 & \frac{1}{2}a_2^2 & \dots & 0 & 0 \\ \dots & \dots & \dots & \dots & \dots \\ 0 & 0 & \dots & \frac{1}{2}a_2^{N-1} & 0 \\ 0 & 0 & \dots & 0 & \frac{1}{2}a_2^N \end{bmatrix}$$

$A = \underbrace{\begin{bmatrix} 1 & 1 & \dots & 1 \end{bmatrix}}_{N}$, $c = \begin{bmatrix} a_1^1 & a_1^2 & \dots & a_1^N \end{bmatrix}$, $b = 1$

The optimization problem reduces to the solution of the following linear system of equations:

$$\begin{cases} a_2^1\varphi_1 + a_1^1 = \beta \\ a_2^2\varphi_1 + a_1^2 = \beta \\ \dots \quad \dots \quad \dots \\ a_2^N\varphi_N + a_1^N = \beta \\ \varphi_1 + \varphi_2 + .. + \varphi_N = b \end{cases} \tag{4.25}$$

The calculated φ_i's in this case will have a closed form solution, which is given by the following equation:

$$\varphi_i = \frac{1}{a_2^i} \cdot \frac{b\prod_{j=1}^{N} a_2^j + \sum_{i=1}^{N} a_1^i \prod_{j=1, j\neq i}^{N} a_2^j}{\sum_{i=1}^{N} \prod_{j=1, j\neq i}^{N} a_2^j} - \frac{a_1^i}{a_2^i} \tag{4.26}$$

We should note at this point that this differential treatment of TCP packets can be the meeting ground of different other renewals that are not discussed here. For example, SYN packets can be strongly protected because a loss of such a packet will result in 6sec delay (a constant value for most TCP implementations)

4.7 Numerical Investigations

In this section the proposed scheme is evaluated, which shows how the bi-objective formulation of the problem can be seen as a unified methodology of the approaches based on minimum power and throughput maximization. We consider a single cell (implications of multiple cells can be taken into account by the so called out-of-cell interference coefficient) with only TCP based traffic. The mobile

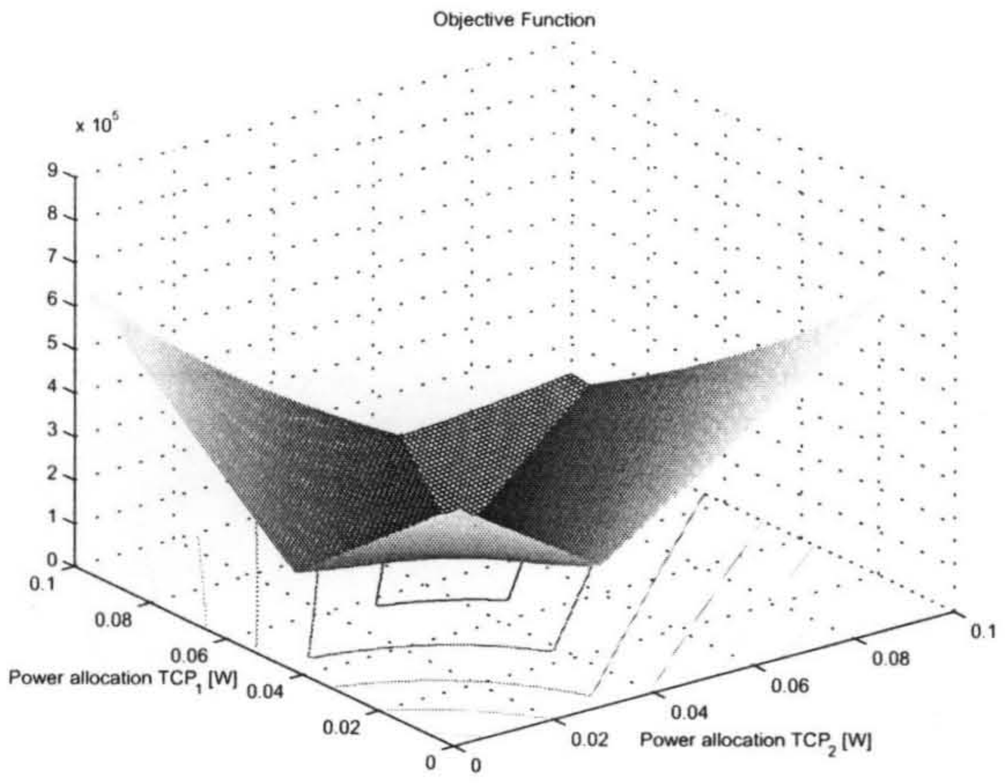

(a)

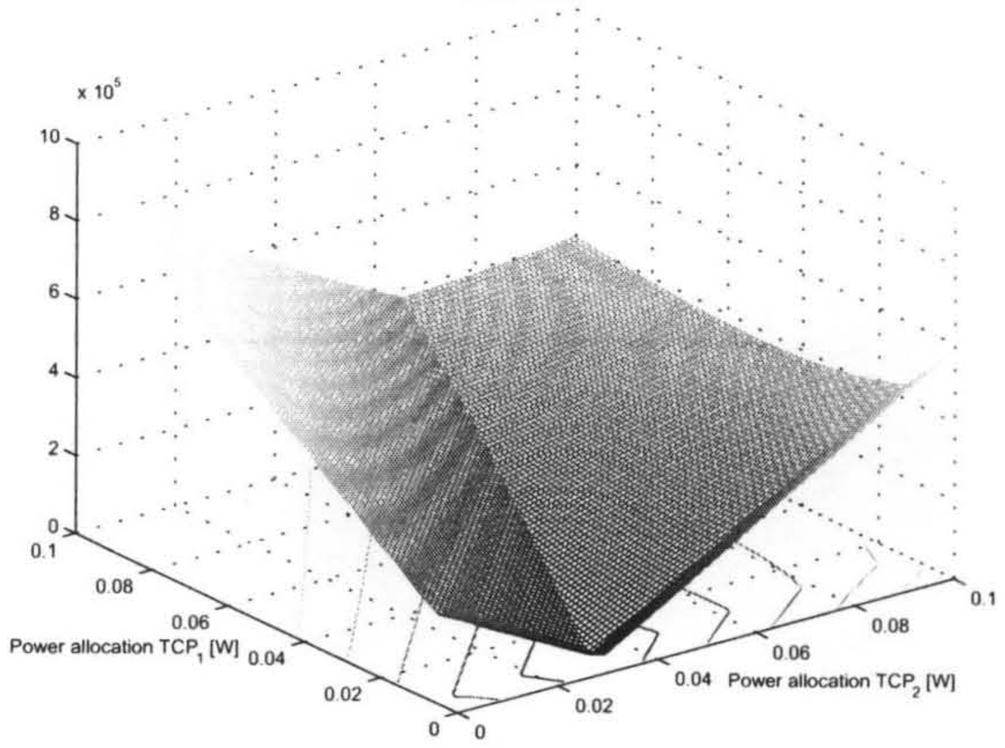

(b)

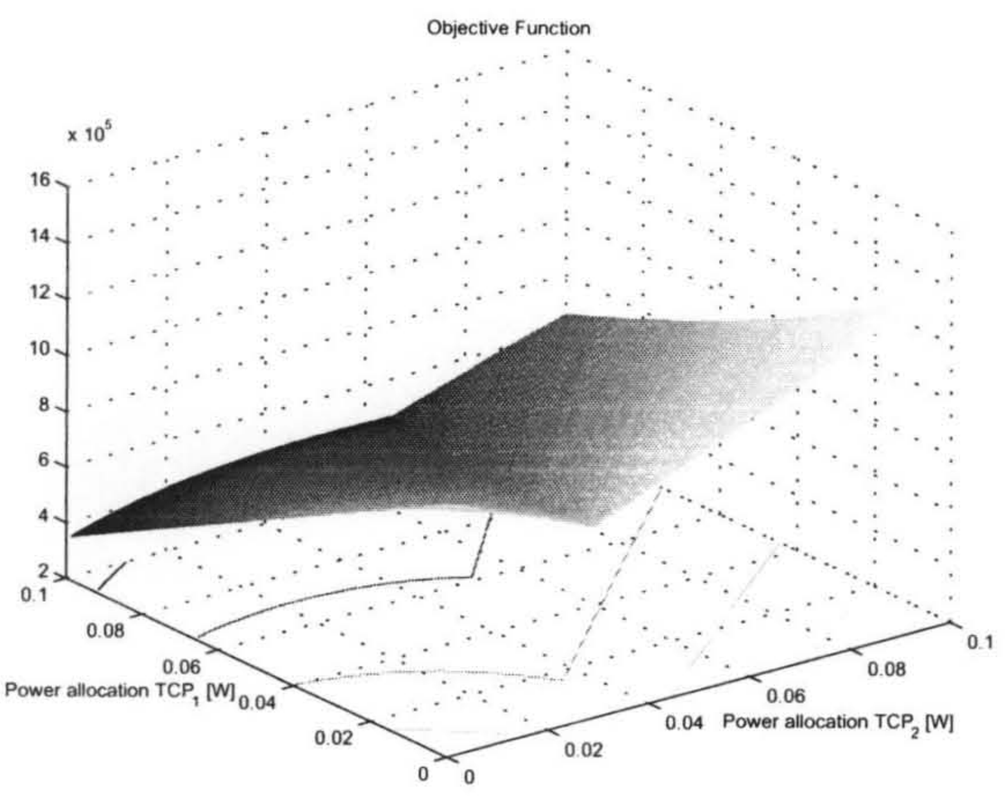

(c)

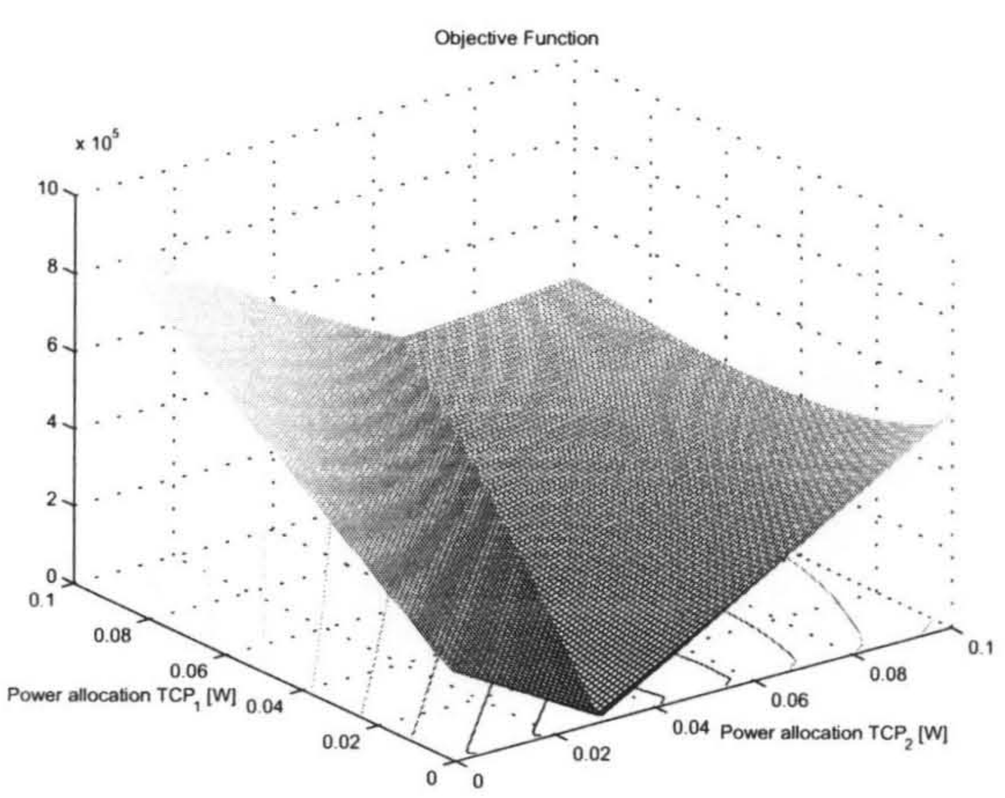

(d)

Figure 4.6: Shape of the objective function in the case of two TCP flows when (a) $cwnd_1 = 32$ - $cwnd_2 = 22$ and equal RTT's and link gains, (b) $cwnd_1 = 4$ - $cwnd_2 = 22$ and equal RTT's and link gains, (c) $RTT_1 = 80ms$ - $RTT_2 = 160ms$ and equal cwnds and link gains, (d) $RTT_1 = 300ms$ - $RTT_2 = 80ms$ and equal cwnds and link gains.

hosts are uniformly distributed and the link gain is modelled as a distance dependent path loss of fourth power while the shadow fading factor is generated from a log normal distribution of zero mean and 8dB standard deviation. The maximum transmitted power of each mobile host is 0.1W and the access point receiver noise power ν is set to be 10^{-12}W. We consider the uplink of the system with a chip rate of W=3.84Mcps, assume that the radio link can support continuous transmission rates, the target E_b/I_0=8 dB and a MSS equal to 200 bytes.

Figure 4.6 depicts how the shape of the objective function defined in equation (4.11) is influenced by TCP parameters for the case of two active TCP-Reno flows. More specifically, in figure 4.6(a)-(b) the effect of the cwnd size on the shape of the objective function is shown. The size of the cwnd plays an important role in how the minimum power point moves around the xy-plane. It can be seen that as the cwnd of the first TCP flow decreases the required power allocation also decreases and this results in a shift of the minimum of the objective function. Figure 4.6(c)-(d) on the other hand shows the effect of the estimated RTT on the shape of the objective function. The figure shows that when the link gains and cwnd sizes remains constant, an increase of the RTT has a net effect of decreasing of the required power for that flow. Thus, as expected, the estimated RTT and the size of the cwnd can be seen as two reciprocal parameters concerning the influence they have on where the minimum of the objective function will lie on the xy-plane.

As indicated in the previous section, the generation of the Pareto front ends the mathematical phase of the multiobjective optimization problem. Thus, whilst the selection of the preferred solution from among the equivalent optimal points can be based on different metaheuristics, we have selected in this case the Euclidean distance from the utopia point. In order to select the solution with the minimum Euclidean distance from the utopia point we need first to perform a polynomial description of the Pareto front. The utopia point where the objective functions reach their theoretical absolute minimum has been chosen to be at (0,0). Fitting a polynomial allows efficient access to the shape of the Pareto front. Figure 4.7 (a) shows the selected point (rectangular box) based on the L_2 norm after fitting the Pareto front with a third order polynomial via least-squares criteria. Figure 4.7 (b) shows the calculated normalized Euclidean distance for all points consisting the Pareto front.

Figure 4.8 depicts the calculated Pareto front in the case of five active TCP flows where the

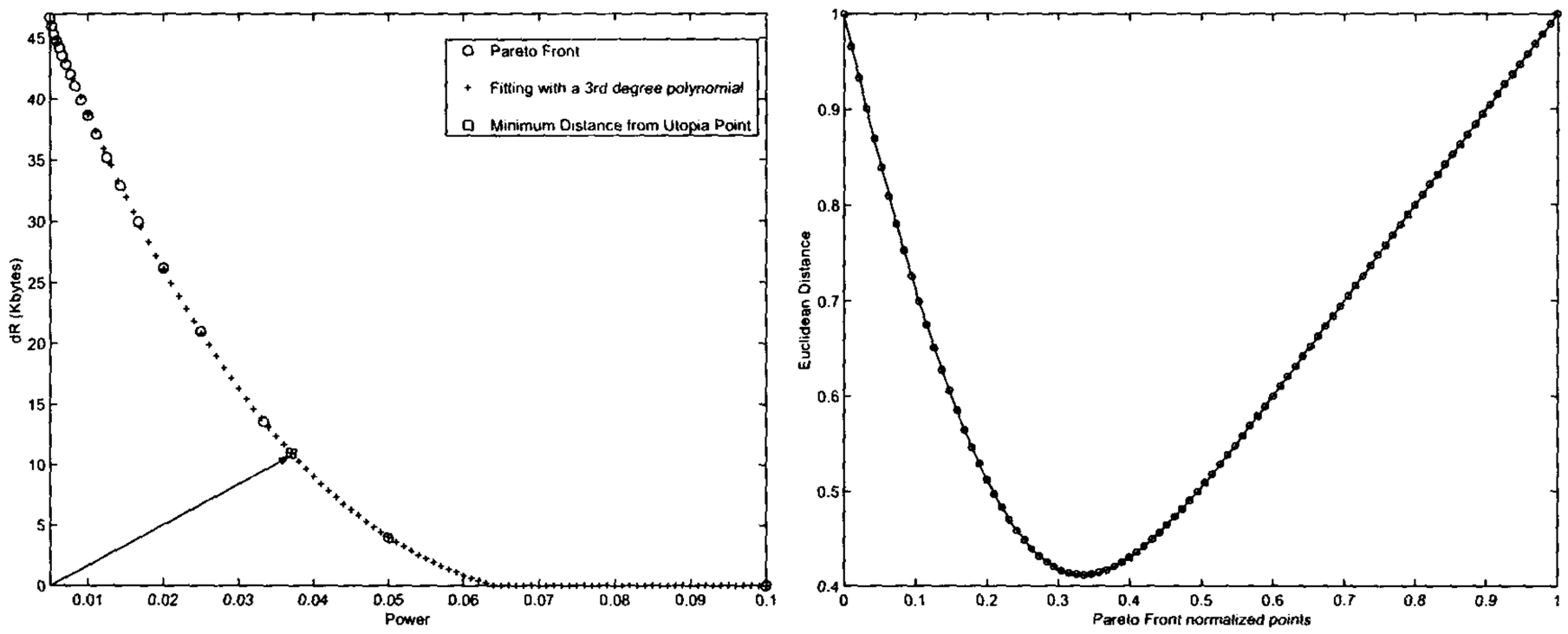

(a) (b)

Figure 4.7: (a) The point with the minimum L_2 norm for the specific shape of the Pareto front, shown with an arrow starting from the utopia point, (b) The L_2 norm for all Pareto front points

three curves represent different characteristics of the flows in the sense of cwnd sizes, RTT's and link gains. The y-axis represent the difference between the allocated rate and the required rate from the TCP and is denoted as dR, while the x-axis denotes the aggregate transmission power. As can be seen from the figure, independently from the parameterization of the TCP flows each curve shows the same behavior; while one objective function improves the other one worsens simultaneously. As expected this depicts the typical characteristics of a Pareto front. Finally, figure 4.9 reveals one of the drawbacks of the ε-constraint method, namely the non even spread sampling of the Pareto front. In this case as mentioned in section 4.4.2 advanced local search techniques can be employed in order to achieve a more even distribution of the solutions consisting the Pareto frontier; although this issue has not been addressed in this chapter. It is important to note that a basic assumption behind the proposed power and rate adaptation scheme that utilizes TCP based information as defined previously, is that the decisions are centralized and based on single cell information. The proposed algorithm can be extended to a multi-cell scenario and implemented in a centralized or decentralized fashion by taking into account technical specifications of 3G systems [27]. The centralized controller lacks scalability because of the requirement for extensive control signalling in the network but it is of

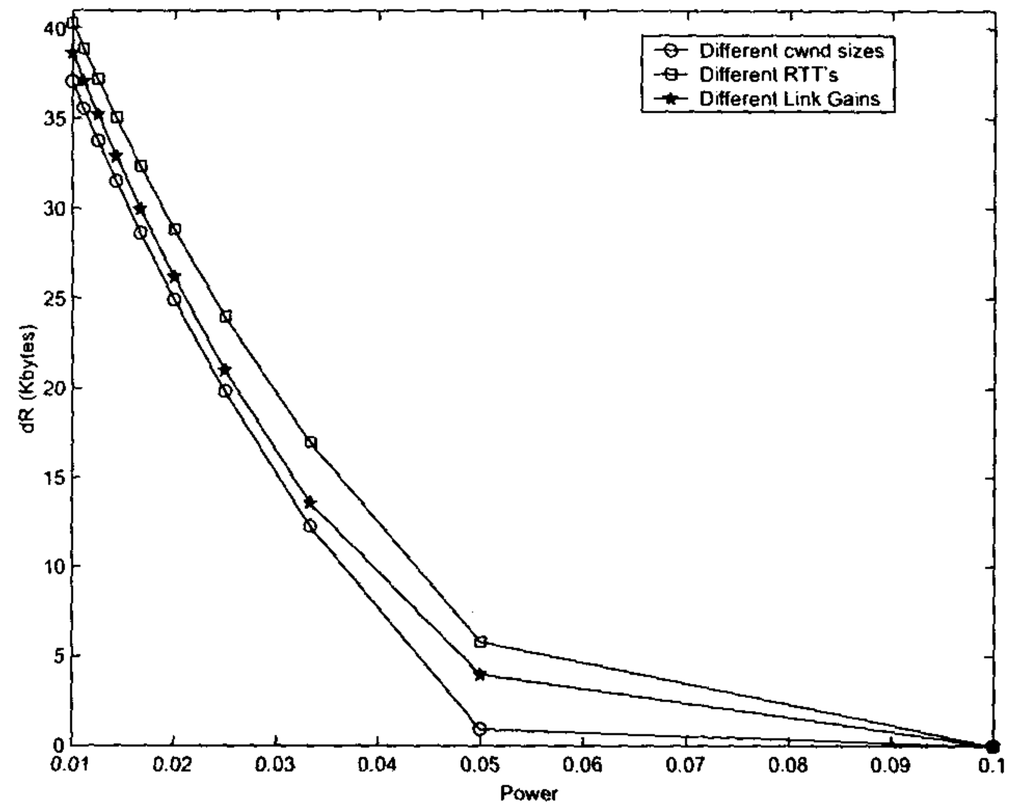

Figure 4.8: Pareto front shape for 5 TCP flows

high importance since it gives the performance bounds of any possible distributed implementation. As opposed to centralized power control, distributed schemes are able to adjust the power levels iteratively using only local measurements. The aim of the numerical investigations of the proposed scheme using a centralized scheme was to provide theoretical limits on the performance, where convergence rate and stability of decentralized algorithms is not an issue. For the case of the greedy algorithm we have also implemented and compared the proposed scheme with the Greedy Rate Packing (GRP) algorithm as proposed in [19]. In GRP the maximum feasible rates are sequentially allocated to flows based on their link gains starting with the flow which has the highest gain. In figure 4.10 the difference between the allocated rate for different TCP flows and the required rate is depicted as a function of different levels of interference in the uplink, i.e., equation (4.7), which can be seen as the main constraint of the system. In this case the interference of the system is increased by holding constant the active TCP flows and increasing their average cwnd size. As can be seen from this figure, when the resource usage in the uplink is increased the absolute difference between the allocated and required rate of the TCP flows is also increased. There is a rapid increase (close to the limit which is less than 1) as there is an upper threshold on the maximum allowed transmission power. Figure 4.11 (a) and 4.11 (b) depict two different snapshots of the allocated rates when the joint power and rate allocation problem as defined in equation (4.11) with inequality constraints is

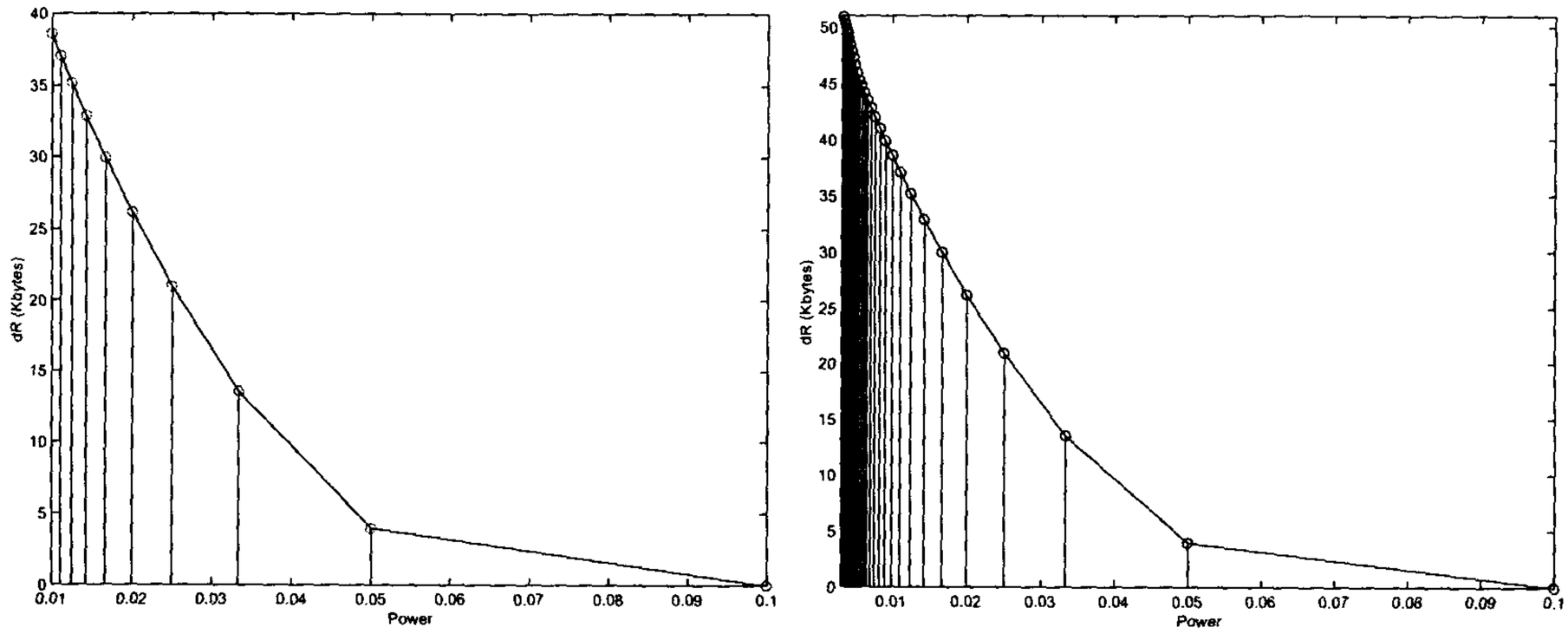

Figure 4.9: The problem of non-uniform distribution of the Pareto front using the ε-constraint method. The right (a) and left (b) figures represent 30 and 10 uniformly distributed samples respectively, from the objective function used as a constraint.

solved using the Sequential Quadratic Programming (SQP) method. An interesting observation is that under an optimum solution it is possible that some flows will be allocated zero transmission rate, which from a system point of view is not desirable.

Figure 4.12 shows the allocation of SIR values to different TCP flows under two different greedy algorithms, i.e., the Greedy Rate Packing and the TCP-aware power and rate adaptation. The figure also shows the required SIR values from the transport layer that can be compared with the allocated values from the two greedy algorithms. The required aggregate SIR in this scenario is 1.29 (greater than one) and the allocated values are less than that required, which in the case of the TCP-aware greedy algorithm are allocated in such way that closely follows the required values, i.e. the required rate. In the case of the Greedy Rate Packing algorithm, as can be seen from the figure, the SIR values are allocated independently of the required rate of each TCP flow and the allocation is only based on channel conditions.

Figure 4.13 (a) shows the theoretical probability of a time out event as given by equation (4.20) which is used to adaptively allocate E_b/I_o values. Based on this different sensitivity to time out events depending on the size of the cwnd, figure 4.13(b) shows how the proposed algorithm differentially

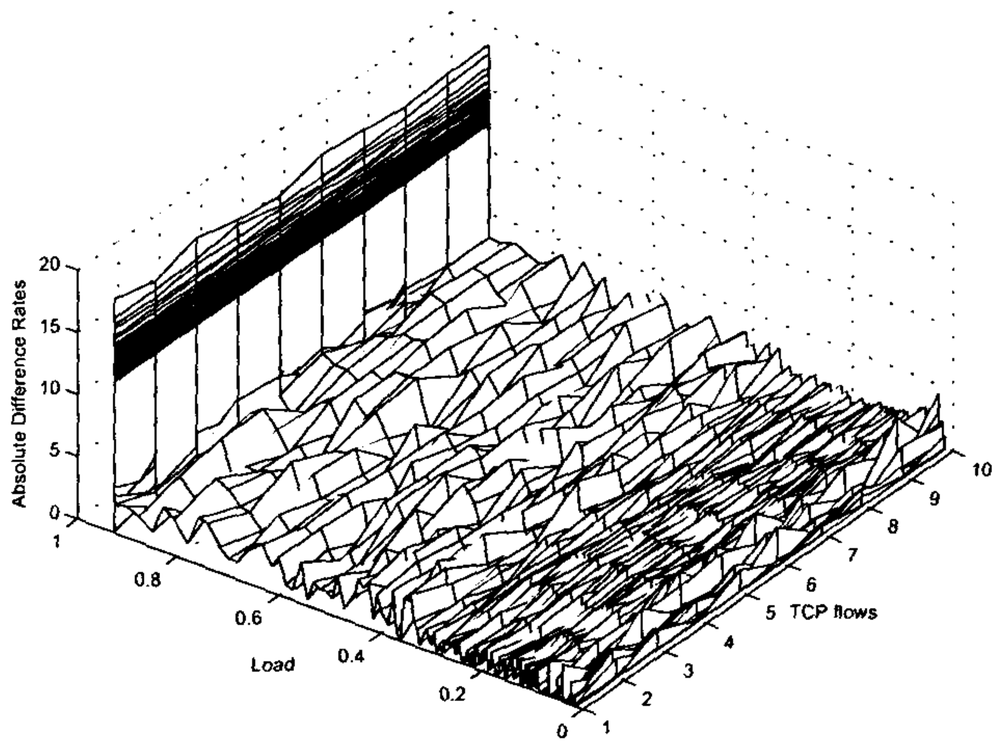

Figure 4.10: Difference between allocated and required rate as a function of system load in the uplink.

allocate E_b/I_o values to different TCP flows versus the traditional approach of a constant assignment. In this case, even though the aggregate budget in both scenarios is the same, for the case of adaptive allocation the maximum value of target E_b/I_o which is 7.2 is allocated to the flow with the minimum cwnd size while the minimum value of target E_b/I_o (5.45) is allocated to the flow with the maximum cwnd size.

4.8 Conclusions

In this chapter a novel joint power and rate allocation scheme has been presented that uses information from the TCP state machine, together with the corresponding family of objective functions. Formerly proposed schemes are agnostic of the required transmission rate and allocate resources based on aggregate optimization criteria such as minimum power consumption or throughput maximization, without taking into account the actual required transmission rate of each flow. The novelty of the proposed scheme is the integration of TCP based information in the objective function, which allows exploration of the difference between the required rate and the actual allocated rate. Based on the above formulation of the problem, that gives insight into the actual required transmission rate, a bi-objective optimization methodology has been proposed; this reveals the trade-off between

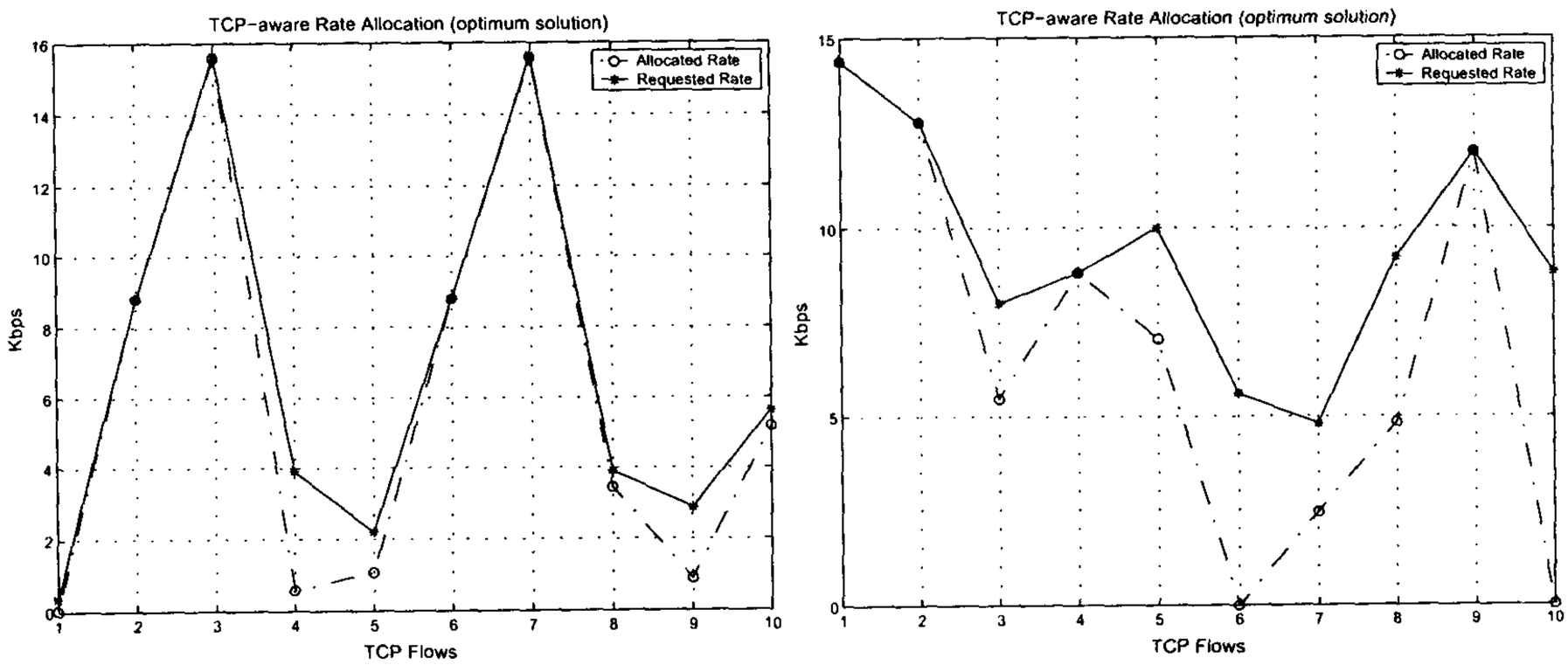

Figure 4.11: TCP-aware allocation of rates based on theoretical optimum solution of the optimization problem

transmission power and data rate satisfaction through the construction of the Pareto frontier. Additionally, a greedy algorithm have been presented in order to achieve linear complexity together with a differentiation on the allocated E_b/N_0 per flow in order to protect flows with small *cwnd* which are vulnerable to timeout events. This is of great importance from the user perception point of view because these events have a deleterious effect on TCP performance because of lengthy recovery times caused by retransmission timeouts. In the next chapter the focus is on how the information of different drop precedence levels of IP packets in the forwarding plane of DiffServ can be integrated into the resource management mechanisms.

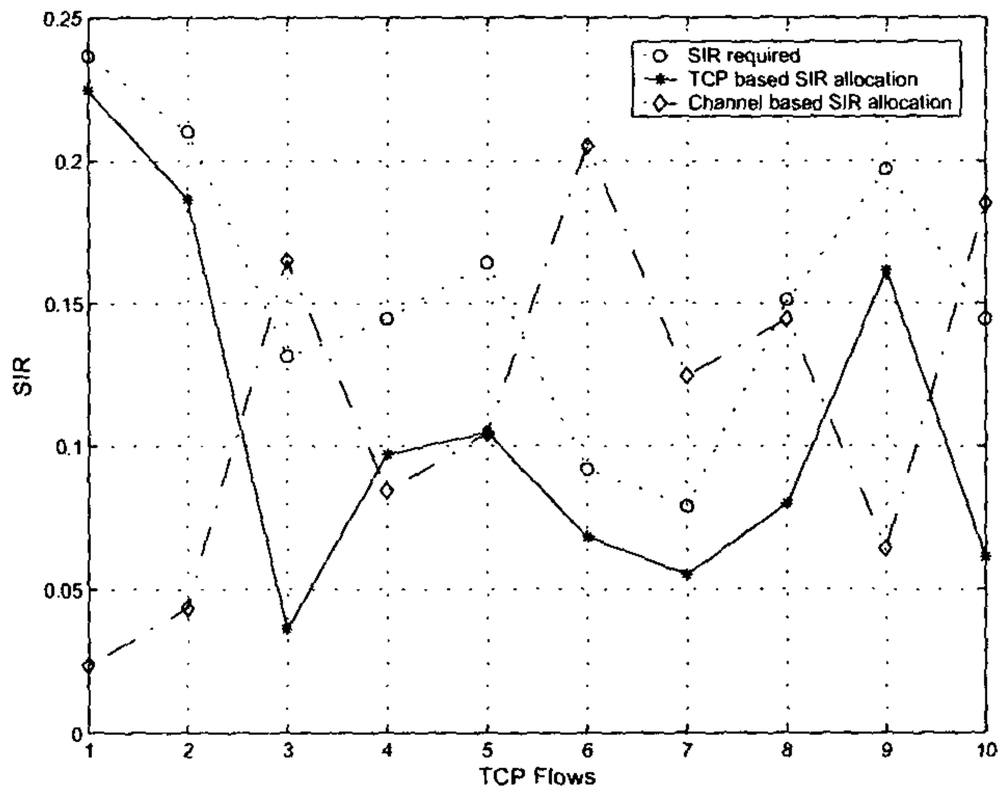

Figure 4.12: Allocation of SIR under the framework of the proposed greedy TCP-aware algorithm and a greedy algorithm that is based only on channel conditions

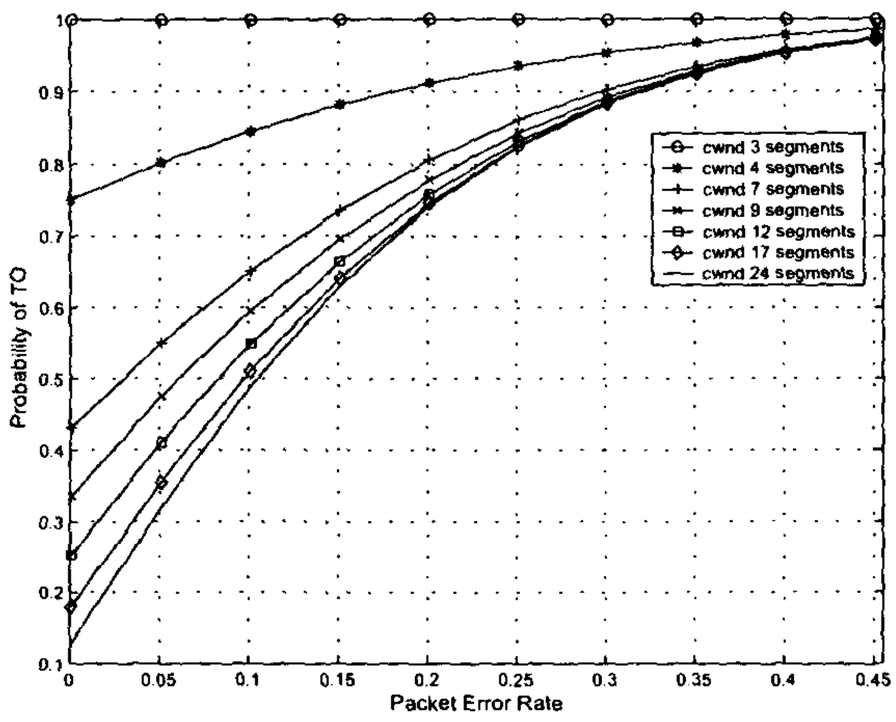

(a)

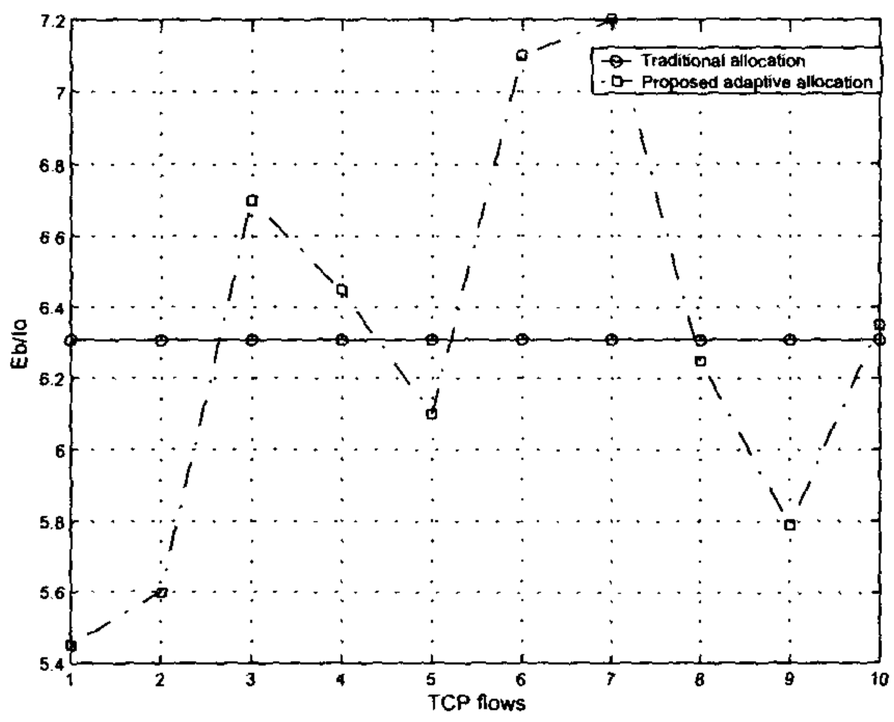

(b)

Figure 4.13: (a) Theoretical probability of time out event as given by equation (4.20), (b) Traditional versus the proposed adaptive allocation of E_b/I_o values on a specific snapshot of the system

Bibliography

[1] A. Sampath, P. Kumar, J. Holtzman, Power control and resource management for a multimedia CDMA wireless system, *In Proc. IEEE PIMRC'95, pp.21-25, 1995*

[2] S. Ramakrisha and J. M. Holtzman, A Scheme for Throughput Maximization in a Dual-Class CDMA System, *IEEE J. Selected Areas in Commun., vol* ***16****, pp. 830-844, June 1998*

[3] S. J. Oh and K. M. Wasserman, Dynamic Spreading Gain Control in Multi-Service CDMA Networks, *IEEE J. Selected Areas in Commun., vol* ***17****, no. 5, pp. 918-927, 1999*

[4] R. Jantti and S-L. Kim, Transmission rate scheduling for the non-real-time data in a cellular CDMA system, *IEEE Commun. Letters, vol.* ***5****, no. 5, pp. 200-202, May 2001*

[5] F. Berggren ,S-L. Kim, R. Jantti, and J. Zander , Joint power control and intra-cell scheduling of DS-CDMA nonreal time data, *IEEE J. Selected Areas in Commun., vol.****19****, no.10, pp. 1860-1870, Oct 2001*

[6] R. Fantacci, S. Nannicini, Multiple access protocol for integration of variable bit rate multimedia traffic in UMTS/IMT-2000 based on wideband CDMA, *IEEE J. Selected Areas in Commun., vol.* ***18****, pp. 1441 - 1454, Aug 2000*

[7] S. Choi and K. G. Shin, An uplink CDMA system architecture with diverse QoS guarantees for heterogeneous traffic, *IEEE/ACM Trans. Networking, vol.****7****, no. 5, pp.616-628, October 1999*

[8] L. Wang, A.H. Aghvami, W.G. Chambers, Design Issues of Media Access Control (MAC) Protocols for Multi-media Traffic Over DS-CDMA Systems, *European Wireless 2002, pp. 151-160, Italy, 2002*

[9] D. I. Kim, E. Hossain, V. K. Bhargava, Downlink Joint Rate and Power Allocation in Cellular Multirate WCDMA Systems, *IEEE Transactions on Wireless Communications, Vol. 2, No. 1, January 2003*

[10] Elmusrati and H. Koivo, Multi-objective distributed power and rate control for wireless communications, *Proc. International Conference on Communications, Vol. 3, pp. 1838-1842, May 11-15, 2003*

[11] M. Allman, V. Paxson, W. Stevens, TCP Congestion Control, *Request for Comments 2581, April 1999*

[12] S-L. Kim, Z. Rosberg, J. Zander, "Combined power control and transmission rate selection in cellular netrworks", *In Proc. of the* 49^{th} *IEEE VTC Fall Conference, Amsterdam, pp.1653-1657,1999*

[13] V. Jacobson, R. Braden, D. Borman, RFC 1323 TCP Extensions for High Performance, *May 1992*

[14] Hao Jiang, Constantinos Dovrolis, Passive Estimation of TCP Round-Trip Times, *ACM SIGCOMM Computer Communications Review (CCR), vol.* ***32****, no. 3, July 2002*

[15] M. Allman, V. Paxson, On Estimating End-to-End Network Path Properties, *In Proceedings of ACM SIGCOMM, Sept. 1999*

[16] I. T. Ming-Chit, Du Jinsong, W. Wang, Improving TCP Performance Over Assymetric Networks, *ACM SIGCOMM Computer Communications Review (CCR), vol.* ***30****, no. 3, July 2000*

[17] A. Calveras, Linares J., J. Paradellas, Window Prediction Mechanism for Improving TCP in Wireless Assymetric Links, *In Proceedings IEEE GLOBECOM, Sydney, Australia, November 1998*

[18] J. Padhye, V. Firoiu, D. Towsley, J. Kurose, Modeling TCP Throughput: A simple model and its empirical validation, *In SIGCOM'98, September 1998*

[19] F. Berggren, Power Control, tranmsission rate control and schedulling in cellular radio systems, *Licentiate Thesis, Royal Institute of Technology, 2001*

[20] Holland J. Adaptation in Natural and Artificial Systems, an introductory analysis with applications to biology, control and artificial intelligence, *The university of Michigan Press, Ann Arbor, USA, 1975*

[21] Kirkpatrick S., Gelatt D., Vecchi P., Optimization by simulated annealing, *Science, vol. **220**, pp. 671-680, 1983*

[22] Glover F., Tabu Search - Part I, *ORSA Journal of Computing, vol **1**, pp.190-206, 1989*

[23] Steuer E., Choo U., An interactive weighted Tchebycheff proedure for multiple objective programming, *Mathematical Programming, vol. **26**, pp. 326-344, 1983*

[24] Das I, Dennis J., Closer look at drawbacks of minimizing weighted sums of objectives for Pareto set generation in multicriteria optimization problems, *Structural Optimization, vol. **14**, pp. 63-69, 1997*

[25] Das I., A Preference Ordering Among Various Pareto Optimal Alternatives, *Structural Optimization, vol. **18**, pp. 30-35, 1999*

[26] Eschenauer H., Koski J., Osyczka E., Multicriteria Design Optimization: Procedures and Applications, *Springer-Verlag, New York, 1990*

[27] Dejan M. Novakovic and Miroslav L. Dukic, Evolution of the Power Control Techniques for DS-CDMA Toward 3G Wireless Communication Systems, *IEEE Communications Surveys & Tutorials, Vol. 3, No. 4, 2000*

Chapter 5

Colour-aware Power and Rate Adaptation in IP-based CDMA Networks

In the previous chapter we have discussed how transport layer information can be integrated and utilized for resource management in the radio access network. In this chapter, a power and rate adaptation approach is proposed that integrates QoS information from the IP layer of the Differentiated Services Architecture (DiffServ) together with lower layer criteria to optimize packet transmission over the wireless interface. With IP technology being the focus of future wireless networks, IP-based resource management is currently receiving increased research attention. An optimization problem is formulated based on the output of a Time Sliding Window three colour marker (TSWtcm) of the ingress DiffServ node in the RAN, where colour aware power and rate control is performed. The critical impetus of the proposed approach, beyond minimization of the transmitted power, is mainly twofold. Firstly, to achieve the required per-class aggregate data rate while prioritizing and ensuring QoS of in-profile packets, and secondly to increase power gains by penalizing out-of-profile packets in sense of the allowed power consumption. The seminal aspect of the proposed scheme is

that tangible power gains can be achieved by differentiating transmission of conformant and non-conformant packets while at the same time the aggregate power gains of AF classes can be utilized to enhance the performance of in-profile traffic. To support the case, meticulous theoretical and simulation results are presented that depict architectural and performance related aspects of the proposed scheme.

5.1 Introduction

Because of the inherent and well known characteristics of the wireless transmission medium the path towards IP based Radio Access Networks (RAN) raises a number of novel and acute research issues both in the forwarding and in the control plane of the architecture. Efficient management of radio resources is essential for wireless networks because they are characterized by scarce radio spectrum, an unreliable propagation channel (with shadowing, multipath fading, interference, etc.) and stochastic user mobility. With W-CDMA being the incumbent standard for 3G networks, one of the critical components of radio resource management in CDMA networks is power control. Power control has been extensively studied in recent years and a number of eloquent solutions have been proposed [11], [12], [13], [14]. Power control has been mainly used to reduce inter and intra-cell interference and to guarantee the required signal to interference ratio (SIR) of ongoing connections, with an ultimum target of achieving a higher degree of utilization and/or better quality of service (QoS).

At the same time, the introduction of IP-based transport in RAN's has been seen as a result of IP's flexibility and its rapidly growing popularity. The Differentiated Services (DiffServ) architecture [1] is currently receiving a wide attention as the main candidate for providing IP QoS both in the Core and Access networks of the UMTS infrastructure [7]. Today's Internet applications have diverse quality of service (QoS) requirements which can be considered as a clear evidence that best effort treatment of traffic mix with heterogeneous characteristics and requirements is less than sufficient. As access to Internet applications from mobile networks is expected to increase steadily over the next few years, IP based mechanisms for transport and resource management are expected to be of critical importance. The integration of such IP layer QoS information with resource management in beyond 3G (B3G) wireless systems is currently growing with exponential pace. Therefore, QoS provisioning

for mobile users in IP based UMTS environments arises as a significant milestone toward the target of achieving the above goals. The situation thus seems to call for a more finely grained analysis and, as such, current efforts for defining future-generation wireless systems emphasize the need for providing unified frameworks with sufficient flexibility to satisfy diverse QoS requirements. Maybe the most relevant previous research work that captures the idea of optimizing resource usage based on DiffServ information can be found in [20], where the authors proposed a call admission control scheme for UMTS networks that utilize power sharing among different AF classes. The difference here is that we are not focusing on admission control policies but on resource management of the on-going admitted flows in different AF classes.

The central thesis of this chapter pivots on the development and investigation of an integrated framework for a DiffServ aware power and rate adaptation scheme for delivering differentiated services in a CDMA environment. The peculiarity of the wireless transmission medium entails that if critical information from the IP layer is explored by lower layers, packet transmission can be further optimized. The upshot thus far is that, even though a large volume of research has been devoted to QoS on different layers these schemes do not consider QoS as a cross-layer issue. The benefits of using information from higher layers to assist optimization of transmission over the wireless link have been discussed in the previous chapter. In that case, a family of objective functions that encompasses TCP based information (i.e, congestion window and round trip time) has been used to define an optimization problem for power and rate adaptation, but did not consider a DiffServ environment. To the best of author's knowledge, this is the first study that considers differentiation of packet transmission over the wireless medium based on the packet drop-precedence (packet colour). Before exploring the potentials of the proposed scheme we should emphasize that even though radio resource management that integrates information from the IP layer (or above) offers many new avenues in the rapidly maturing research area of cross-layer schemes, the issues that naturally arise from such designs should carefully taken into account.

The rest of the chapter is organized as follows. In section 5.2 a retrospective of IP QoS support in radio access networks is presented together with the related DiffServ functionalities in the ingress node. In section 5.3 the motivation behind the proposed colour aware power and rate adaptation scheme is presented. This is followed with section 5.4 where the proposed scheme is analyzed. In

section 5.5 the outage probability is calculated for the colour aware scheme. In section 5.6 a rate truncation scheme for the out of profile packets is presented and in section 5.7 validation and experimental results of the proposed schemes are discussed. Finally, the chapter closes with the conclusions in section 5.8.

5.2 IP QoS in Wireless Networks

5.2.1 Differentiated Services Architecture

The Differentiated Services Architecture (DiffServ) allows an approach to IP Quality of Service that is modular, incrementally deployable and scalable, while introducing minimal per-node complexity [1]. The aim within IETF was to define the general architecture for differentiated services by mainly focusing on the forwarding plane and therefore to define different required "behaviors" in routers, which are known as per-hop forwarding "behaviors" (or PHBs). Additionally, DiffServ architecture also defines the functionality required at the edges of the scope domain to classify and condition (e.g., policing and shaping) traffic according to specific rules. In a mobile network for example the edge DiffServ router can be the gateway router to the Internet (in the core network) and the radio network controller in the access network. On the other hand, per-flow resource reservation solutions (such as IntServ) suffer from scalability issues because of the requirement for managing state information in each node. This requirement is not only relevant for backbone networks but also for mobile networks. The scalability problem in this case results from the extensive signalling load introduced by reservation protocols (such as RSVP) because of changes in the attachment point of mobile users. Even though a number of solutions have been proposed to extend RSVP to accommodate mobility issues, there is still a lack of a widely accepted solutions [4]. Another important issue, beyond mobility, that has not been widely emphasized is the interaction between rate adaptation mechanisms over the air-interface and per-flow resource reservation mechanisms. In UTRAN the transmission rate for a mobile node using a dedicated channel can change every 10msec [1] (i.e on a frame by frame basis). This rate adaptation may force a new negotiation phase from RNC to Node B even though the route has not changed. The independent operation between rate assignment and

[1] In High Speed Downlink Packet Access (HSDPA) mode the transmission rate can change even faster, i.e every 2msec

per-flow resource reservation in UTRAN means that additional signalling overhead can be generated by the triggering of new reservation of resources to match the updated assigned rate [2]. From this perspective, a compromise between resource reservation and rate adaptation can also lead to better utilization of the resources in the radio access network. As will become more evident subsequently, the proposed scheme supports such coupling between rate control and aggregate per-class allocation of resources which can be used for dynamic (re)allocation of bandwidth between different AF classes. In this chapter we will assume that services belong to the Assured Forwarding (AF) [3] Per Hop Behavior (PHB) class that provides better than best effort services (even though the framework can also be used for the Expedited Forwarding (EF) [2] class).

5.2.2 Ingress Marking

Traffic aggregates are characterized using the DiffServ Code Point (DSCP) and the AF PHB RFC proposes four classes and three-drop preferences per class. AF can be seen as an extension of the RIO scheme [5], which uses a single FIFO queue and two-drop preferences. Most of the current studies of differentiated drop mechanisms are based on the RIO approach. The discussion in this paper is based on the most general case and thus assumes a three level drop preference. The three level drop mechanism utilizes the RED (Random Early Detect) queue for performing differentiated dropping of packets during congestion at the node. The three level drop mechanism scheme utilizes a single queue. All user packets are directed to and served from the same queue.

Metering and marking functionalities of packets inside AF classes are on per flow basis (even though these policies can also be applied for aggregated flows). Marking incoming traffic at the ingress DiffServ router is one of the most important functionalities. This building block is responsible for marking sender's traffic according to a specific profile. Traffic that conforms with the service profile will be handled with a low drop precedence, while non-conforming traffic will be handled with high drop precedence. Depending on the mechanism used to measure the conformity of the traffic, traffic marking can be in general classified in two general categories; *Token bucket* and *Average rate estimation.* In the next section we use, as a case study, a marking algorithm from the second

[2] An obvious solution to this problem would be that reservation in the wired (or point-to-point wireless) part of UTRAN network is based on the maximum contracted rate by the user. This scheme is the less optimum because it would lead to maximum waste of resources.

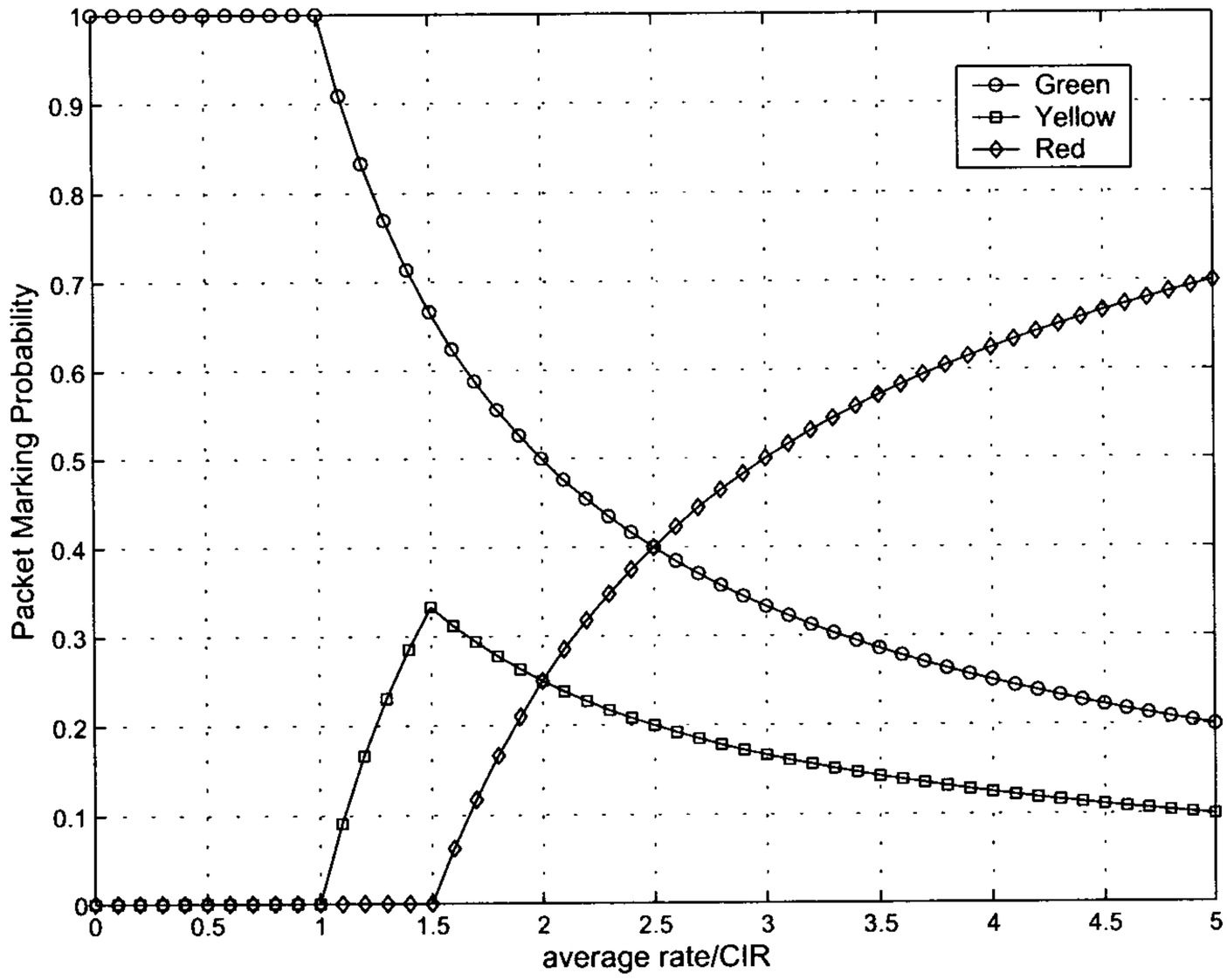

Figure 5.1: Graphical representation of the marking probability of the TSWtcm algorithm

family, even though the proposed rate adaptation scheme is independent from the actual marking algorithm. The rate estimating algorithm used is the **T**ime **S**liding **W**indow **t**hree **c**olour **m**arking (**TSWtcm**) [6], where the arrival rate is calculated according to the weighted average of the arrival rate over a certain time window. In TSWtcm, whenever a packet arrives, the marker calculates the estimated arrival rate. If the estimated arrival rate is less than the Committed Information Rate (CIR), arriving packets are marked as green; otherwise, they are marked as green, yellow or red according to a calculated probability which also depends on Peak Information Rate (PIR) contructed. If by r_i we denote the measured average rate of flow i, the pseudo code of the TSWtcm can be described as follows,

---

TSWtcm Algorithm

---

if $r_i \leq CIR$,

```
    mark packet as green
```

`else if` $(CIR < r_i \leq \text{PIR})$

`calculate` $p_0 = \dfrac{r_i - CIR}{r_i}$

`with probability` p_0 `mark packet as yellow`

`with probability` $1 - p_0$ `mark packet as green`

`else`

`calculate` $p_1 = \dfrac{r_i - PIR}{r_i}$, `and` $p_2 = \dfrac{PIR - CIR}{r_i}$

`with probability` p_1 `mark packet as red`

`with probability` p_2 `mark packet as yellow`

`with probability` $1 - (p_1 + p_2)$ `mark packet as green`

Figure 5.1 shows how the probability of marking a packet as green, yellow or red changes based on the normalized arrival rate (we have used $PIR = 1.5 \cdot CIR$). Providing end-to-end differentiated service, on the other hand, can be obtained by concatenation of per-domain services and Service Level Specifications [3] (SLS) between adjoined domains along the path that the traffic crosses in going from source to destination and is beyond the scope of this paper. As mentioned before, we continue to stress the line that DiffServ over MPLS has been adopted in UMTS standardization body (3GPP) both at the Terrestrial Radio Access segment (UTRAN) and at the Core Network for providing traffic differentiation. In such enhanced UMTS platform, where IP with QoS guarantees will more likely be the reference transport solution in every segment of the system we envision that the Radio Network Controller (RNC) node will perform all the related functionalities of an edge DiffServ node as shown in figure 5.2.

5.2.3 Resource Management

We consider a single cell in a CDMA network with n_j active mobile nodes in each AF class ($1 \leq j \leq \Theta$ classes). With a fixed chip rate in the system, the total bandwidth W is shared among all users and different rates are achieved through orthogonal variable spreading factor (OVSF) codes. We also assume IP packets of constant length (P bits) and the emphasis will be on the downlink transmission,

[3] The notions of Service Level Agreement (SLA) and Traffic Conditioning Agreement (TCA) used in the initial DiffServ proposed architecture (RFC 2475), have changed in RFC 3260 to Service Level Specification (SLS) and Traffic Conditioning Specification (TCS) in order to reflect better the technical parameters that represent rather than any pricing or business model.

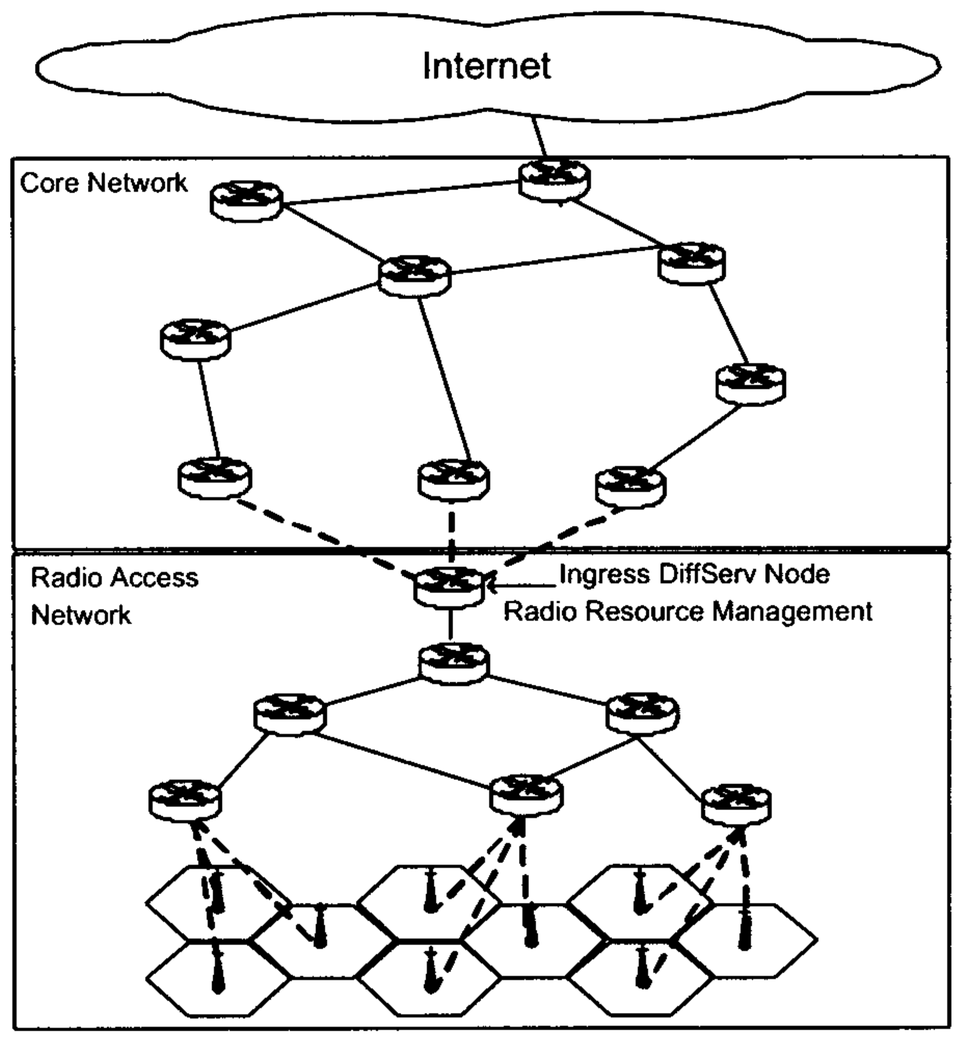

Figure 5.2: All IP based architecture where the RNC node can be considered as the ingress DiffServ node for the access network

where the maximum transmission power at the access point is equal to p_{max}. As has been discussed in the previous chapter the received SIR of mobile i,is defined by:

$$SIR_i(\mathbf{p}) \stackrel{\text{def}}{=} \frac{g_i p_i}{\theta_i \cdot g_i \sum_{j \neq i} p_j + I_i + \nu}, \; 1 \leq i \leq N \tag{5.1}$$

We also note that the DiffServ classes may have different bit-energy-to-interference-power-spectral-density ratio, E_b/I_0, requirements. With a per class target $(E_b/I_0)_j = \Gamma_j, 1 \leq j \leq \Theta$ at the receiver, which gives a constant bit-error independent of the bit-rate, the relationship between rate r_i and SIR (denoted as γ_i in the sequel for notation convenience) will have the form:

$$\frac{r_i}{\gamma_i} = \frac{W}{\Gamma_j} \tag{5.2}$$

In this case, the optimum feasible allocation of rates (or $SIR's$) for achieving throughput, $\widetilde{R}$ in the cell will be the solution of the following rate and power control problem in terms of target $SIR's$

values,

$$\min_{\gamma_i} \quad \frac{1}{1-\sum_{i=1}^{N}\frac{\theta\gamma_i}{1+\theta\gamma_i}}\sum_{i=1}^{N}\frac{\gamma_i}{1+\theta\gamma_i}\cdot\frac{I_i+\nu}{g_i}$$

$$s\,t. \quad \sum_{i=1}^{N}\frac{\gamma_i}{1+\theta\gamma_i}\cdot\frac{I_i+\nu}{p_{max}g_i}\leq 1 \tag{5.3}$$

$$\sum_{i=1}^{N}\gamma_i=\widetilde{\gamma}, \quad \left(\frac{E_b}{I_0}\right)_j=\Gamma_j, \quad \forall\, j,i$$

The above problem formulation minimize the power consumption without any specific QoS requirements (except from the BER and aggregate throughput requirements). In the following section, and before we enhance the above model with DiffServ per class QoS requirements we discuss the motivation behind the proposed scheme.

5.3 Motivation behind the proposed scheme

In order to explore the benefits of utilizing IP layer information, an insight into the interference produced by packet transmission is presented in this section. We concentrate on the downlink and the effect of altering the transmission time, τ_i, (i.e, increasing or decreasing the transmission rate) of user i on the total interference and transmitted power. Equation (6.3) can be written as,

$$p_i-\frac{\theta\Gamma_j}{W\tau_i}\sum_{j\neq i}p_j=\frac{\Gamma_j(I_i+\nu)}{g_iW\tau_i}$$

The above linear system of equations can be written in matrix form as,

$$\mathbf{(I-H)P=n}$$

where $\mathbf{P} = [p_1, \cdots, p_{n_j}]^T$, $\mathbf{n} = \left[\frac{\Gamma_j(I_1+\nu)}{g_1 W \tau_1}, \cdots, \frac{\Gamma_j(I_1+\nu)}{g_1 W \tau_{n_j}}\right]^T$ and

$$[\mathbf{H}]_{\mathbf{ij}} = \begin{cases} 0 & \text{if } i = j \\ \dfrac{\theta \Gamma_j}{W \tau_i} & \text{if } i \neq j \end{cases}$$

The sum of transmitted powers would be,

$$P_{\text{sum}} = \mathbf{1^T}(\mathbf{I} - \mathbf{H})^{-\mathbf{1}}\mathbf{n} \tag{5.4}$$

By calculating the gradient of the above equation with respect to the transmission times we can find which users cause large interference and contribute more to the overall transmitted power. By utilizing the gradient information and the related colour of the packet, if the transmitted time of yellow or red packets that contribute more to the interference is reduced this would greatly increase system performance. From (5.4) we have,

$$\begin{aligned} \delta_i =& \frac{\partial P_{\text{sum}}}{\partial \tau_i} = \frac{\partial(\mathbf{1^T}(\mathbf{I}-\mathbf{H})^{-\mathbf{1}}\mathbf{n})}{\partial \tau_i} \\ =& \mathbf{1^T}\left[(\mathbf{I}-\mathbf{H})^{-\mathbf{1}}\frac{\partial \mathbf{n}}{\partial \tau_\mathbf{i}} - (\mathbf{I}-\mathbf{H})^{-\mathbf{1}}\frac{\partial(\mathbf{I}-\mathbf{H})}{\partial \tau_\mathbf{i}}(\mathbf{I}-\mathbf{H})^{-\mathbf{1}}\mathbf{n}\right] \\ =& \mathbf{1^T}(\mathbf{I}-\mathbf{H})^{-\mathbf{1}}\left[\frac{\partial \mathbf{n}}{\partial \tau_\mathbf{i}} - \frac{\partial(\mathbf{I}-\mathbf{H})}{\partial \tau_\mathbf{i}}(\mathbf{I}-\mathbf{H})^{-\mathbf{1}}\mathbf{n}\right] \\ =& \mathbf{1^T}(\mathbf{I}-\mathbf{H})^{-\mathbf{1}}\left[\frac{\partial \mathbf{n}}{\partial \tau_\mathbf{i}} + \frac{\partial \mathbf{H}}{\partial \tau_\mathbf{i}}\mathbf{P}\right] \end{aligned} \tag{5.5}$$

If we define by $\mathbf{D}_i$ ($n_j \times n_j$ matrix) and $\mathbf{u}_i$ ($n_j \times 1$ matrix) as

$$[\mathbf{D}_i]_{jk} = \begin{cases} -\dfrac{1}{\tau_i} & , \ i = j = k \\ 0 & , \ \text{otherwise} \end{cases}$$

$$[\mathbf{u}_i]_j = \begin{cases} -\dfrac{\Gamma_j(I_1+\nu)}{g_1 W \tau_i^2} & , \ j = i \\ 0 & , \ \text{otherwise} \end{cases}$$

then equation (5.5) can be written as,

$$\delta_i = \mathbf{1^T}(\mathbf{I} - \mathbf{H})^{-1}\left[\mathbf{D_i H P} + \mathbf{u_i}\right] \tag{5.6}$$

by expanding (5.6) the i^{th} element of the gradient can be written as,

$$\begin{aligned}\delta_i &= -\frac{c_i \Gamma_j}{W \tau_i^2}\left[\left(\frac{\sum_{j\neq i}\theta g_i p_j + I_i + \nu}{g_i p_i}\right) p_i\right] \\ &= -\frac{c_i \Gamma_j}{W \tau_i^2} \cdot \frac{p_i}{\gamma_i} \\ &= -\frac{c_i p_i}{\tau_i}\end{aligned} \tag{5.7}$$

where $c_i = \mathbf{1^T}(\mathbf{I} - \mathbf{H})^{-1}\mathbf{v_i}$ and $\left[\mathbf{v}_i\right]_j = \begin{cases} 1 & , \ j = i \\ 0 & , \ \text{otherwise} \end{cases}$

The gradient represents how individual mobile users affect the rate of change of the transmitted power, while c_i coefficient represent the severeness of the interference produced by individual mobile users. Here, we are mainly interested in the magnitude of the gradient rather than on directionality (which depict the steepest downhill direction). Taking as a case study a two user scenario, figure 5.3 shows the required power for transmission range between 64Kbps to 128Kbps, under lognormal shadowing and normalized distance from the base station 0.2 and 0.9 respectively. As shown in the same figure, the second user which is on the border of the cell requires much higher power, while at the same time, the total power consumed is mostly effected by changes of the transmission time of the second user rather than of the user that is close to the base station. This is more clearly depicted in figure 5.4 where numerical gradients have been computed for the above scenario. As can be seen, the gradient of the second user is the dominant one compared with that of the first user. It is interesting to note that there is an intersection area of the gradients (equal contribution to interference levels) where the difference in the transmission rate between the mobile users is approximately 37Kbps. If we now assume, that the second user, which is located on the cell boundary, transmitting out-of-profile packets, i.e, yellow, or (even worst) red packets, then a reduction on the allocated transmission time will significantly reduce the interference that is produced by this user. By penalizing mobile user 2, which can transmit beyond the contracted rate agreement and at the same time because of

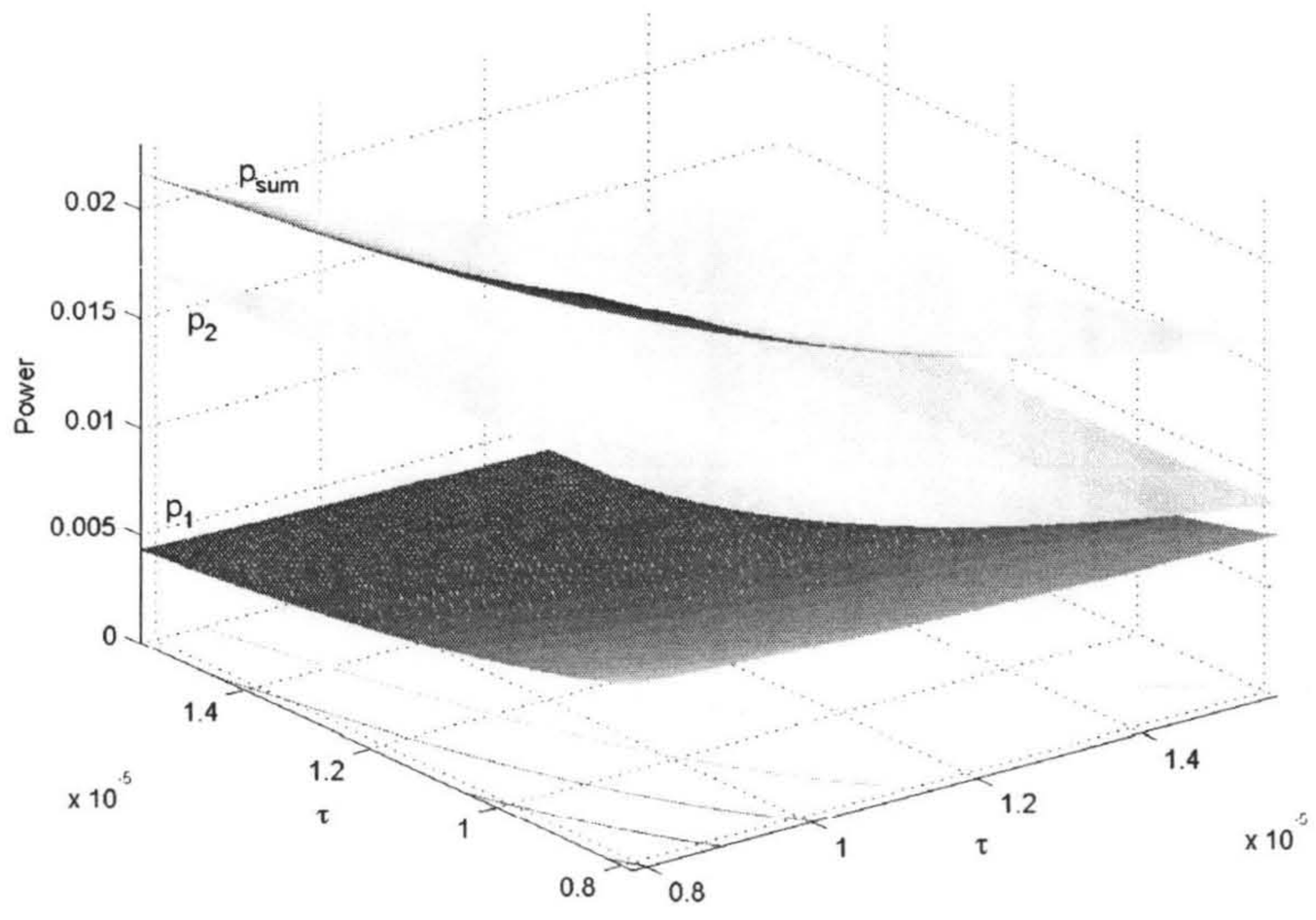

Figure 5.3: Power consumption with transmission range between 64Kbps to 128Kbps, under lognormal shadowing and normalized distance from the base station 0.2 and 0.9 respectively

channel conditions contribute highly to the total interference, the system performance can be greatly increased. The rate reduction for the out-of-profile packets is justified by the fact that the actual transmission rate (as discussed in section 5.2) is greater than the CIR. This approach goes beyond a traditional optimization approach that was based solely on lower layer criteria and static QoS per class information for packet transmission. It is in this spirit that we now present an approach for jointly utilizing information from channel conditions and packet colour.

5.4 Colour awareness on power and rate adaptation

Traditional power and rate adaptation techniques treat all packets equally and any differentiation is based only on lower layer criteria such as channel conditions and inter-cell interference for each user. In that sense, allocated power and rate vectors for packets in the same or different DiffServ classes are colour blind. We now propose an integrated framework for power and rate adaptation that is colour aware, takes into account lower layer information and provides the required aggregate per class transmission rate. Using a different weighting factor ($\xi_{\text{green}}, \xi_{\text{yellow}}, \xi_{\text{red}}$) depending on the

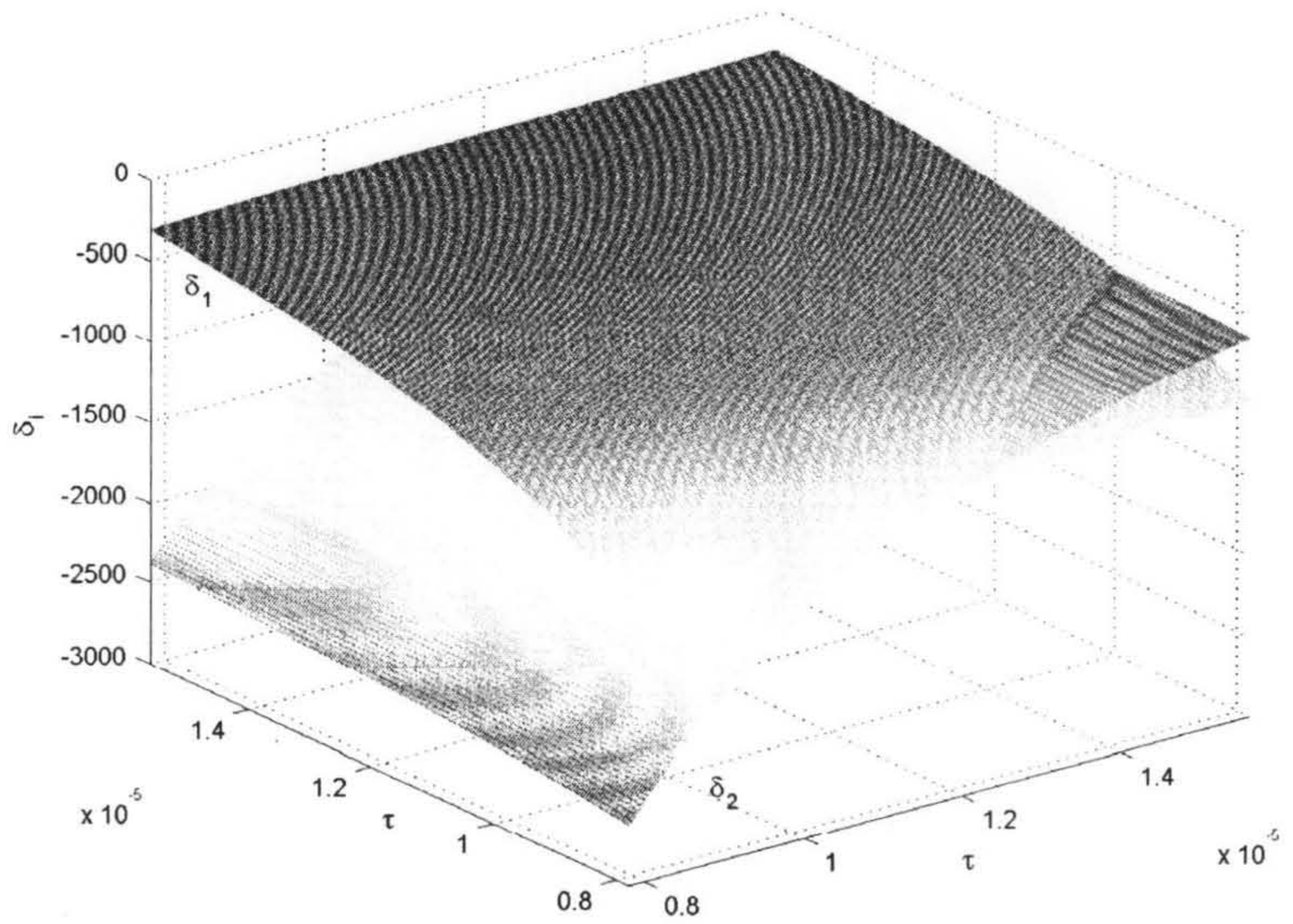

Figure 5.4: Gradient of power consumption with respect to transmission time

colour of the packets, transmission times and related power allocations will be differentiated firstly to prioritize in-profile packets and secondly to reduce required power consumption for out-of-profile packets. Instead of fixed degradation of the out-of-profile packets, the weighting factors increased linearly depending on channel conditions and inter-cell interference as shown in figure 5.5(a). As can be seen in the figure, there is no degradation for green packets while the difference between the yellow and red packets can be controlled by the $d\xi$ parameter. Based on this framework the actual transmission time of user i for a yellow or red packet will be augmented by ξ_i. Also, we have selected that the maximum degradation for a red packet to be equal to $\xi_{\text{red}} = 0.5\tau$ (where τ denote the average transmission time per user in the AF class in order to achieve the required aggregate data rate). If by τ_i we denote the transmission time for mobile host i, then based on the output of the TSWtcm the average transmitted rate can be written as,

$$R_i = [p_i^g \tau_i + p_i^y(\tau_i + \xi_y) + p_i^r(\tau_i + \xi_r)]^{-1} \tag{5.8}$$

where p_i^g, p_i^y and p_i^r represent the probability that a packet from user i is marked as green, yellow or red respectively. A significant observation on the proposed linear function of degradation is that it is reminiscent of the RIO technique where instead of the queue length the channel and inter-cell interference are taken into account and it is deterministic rather than probabilistic.

We will first consider a power minimization problem with constraints on the transmission time per class. As have been discussed previously, for a given power vector $\mathbf{p} = (p_1, p_2, ..., p_N)^T$, the received SIR of mobile i,can be defined as:

$$\mathrm{SIR}_i(\mathbf{p}) \stackrel{\mathrm{def}}{=} \frac{g_i p_i}{\theta_i \cdot g_i \sum_{j \neq i} p_j + I_i + \nu}, \; 1 \leq i \leq N \tag{5.9}$$

The power vector now that supports every mobile with the minimum power can be found by solving the linear system of equations in (6.3),

$$p_i^* = \frac{\gamma_i}{1 + \theta\gamma_i} \left(\frac{\sum_{j=1}^{N} \frac{\theta\gamma_j}{1+\theta\gamma_j} \frac{I_j + \nu}{g_j}}{1 - \sum_{j=1}^{N} \frac{\theta\gamma_j}{1+\theta\gamma_j}} + \frac{I_i + \nu}{g_i} \right) \tag{5.10}$$

If we substitute in the optimum power vector (equation 6.5) the γ_i with the corresponding transmission rates r_i using (6.4) and subsequently the transmission rates with the corresponding transmission times τ_i we have:

$$p_i^* = \frac{\Gamma}{W\tau_i + \Gamma\theta} \left(C + \frac{I_i + \nu}{g_i} \right)$$

In that case, the constrained optimization problem that will be explored next can be written as follows,

$$\min_{\tau_i} \quad \frac{1}{1 - \sum_{i=1}^{n_j} \frac{\theta\Gamma_j}{W(\tau_i + \xi_i) + \theta\Gamma_j}} \sum_{i=1}^{n_j} \frac{\Gamma_j}{W(\tau_i + \xi_i) + \theta\Gamma_j} \cdot \frac{I_i + \nu}{g_i}$$

$$s\,t. \quad \sum_{i=1}^{n_j} \frac{\Gamma_j}{W(\tau_i + \xi_i) + \theta\Gamma_j} \cdot \left(\frac{I_i + \nu}{p_{n_j} g_i} + \theta \right) \leq 1 \tag{5.11}$$

$$\sum_{i=1}^{n_j} \frac{1}{\tau_i + \xi_i} = R_j, \quad \left(\frac{E_b}{I_0} \right)_j = \Gamma_j, \quad \forall\, j, i$$

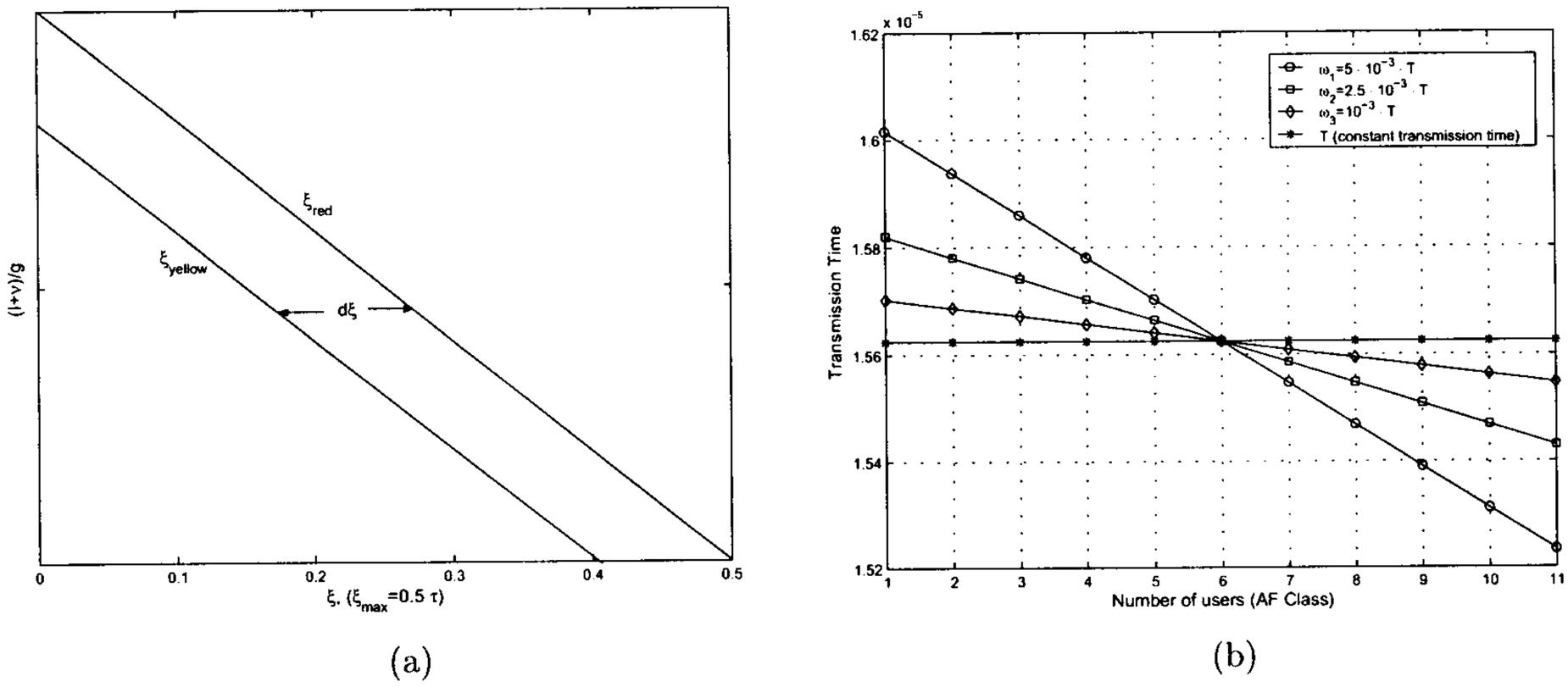

(a) (b)

Figure 5.5: (a) A linear function that represent the additional delay introduced for non-conforming packets (yellow, red) (b) Constant versus adaptive allocation of transmission times for users sorted according to channel and inter-cell interference conditions (shown for different values of ω).

Lemma 5.4.1. *If we assume that*

$$\frac{I_1 + \nu}{g_1} \geq \frac{I_2 + \nu}{g_2} \geq \ldots \geq \frac{I_N + \nu}{g_N} \tag{5.12}$$

a necessary condition for optimality is

$$\tau_i \geq \tau_{i+1} \tag{5.13}$$

Proof. Assuming a feasible reassignment of transmission times that minimize A but does not satisfy 5.13. Based on the feasible reassignments, we can find a pair of τ_i and τ_j such as $\tau_j > \tau_i$ for $1 \leq i < j \leq M$. Then we can write $\tau_j = \tau_i + \omega$ where $\omega > 0$. If we now compare the assumed optimal allocation,

$$\frac{\Gamma P\left(C + \dfrac{I_i + \nu}{g_i}\right)}{W\tau_i + \Gamma P\theta} + \frac{\Gamma P\left(C + \dfrac{I_j + \nu}{g_j}\right)}{W\tau_j + \Gamma P\theta} \tag{5.14}$$

$$= \frac{\Gamma P\left(C + \frac{I_i + \nu}{g_i}\right)}{W\tau_i + \Gamma P\theta} + \frac{\Gamma P\left(C + \frac{I_j + \nu}{g_j}\right)}{W(\tau_i + \omega) + \Gamma P\theta}$$

with the following one,

$$\frac{\Gamma P\left(C + \frac{I_i + \nu}{g_i}\right)}{W\tau_j + \Gamma P\theta} + \frac{\Gamma P\left(C + \frac{I_j + \nu}{g_j}\right)}{W\tau_i + \Gamma P\theta} \tag{5.15}$$

$$= \frac{\Gamma P\left(C + \frac{I_i + \nu}{g_i}\right)}{W(\tau_i + \omega) + \Gamma P\theta} + \frac{\Gamma P\left(C + \frac{I_j + \nu}{g_j}\right)}{W\tau_i + \Gamma P\theta}$$

By subtracting equation (5.14) from (5.15) and after some algebra it can be shown that the power required for the assumed optimal allocation is higher, i.e,

$$\frac{\Gamma\omega}{(W\tau_i + \Gamma P\theta)(W\tau_j + \Gamma P\theta)}\left[\frac{I_i + \nu}{g_i} - \frac{I_j + \nu}{g_j}\right] > 0$$

Thus for any i, j with $\frac{I_i + \nu}{g_i} \geq \frac{I_j + \nu}{g_j}$, an optimal assignment should have $\tau_i \geq \tau_j$ □

The lemma states that it is possible to reduce the aggregated transmitted power per DiffServ class by allocating less rate to mobile hosts that experience small link gains and high inter cell interference. The above results suggest the form of the optimum solution and point out the fact that in an optimum allocation transmission times will be sorted according to channel and inter-cell interference. Based on the above result we proceed with an analytical comparison of power consumption for a specific AF class between an adaptive per class allocation with an allocation that gives the same aggregate per class rate but with equal transmission times. As shown in figure 5.6 we assume that the adaptive allocation of transmission times for an AF class with n users are separated by a constant time ω, while for the case of equal transmission times all users are allocated a transmission time equal to $\tau = \tau_{(n+1)/2}$. Even though a transmission rate allocation with equal steps is not optimum it gives an insight into the power consumption savings from a traditional equal treatment of packets which belong in the same DiffServ class.

Before considering optimum allocated transmission times we compare power consumption between an adaptive per class allocation with an allocation that gives the same aggregate per class rate but

with equal transmission times. This would have the following form,

$$\sum_{i}^{n_j}\widehat{p}-\sum_{i}^{n_j}p_i=\underbrace{\left(\sum_{i}^{n_j}\frac{\Gamma PC}{W\tau+\Gamma P\theta}-\sum_{i}^{n_j}\frac{\Gamma PC}{W\tau_i+\Gamma P\theta}\right)}_{A}+\Gamma P\underbrace{\left(\sum_{i}^{n_j}\frac{\frac{I_i+\nu}{g_i}}{W\tau+\Gamma P\theta}-\sum_{i}^{n_j}\frac{\frac{I_i+\nu}{g_i}}{W\tau_i+\Gamma P\theta}\right)}_{B} \tag{5.16}$$

If we define $\beta_{k,l}$ with $1\leq k,l\leq n_j$ as,

$$\beta_{k,l}=\prod_{\substack{i=1\\ i\neq k,l,(n_j+1)/2}}^{n_j}[W\tau_i+\Gamma P\theta]$$

Then, after some algebra, it can be shown that part A of the equation (5.16) can be written as,

$$A=\omega W^2((n+1)/2-1)\beta_{1,n}(\tau_n-\tau_1)+\omega W^2((n+1)/2-2)\beta_{2,n-1}(\tau_{n-1}-\tau_2)+\ldots$$
$$+\omega W^2\beta_{(n+1)/2+1,(n+1)/2-1}(\tau_{(n+1)/2+1}-\tau_{(n+1)/2-1})$$

but from equation (5.13) $A<0$. With the same rational, and if for the sake of simplicity we assume that $K_i=\dfrac{I_i+\nu}{g_i}$ and $a_i=(n+1)/2-i$ where $1\leq i\leq(n+1)/2-1$ ($a_{(n+1)/2-1}=1$), and substitute $(n+1)/2-1$ with n^- and $(n+1)/2+1$ with n^+ then, part B of equation (5.16) can be written as,

$$B=a_1\left[\frac{K_1}{W\tau_1+\Gamma P\theta}-\frac{K_{n_j}}{W\tau_{n_j}+\Gamma P\theta}\right]+$$
$$a_2\left[\frac{K_2}{W\tau_2+\Gamma P\theta}-\frac{K_{n_j-1}}{W\tau_{n_j-1}+\Gamma P\theta}\right]+\ldots$$
$$a_{n^-}\left[\frac{K_{n^-}}{W\tau_{n^-}+\Gamma P\theta}-\frac{K_{n^+}}{W\tau_{n^+}+\Gamma P\theta}\right]$$

Using the fact that link gains and inter-cell interference are sorted as depicted in equation (5.12), we can assume that for all the $(n+1)/2-1$ pairs of the above equation we have $K_n=K_1+\lambda_1$, $K_2=K_{n_j-1}+\lambda_2$, …, $K_{n^+}=K_{n^-}+\lambda_{n^+}$,

$$B=a_1\left[\left(\frac{K_1}{W\tau_1+\Gamma P\theta}-\frac{K_1}{W\tau_{n_j}+\Gamma P\theta}\right)-\frac{\lambda_1}{W\tau_{n_j}+\Gamma P\theta}\right]+$$
$$a_2\left[\left(\frac{K_2}{W\tau_2+\Gamma P\theta}-\frac{K_2}{W\tau_{n_j-1}+\Gamma P\theta}\right)-\frac{\lambda_2}{W\tau_{n_j-1}+\Gamma P\theta}\right]+$$
$$\ldots a_{n^-}\left[\left(\frac{K_{n^-}}{W\tau_{n^-}+\Gamma P\theta}-\frac{K_{n^-}}{W\tau_{n^+}+\Gamma P\theta}\right)-\frac{\lambda_{n^+}}{W\tau_{n^+}+\Gamma P\theta}\right]$$

using the above formulation and given equation (5.13), $B < 0$.

Figure 5.6 shows numerically the difference on power consumption between the two schemes. As shown in the figure, the difference in power consumption is increased as ω increased. The downfall of this is that fairness between flows in the same AF class is decreased. As will be discussed next, where optimum allocations are investigated using gradient-based optimization techniques, the fairness between flows can be controlled based on the upper and lower bounds on the optimization solution space.

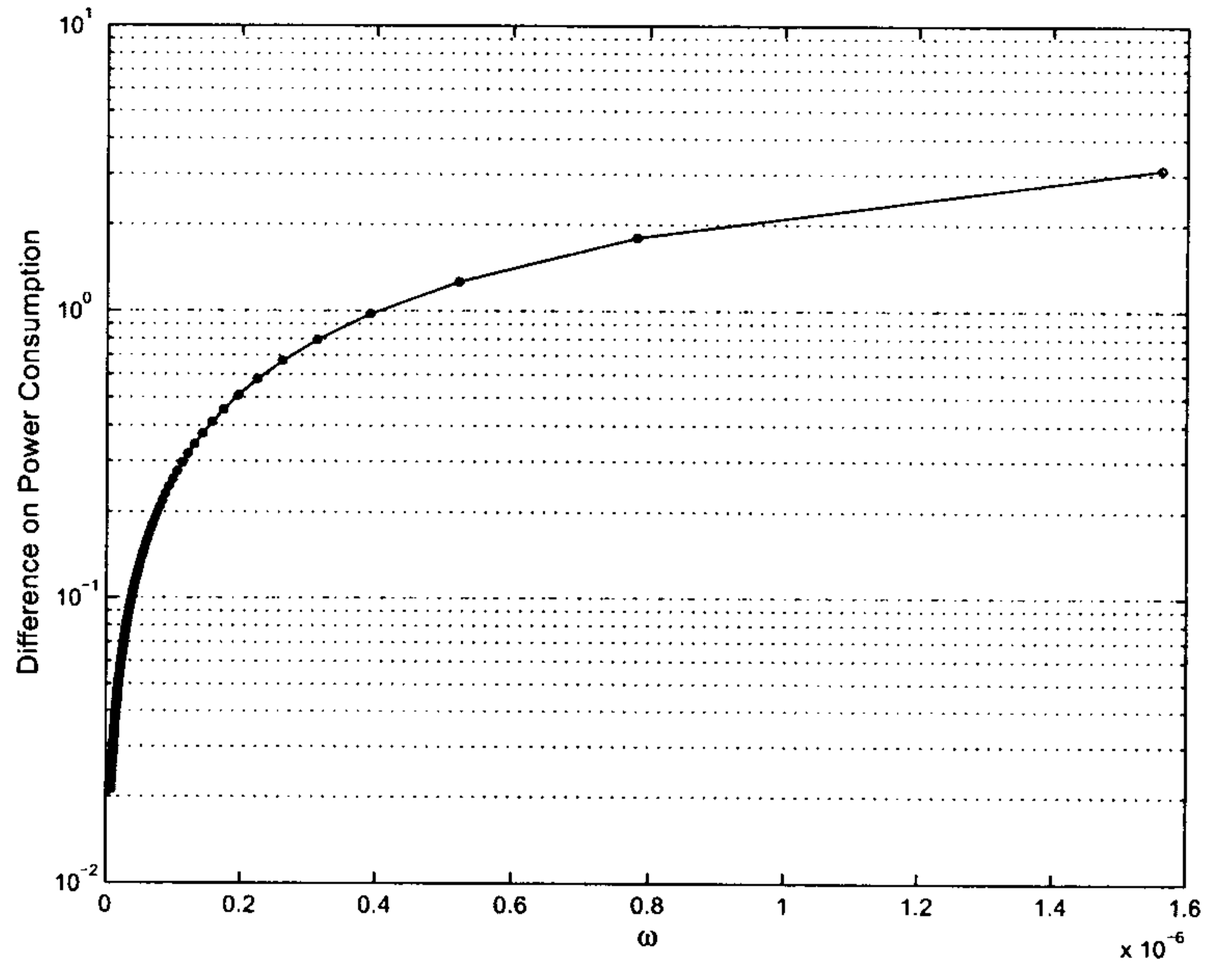

Figure 5.6: Difference on power consumption between a constant aggregate allocation and adaptive allocation as a function of ω

5.5 Calculation of Outage Probability

In this section we compare the outage probability between a traditional colour blind transmission and the proposed rate reduction scheme for the out-of-profile packets. For the inter-cell interference we can assume statistically uniform distribution of the load and that each base station accommodates a maximum number of sessions and so the transmitted power is maximum (worst case scenario). In

this case the inter-cell interference to the i^{th} mobile user is given by,

$$I_i^{\text{inter}} = \sum_{j=1}^{K} P_j \cdot g_j \tag{5.17}$$

where K is the number of neighbor cells that are considered to contribute to the inter-cell interference, P_j is the total transmitted power from base station j and g_j is the link gain from the j^{th} base station to the i^{th} mobile user. If we also assume that φ_i denote power fraction allocated for mobile host i then the received E_b/I_0 would be given by,

$$(E_b/I_0)_i = \frac{W}{R_i} \cdot \frac{g_i \varphi_i P_T}{g_i \varphi P_T + \sum_{j=1}^{K} P_j \cdot g_j + n}$$

Assuming that the background noise is negligible compared with the total transmitted power and by subsisting $S_i = g_i P_T$ we have,

$$(E_b/I_0)_i = \frac{W}{R_i} \cdot \frac{\varphi_i}{\varphi + \dfrac{I_i^{\text{inter}}}{S_i}} \tag{5.18}$$

From equation (5.18) it can be seen that the fraction of power required for mobile user i would be,

$$\varphi_i = \frac{(E_b/I_0)_i \, R_i}{W} \cdot \left(\varphi + \frac{I_i^{\text{inter}}}{S_i} \right) \tag{5.19}$$

Assuming a uniform distribution of users within the cell, the average inter-cell interference power to total power from the assigned BS ratio is approximately $n \approx 0.4$ times that compared with the worst case where all users are located at the cell boundary [23]. By taking into account the average downlink power factor n and (5.8), the outage probability can be written as

$$\mathrm{P}_{\text{out}} = \Pr\left[\sum_{i=1}^{n_j} \rho_{ij} \varphi_i^j > \frac{1}{n} \right] = \Pr\left[\frac{(E_b/I_0)_i \sum_{i=1}^{n_j} \rho_{ij} \cdot \left(\varphi + \dfrac{I_i^{\text{inter}}}{S_i} \right)}{W(p_i^g \tau_i + p_i^y [\tau_i + \xi_y] + p_i^r [\tau_i + \xi_r])} > \frac{1}{n} \right] \tag{5.20}$$

where ρ_i is the activity or duty cycle of a service for mobile user i belonging in AF class j [23]. Based on (5.17), the ratio of inter-cell interference power to received power at the mobile host represent a

random variable that is the sum of lognormal variables. Although no exact closed-form expression for the probability density function of the sum of lognormally distributed random variables is known, it is widely accepted that the sum can be approximated by another lognormal distribution (in most cases the first two moments are used) [24]. Since the sum of lognormal variables can be approximated as a lognormal variable, the ratio can be approximated as a lognormal random variable with a mean value m_I (dB) and standard deviation value of σ_I (dB). With the same reasoning we can approximate the left hand side of inequality in (5.20) with another lognormal variable Z, since it represents the sum of i.i.d lognormal variables. Given the fact that $\widehat{Z} = 10\log(Z)$ is a normally distributed random variable, the outage probability can be written in a closed form as follows,

$$\mathrm{P_{out}} = \Pr\left[\widehat{Z} = 10\log(Z) > -10\log(n)\right] = Q\left(\frac{-10\log(n) - E[\widehat{Z}]}{\sqrt{var[\widehat{Z}]}}\right) \tag{5.21}$$

where $Q(y) = \int_y^\infty e^{-y^2/2} dy$

5.6 Performing Rate Truncation on the Out Of Profile Packets

If we assume different link gain threshold levels ϕ_j depending on the packet drop precedence, i.e, $j \in$ {green, yellow,red}, then based on the output of the TSWtcm the rate truncation scheme which depends on the actual link gain conditions can be written formally as follows,

$$R_i = \begin{cases} r_i & \text{if in-profile} \\ r_i & \text{if } g_i \geq \varphi_j \text{ and out-of-profile} \\ 0 & \text{if } g_i < \varphi_j \text{ and out-of-profile} \end{cases} \tag{5.22}$$

Assuming the P_R express the average received power, then the average required $-$ normalized, i.e, assuming required received power equal to one $-$ transmission power taking into account lognormal

shadowing and path loss can be written as [25],

$$P_T = P_R \cdot E\{1/g\} = P_R \left(\Pr[\text{in}] \int_0^\infty \frac{1}{s} P(s) ds + \Pr[\text{out}] \int_{\varphi_j}^\infty \frac{1}{s} P(s) ds \right) =$$

$$= P_R \left(\Pr[\text{in}] \int \int_{x^{-\mu} \cdot 10^{r/10} \geq 0} x^\mu \cdot 10^{-r/10} P(x,r) dr dx + \right.$$

$$\left. + \Pr[\text{out}] \int \int_{x^{-\mu} \cdot 10^{r/10} \geq \varphi_j} x^\mu \cdot 10^{-r/10} P(x,r) dr dx \right) =$$

$$= P_R \left(\Pr[\text{in}] \int_0^1 x^\mu \left[\int_0^\infty e^{-br} \frac{1}{\sqrt{2\pi}\sigma} e^{-\frac{r^2}{2\sigma^2}} dr \right] 2x dx + \right. \tag{5.23}$$

$$\left. + \Pr[\text{out}] \int_0^1 x^\mu \left[\int_{10 log_{10}(\varphi_j x^\mu)}^\infty e^{-br} \frac{1}{\sqrt{2\pi}\sigma} e^{-\frac{r^2}{2\sigma^2}} dr \right] 2x dx \right) =$$

$$= P_R e^{\sigma^2 b^2/2} \left(\Pr[\text{in}] + \Pr[\text{out}] Q \left(\frac{10 log_{10}(\varphi_j x^\mu)}{\sigma} + \sigma b \right) \right)$$

where

$$b = \ln 10/10 \text{ and } Q(\tau) \stackrel{\text{def}}{=} \frac{1}{2\pi} \int_\tau^\infty e^{-\frac{u^2}{2}} du$$

The probability that an out-of-profile packet with drop preference j and cutoff fade depth φ_j is transmitted would be,

$$\begin{aligned} p(\varphi_j) &= \Pr\{g_i \geq \varphi_j\} \\ &= \int \int_{x^{-\mu} \cdot 10^{r/10} \geq \varphi_j} P(x,r) dr dx \\ &= \int_0^1 \left[\frac{1}{\sqrt{2\pi}} \int_{\frac{10 log_{10}(\varphi_j x^\mu)}{\sigma}}^\infty e^{-\frac{u^2}{2}} du \right] 2x\, dx, \quad u = r/\sigma \\ &= \int_0^1 Q\left(\frac{10 \cdot log_{10}(\varphi_j x^\mu)}{\sigma} \right) 2x\, dx \end{aligned} \tag{5.24}$$

This probability gives the fraction of time that out-of-profile packets are actually transmitted and depends on the cut-off threshold φ_j and the link gain variations (σ). Based on whether or not the packet is delayed or actually dropped the following implementation can take place.

5.6.1 Rate Truncation with packet delay

In this case the out-of-profile packets will be delayed for a time period equal to the time that the channel remains below the cut-off threshold. If we assume that channel conditions are independent between sequential packet transmissions then the average number of packet transmission time intervals where the out-of-profile packet will cease transmission would be,

$$E\{n\} = \sum_{i=1}^{\infty} n(1 - \Pr\{g_i \geq \varphi_j\})^n = \frac{1 - \int_0^1 Q\left(\frac{10 \cdot log_{10}(\varphi_j x^{\mu})}{\sigma}\right) 2x\, dx}{\left(\int_0^1 Q\left(\frac{10 \cdot log_{10}(\varphi_j x^{\mu})}{\sigma}\right) 2x\, dx\right)^2} \tag{5.25}$$

Thus, if the packet size is equal to B bits and the bit rate equal $r_i$bps the average delay introduced would be,

$$E\{d\} = \frac{B}{r_i} E\{n\} \tag{5.26}$$

In this case, the average transmission rate that depends on the percentage of the out-of-profile and in-profile packets would be,

$$E\{R_i\} = \begin{cases} r_i & r_i \leq CIR \\ (1 - p_0)p(\phi_{green})r_i + p_0 p(\phi_{yellow})r_i & CIR < r_i \leq PIR \\ [1 - (p_1 + p_2)]\, p(\phi_{green})r_i + p_2 p(\phi_{yellow})r_i + p_1 p(\phi_{red})r_i & r_i > PIR \end{cases} \tag{5.27}$$

The released radio resources resulting from rate truncation of the out-of-profile packets can be characterized by the average power consumption savings. The aggregate power gains would be,

$$P_s = \begin{cases} \beta \sum_{j=1}^{\Theta-1} \sum_{i=1}^{n_j} i p_0 p(\varphi_{yellow}) P_T, & CIR < r_i \leq PIR \\ \beta \sum_{j=1}^{\Theta-1} \sum_{i=1}^{n_j} i[p_2 p(\varphi_{yellow}) + p_1 p(\varphi_{red})] P_T, & r_i > PIR \end{cases} \tag{5.28}$$

where

$$\beta = \frac{2e^{\sigma^2 b^2/2} Q(\sigma b)}{\mu + 2}$$

5.6.2 Rate Truncation with packet dropping

When packet dropping is performed in conjunction with rate truncation there will not be any additional delay imposed by the out-of-profile packets to the conformant packets. This is because the head of the line effect from a non-conformant packet ceasing transmission and delaying packets in the queue will be eliminated. The negative effect of dropping an out-of-profile packet is related to flows that use TCP as a transport protocol. TCP implements congestion control and avoidance mechanisms that interpret packet drops as congestion signals. Therefore, this scheme may affect the performance of TCP and can result in reduction of the achieved throughput.

5.6.3 Hybrid scheme – Rate Truncation with packet delay and dropping

In this scheme the advantages of both previous schemes can be combined to give more flexible management of non-conformant traffic. The benefit of the first scheme is that it allows transmission of all packets at the expense of delay, whereas the advantage of the second scheme is that it does not introduce delay but penalizes non-conformant traffic in the sense of dropping out-of-profile packets. In what follows, we briefly explain the algorithm of GRED and discuss how information from GRED can be used for the rate truncation algorithm. [4] GRED [26] is an improvement of RED (Random Early Detection) proposed in [27]. For every packet arrival, the average queue length $\bar{q}$ is updated as

$$\bar{q} \longleftarrow (1 - w_q)\bar{q} + w_q q$$

[4] Actually in the DiffServ environment there will be different GRED algorithms for the different packet colors

where q is the actual queue length and w_q controls the weight of exponential averaging filter. Based on this information GRED calculates the packet drop probability as

$$p_b = \begin{cases} 0 & \text{if } \overline{q} < \min_{th} \\ \max_p \left(\dfrac{\overline{q} - \min_{th}}{\max_{th} - \min_{th}} \right) & \text{if } \min_{th} \leq \overline{q} < \max_{th} \\ (1 - \max_p) \left(\dfrac{\overline{q} - \max_{th}}{\max_{th}} \right) & \text{if } \max_{th} \leq \overline{q} < 2\max_{th} \\ 1 & \text{if } \overline{q} > 2\max_{th} \end{cases} \tag{5.29}$$

by $\min_{th}$, $\max_{th}$ we denote the minimum and maximum threshold respectively and max_p is the maximum packet drop probability. Actually, GRED randomly drops a packet with probability p_a defined as,

$$p_a = \frac{p_b}{1 - count \times p_b} \tag{5.30}$$

where *count* is the number of packets that have arrived at a router since the last packet dropping. Assuming that this is the GRED algorithm applied for the red packets then in the proposed hybrid scheme we can combine the previous two schemes by introducing a maximum time interval T where out-of-profile packets can be delayed. If channel conditions remain below the threshold for a time interval greater than T, then the packet will be dropped. During this time interval, the packet will be dropped with probability p_a. In this case the algorithm takes also into account the average length of the queue as measured by GRED and increases according to the same algorithm the probability of dropping a packet when the network is congested. Equation 5.26 for the hybrid case can be written as $E\{d\} = \frac{P}{r_i} E\{n\} \leq T$. The probability that an out-of-profile packet actually being transmitted in this case is actually more difficult to be computed because it depends on the instantaneous queue size, $p_t = Prob[GRED_{drop}] \cdot Prob[n \cdot slot_d \leq T]$.

The benefit of the proposed hybrid scheme is that it can combine information from the active queue management algorithm, i.e, being cognizant of the current congestion situation, and channel conditions, to trade-off the delay introduced with packet dropping. For elastic applications, further observation reveals that this trade-off between packet dropping and delay can significantly increase the performance because this traffic is more prone to packet loss rather than packet delay. This is because elastic traffic mainly utilizes different flavors of the TCP protocol suite, where the actual

throughput obtained is heavily depended on the packet loss rate and it is less sensitive to RTT fluctuations (which can potentially lead to pre-mature timeout events) [27]. Dropping out of profile packets, as discussed in section 5.6.2, heavily influence the TCP state machine which will respond by drastically reducing the sending rate.

5.7 Experimental Results and Validation

A single cell CDMA network is considered and we focus on a single AF class that utilizes a constant fraction of the total transmitted power. The mobile hosts are uniformly distributed and the link gain is modelled as a distance dependent path loss of fourth power while the shadow fading factor is generated from a long normal distribution of zero mean and 8dB standard deviation. The maximum transmitted power of the base station is 30W and the receiver noise power ν is set to be 10^{-12}W for all mobile nodes. We consider downlink transmission in the system with a chip rate of W=3.84Mcps under the assumption that the radio link can support continuous transmission rates for specific target E_b/I_0 equal to 8 dB. We also assume that the buffer size in the access point to be infinite so that packet loss can only occur due to errors in the wireless channel. Table 6.1 summarizes the parameters used in the numerical investigations.

PARAMETER	VALUE
Total power	30W
Number of users (N)	16
noise, ν	$10^{-12}W$
Processing Gain [W]	3.84Mcps
Carrier frequency [MHz]	2000
Path loss exponent	4
σ of log-normal shadowing [dB]	8
Slot duration [msec]	10
MSS of TCP/UDP packets [bytes]	150
BER(φ) [DPSK]	$\frac{1}{2}e^{-\varphi}$
Number of AF classes	1

Table 5.1: Parameters for the numerical investigations

The optimization problem described in (5.11) has been numerically solved using the quasi-Newton BFGS (Broyden-Fletcher-Goldfarb-Shanno) method. The formula for the gradient of the objective

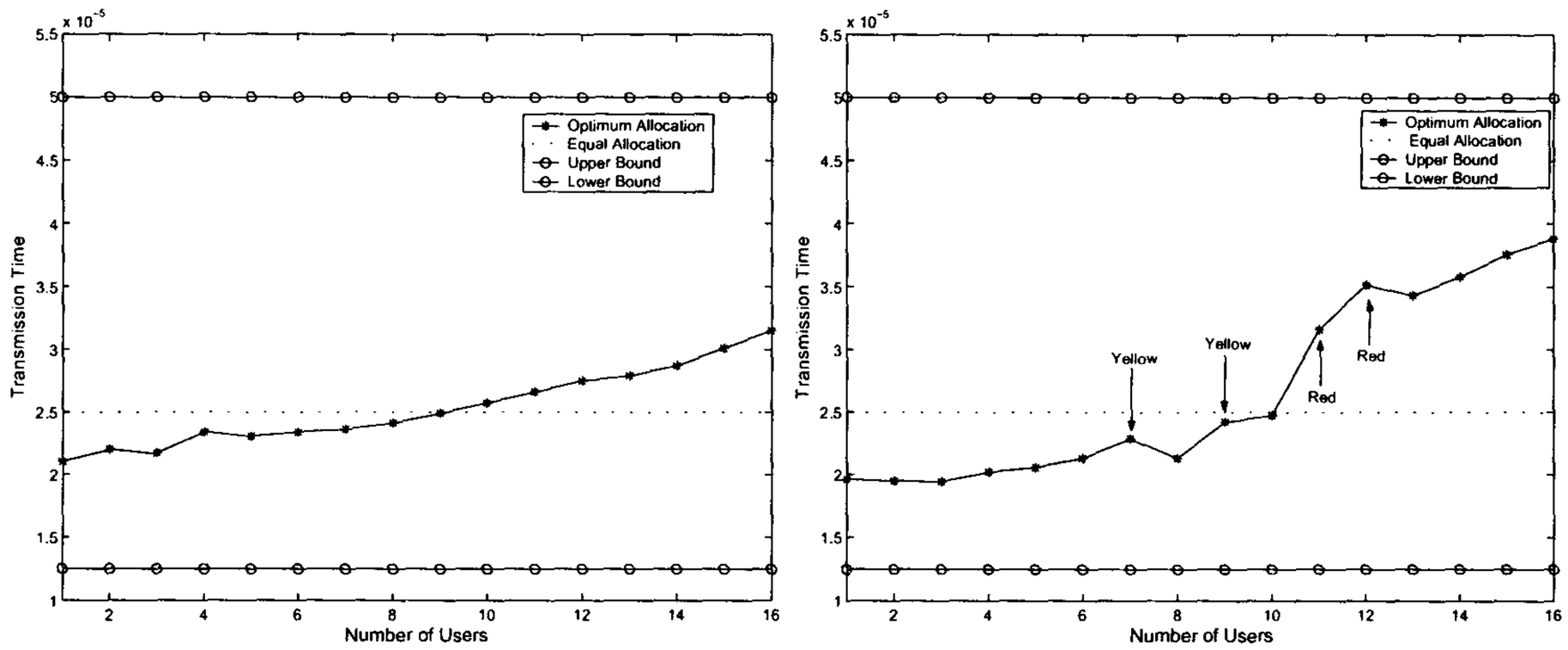

(a) (b)

Figure 5.7: (a) Optimum allocated transmission times with only green packets.(b) Optimum allocated transmission times when transmitting yellow packets for users 7, 9 and red packets for users 11 and 12.

function has been provided as a subroutine and thus the gradients have not been approximated numerically. Figure 5.7 shows the optimum allocation of transmission times for the N AF users which have been sorted based on the channel conditions and inter-cell interference. The aggregate transmission rate for the AF class has been set to 640Kbps, which give an average rate of 40Kbps per user. Figure 5.7(a) depicts the case when all the transmitted packets are marked as green, while 5.7(b) shows how transmission times are affected when a specific number of transmission packets, $K = 4$, have been marked as yellow and red assuming the same conditions. The bounds of the optimization problem control the worst case unfairness between active flows. As the distance between the bounds and the average transmission time is decreased so does the unfairness on assigned rates between flows. The additional delay introduced to the non-conforming traffic has been calculated based on channel conditions and inter-cell interference as has been shown in figure 5.5(a) in section 5.4. The upper and lower limits of the linear function are dynamically updated influenced by the best and worst channel and inter-cell interference of the N active users, while the $d\xi$ parameter has been chosen to be equal to 0.04τ (τ is the average transmission time). We should point out that not only the transmission times of the yellow or red packets are affected but the transmission time of all

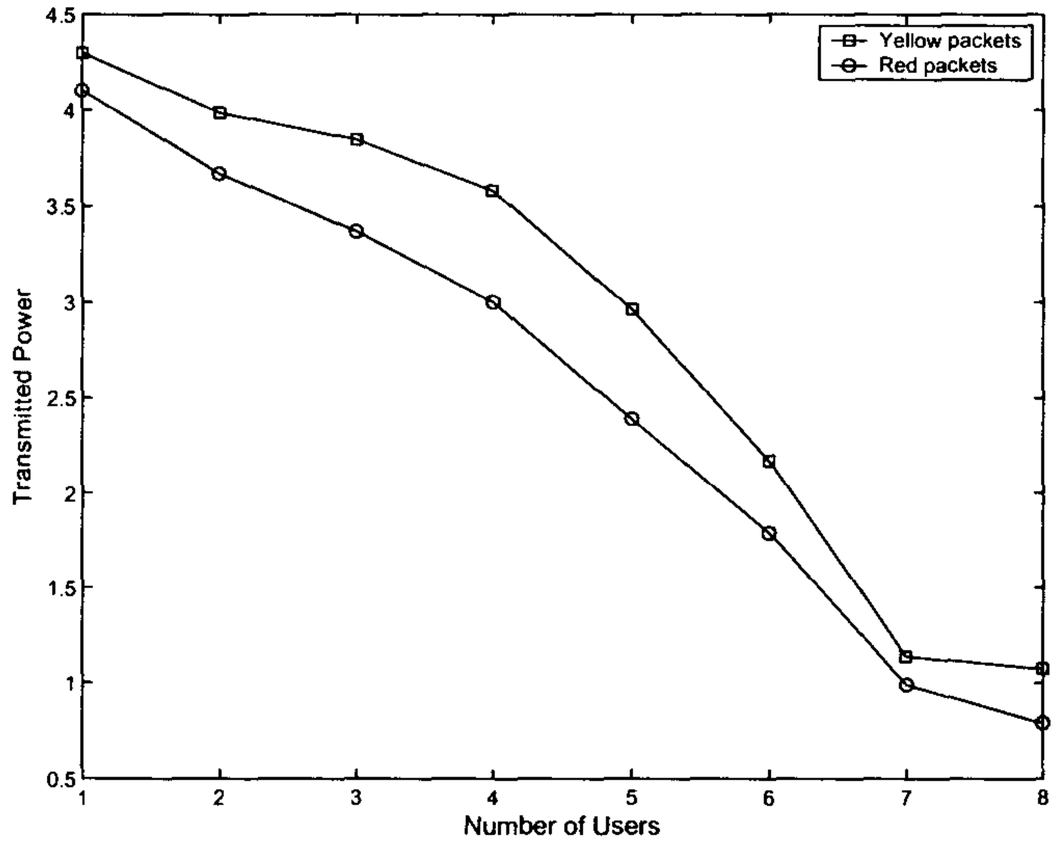

Figure 5.8: Consumed power for yellow and red packet transmission.

users. This should come by no surprise and the simple explanation of this behavior is based on the fact that the local (or global) minimum will not only change in the K-dimensional subspace defined by the yellow and red packets but in the whole N-dimensional space because they are not linearly independent. Figure 5.8 depicts the evolution of power consumption for eight users levels in the AF class when the packets transmitted are yellow or red. As the number of packets transmitted that correspond to non-conforming traffic increases the required power is decreasing. Under the same scenario, the required power consumption when all packets transmitted were in-profile (i.e, green) was 5.01W. Comparing this value with the case when all transmitted packets are red, which require the minimum possible power, we can see from figure 5.8 that power requirements can be reduced as much as 80%. The difference between the required power consumption for red and yellow packets can be controlled by the $d\xi$ parameter and this case was constant and equal to 0.04τ as in previous experiments.

By the same token, figure 5.9 depicts how the outage probability changes for one AF class when the normalized transmission rate changes in the interval $[0, 3\text{CIR}]$ for all eight users (having all the same rate at each transmission rate value). According to the TSWtcm algorithm the probability of

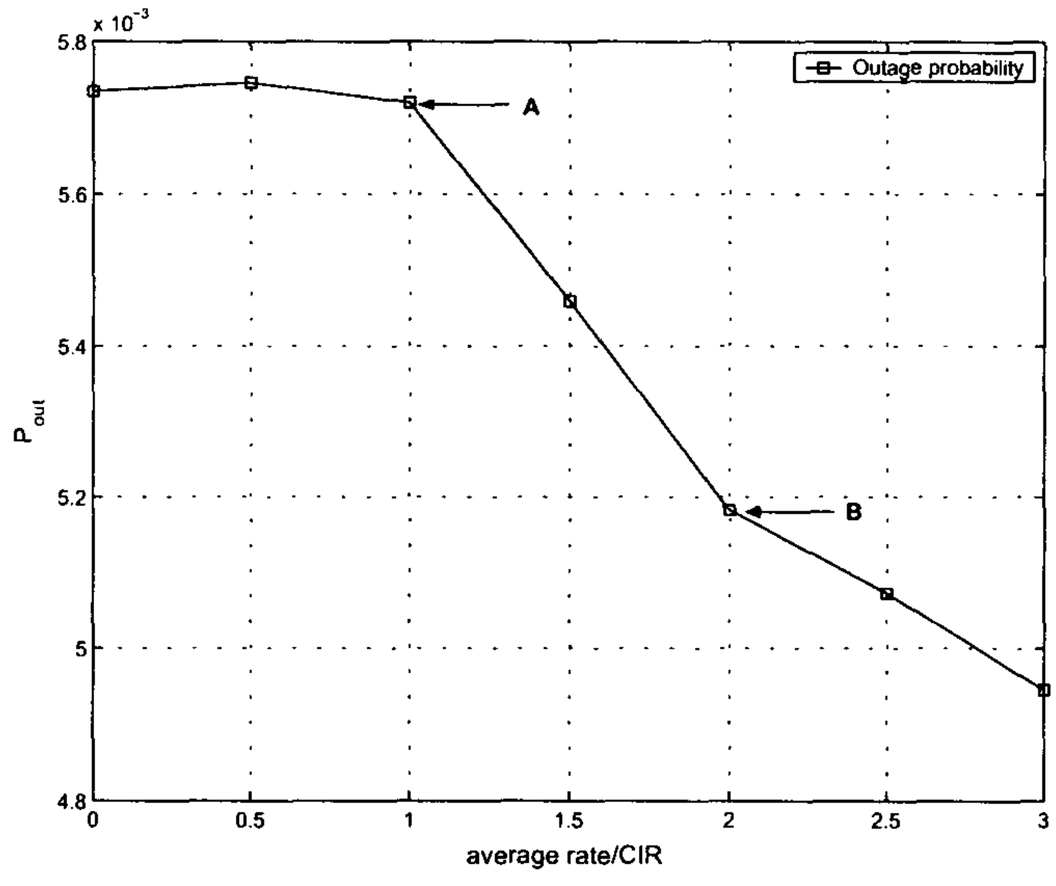

Figure 5.9: Outage probability as a function of the normalized transmission rate ($PIR = 1.5CIR$)

marking packets as yellow and red increases and thus the outage probability decreases depending on the mixture of conforming and non-conforming packets. As can be seen in the figure the outage probability calculated according to section 5.5 remains constant until the average rate reaches the CIR because there are only in-profile packets transmitted. If we compare the outage probability when all average rates are equal to CIR (point A in figure) with the case of transmission rates equal to two times the PIR (point B in figure) we see that the outage probability is reduced by 9%. Transmitting at twice the contracted PIR rate means, according to the TSWtcm algorithm, that only 50% of the packets will be marked as green while the other 50% will be equally split between yellow and red packets. The increased transmission times for the yellow and red packets as affected inside the optimization problem by the factors of ξ_y and ξ_r respectively explains why the outage probability decreases. In the case of rate truncation the corresponding average rate that takes into account the probability of transmission for packets marked as yellow and red is depicted in figure 5.10(a), (b) respectively. The average rate for the in-profile, i.e., green, packets that are transmitted independently of channel conditions, is shown in figure 5.11(a). Therefore depending on the chosen thresholds for the cutoff fade depth of the out-of-profile packets (yellow and red) their transmission is suppressed releasing resources for in-profile packets.

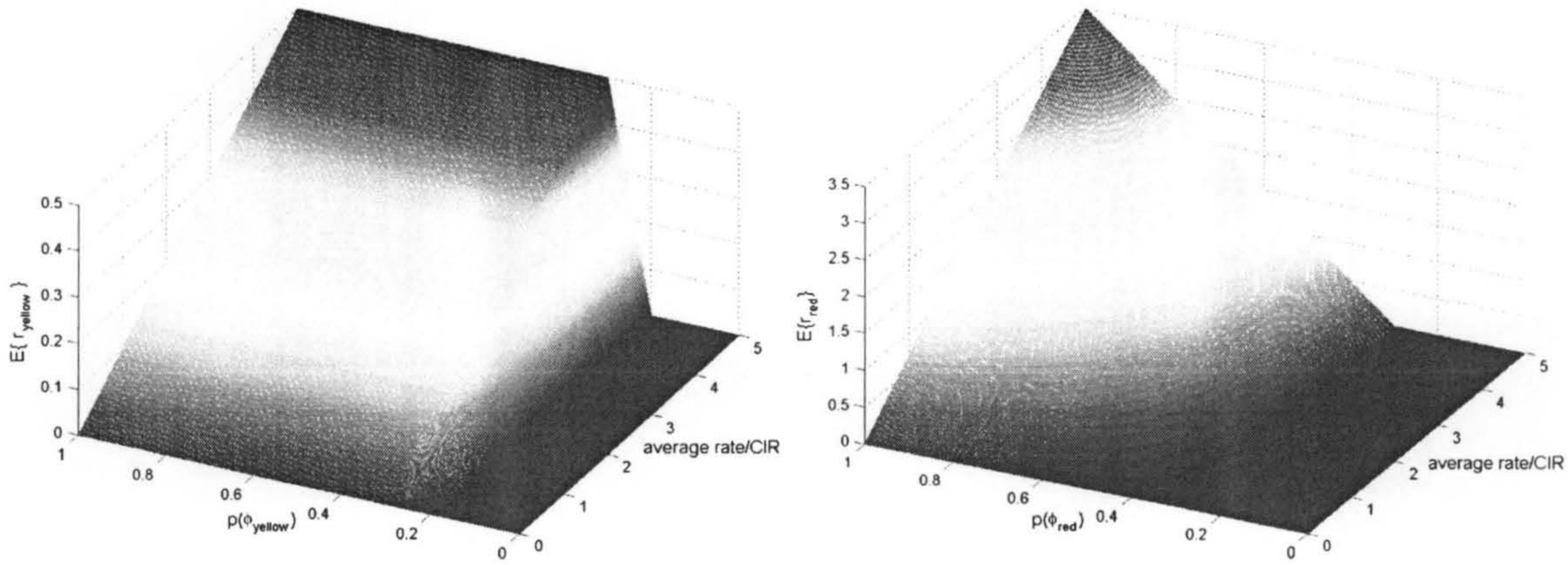

(a) (b)

Figure 5.10: The average transmission rate of yellow and red marked packets respectively as a function of the normalized incoming rate and probability of transmission($PIR = 1.5 \cdot CIR$)

Figure 5.11(b) depicts the difference between the power consumption for a single flow between the traditional approach, where link gains are compensated for all packets independently of drop precedence, and the proposed scheme where rate truncation is performed for the out-of-profile packets. Figure 5.11 indicates that for $\sigma = 10$dB, average rate equal to PIR and probability of packet transmission around 95% the power savings are approaching almost 25%. Finally, an important additional benefit of the proposed technique is that it discourages greedy sources to transmit out-of-profile packets (which are beyond the agreed SLA) because they provide no benefit to the mobile host.

5.8 Conclusions

Providing QoS in pure IP RAN's currently appears to have a chequered future. On one hand, per-flow and stateless approaches are still immature and clearly the pendulum has not settled in neither direction. On the other hand, research on the integration of IP level QoS information with resource management functionalities has been mainly considered independently. In that respect, research

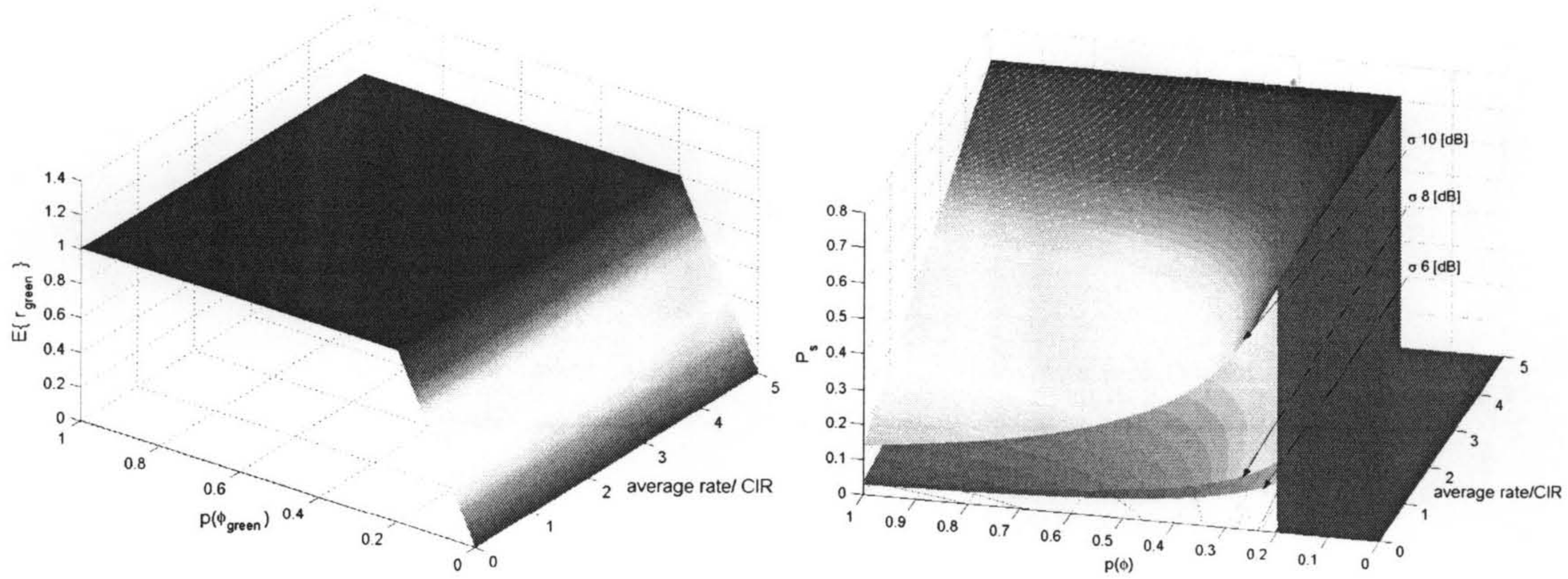

Figure 5.11: (a)The average transmission rate of green packets as a function of the normalized incoming rate and probability of transmission($PIR = 1.5 \cdot CIR$) (b) Power gains of the proposed rate truncation scheme as a function of the normalized incoming rate and probability of transmission for different background noise levels.

regarding how QoS information from the IP layer can be utilized within resource management functionalities is still in early stages. This chapter has focused on the second problem and proposes an approach for providing differentiated services and resource management in IP-based CDMA networks. The key aspect of the proposed scheme is that power and rate adaptation mechanisms are aware of the IP QoS requirements (forwarding plane of DiffServ). This higher degree of integration between the IP layer QoS mechanisms and radio network resource management leads to a better utilization of the scare resources of the air-interface.

Another interesting direction of research would be to adaptively share the resources between different AF classed to optimize utilization of the total available bandwidth. Additionally, this approach that penalizes non-conforming packets has the desirable side affect of reducing of the outage probability. The optimization problem considered here deals with aggregate rate and power consumption. Future ramifications of the current work will augment this model by also taking into account delay constraints. Finding the optimum trade-off between the consumed power and transmitting packet delay can actually be considered as a multi-objective optimization problem and would be of high interest to unfold the Pareto frontier.

Also a family of rate truncation algorithms has been presented for the out-of-profile DiffServ packets with different thresholds depending on the drop precedence of the packet. According to channel conditions and the percentage of out-of-profile DiffServ packets, rate truncation enhances the QoS experienced by the in-profile packets while at the same time providing significant aggregate power savings. An implicit feature of the proposed scheme is that greedy users are actually penalized and therefore are discouraged from violating contracted rates. Optimization or adaptation of the different threshold levels for performing rate truncation on the out-of-profile packets based on traffic conditions and the degree of congestion will be an issue of future research. In the next chapter a case study is presented of how higher layer information can be used for power and rate control by considering MPEG-4 streaming video transmission.

Bibliography

[1] S. Blake et. al., An Architecture for Differentiated Services, *RFC 2475, Internet Request for Comments, December 1998*

[2] V. Jacobson et. al. An Expedited Forwarding PHB, *RFC 2598, Internet Request for Comments, June 1999*

[3] J. Heinanen et. al. Assured Forwarding PHB Group, *RFC 2597, Internet Request for Comments, June 1999*

[4] R. Hancock et al. Next Steps in Signaling: Framework, *Network Working Group, Internet Draft, October 2003*

[5] D. Clark, W. Fang, Explicit Allocation of Best-Effort Packet Delivery Service, *IEEE/ACM Transaction on networking, 1998, 6(4): 362-373*

[6] W. Fang, N. Seddigh, B. Nandy, A time sliding window three colour marker (TSWtcm), *RFC 2859, June 2000.*

[7] 3^{rd} Generation Partnership Project, IP Transport in UTRAN - Work Task Technical Report, *TR 25.933, 2003*

[8] J. Zander, Performance of optimum transmitter power control in cellular radio systems, *IEEE Transactions of Vehicular Technology, vol. 41, pp. 5762, Feb. 1992.*

[9] S. A. Grandhi, R. Vijayan, D. J. Goodman, and J. Zander, Centralized power control in cellular radio systems, *IEEE Transactions of Vehicular Technology, vol. 42, pp. 466468, Nov. 1993.*

[10] G. J. Foschini and Z. Miljanic, A simple distributed autonomous power control algorithm and its convergence, *IEEE Transactions of Vehicular Technology, pp. 541646, 1993.*

[11] A. Sampath, P. Kumar, J. Holtzman, "Power control and resource management for a multimedia CDMA wireless system" *In Proc. IEEE PIMRC'95, pp.21-25, 1995*

[12] S. Ramakrisha and J. M. Holtzman, A Scheme for Throughput Maximization in a Dual-Class CDMA System, *IEEE J. Selected Areas in Commun., vol **16**, pp. 830-844, June 1998*

[13] S. J. Oh and K. M. Wasserman, Dynamic Spreading Gain Control in Multi-Service CDMA Networks, *IEEE J. Selected Areas in Commun., vol **17**, no. 5, pp. 918-927, 1999*

[14] R. Jantti and S-L. Kim, Transmission rate scheduling for the non-real-time data in a cellular CDMA system, *IEEE Commun. Letters, vol. **5**, no. 5, pp. 200-202, May 2001.*

[15] F. Berggren ,S-L. Kim, R. Jntti, and J. Zander , Joint power control and intra-cell scheduling of DS-CDMA nonreal time data, *IEEE J. Selected Areas in Commun., vol.**19**, no.10, pp. 1860-1870, Oct 2001.*

[16] R. Fantacci, S. Nannicini, Multiple access protocol for integration of variable bit rate multimedia traffic in UMTS/IMT-2000 based on wideband CDMA,*IEEE J. Selecte. Areas in Commun., vol. **18**, pp. 1441 - 1454, Aug 2000.*

[17] S. Choi and K. G. Shin, An uplink CDMA system architecture with diverse QoS guarantees for heterogeneous traffic, *IEEE/ACM Trans. Networking, vol.**7**, no. 5, pp.616-628, October 1999.*

[18] L. Wang, A.H. Aghvami, W.G. Chambers, Design Issues of Media Access Control (MAC) Protocols for Multi-media Traffic Over DS-CDMA Systems. *European Wireless 2002, pp. 151-160, Italy, 2002*

[19] D. I. Kim, E. Hossain, V. K. Bhargava, Downlink Joint Rate and Power Allocation in Cellular Multirate WCDMA Systems, *IEEE Transactions on Wireless Communications, Vol. 2, No. 1, January 2003*

[20] Ehab S. Elmallah, Hossam S. Hassanein, A Power-aware Admission Control Scheme for Supporting the Assured Forwarding Model in CDMA Cellular Networks, *Proceedings of the 27th Annual IEEE Conference on Local Computer Networks, (LCN 2002)*

[21] H. Holma, A. Toskala, WCDMA for UMTS, *Wiley, New York, 2000*

[22] S-L. Kim, Z. Rosberg, J. Zander, "Combined power control and transmission rate selection in cellular netrworks", *In Proc. of the* 49^{th} *IEEE VTC Fall Conference, Amsterdam, pp.1653-1657,1999*

[23] W. Choi and J. Y. Kim, Forward-link capacity of a DS/CDMA systsm with mixed multirate sources, *IEEE Transactions Veh. Technol., vol. 50, no. 3, pp. 737749, May 2001.*

[24] L. F. Fenton, The sum of log-normal probability distributions in scatter Transmission systems, *IRE Trans. Commun. vol. COM-8, pp. 57-67, March 1960*

[25] Sang Wu Kim, Andrea Goldsmith, Truncated Power Control in Code-Division Multiple-Access Communications, *IEEE Transactions on Vehicular Technology, Vol. 49, No. 3, May 2000*

[26] S. Floyd, Recommendations on using the gentle variant of RED, *available at* `http://www.aciri.org/floyd/red/gentle.html`, *May 2000*

[27] S. Floyd, V. Jacobson, Random Early Detection Gateways for Congestion Avoidance, *IEEE/ACM Transactions on Networking, 1(4):397-413, August 1993*

[28] J. Padhye, V. Firoiu, D. Towsley, J. Kurose, Modeling TCP Throughput: A simple model and its empirical validation, *In SIGCOM'98, September 1998*

Chapter 6

TFRC MPEG-4 Streaming Video via Power and Rate Control

In previous chapters a general framework for providing and utilizing higher layer information for resource management has been developed. As a case study of this proposed framework, in this chapter we articulate a power and rate adaptation scheme for MPEG-4 streaming video over RTP. The proposed scheme utilize information from the **TCP Friendly Rate Control** (TFRC) transport protocol and the type of MPEG-4 frame (i.e, Intra, Predictive or Bidirectional) together with lower layer criteria to optimize packet transmission over the wireless link. A multi-objective optimization problem is formulated based on the weighted sum of two competing objectives and is solved using derivative based optimization techniques. The first objective expresses the absolute difference between the required transmission rate, as defined by the TFRC and the allocated rate, the second is the total consumed power.

Furthermore, in the proposed scheme, the allocated bit-energy-to-interference-power-spectral-density ratio, E_b/I_0, depends on the type of video frame being transmitted. Based on a derived condition for optimal allocation, heuristic allocation is performed. Finally, through simulation results the proposed scheme is evaluated and possible different ramifications of the scheme are discussed.

6.1 Introduction

Providing effective ubiquitous connectivity to Internet services such as streaming video over 3G and beyond wireless networks is anticipated to be of critical importance to network operators. The high volume and rate variability of streamed video traffic together with the corresponding timing constraints call for adaptive resource allocation algorithms that utilize information from the video flow to achieve efficient utilization of the resources over the wireless link. Notwithstanding the importance of video streaming delivery, efficient resource management schemes for multiple video streams that utilize information from the encoded video stream for efficient packet transmission in an all IP-based 3G network infrastructure has attracted less attention than per-flow optimization of video transmission.

Video streaming over wireless channels is challenging because of the fluctuations of the radio link, the scarcity of wireless resources and stochastic user mobility. Therefore, the peculiarities of the wireless transmission medium raise a number of interesting issues on how to optimize packet transmission. Even though there has been extensive research efforts to enhance per flow video transfer over both the Internet and wireless networks, joint optimization of different video flows from a radio resource management perspective have attracted little attention. The proposed techniques that aim to enhance perceived video quality can be grouped into three different approaches. The first one is through retransmission based error recovery (REC) [1], [2]. The main motivation behind these schemes is that even though a retransmitted packet can arrive after the play-out delay it can still be used to reduce the effect of error propagation. The second category focus on the utilization of Forward-Error-Correction (FEC), in the sense of joint source-channel coding techniques. The idea here is that of combining scalable coding with unequal error protection (UEP) in order to achieve a graceful degradation of the quality [3], [4], [5], [6]. Layer coding finally, has been used to partition the video stream into different layers and to protect each layer independently [7]. This approach is interesting as it can utilize the Fine Granular Scalability (FGS) mechanisms of MPEG-4 video [8].

In this chapter, and in relation to the previous mentioned work, a different path is followed for optimizing transmission of streamed video over wireless. In this case, video encoding related information is utilized by the resource management controller in the radio access network to optimize packet transmission over the wireless interface. Therefore, the problem to be considered is the

optimization of resource usage for multiple video streaming flows. In that respect, a novel power and rate adaptation approach is proposed that integrates information from the RTP packet header such as required transmission rate from the TFRC and the type of frame. With CDMA being the incumbent standard for 3G networks (ARIB/ETSIs W-CDMA [9] or TIAs cdma2000 [10]), one of the most critical components for radio resource management in such networks is power control. As already mentioned in the previous chapters, power control has been extensively studied in recent years and a number of different solutions have been proposed [11], [12], [13], [14]. In some previously developed MAC protocols that aim to support multi-media traffic over DS-CDMA systems [15], [16], [17] the focus was on link layer performance in terms of throughput and/or delay. These MAC protocols are agnostic to the different transport/application protocols that are used to carry the traffic. Therefore the above schemes, cannot use selective information from higher layer protocols to optimize the transmission across the air-interface. Also in [18] an adaptive rate allocation scheme have been proposed by modelling the Signal-to-Interference ratio (SIR) but the authors did not discuss the performance observed by higher layers. In [19] the authors propose a joint source coding and data rate adaptation scheme using Lagrangian relaxation and Dynamic Programming. The aim of the proposed scheme was to provide energy efficient video transmission subject to video quality and delay constraints. As a result, tradeoffs between packetization, source coding, rate control and scheduling have been considered. Additionally, in [20] theoretical tradeoffs between average power consumption and average queueing delay constraints have been studied. The main characteristic of the proposed adaptive power and rate adaptation scheme described in this chapter is that it explores information both from the transport layer (i.e., the required rate from the TFRC) and the application layer (i.e., type of frame carried by the packet under transmission).

The rest of the chapter is organized as follows. In section 6.2 background information on MPEG-4 video encoding is presented, together with the corresponding issues on carriage of MPEG-4 content over IP and the use of TCP friendly protocols in conjunction with video streaming. In section 6.3 a review of resource management in CDMA networks is presented with emphasis on the minimum power allocation vector. This is followed by section 6.4, where the proposed power and rate adaptation scheme is presented and in section 6.5 experimental results are reported. Finally, the paper closes with the conclusions in section 6.6.

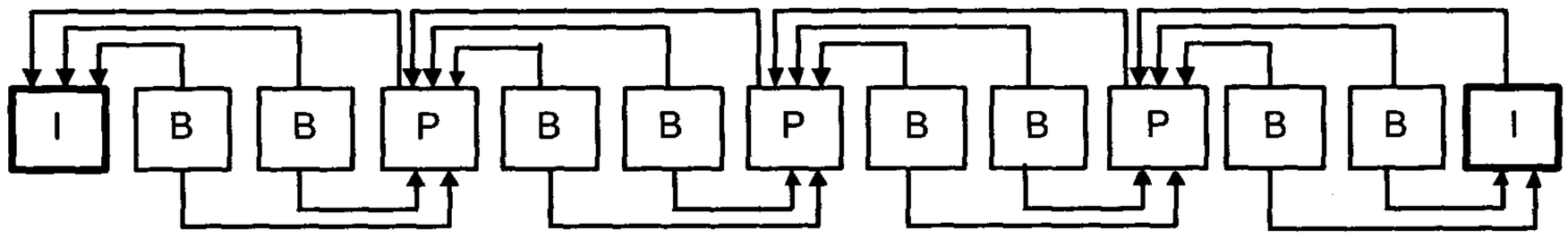

Figure 6.1: The dependency between Intra (I), Predicted (P) and Bi-directional (B) frames in MPEG-4.

6.2 MPEG-4 Object Based Streaming

The strength of MPEG-4 stems from its radical object-oriented paradigm, which has been considered to be of critical importance for wireless networks with limited resources. This is because low bit-rates can be accommodated by the use of scalable objects in MPEG-4. The MPEG-4 scene consists of a number of audio and video media objects. Several of them are typically background, such as audio clips or static images. The information for each streaming media object is brought within one or more elementary streams. The basic object in MPEG-4 is a Video Object Plane (VOP), which in general can have any shape. The VOP term is used in MPEG-4 instead a frame, but because the analysis in this paper involves only one layer the terms VOP and frame are used interchangeably. Mainly, the object oriented approach of MPEG-4 allows scaling of video transmission, where the base layer conveys all the information in some basic quality, and one or more enhancement layers can be used to get a higher quality picture if network resources are available. When a scene is composed of different objects, it is even possible to send only the most important of them. This kind of scalability makes MPEG-4 a very strong candidate for delivering video over 3G wireless networks which have limited resources. The approach also allows unequal error protection, i.e., protecting the most important objects best. The MPEG standard defines four distinct encoding pictures: Intra-coded Picture (I-Picture), Predictive- Coded Picture (P-Picture), Bidirectional-Predictive-Coded Picture (B-Picture) and DC-Coded Picture (D-Picture). The I-Picture is coded using information only from the picture itself. The P-Picture is coded using motion compensation prediction in reference to a previous I-Picture or another P-Picture. B-Picture is coded in reference to either previous or future I-Pictures or P-Pictures. Finally, the D-Picture stores the DC component of each Discrete Cosine Transform (DCT) block. The I, B and P pictures are arranged in a periodic pattern known

as a Group of Pictures (GOP). Figure 1 shows the GOP of MPEG-4 video that we used in our experiments, and the relationships among pictures. The MPEG-4 Group of Pictures (GOP) is made of 12 frames in the following order: IBBPBBPBBPBB. The first two B pictures (2 and 3) are bidirectionally coded using the past frame (I frame 1) and the future frame P (frame 4). Therefore, each B picture is encoded based on the previous and following I and/or P pictures. P pictures on the other hand are dependent of previous I or P pictures. It is worth mentioning that because of these dependencies the decoding order will be different from the encoding order. The P frame 4 must be decoded before B frames 2 and 3, and I frame 1 (the last I frame) before B frames 11 and 12. Therefore, the actual MPEG-4 video transmission sequence order over the wireless link would be 1, 4, 2, 3, 7, 5, 6, 10, 8, 9, 1, 11, and 12. From figure 6.1 and the above discussion about the dependencies between different frames, it is easy to conclude that I-Pictures are the most important ones since they contain the actual video content and all other pictures are error-coded based on the I frames. In the probabilistic model that will be developed in the sequel, which is based exactly on the dependencies between different frame types, we will assume an open GOP model. Finally, if by N_P we denote the number of P frames in the GOP and by N'_B the number of B frames between two P frames then the number of B frames will be $N_B = (1 + N_P) \times N'_B$.

6.2.1 MPEG-4 over IP

The specifications on the carriage of MPEG-4 contents over IP networks mainly involve standardization efforts on the payload format of the Real Time Protocol inside IETF. Currently, in the Audio/Video Transport (avt) working group in IETF, the efforts related to MPEG-4 transport over IP are reflected in a vast number of RFC's and Internet Drafts.

Real-Time Transport Protocol (RTP)

RTP [28] provides end to end delivery services to support applications transmitting real-time data. Services provided include payload type identification, sequence numbering, timestamping and source identification. RTP does not include any functionalities to transfer packets across the network and assumes that other transport layer protocols such as TCP or UDP are available. Thus, we should stress that RTP is an application layer protocol and not a transport protocol since RTP headers are

created by the sending application, before the packet is further encapsulated by a transport protocol. However, packetization using RTP instead of some proprietary standard, enhances interoperability between different applications. In order to support TFRC functionalities, the RTP protocol need to be modified to include additional information such as bit-rate and round trip time [29]. In the proposed scheme we assume that the radio network controller has access the the header fields of the RTP protocol.

Real-Time Control Protocol (RTCP)

Periodically, feedback on the quality of the media distribution is provided to the sender, using the control plane of RTP which is the Real-Time Control Protocol (RTCP) [28]. The feedback is in the form of a report that includes statistical information such as fraction of packets lost since the last report was sent, cumulative number of packets lost since the beginning, and interarrival jitter. The RTCP can be seen as the natural candidate to transport feedback from a TFRC receiver. Despite this fact, to include TFRC information in RTCP, the timing for sending these reports must be changed to a time scale close to that of a RTT interval. To achieve feedback of information in such small time scales the RTCP protocol may need to be modified. Because the algorithm that is used in the standard requires that traffic reports should be restricted to 5% of the session bandwidth, with the control bandwidth split between the sender and the receivers at a ratio of 3:1. The frequency of feedback information from the receiver to the TFRC sender is still an open issue. For example, video streaming over wireless with a data rate of less than 5Mbps may require transmitting RTCP packets at higher frequency than the recommended minimum interval [30].

TCP–Friendly Rate Control (TFRC)

TFRC is a rate regulation algorithm that allows a non-TCP connection to behave similarly to a TCP connection under the same network conditions. Therefore, a TFRC connection reacts to congestion in the network, which are indicated by packet losses, in a similar but smoother fashion to TCP. To accommodate this, the TFRC sender estimates network conditions by exchanging control packets between the end systems and collecting the feedback information using RTCP functionalities as mentioned in the previous section 6.2.1. The TFRC sender may transmit one or more control packets

to the sender in a RTT horizon and upon receiving the control packet the receiver returns feedback information required for calculating RTT and packet loss probability p. The sender then derives the estimated throughput of a virtual TCP connection which would have competed for bandwidth on the same path that the TFRC connection traverses. For connections with large bandwidth-delay products, where the probability of a timeout event is very small, it has been shown that the following, so-called *square root formula*, can model accurately the actual throughput [21]

$$T = MSS \cdot \min\left[\frac{1}{\overline{RTT}}\sqrt{\frac{c}{p}}, \frac{W_{\max}}{\overline{RTT}}\right] \tag{6.1}$$

where MSS is the maximum segment size, W_{max} the advertised receiver window size, $\overline{RTT}$ denotes the average RTT of the connection, c is a constant that depends on the version of the TCP used and the process of inter-loss times [26] and p is the probability of packet loss (packet loss ratio). Actually, for TFRC a more accurate model of TCP throughput is used [27], that takes into account the effect of timeout events T_o,

$$R_{\mathrm{TCP}} = \frac{\mathrm{PacketSize}}{\overline{RTT}\sqrt{\frac{2p}{3}} + 3T_o\sqrt{\frac{2p}{8}}p(1+32p^2)} \tag{6.2}$$

The above equation gives the allowed rate for non-TCP traffic to achieve a fair allocation of the available bandwidth between different flows and it is envisioned that for real implementations this would be given in a look-up table format. We should note that TFRC is not a transport protocol per se, thus, it should be deployed together with a transport protocol such as UDP. Finally, an important point to emphasize is that for video streaming over wireless there can be two different sources of packet loss. The first one is caused by congestion in the wireline part of the path and the second one by impairments in wireless channel. Concerning TCP, there are several proposals for loss differentiation [22], [23], [5], which they can also be adapted for TCP-friendly protocols. Loss differentiation schemes for TFRC are currently attracting wide research attention – especially for end-to-end solutions – because efficient loss differentiation algorithms can increase the performance of the application (see [25] and references therein).

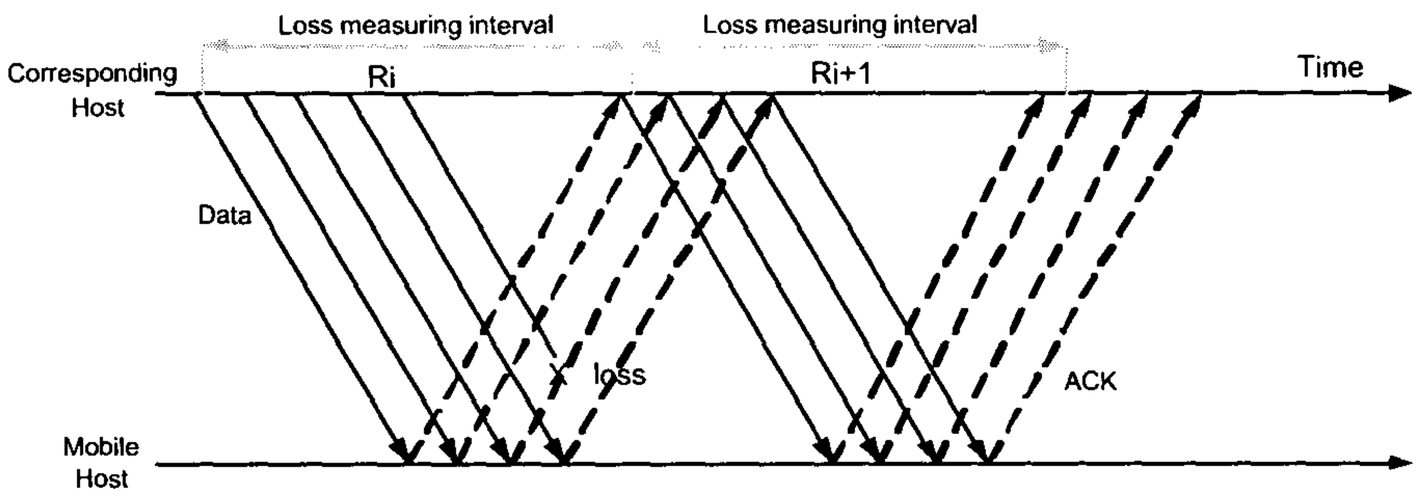

Figure 6.2: Measuring interval of losses for TCP-friendly rate control.

6.3 Resource Management

As in the previous chapters, we consider a single cell CDMA network with n_j active mobile nodes (this number can also be considered as an admission feasibility policy which is based on user requirements). The chip rate for all users is fixed, the total bandwidth W is shared among all users and the IP packets are considered to be of constant size (P bits). The emphasis will be on the downlink transmission where the maximum transmission power at the access point is equal to $p_{\max}$. A small time interval Δt is considered such that the link gain between each mobile i and the access point is stationary and given by g_i $(1 \leq i \leq N)$. For a given power vector $\mathbf{p} = (p_1, p_2, ..., p_N)^T$, and by making the standard Gaussian approximation for the statistics of the inter-cell and intra-cell interference, the received SIR of mobile i,is defined by:

$$\mathrm{SIR}_i(\mathbf{p}) \stackrel{\text{def}}{=} \frac{g_i p_i}{\theta_i \cdot g_i \sum_{j \neq i} p_j + I_i + \nu}, \; 1 \leq i \leq N \tag{6.3}$$

Where $\nu > 0$ and I_i is the lumpsum power of background, thermal noise and the inter-cell interference respectively at the mobile host i. The orthogonality factor, θ_i, depends mainly on the multipath effects and throughout the paper will be considered as constant for all mobile hosts. Typical values for the orthogonality factor are between $[0.1, 0.6]$, for more details see [9]. We assume a generic framework where video streaming traffic belongs to a specific DiffServ class (different classes can in general have different bit-energy-to-interference-power-spectral-density ratio, E_b/I_0 requirements) which utlize a constant fraction of the total available power at the base station. With a per class

target $(E_b/I_0)_j = \Gamma_j, 1 \leq j \leq \Theta$ at the receiver, which gives a constant bit-error independent of the bit-rate, the relationship between rate r_i and SIR (denoted as γ_i hereafter for notation convenience) will have the form:

$$\frac{r_i}{\gamma_i} = \frac{W}{\Gamma_j} \tag{6.4}$$

With a predefined assignment of γ_i targets, the power vector that supports every mobile with the minimum power can be found by solving the linear system of equations in (6.3),

$$p_i^* = \frac{\gamma_i}{1+\theta\gamma_i}\left(\frac{\sum_{j=1}^{N}\frac{\theta\gamma_j}{1+\theta\gamma_j}\frac{I_j+\nu}{g_j}}{1-\sum_{j=1}^{N}\frac{\theta\gamma_j}{1+\theta\gamma_j}} + \frac{I_i+\nu}{g_i}\right) \tag{6.5}$$

Additionally, the constraint of the maximum transmission power on the downlink (i.e, in CDMA the downlink is considered to be *power limited*) can be formally written as,

$$\sum_{i}^{N} p_i \leq p_{\max}, \text{ with } N = \sum_{j=1}^{\Theta} n_j \tag{6.6}$$

6.3.1 Minimum Power Consumption

Based on the discussions on previous chapters, we have already explained that the above derived minimum power vector, i.e equation (6.5), assumes an arbitrary allocation of target $SIRs$. Therefore, the optimum feasible allocation of rates (or $SIRs$) that would provide throughput, $\widetilde{R}$ in the target cell will be the result of the following optimization problem,

$$\begin{aligned} &\min_{p,\gamma} \quad \sum_{i=1}^{N} p_i \\ &\text{subject to} \quad \sum_{i=1}^{N} p_i \leq p_{\max} \\ &\sum_{i=1}^{N} r_i = \widetilde{R}, \left(\frac{E_b}{I_0}\right)_j = \Gamma_j, \quad 1 \leq j \leq \Theta \end{aligned} \tag{6.7}$$

Using equations (6.4), (6.5) and (6.6) the above problem can be solved in terms of target $SIR's$ as follows,

$$\min_{\gamma_i} \quad \frac{1}{1-\sum_{i=1}^{N}\frac{\theta\gamma_i}{1+\theta\gamma_i}} \sum_{i=1}^{N} \frac{\gamma_i}{1+\theta\gamma_i} \cdot \frac{I_i+\nu}{g_i}$$

$$\text{subject to} \quad \sum_{i=1}^{N} \frac{\gamma_i}{1+\theta\gamma_i} \cdot \frac{I_i+\nu}{p_{max}g_i} \leq 1 \tag{6.8}$$

$$\sum_{i=1}^{N} \gamma_i = \widetilde{\gamma}, \quad \left(\frac{E_b}{I_0}\right)_j = \Gamma_j, \quad \forall\, j,i$$

Based on this analysis, we define next the proposed power and rate adaptive scheme that incorporate information from the TFRC and type of frame of the MPEG-4 video.

6.4 A Joint MPEG4–TFRC aware Power & Rate Adaptation Scheme

Contemporary video coding, such as MPEG-4 uses predictive coding which is sensitive to error propagation (the same is true also for H.263). Because the Intra frames are utilized by the motion compensated prediction algorithms and therefore errors inside these frames has as a net effect a possible propagation of errors both in the temporal and spatial domain. MPEG-4 especially, is based on a motion-compensation and variable-length coding (VLC) scheme to reduce temporal and statistical redundancies between frames. These techniques lead to better compression ratios but the quality is susceptible to transmission errors. Even though errors that occur in VLC coded symbols are mainly responsible for synchronization errors and are of great importance for the end user perceived quality of service, we will rather focus in this paper on error propagation between frames. In that sense, the perceived quality of the decoded video stream on the mobile user site is heavily affected by the degree of erroneous reception of the intra-coded images (I-frames). Predictively coded images (P-frames) are also important because bi-directional coded images (B-frames) are decoded based on I or P frames. Thus, in MPEG-4, since loosing an I-frame would cause distortion on all frames in

the GOP, these intra-coded images contain vital information that should be protected. If there is a P-frame this will only affect adjacent B-frames and finally erroneous reception of a B-frame would not affect other frames.

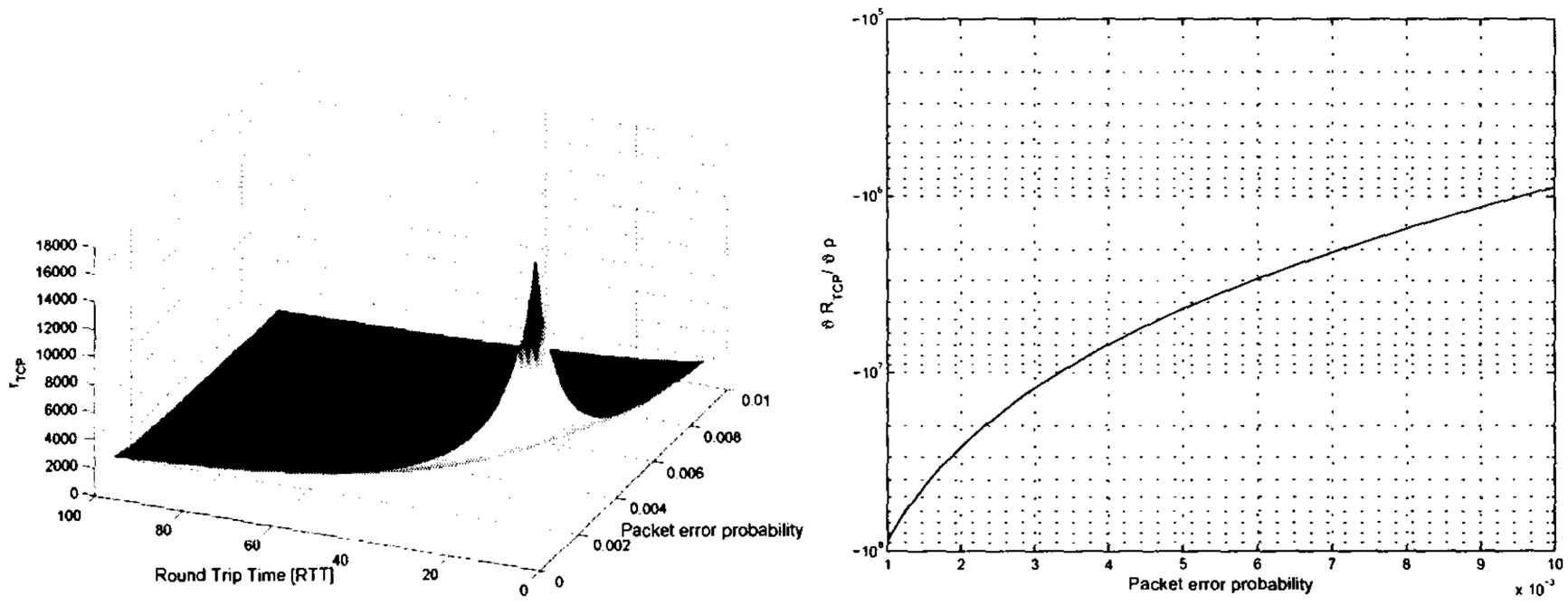

Figure 6.3: (a) TCP Friendly rate adjustment as a function of the RTT and the probability of packet in error - MTU = 500bits (b) Gradient of the TCP-friendly rate adjustment with respect to the packet error probability $\left(\frac{\vartheta R_{TCP}}{\vartheta p}\right)$

On the other hand, since the bit-rate of streaming video is controlled by a TCP-friendly algorithm, flows with a small transmission rate should be protected because an increase in the measured accumulated error will result in additional decrease on the transmission rate as given by the TFRC. It is clear that the packet error rate during the specific measured interval is of high importance. If for the sake of illustration we assume the case of an additive white Gaussian noise channel (no-fading) the bit error rate can be given as a function of the received $\Gamma = Eb/No$ [1], i.e,

$$P_b = f(\Gamma)$$

If we assume no error detection and correction capabilities the bit errors are i.i.d and the the packet

[1] For example in the case of DPSK (Differential Phase Shift Keying) modulation $f(\Gamma) = \frac{1}{2} \cdot e^{-\Gamma}$, or for BPSK/QPSK $f(\Gamma) = \frac{1}{2} \cdot erfc(\sqrt{\Gamma})$, where $erfc(.)$ is the complementary error function.

error probability can be written as,

$$P_e = 1 - (1 - P_b)^L$$

where L is the number of bits per packet. If the error correction capability of the error correcting code is c bits, then the probability that a packet is received successfully, under the assumption that the errors in the packet occur independently, would be:

$$P_e(\Gamma) = 1 - \sum_{j=0}^{c} \binom{L}{j} P_b^j (1 - P_b)^{L-j}, \tag{6.9}$$

Having this in mind, the previously presented argument can now be explained thoroughly using figure 6.3. The left graph 6.3(a) represents how the transmission rate is updated as a function of the RTT and probability of packet loss as given by equation 6.2. As can be seen in the figure, for the range of packet error rates of interest ($0.5\% - 4.8\%$ or $10^{-6} - 10^{-5}$ in terms of bit-error-rate) the permutations of the transmission rate are very significant. This sharp change on the transmission rate is more clearly shown in figure 6.3(b) which depicts the gradient of the R_{TCP} with respect to the probability of packet error. Therefore, it is crucial to differentiate and protect, in terms of E_b/N_o value or FEC streaming video flows with small transmission rate so as to avoid any sharp reduction in their rate which would result in degradation of the perceived video quality.

The proposed power and rate adaptation scheme utilizes information from both the transmission rate of the TCP-friendly flows and the type of video frame transmitted (I, P or B).

6.4.1 Differentiation of E_b/N_o value based on the type of frame

In order to differentiate target E_b/N_o values for packets carrying different types of frame, we first analyze the influence that erroneous frames have in the probability of successful decoding of a GOP. If we assume that n packets in error result in a non displayable frame, then the probability that an I frame is correctly displayed can be written as

$$P(I_S) = 1 - \sum_{i=n}^{S_I} \binom{S_I}{i} p^i (1 - p)^{S_I - i} = 1 - p_I$$

where S_I expresses the number of packets in the I frame. With the same reasoning, and based on the interdependencies between the different type of frames as discussed in section 6.2, the probability of the successful display of a P and B frame can be written as follows (similarly, S_P, S_B express the number of packets in the P and B frame respectively),

$$P(P_{1,S}) = P(I_S)\left[1 - \sum_{i=n}^{S_P}\binom{S_P}{i}p^i(1-p)^{S_P-i}\right] = P(I_S)\left[1-p_P\right]$$

$$P(P_{i,S}) = P(P_{(i-1),S})\left[1 - \sum_{i=n}^{S_P}\binom{S_P}{i}p^i(1-p)^{S_P-i}\right] = P(P_{(i-1),S})\left[1-p_P\right]$$

$$P(B_{0,j,S}) = P(I_S)P(P_{1,S})\left[1 - \sum_{i=n}^{S_B}\binom{S_B}{i}p^i(1-p)^{S_B-i}\right] = P(I_S)P(P_{1,S})\left[1-p_B\right]$$

$$P(B_{i,j,S}) = P(P_{i,S})P(P_{(i-1),S})\left[1 - \sum_{i=n}^{S_B}\binom{S_B}{i}p^i(1-p)^{S_B-i}\right] = P(P_{i,S})P(P_{(i-1),S})\left[1-p_B\right]$$

$$P(B_{N_p,jS}) = P(I_S)P(P_{N_p,S})\left[1 - \sum_{i=n}^{S_B}\binom{S_B}{i}p^i(1-p)^{S_B-i}\right] = P(I_S)P(P_{N_p,S})\left[1-p_B\right]$$

The probability of successful packet transmission is a non-decreasing function of the E_b/N_o value and depends on the modulation/demodulation scheme and the channel coding algorithm that is used. Based on the above discussion the probability of successful display of the GOP can be written as,

$$\begin{aligned} P'(GOP_S) &= \prod_f P'(f_S) \\ &= \prod_{i,j} P'(I_S)P'(P_{i,S})P'(B_{i,j,S}) \end{aligned} \tag{6.10}$$

By taking the logarithm of the above equation we have,

$$\log P'(GOP_S) = \log P'(I_S) + \sum_{i=1}^{N_p}\log P'(P_{i,S}) + \sum_{i=0}^{N_p}\sum_{j=1}^{N_{\hat{B}}}\log P'(B_{i,j,S}) \tag{6.11}$$

because $\log x$ is monotonic increasing in $\{x|x > 0\}$ the analysis will hold equivalently for the following equation where we have dropped the logarithms,

$$\begin{aligned} P(GOP_S) &= \sum_f P(f_S) = \\ &= P(I_S) + \sum_{i=1}^{N_p} P(P_{i,S}) + \sum_{i=0}^{N_p} \sum_{j=1}^{N_{\hat{B}}} P(B_{i,j,S}) \\ &= P(I_S) \left\{1 + P(P_S) + [P(P_S)]^2 + [P(P_S)]^3\right\} + [P(I_S)]^2 P(B_S) P(P_S) \left\{1 + 2[P(P_S)]^2 + [P(P_S)]^4\right\} \end{aligned} \tag{6.12}$$

Under the assumption of the same probability of losing a packet among different frame types, the probabilities p_I, p_P and p_B depend on the number of packets in each frame and the number of packets in error that lead to an erroneous frame decoding. Without loss of generality and to simplify the notation and analysis we will assume now that these probabilities are equal. In that case, the probability of successful display for the different frames types would be, $P(I_S) = 1 - p_I$, $P(P_S) = 1 - p_P$ and $P(B_S) = 1 - p_B$. Using the above analysis we can now show that differentiation of E_b/N_o values between different frames can increase the aggregate probability of successful GOP decoding as shown in equation 6.12.

Proposition 6.4.1. *Let us assume a specific pattern of GOP such as the one shown in figure 6.1. Then, among the target - constant - $(E_b/N_o)_t$ values, the ones that satisfy the inequality*

$$(E_b/N_o)_I \geq (E_b/N_o)_P \geq (E_b/N_o)_B \tag{6.13}$$

under the constraint of $E\{(E_b/N_o)_I + (E_b/N_o)_P + (E_b/N_o)_B\} = (E_b/N_o)_t$ increases the $P(GOP_S)$ which is equivalent of increasing the aggregate probability of successful GOP decoding ($P'(GOP_S)$).

Proof. As mentioned before the probability of packet error is a non-decreasing function with respect to (E_b/N_o) value and we can assume that the target $(E_b/N_o)_t$ value leads to a packet error equal to p. A constant (E_b/N_o) value means that $p_I = p_P = p_B = p$ and the probability of successful GOP decoding would be $P_c(GOP_S)$. From the different possible allocations that satisfy equation 6.13 and the corresponding constraints we can define one such as $p_I = p - \psi$, $p_P = p$, and $p_B = p + \psi$ where ψ is positive ($\psi < 1 - p$). If with this allocation the probability of successful GOP decoding

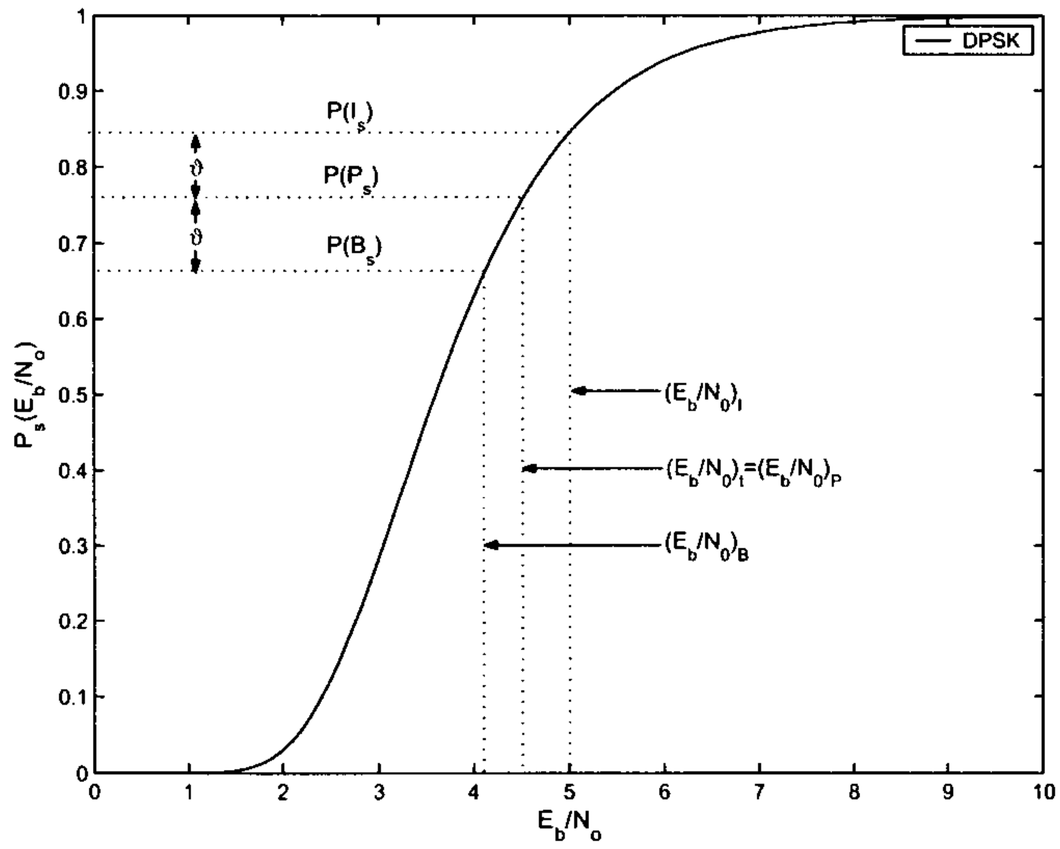

Figure 6.4: Proposed differentiation of allocated E_b/N_0 values for different type of frames inside a GOP's.

is equal to $P_\psi(GOP_S)$, then we should show that

$$P_\psi(GOP_S) \geq P_c(GOP_S) \tag{6.14}$$

In the first case, where we have equal allocations of target (E_b/N_o) values the probability $P_c(GOP_S)$ can be written as

$$P_c(GOP_S) = (1-p)\underbrace{\left[1+(1-p)+(1-p)^2+(1-p)^3\right]}_{u} + (1-p)^3\underbrace{\left[(1-p)+2(1-p)^3+(1-p)^5\right]}_{w} \tag{6.15}$$

For the second case, the probability $P_\psi(GOP_S)$ can be written as,

$$\begin{aligned}
P_\psi(GOP_S) &= (1-p+\psi)\underbrace{\left[1+(1-p)+(1-p)^2+(1-p)^3\right]}_{u}+ \\
&+(1-p+\psi)^2(1-p-\psi)\underbrace{\left[(1-p)+2(1-p)^3+(1-p)^5\right]}_{w} \\
&=(1-p+\psi)u+(1-p+\psi)^2(1-p-\psi)w \\
&=\left\{(1-p)u+(1-p)^3w\right\}+\psi u-(1-p)^3\psi w+\left[2\psi(1-p)+\psi^2\right](1-p-\psi)w \\
&=P_c(GOP_S)+\psi u-(1-p)^2\psi w+\left[2\psi(1-p)+\psi^2\right](1-p-\psi)w
\end{aligned} \tag{6.16}$$

So, we have to show that

$$\psi u-(1-p)^2\psi w+\left[2\psi(1-p)+\psi^2\right](1-p-\psi)w\geq 0 \tag{6.17}$$

Equation 6.17 can be written as

$$\begin{aligned}
&\psi\left[u-(1-p)^2w+2(1-p)(1-p-\psi)w+\psi(1-p-\psi)w\right] \\
&=\psi\left[u-(1-p)^2w+2(1-p)w-2\psi(1-p)w+\psi(1-p)w-\psi^2w\right] \\
&=\psi[u+w\underbrace{\left[(1-p)^2-\psi(1-p)-\psi^2\right]}_{K}]
\end{aligned} \tag{6.18}$$

But because $\psi<1-p$ (since $p+\psi<1$) we can write $\psi=a\cdot(1-p)$ where $a<1$. So,

$$\begin{aligned}
K=&(1-p)^2-a(1-p)(1-p)-a^2(1-p)^2 \\
=&(1-p)^2\left[1-a(1+a)\right]
\end{aligned} \tag{6.19}$$

so $K>0$ (because $a\ll(\sqrt{5}-1)/2$) and thus inequality 6.14 holds true. □

Remark The above result holds independently of the value of n, i.e., the number of packets in error that result in an erroneous frame display.

The effect of E_b/N_0 differentiation on the quality of still images can be seen in 6.5. In this figure the original 'Lena' picture is depicted together with three different transmitted versions with $E_b/N_0=$

(a)

(b)

(c)

(d)

Figure 6.5: Effect of E_b/N_0 differentiation on the quality of still images (with $\psi = 1.58dB$[dB]) (a) Original 512x512 8bit grayscale 'Lena' image, (b) $E_b/N_0 = 10 + \psi$[dB] representing the case of an Intra-frame (PSNR = +44.70 dB), (c) $E_b/N_0 = 10$[dB] representing the case of a Predictive-frame (PSNR = +36.41 dB), (d) $E_b/N_0 = 10 - \psi$[dB] representing the case of a Bi-directional-frame (PSNR = +27.31 dB).

10[dB] and $\psi = 1.58dB$[dB].

6.4.2 Weighted sum based optimization for power and rate control

With fixed E_b/N_o values for the different frame types the optimization problem can be formulated as a weighted sum of the difference between the transmission rate and the TFRC rate ($\widetilde{r}$) and the total required transmission power as follows,

$$\min_{p,\gamma} \quad w_1 \sum_{i=1}^{N} \left| \frac{1}{c_i} \int_0^{c_i} [r_i(t) P_s(\Gamma_f)]\, dt - \widetilde{r}_i \right| + w_2 \sum_{i=1}^{N} p_i$$

$$\text{subject to} \quad \sum_{i=1}^{N} \frac{\gamma_i}{1+\theta\gamma_i} \cdot \frac{I_i + \nu}{\phi p_{max} g_i} \leq 1 \tag{6.20}$$

$$\sum_{i=1}^{N} \gamma_i = \widetilde{\gamma}, \quad w_1 + w_2 = 1, \quad \left(\frac{E_b}{I_0}\right)_f = \Gamma_f, \quad f \in \{I, P, B\}$$

where c_i expresses the time interval where the optimization problem take place, w_1,w_2 are the weights for the two different metrics used in the objective function and ϕ is the fraction of the total power allocated for the aggregate streaming video (this can be for example the fraction of power allocated in an AF DiffServ class). Finally, $\widetilde{\gamma} = \frac{\Gamma_t}{W} \sum_i r_i$ where Γ_t is the average E_b/N_o value. In practical terms the integration interval will be over the horizon of one packet transmission interval c_i with a constant transmission rate. If we additionally substitute rate and power with the equivalent expression based on SINR (γ), the optimization problem that is actually implemented will have the following form,

$$\min_{\gamma} \quad \frac{w_1}{\sum_i \widetilde{r}_i} \sum_{i=1}^{N} \left| \frac{P_s(\Gamma_i) W g_i p_i}{\Gamma_i \left(\theta_i \cdot g_i \sum_{j \neq i} p_j + I_i + \nu\right)} - \widetilde{r}_i \right| + \frac{w_2}{\phi p_{max}} \frac{1}{1 - \sum_{i=1}^{N} \frac{\theta\gamma_i}{1+\theta\gamma_i}} \sum_{i=1}^{N} \frac{\gamma_i}{1+\theta\gamma_i} \cdot \frac{I_i + \nu}{g_i}$$

$$\text{subject to} \quad \sum_{i=1}^{N} \frac{\gamma_i}{1+\theta\gamma_i} \cdot \frac{I_i + \nu}{\phi p_{max} g_i} \leq 1 \tag{6.21}$$

$$\sum_{i=1}^{N} \gamma_i = \widetilde{\gamma}, \quad , w_1 + w_2 = 1, \quad \left(\frac{E_b}{I_0}\right)_f = \Gamma_f, \quad f \in \{I, P, B\}$$

The above problem formulation that aggregates the two components into one objective function using a weighted scheme can be seen as the simplest form of multi-objective optimization [34]. The

weights w_1 and w_2 control the relative importance of the objectives and are fixed at the outset. It is clear that this process of choosing the weights involves *a priori* assumptions on the relative worth of the objectives, and in the above case equal importance for the two functions (i.e, $w_1 = w_2 = 0.5$) have been chosen. This can be seen as a fair trade-off between throughput maximization (first objective) and power consumption (second function objective). Note that, with $w_1 = 0$ the above problem is reduced to a minimum transmission power, while with $w_2 = 0$ becomes a throughput maximization problem.

6.5 Numerical Investigations and Validation

A single cell CDMA network is considered and we focus in a single class that is used to transmit video content and utilize a constant fraction of the total transmitted power of the base station. The mobile hosts are uniformly distributed and the link gain is modelled as a distance dependent path loss of fourth power, while the shadow fading factor is generated using a long normal distribution of zero mean and 8dB standard deviation. The maximum transmitted power of the base station is 30W and the receiver noise power ν is set to be 10^{-12}W for all mobile nodes. We consider downlink transmission in the system with a chip rate of W=3.84Mcps under the assumption that the radio link can support continuous transmission rates for an average target of $(E_b/I_0)_t$ equal to 7.8 dB. We also assume an infinite buffer size at the access point, so that packet loss can only occur due to errors in the wireless channel. Table 6.1 summarizes the parameters used in the numerical investigations.

The Peak-Signal-to-Noise- Ratio (PSNR) is probably the most widely accepted criterion for characterizing image quality, since several studies confirm that more complicated and sophisticated metrics do not actually outperform the PSNR metric in predicting actual human perception on image quality [31] (especially for high bit rates). For video images of size $X \times Y$ pixels, the PSNR of the video sequence between images i to j is defined by [32]

$$\mathrm{PSNR}(i,j) = 10 \cdot log_{10} \frac{P^2}{\mathrm{MSE}(i,j)}$$

PARAMETER	VALUE
Total power	30W
Number of users (N)	16
noise, ν	$10^{-12}W$
Processing Gain [W]	3.84Mcps
Carrier frequency [MHz]	2000
Path loss exponent	4
σ of log-normal shadowing [dB]	8
Slot duration [msec]	10
MSS of TCP/UDP packets [bytes]	150
BER(φ) [DPSK]	$\frac{1}{2}e^{-\varphi}$
Number of AF classes	1

Table 6.1: Parameters used in the numerical investigations

PSNR [dB]	**MOS**	**Quality**	**Impairment**
> 37	5	Excellent	Imperceptible
31 - 37	4	Good	Perceptible, but not annoying
25 - 31	3	Fair	Slightly annoying
20 - 25	2	Poor	Annoying
< 20	1	Bad	Very annoying

Table 6.2: PSNR to MOS translation of ITU-R quality and impairment scale

where P is the maximum value of a pixel (which is equal to 255 for an 8bit grayscale image), and MSE(i,j) is defined as

$$\mathrm{MSE}(i,j) = \frac{1}{X \cdot Y \cdot (j-i+1)} \sum_{n=i}^{j} \sum_{x=1}^{X} \sum_{y=1}^{Y} \left[I(x,y,n) - \widehat{I}(x,y,n) \right]^2$$

where $I(x,y,n)$ and $\widehat{I}(x,y,n)$ express the gray level pixel values (we use the Y-luminance information and not the U and V which are the colour components) of the original and decoded image respectively. The PSNR metric is related with the mean opinion scale (MOS), which describes the human quality impression by a subjective quality metric, as shown in table 6.2 The analysis is based on a short MPEG-4 video clip of 828 frames encoded in the CIF format [35]. This clip was obtained by

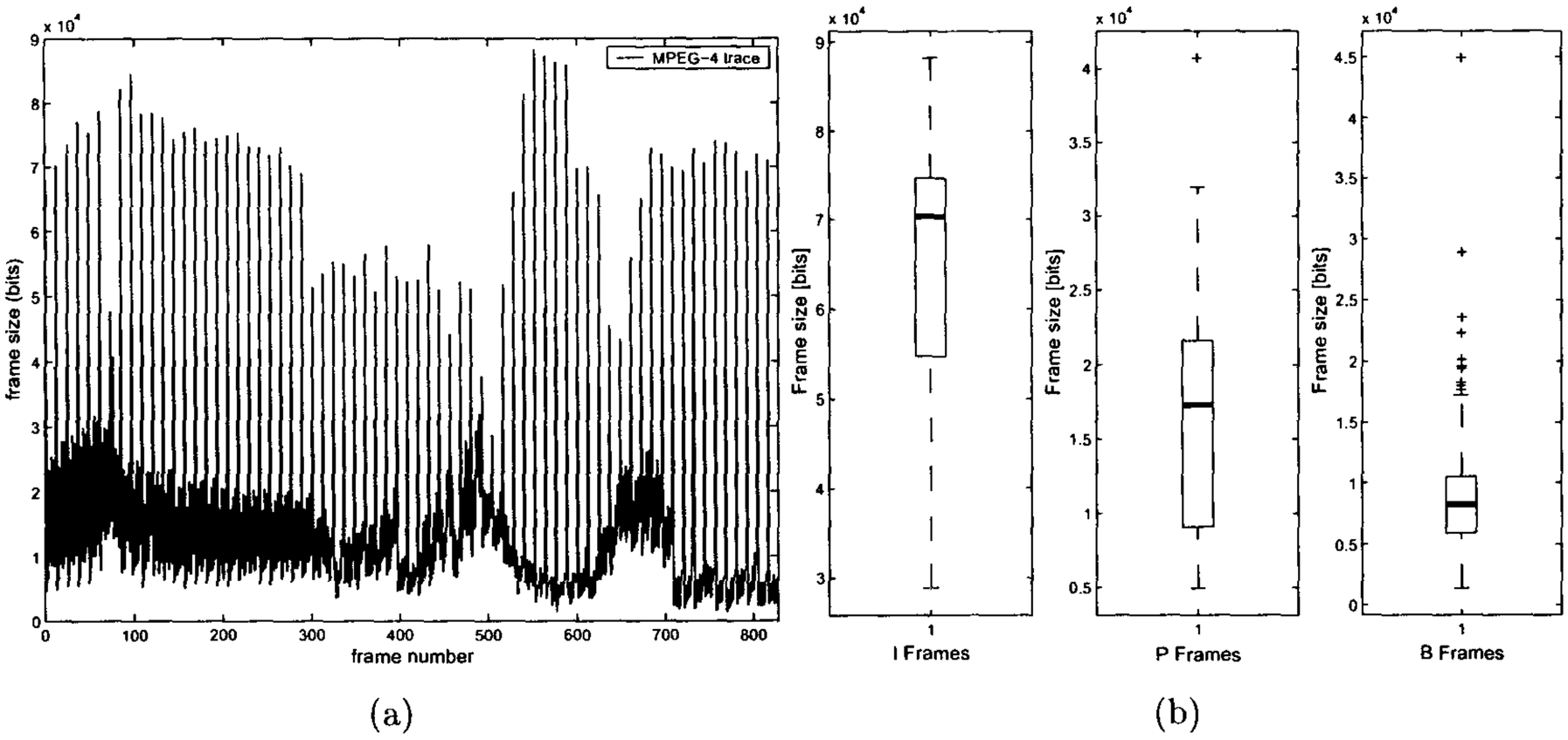

Figure 6.6: (a) Frame size of the base layer MPEG-4 video trace (b) Box plot graph of the Intra, Predicted and Bidirectional frames of MPEG-4 trace.

concatenating the wellknown sequences of 'coastguard', 'foreman', and 'table' and the trace has been segmented into 4 scenes: $T_1 = 1$, $T_2 = 301$, $T_3 = 601$, $T_4 = 732$ (more details on the actual traces can be found in [35]). Figure 6.6(a) shows the size per frame (in bits) in the MPEG-4 trace and 6.6(b) provides a visual summary of both the central tendencies and dispersions of frame sizes using the box plots for the Intra, Predictive and Bi-directional frames in the video sequence. It is interesting to note that the median in I and P frames compared with the median in B frames is approximately 7 and 2 times larger respectively. Based on this distribution, figure 6.9 shows the probability of successful GOP display based on the analysis explained in section 6.4.1 for constant and adaptive Eb/No allocation with $\psi = 0,3$ and $\psi = 0,6$. As can seen from these figures the probability of successful GOP display is largely improved compared with current approaches, where the allocated E_b/N_o considered constant for the whole video transfer. We should also point out that the performance of the adaptive allocation scheme is decreased when ψ increases above a certain value. Heuristically, through simulations, we have found out that the ψ value should not exceed 5% of the average E_b/N_o. This adaptive allocation of the target E_b/N_o could be used for example in the High-Speed Downlink Shared Channels (HS-DSCH) of W-CDMA standard. In High Speed Downling

Packet Access (HSDPA) the power is held constant over the transmission interval (i.e., 2msec) and instead of power control, adaptive modulation and coding (AMC) techniques are used with constant target E_b/N_o. Therefore if in HSDPA video streaming packet transmission the E_b/N_o is not held constant but is differentiated depending on the type of frame being transmitted (using suitable values of ψ), the performance of the system can be increased. For a 500Kbps video transmission and based on the box plots median values shown in figure 6.6(b) the average time of altering target E_b/N_o values is 140msec for I frames, 16msec for P frames and 9msec for B frames. These required time intervals are approximately between one and two orders of magnitude larger when compared with scheduling decisions in a HSDPA enabled UMTS network. Thus, from the complexity perspective, such adaptive allocation of E_b/N_o values is feasible.

Figure 6.7 depicts how the probability of successful decoding of different type of frames is changing over a specific range of packet error rate and threshold parameter θ. With constant weights, w_i,

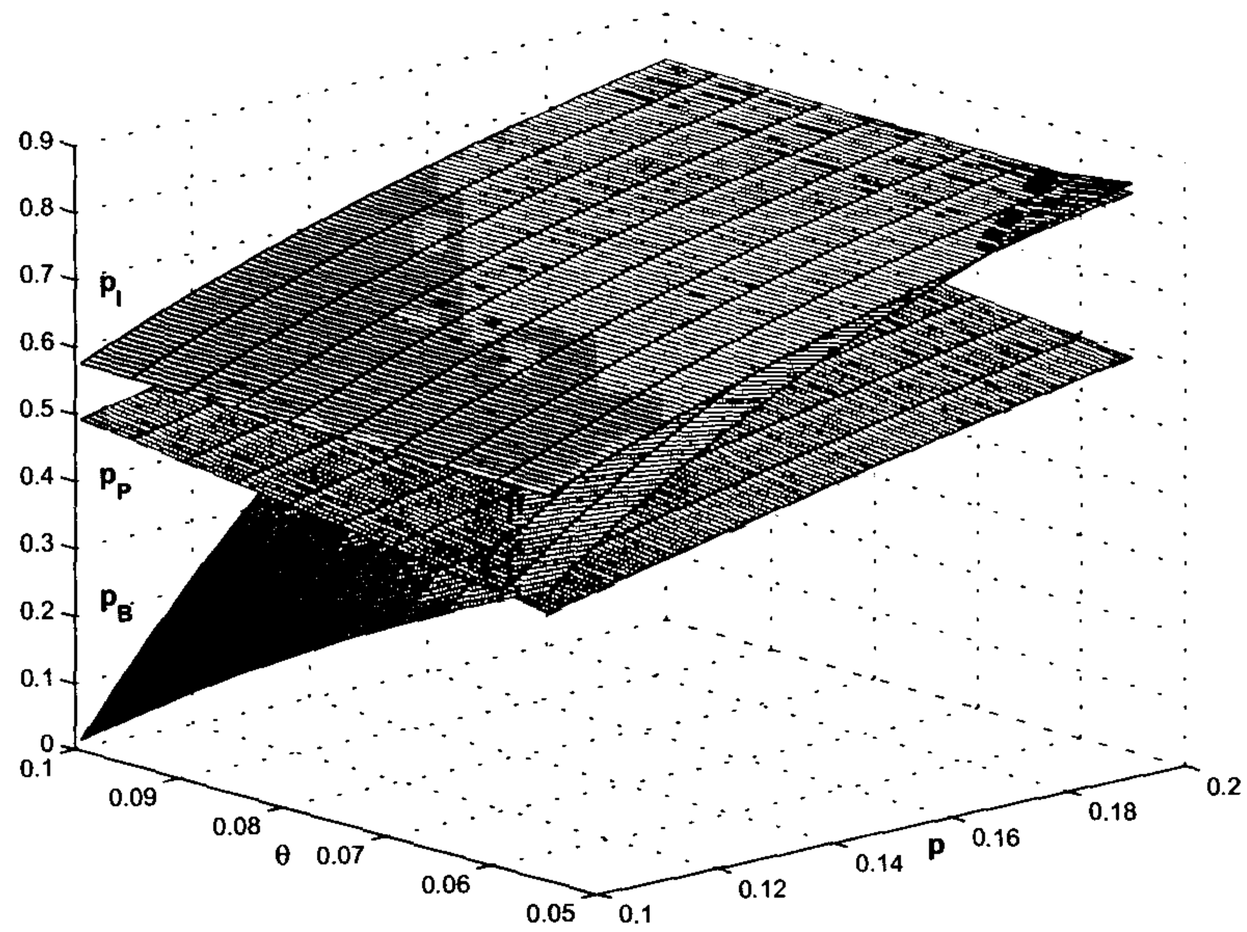

Figure 6.7: Probability of successful decoding of different frame types over a specific range of packet error rate $[0.1, 0.2]$ and threshold parameter θ $[0.05, 0.1]$.

the solution of the bi-objective optimization problem described in section 6.4.2 provides only one

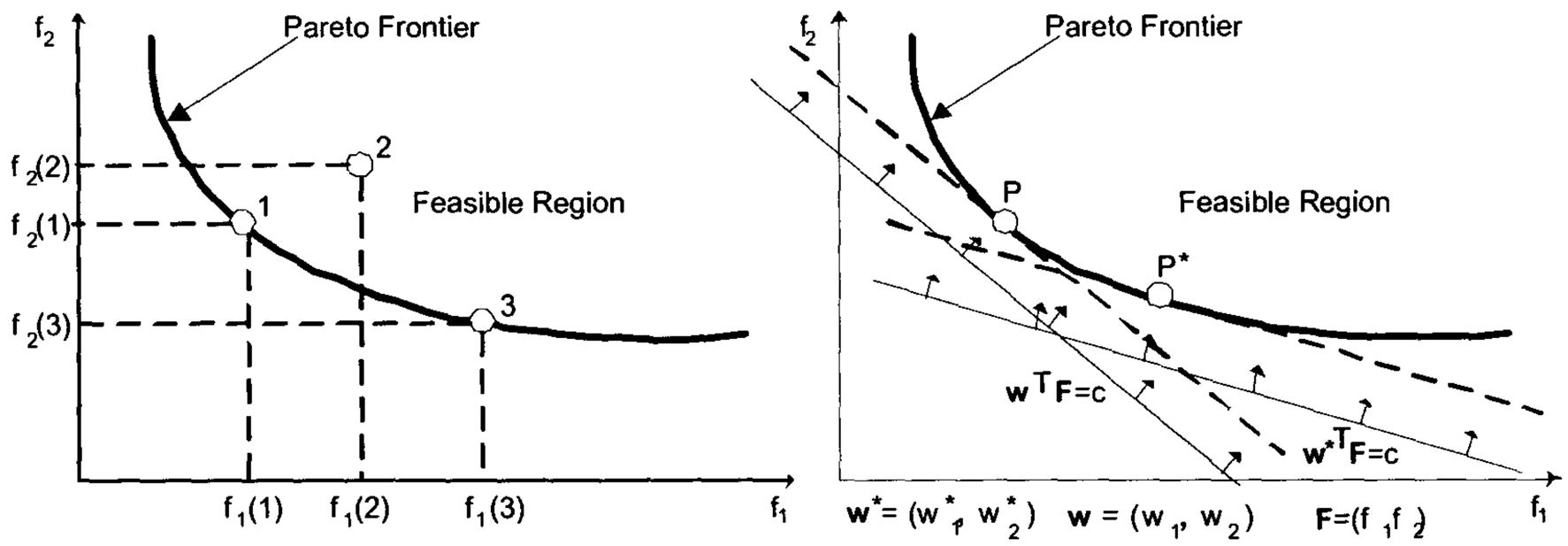

Figure 6.8: (Right) In the Pareto frontier of the bi-objective optimization problem depicted points 1 and 3 are an example of Pareto non-dominated optimal solutions. Solution 2 is not Pareto optimal because solution 1 has simultaneously smaller values for both objectives. (Left) Geometrical representation of the weighted sum strategy.

non-dominated (or non-inferior) solution. By varying the weights, it is possible to unfold the whole Pareto frontier (i.e., the whole set of non-dominated solutions). More formally, and for the case of two objective functions f_1 and f_2 (with $f_i : \mathcal{S} \rightarrow \mathcal{R}$), a solution x dominate solution y ($x, y \in \mathcal{S}$) if $\exists i \in \{1,2\}$ such that $f_i(x) > f_i(y)$ and $\forall j \in \{1,2\}$, $f_j(x) \geq f_j(y)$. Therefore, a solution is Pareto-optimal if it is not dominated by any other solution. Figure 6.8 (left) shows the Pareto frontier of a bi-objective optimization problem where solutions 1 and 3 are Pareto optimal and solution 2 is inferior because solution 1 for example has simultaneously smaller values for both objectives. The geometrical interpretation of the weighted sum strategy for solving the bi-objective optimization problem is depicted in figure 6.8 (right). For a given set of weights a straight line in the objective function space is formed and the solution is the point where the objective line becomes tangent to the feasible objective space (Pareto front). As shown in the same figure, by changing the weights the slope of the objective line is changing which therefore lead to a different solution. The ideal scenario would be to unfold the whole Pareto frontier, but this would require exhaustive search among all possible combinations of the weights. Figure 6.10(a) shows the allocation of bit-rates for three MPEG-4 streams over the whole spectrum of different allocated weighting factors, based on the optimization problem defined in equation 6.21. The minimization problem has been numerically solved using the well known quasi-Newton BFGS (Broyden-Fletcher-Goldfarb-Shanno)

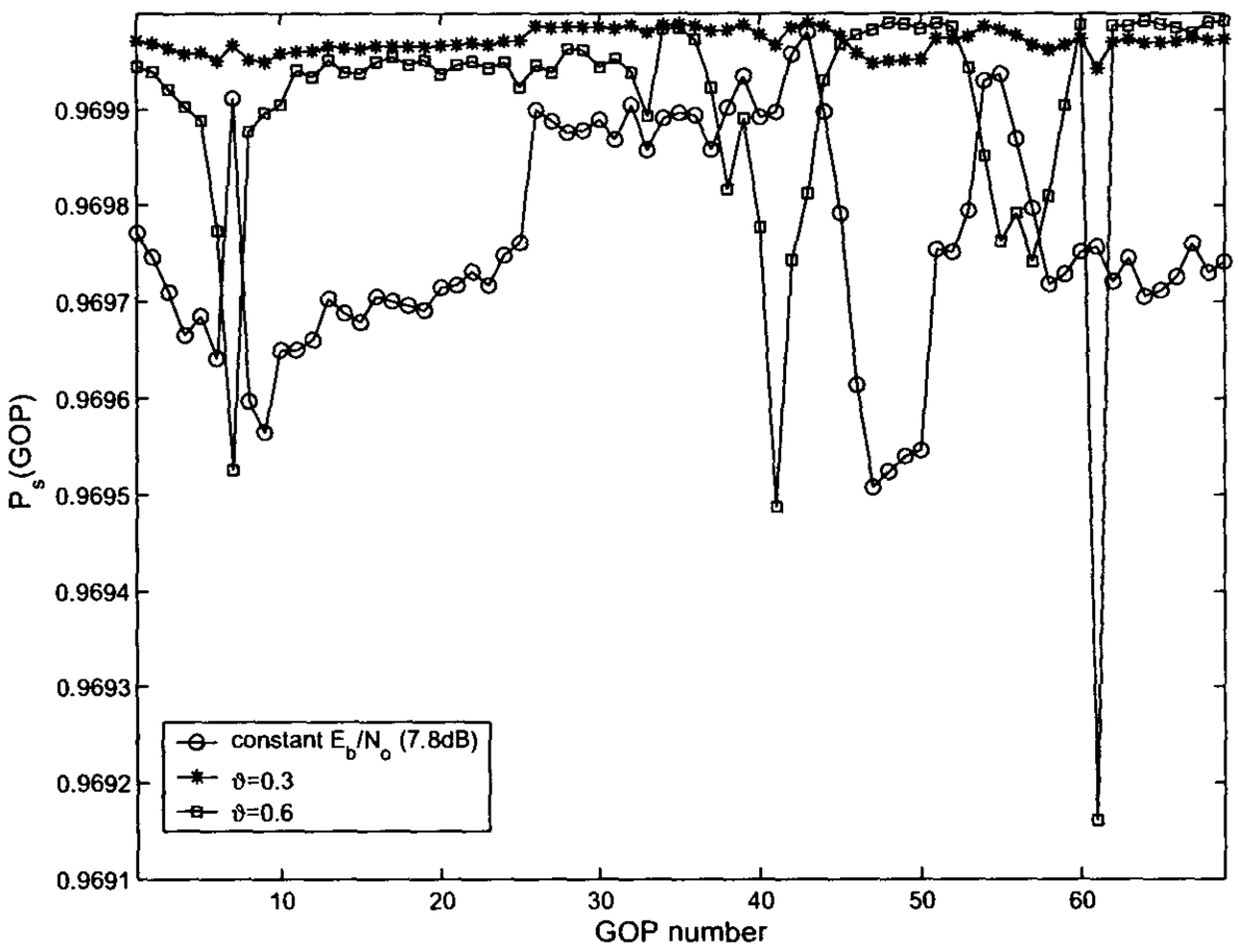

Figure 6.9: Probability of successful GOP display for constant and adaptive E_b/N_o with $\psi = 0,3$ and $\psi = 0,6$.

method, which is available in the optimization toolbox of MATLAB. As can be seen in figure 6.10(a) as the weighting factor for the objective function that expresses the difference between the required rate from the TFRC and the actual allocated rate increases, the optimization becomes a throughput maximization. Under feasibility conditions, as w_1 approaches one the allocated rates will be equal to the TFRC rates. Figure 6.10(b), on the other hand, shows the power consumption under the same scenario. In this case we have the requirement for minimum rate allocation that emphasizes the fact that as the value of w_2 approaches one the transmission power goes to zero. Thus, the proposed algorithm give a flexibility on the trade off between throughput maximization and power consumption.

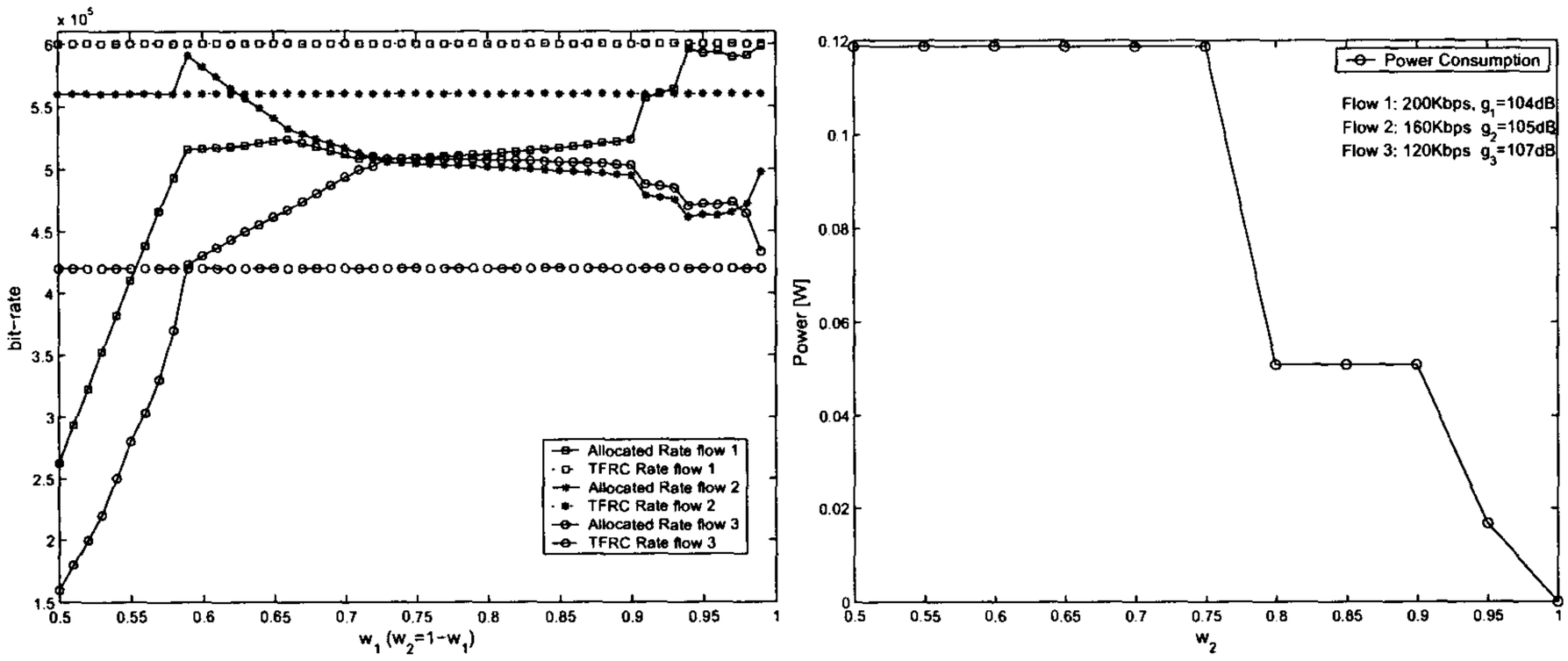

(a) (b)

Figure 6.10: (a) Frame size of the base layer MPEG-4 video trace (b) Power consumption as a function of the weighting factor w_2 of the optimization problem – without minimum rate guarantees.

6.6 Conclusions

In this chapter a power and rate adaptation approach for CDMA networks that utilize higher layer information, such as the required rate from the transport layer (in terms of the TCP-friendly protocol used) and the type of frame inside the GOP (i.e, Intra, Predictive or Bi-directional) has been

presented. The novelty of the proposed scheme compared with previous proposals that are based on lower layer criteria is the utilization of information that is encapsulated in the RTP protocol. Therefore, in the optimization scheme proposed the required rate of the TFRC algorithm and the type of frame in the video stream are combined with traditional lower layer information such as channel conditions. Using this information, a multi-objective optimization problem has been formulated based on the weighted sum of two competing objectives, i.e the difference between the assigned rate and required rate (as depicted by the TFRC) and the total consumed power. Furthermore, the scheme uses adaptive allocation of the target E_b/N_o values in order to increase the probability of successful GOP display.

In the proposed power and rate adaptation scheme the video has been considered as a single layer encoded stream. MPEG-4 allows encoding into a *Base Layer* (BL) and a number of *Enhancement Layers* (ELs) [8]. The decoded BL would provide minimal rendered quality and additional decoded ELs would increase the quality. As a future direction, the proposed scheme can be augmented for multiple encoded layers in the MPEG-4 video stream, satisfy BL transmission for all video streams and allocate resources for subsequent ELs based on channel conditions and overall power consumption constraints. In that respect, adaptive E_b/N_o allocation will not only depend on the type of frame but also on the specific type of the encoded layer. The situation thus seems to call for a more finely grained analysis.

The TFRC-aware scheme can also be used in conjunction with, and in an ancillary fashion to, previously proposed mechanisms that aim to improve the quality of video transmission over error prone channels such as REC, FEC and UEP. This is because the output of the proposed power and rate control mechanism can be seen as an orthogonal issue related to the decisions of dynamic FEC tuning, adaptive REC or unequal error protection.

6.7 Appendix

6.7.1 Derivative Based Optimization Techniques

This section provides a retrospective on the derivative optimization techniques that have been used in previous sections. Let's first assume the following unconstrained minimization problem

$$\min_{x \in \mathbb{R}^n} f(x) \tag{A-22}$$

where f is twice continuously differentiable. In that case, the first order necessary condition depicts that if f achieves its minimum at a point x, then

$$\nabla f(x) = 0 \tag{A-23}$$

Newton's method solves equation A-23 iteratively. Assume that $\tilde{x}$ is the current approximate solution of A-23. To compute the next approximate solution we consider the Taylors expansion of $\nabla f(x)$ at $\tilde{x}$,

$$\nabla f(x) = \nabla f(\tilde{x}) + \nabla^2 f(\tilde{x})(x - \tilde{x}) + o(\|x - \tilde{x}\|) \tag{A-24}$$

If we set,

$$a(x) = \nabla f(\tilde{x}) + \nabla^2 f(\tilde{x})(x - \tilde{x}) \tag{A-25}$$

Then, if we solve the above linear system of equations we obtain a a new approximate solution of A-23. Therefore, and more formally, in the general case the Newton's iterative method can be written as,

$$x_{i+1} = x_i - \nabla^2 f(\tilde{x_i})^{-1} \nabla f(\tilde{x_i}), \quad i = 0, 1, 2, ... \tag{A-26}$$

where $\nabla^2 f(\tilde{x})$ express the Hessian matrix and $\nabla f(\tilde{x})$ is the derivative of the matrix.

6.7.2 Quasi−Newton's methods

The drawback in Newton's method is that we need to calculate the Hessian of f at each iteration. As the dimensionality of problem increases, calculating the Hessian of f becomes more difficult and

also the computational time increases. The Quasi−Newton's method modifies Newton's method by avoiding the computation of the Hessian while retaining the fast local convergence of Newtons method. The idea behind Quasi−Newton's is to calculate a series of sequence $\{G_k\}$ instead of $\{\nabla^2 f(x)\}$. The series of sequence $\{G_k\}$ is calculated as follows: Assume that in the first step we have calculated $\nabla f(x_0)$, $\nabla^2 f(x_0)$ and x_1 (using original Newton's method). We can write,

$$\nabla f(x_0) - \nabla f(x_1) = \nabla^2 f(x_1)(x_0 - x_1) + o(\|x - \tilde{x}\|) \tag{A-27}$$

The aim is instead of calculating $\{\nabla^2 f(x_1)\}$ to calculate a matrix G_1 that satisfy,

$$\nabla f(x_0) - \nabla f(x_1) = G_1(x_0 - x_1) \tag{A-28}$$

or if we substitute G_1^{-1} with H_1 we have the so-called quasi-Newton condition:

$$H_1(\nabla f(x_0) - \nabla f(x_1)) = x_0 - x_1 \tag{A-29}$$

Generally, in an iterative fashion the quasi-Newton condition is written as,

$$H_{i+1}\gamma_i = \delta_i \tag{A-30}$$

where $\gamma_i = \nabla f(x_{i+1}) - \nabla f(x_i)$ and $\delta_i = x_{i+1} - x_i$. The matrix H_{i+1} is constructed iteratively from H_i using the gradient information at both x_{i+1} and x_i. A simple way of doing this is through an update from H_i as follows,

$$H_{i+1} = H_i + wuu^T \tag{A-31}$$

If we now substitute H_{i+1} into the quasi-Newton condition equation A-29 we have,

$$H_i\gamma_i + wuu^T\gamma_i = \delta_i \tag{A-32}$$

By choosing $u = \delta_i - H_i\gamma_i$ and $w = \left[\gamma_i^T(\delta_i - H_i\gamma_i)\right]^{-1}$ the update formula will have the form,

$$H_{i+1} = H_i + \frac{(\delta_i - H_i\gamma_i)(\delta_i - H_i\gamma_i)^T}{(\delta_i - H_i\gamma_i)^T\gamma_i} \tag{A-33}$$

6.7.3 The Quasi Newton Broyden, Fletcher, Goldfarb, and Shanno (BFGS) Method

The quasi-Newton's formula expressed in equation A-29can also be written as follows,

$$\gamma_i = G_{i+1}\delta_i \tag{A-34}$$

Assuming that we have calculated G_i then in the next iteration G_{i+1} can be calculated using equation A-33 by substituting H_{i+1} with G_{i+1} and H_i with G_i. Therefore from the following equation,

$$H_{i+1} = H_i + \frac{\delta_i\delta_i^T}{\delta_i^T\gamma_i} - \frac{H_i\gamma_i\gamma_i^T H_i}{(H_i\gamma_i)^T\gamma_i} \tag{A-35}$$

we obtain,

$$G_{i+1} = G_i + \frac{\delta_i\delta_i^T}{\delta_i\gamma_i} - \frac{G_i\gamma_i\gamma_i^T G_i}{(G_i\gamma_i)^T\gamma_i} \tag{A-36}$$

We can therefore calculate G_{i+1}^{-1} as follows,

$$G_{i+1}^{-1} = G_i^{-1} + \left(1 + \frac{\gamma_i^T G_i^{-1}\gamma_i}{\delta_i^T\gamma_i}\right)\frac{\delta_i\delta_i^T}{\delta_i^T\gamma_i} - \left(\frac{\delta_i\gamma_i^T G_i^{-1} + G_i^{-1}\gamma_i\delta_i^T}{\delta_i^T\gamma_i}\right) \tag{A-37}$$

Then, if we let $H_{i+1} = G_{i+1}^{-1}$ and $H_i = G_i^{-1}$, the BFGS formula can be written as,

$$H_{i+1} = H_i + \left(1 + \frac{\gamma_i^T H_i\gamma_i}{\delta_i^T\gamma_i}\right)\frac{\delta_i\delta_i^T}{\delta_i^T\gamma_i} - \left(\frac{\delta_i\gamma_i^T H_i + H_i\gamma_i\delta_i^T}{\delta_i^T\gamma_i}\right) \tag{A-38}$$

Constrained optimization problems can be solved using Sequential Quadratic Programming (SQP) where at each iteration an approximation is made of the Hessian of the Lagrangian function using the BFGS method.

Bibliography

[1] Injong Rhee, Error control techniques for interactive low-bit rate video transmission over the Internet, *Proc. SIGCOMM 1998*

[2] C. Papadopoulos, G. Parulkar, Retranmsission-based error control for continious media applications, *Proc. 6^{th} Workshop on Network and Operating System Support for Digital Audio and Video, pp. 5-12, 1996*

[3] Hong and A. Nostratinia, Rate-constrained scalable video transmission over the internet, *Proc. 12th Packet Video Workshop, Pittsburgh, PA, Apr. 2002*

[4] G. Wang, Q. Zhang, W. Zhu and Y. Zhang, Channel adaptive unequal error protection for scalable video transmission over wireless channel, *Proc. SPIE VCIP '01, vol. 4310, San Jose, CA, pp.648-655, Jan. 2001*

[5] T. Stockhammer, Progressive Video Transmission for Packet-Lossy Channels exploiting Feedback and Unequal Erasure Protection, *IEEE International Conference on Image Processing 2002 (ICIP 2002), Rochester, NY, Sept. 2002*

[6] J. Vass and X. Zhuang, Adaptive and Integrated Video Communication System Utilizing Novel Compression, Error Control and Packetization Strategies for Mobile Wireless Environments, *In Proc. of International Packet Video 2000, Cagliari, Sardinia, Italy, 1-2 May 2000*

[7] N. Normura, T. Fujii, N. ohta, Layered Packet Loss Protoection for Variable Rate Coding Using DCT, *In Proc. of International Workshop on Packet Video, 1998*

[8] Radha, H., van der Schaar, M., Chen, Y., The MPEG-4 fine-grained scalable video coding method for multimedia streaming over IP, *IEEE Transactions on Multimedia 3, pp. 5368, 2001*

[9] Harri Holma (Editor), Antti Toskala (Editor), WCDMA for UMTS: Radio Access for Third Generation Mobile Communications – Third Edition, *John Wiley & Sons, 2004*

[10] Kamran Etemad, CDMA2000 Evolution: System Concepts and Design Principles, *John Wiley & Sons, 2004*

[11] J. Zander, Performance of optimum transmitter power control in cellular radio systems, *IEEE Transactions of Vehicular Technology, vol. 41, pp. 5762, Feb. 1992*

[12] S. A. Grandhi, R. Vijayan, D. J. Goodman, and J. Zander, Centralized power control in cellular radio systems, *IEEE Transactions of Vehicular Technology, vol. 42, pp. 466468, Nov. 1993*

[13] G. J. Foschini and Z. Miljanic, A simple distributed autonomous power control algorithm and its convergence, *IEEE Transactions of Vehicular Technology, pp. 541646, 1993.*

[14] A. Sampath, P. Kumar, J. Holtzman, Power control and resource management for a multimedia CDMA wireless system, *In Proc. IEEE PIMRC'95, pp.21-25, 1995*

[15] R. Fantacci, S. Nannicini, Multiple access protocol for integration of variable bit rate multimedia traffic in UMTS/IMT-2000 based on wideband CDMA,*IEEE J. Selecte. Areas in Commun., vol.* ***18****, pp. 1441 - 1454, Aug 2000*

[16] S. Choi and K. G. Shin, An uplink CDMA system architecture with diverse QoS guarantees for heterogeneous traffic, *IEEE/ACM Trans. Networking, vol.****7****, no. 5, pp.616-628, October 1999*

[17] L. Wang, A.H. Aghvami, W.G. Chambers, Design Issues of Media Access Control (MAC) Protocols for Multi-media Traffic Over DS-CDMA Systems. *European Wireless 2002, pp. 151-160, Italy, 2002*

[18] D. I. Kim, E. Hossain, V. K. Bhargava, Downlink Joint Rate and Power Allocation in Cellular Multirate WCDMA Systems, *IEEE Transactions on Wireless Communications, Vol. 2, No. 1, January 2003*

[19] Carlos E. Luna, Yiftach Eisenberg, Randall Berry, Thrasyvoulos N. Pappas, and Aggelos K. Katsaggelos, *Joint Source Coding and Data Rate Adaptation for Energy Efficient Wireless Video Streaming, IEEE Journal on Selected Areas in Communications, Vol. 21, No. 10, December 2003*

[20] R. Berry and R. Gallager, Communication over fading channels with delay constraints, *Transactions on Information Theory, vol. 48, pp. 11351149, May 2002*

[21] Teunis J. Ott, J.H.B. Kemperman, and Matt Mathis, The Stationary Behavior of Ideal TCP Congestion Avoidance, *accesible via* `ftp://ftp.bellcore.com/pub/tjo/TCPWindow.ps`, *August 1996*

[22] H. Balakrishnan, V. Padmanabhan, S. Seshan, R. Katz, A comparison of mechanisms for improving TCP performance over wireless links, *ACM SIGCOMM96, pp.256 - 269*

[23] S. Biaz, N. H. Vaidya, Distinguishing congestion losses from wireless transmission losses: a negative result, *Computer Communications and Networks, 1998*

[24] V. Tsaoussidis and I. Matta, Open issues on TCP for Mobile Computing, *The Journal of Wireless Communications and Mobile Computing, Wiley Academic Publishers, Issue 2, Vol. 2, March 2002*

[25] Song Cen, Pamela C. Cosman, and Geoffrey M. Voelker, End-to-End Differentiation of Congestion and Wireless Losses, *IEEE/ACM Transactions on Networking, Vol. 11, No. 5, October 2003*

[26] Altman, K. Avrachenkov, and C. Barakat, A stochastic model of TCP/IP with stationary random losses, *ACM SIGCOMM, Stockholm, pp.231-242, August 2000*

[27] J. Padhye, V. Firoiu, D. Towsley, J. Kurose, Modeling TCP Throughput: A simple model and its empirical validation, *In SIGCOM'98, September 1998*

[28] H. Schulzrinne, S. Casner, R. Frederick, and V. Jacobson, RTP: A Transport Protocol for Real-Time Applications, *IETF RFC 3550 July 2003*

[29] Michael Zink, Carsten Griwodz, Jens Schmitt, and Ralf Steinmetz, Scalable TCP-friendly Video Distribution for Heterogeneous Clients, *SPIE Conference on Multimedia Computing and Networking (MMCN) 2003*

[30] Ladan Gharai, RTP Profile for TCP Friendly Rate Control, *IETF Internet Draft, draft-ietf-avt-tfrc-profile-00.txt, June 2004*

[31] A. M. Rohaly and al., Video Quality Experts Group: Current Results and Future Directions, *Proc. SPIE Visual Communications and Image Processing, vol. 4067, pp. 742753, Perth, Australia, June 2000*

[32] S. Olsson, M. Stroppiana, and J. Baina, Objective Methods for Assessment of Video Quality: State of the Art, *IEEE Trans. on Broadcasting, vol. 43, no. 4, pp. 487495, December 1997*

[33] Kikuchi, T. Nomura, S. Fukunaga, Y. Matsui, H. Kimata RTP Payload Format for MPEG-4 Audio/Visual Streams, *IETF RFC 3016, November 2000*

[34] Steuer E., Choo U., An interactive weighted Tchebycheff proedure for multiple objective programming, *Mathematical Programming, vol.* **26**, *pp. 326-344, 1983*

[35] Martin Reisslein, Jeremy Lassetter, Sampath Ratnam, Osama Lotfallah, Frank H.P. Fitzek, Sethuraman Panchanathan, Traffic and Quality Characterization of Scalable Encoded Video: A Large-Scale Trace-Based Study, Part 1: Overview and Definitions, *Arizona State University, Techical Report, December 2003*

Chapter 7

Final Remarks, Extensions & Conclusions

This chapter gives a brief overview and summary of the research results together with a list of the publications. We also discuss how the general approach followed in this thesis can be used to propel future research directions and to some extent examples of these research themes are presented.

7.1 Introduction

The main contemporary protocol stack design was based on the architectural principle of drawing clear lines of demarcation between functionalities performed at different layers. Even though this approach proven to be a successful model for fixed networks, the critical architectural issue of whether this layering is suitable for wireless packet based networks is becoming, over the last few years, a prominent question. Therefore, over the last few years we are witnessing a new paradigm shift from the traditional protocol stack architecture. With an increased heterogeneity of wireless networks and IP technology being the defacto network layer solution, adherents of cross-layer designs believe that only through breaking the traditional communication flow between layers the performance of the system can be further stretched to its limits. On the other hand, there is a general skepticism on cross-layer solutions in the sense that these designs may have rather short

term benefits and can potentially lead to very complicated network architectures. Clearly, a sound network architecture should have a modular design and based on long term considerations. This will allow the required abstraction that developers need in order to provide new enhanced components, while at the same time being assured that the whole system will interoperate. Two of the most

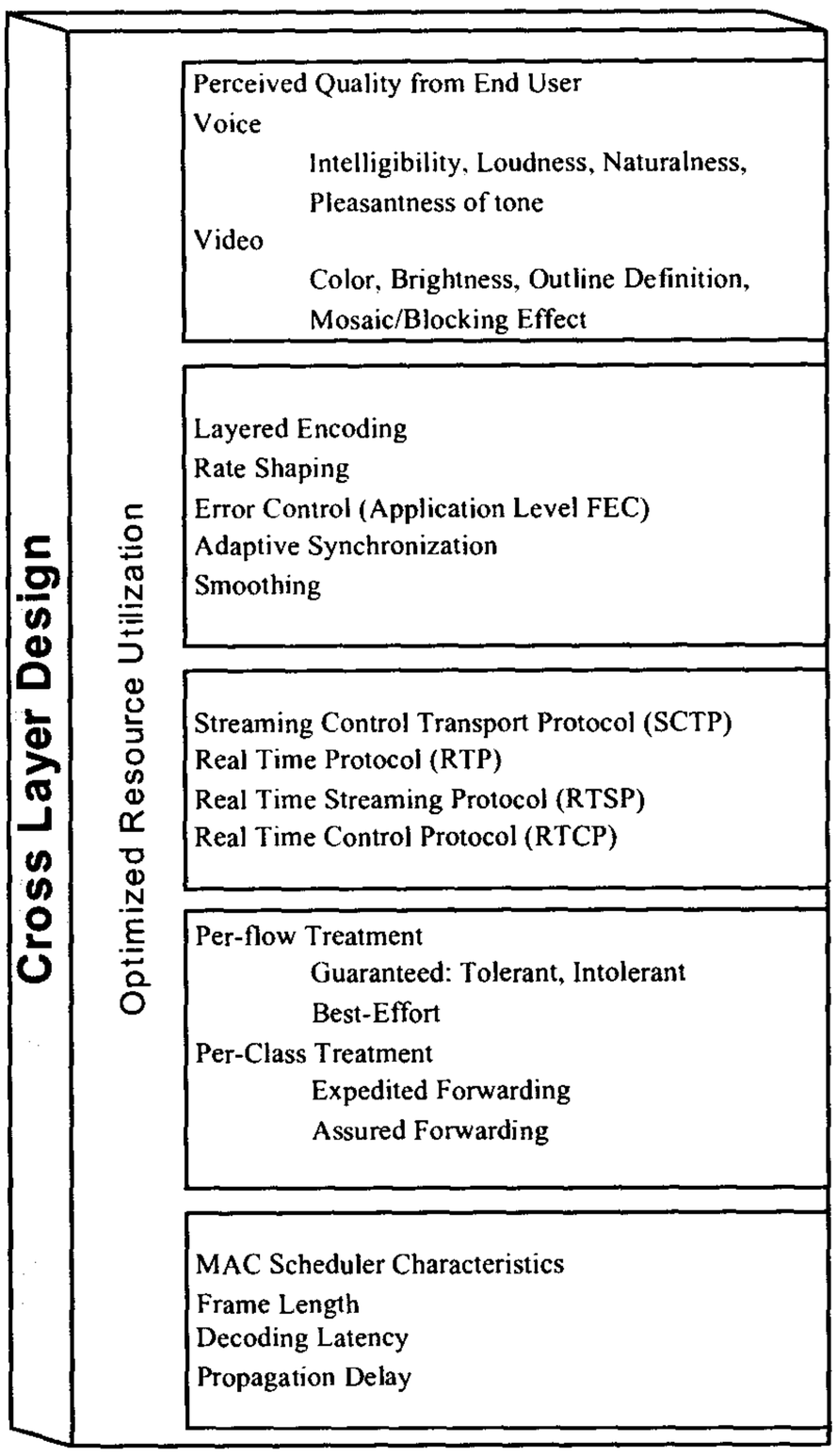

Figure 7.1: The evolution of the protocol stack

fundamental and important aspects of wireless communication systems is the time variability of the channel and the limited resources of the air-interface. that should be optimally shared among the spatially distributed mobile users. Therefore, to achieve optimal allocation of the resources, such as power, data rate and bandwidth, among the spatially distributed mobile users, information about channel conditions should be included. Based on these fundamental differences between wireline

connectivity and single/multi hop wireless connectivity, we can loosely identify the following basic reasons behind a cross layer architectural design:

– Applications can adapt based on both channel and network characteristics.

– Network entities can adapt to the application and wireless channel characteristics.

– Adaptive QoS can be seen as a functionality that is supported in all the layers of the protocol stack for optimized performance.

As shown in figure 7.1 cross layer designs for providing QoS adaptation can potentially utilize information from all layers of the protocol stack. Because these cross-layer designs can lead to complicated protocol stack interactions, the most important requirement for such solutions to be adopted is to ensure sufficient longevity and modularity of the architecture. We should therefore acknowledge that there are many advantages to a layered approach. Layered architectural solutions tend to be modular, therefore it is easier to modify or debug portions of an implementation. Due to the fact that different modules and layers are not tightly integrated, their correctness can be verified independently. These benefits have outweighed the limited optimizations that are possible in traditional systems and have been extensively used for wireline networks. But, as have been discussed in previous chapters, wireless packet based transmission impose a tradeoff between rate, power/energy and delay constraints due to the capacity-limited and stochastic impairments of the broadcast wireless communication channel. Therefore due to the nature of the wireless transmission medium (which in general can also be considered as multi-hop wireless) careful implementation of cross-layer designs has shown to increase the performance of the system [8].

7.2 Summary

Based on the above general framework, the research work presented in the previous chapters focused on mechanisms that utilize TCP/IP based information in order to optimize the transport of packets in heterogeneous wireless networks that fully support IP technology.

Core-centric approach

From the core network perspective of the wireless network architecture, we have seen that IP transport should performed with the minimum number of traffic classes, independently of the number of traffic classes supported on the wireless link. A number of arguments have been discussed explaining the benefits of a core–centric network design. The leading exponent of these arguments is based on the fact that bandwidth provision on the core network, which is actually a wireline network, is less problematic compared with the scarce resources available on the radio access network (limited resources on RANs becomes a prominent issue for QoS provision not only because of the last wireless hop but also because of the possible wireless point-to-point links). From another perspective, we have also argued that core network design should be disassociated with a particular RAN because in the future the same core network will support a plethora of different access network technologies. In such environment the core network can be considered as the least common denominator of all these heterogeneous networks, that will provide the required QoS guarantees to different RANs and therefore should not be constrained by a RAN with a specific QoS design. Extensive simulation results supported these arguments by depicting that the degree of required over-provisioning for reducing the number of traffic classes in the core network is not prohibited. Also, as have been explained a core network with the minimum required number of traffic classes leads to a more simplified control plane in the architecture.

Hop Based Queueing

In all IP wireless network architecture, TCP traffic is envisioned to constitute a significant percentage of the overall aggregate traffic. Wireless networks can be considered as stub networks on the periphery of the Internet and therefore ingress traffic will have different hop counts. Because of the dimension of the Internet there can be a large variability on the number of hops that packets traverse before reaching their destination. The number of routers traversed by IP packets can be linked with the average Round-Trip-Time (RTT) of the connection even though due to random queueing delays this may not be true for instantaneous values. Since TCP throughput is biased towards the RTT, we have proposed an active queueing mechanism that take into account the number of routers traversed by examining the TTL field of the IPv4 packet (or the Hop Limit field in IPv6). In that case the

aim and characteristics of the proposed Hop Based Queueing (HBQ) algorithm can be summarized as follows,

- Equalize achieved throughput of TCP connections with different RTTs
- Minimize the resources consumed from the IP packets in the path from source to destination
- Enhance the performance of TCP flows that span over a large number of hops
- HBQ can be seen as an add-on feature of the Random Early Detection algorithm
- Two different implementation proposed; one that use the exact information from the number of routers traversed by the enqueued packets and another one that is use a threshold on the number of hops
- In an ad hoc network, HBQ algorithm reduces the aggregate energy consumption

Active queueing mechanisms will be an important part of all IP based mobile network architectures. Detecting incipient congestion early enough and conveying a congestion notification to the end-hosts (even by dropping or marking), will allow them to reduce their transmission rate before queues in the network overflow and more packets are dropped. HBQ aims to fulfill these critical aims, as have been considered by the RED algorithm, but also to take into account the number of traversed routers of packets in order to minimize consumption of resources and TCP bias towards RTT.

A New Family of Power and Rate Control Algorithms

In this trend towards the convergence of fixed IP networks with mobile networks the interactions of IP mechanisms with radio link layer mechanisms are inevitable. In that respect, and concerning on the wireless access network a family of power and rate adaptation algorithms have been proposed for CDMA networks. Traditional power and rate control algorithms, utilize information form the link and/or physical layer (such as queueing delay and channel conditions) to optimize packet transmission. The novelty of the proposed mechanisms is that they utilize information from the TCP/IP layer.

In wireline networks TCP reacts to congestion, i.e., packet loss, by decreasing its congestion window, thus reducing network utilization. However, in wireless networks, losses may occur because of the

high bit-error rate of the wireless medium due to shadowing/fading and/or mobility. Even though these losses are not related to congestion, TCP still reacts according to the congestion control state machine, having as a net result an unnecessary reduction of the throughput. A number of different solutions have been proposed in order to increase the efficiency of TCP over wireless networks. The proposed scheme in this thesis can be considered as a cross-layer solution, where the link layer is aware of the TCP state machine in the sense of the size of the *cwnd* and RTT of the connection. The power and rate adaptation algorithm minimize the difference between the allocated rate (r_a)and the required rate (r_{req}) as depicted by the TCP state machine ($r_{req} = cwnd/RTT$).

Additionally, a DiffServ-aware power and rate controlled downlink transmission scheme was proposed in order to provide quality of service (QoS) support over IP-based CDMA systems. The proposed algorithms exploit the packet drop precedence (packet colour) of the IP packets in the assured forwarding (AF) class of DiffServ, and prioritizes the downlink power allocation by the packet colour. Also, a novel rate truncation scheme for the out-of-profile packets of the Assured Forwarding (AF) Per Hop Behavior (PHB) is proposed, aiming to reduce the required transmitted power and increase the QoS experienced by the in-profile packets.

7.3 Future Work

The potential extensions of the research work can be categorized in two different directions (even though they share many common elements). The first direction is to analyze the effect and implications of the proposed architectural semantics (i.e., higher coupling between layers) in the High Speed Downlink Packet Access (HSDPA) system of 3GPP as explained in 7.3.1. The second direction is a rather theoretical one and concerns with algorithmic solutions for the related optimization problems involved in adaptive power and rate control mechanisms. As mentioned before, practical implementations of adaptive power and rate allocation schemes require algorithms that are able to run in real-time. Therefore, traditional constrained optimization techniques that are based on gradient, steepest descents or Newton's method are not applicable because of the inherent complexity. As discussed in section 7.3.2, approximate dynamic programming methods can be used in order to tackle complexity issues.

7.3.1 Application in High Speed Downlink Packet Access

General Features

The **H**igh **S**peed **D**ownlink **P**acket **A**ccess (HSDPA) is a set of mechanisms proposed within 3GPP in order to enhance the maximum downlink transmission rate and efficiency of W-CDMA systems [1]

User data are multiplexed in the high speed physical packet downlink shared channel (HS-PDSCH) of HSDPA in a time division fashion. The frame transmission duration in the channel HS-PDSCH is 2 ms, which corresponds to 3 slots, by the MAC layer scheduler in Node B. Therefore, this short interval frame transmission enables better exploitation of the – independent – fast fading channels among users. In that respect, efficient multi-user diversity techniques can be deployed in order to take advantage of rather than compensate of channel fading. Other important core functionalities of HSDPA include the adaptive modulation and coding scheme (AMCS), hybrid ARQ (HARQ), and MAC layer scheduling.

HSDPA uses codes with a spreading factor of 16 (fixed). A maximum of 15 different codes are available, which can be assigned to a single user or distributed among up to 15 users. The number of codes assigned to a user depends on propagation conditions and of course the capabilities of the mobile terminal. Concerning the modulation, either QAM or 16QAM is used with each code. Based on the feedback from mobile terminal on the channel quality information (CQI) modulation and coding scheme (AMCS) are adaptively selected [6].

The HARQ provides an acknowledge-based ARQ mechanism that is more efficient than traditional ARQ schemes. HARQ mounts a memory on the mobile terminal to keep the soft information of an erroneous frame for later utilization. The mobile terminal sends a negative acknowledge (NACK) message to the Node B if a frame in error is detected through a cyclic redundancy check (CRC). If a NACK message is received, the Node B retransmits the same data block using the same MCS. The retransmitted frames are softly combined with the original frame at the mobile terminal, thus utilizing the previous erroneous frame which would otherwise become waste. The HARQ employs a stop-and-wait (SAW) mechanism, and due to the feedback delay for the acknowledgement, a single HARQ process has to wait a number of frames for the next transmission. Thus in HSDPA, multiple HARQ processes (sometimes referred to as N-channel SAW) are enabled to work in parallel for a

single user.

The MAC scheduler is responsible to choose in every 2 ms frame which user to transmit on the HS-PDSCH. The scheduler is open to implementation and a number of scheduling algorithms have been proposed; a typical scheduler would be a round robin (RR), maximum C/I (MaxC/I), or proportionally fair (PF) scheduler. In a MaxC/I or PF scheduler, the Node B utilizes the channel quality information reported at periodic intervals from the mobile terminals. A MaxC/I scheduler selects the user with the best channel quality, whereas a PF scheduler selects the user with the best relative quality to the average quality for the user. The RR scheduler provides fair sharing of the radio resources among all users but with the lowest aggregate throughput, whereas the MaxC/I scheduler provides the worst fairness but the highest aggregate throughput. The PF scheduler provides a more balance treatment between fairness and throughput compared to RR and MaxC/I [4].

Scheduling Algorithms utilizing IP QoS Information

An important feature of HSDPA that has not been emphasized in the literature is the priority queuing mechanism. The scheduling is handled in the MAC layer of the HSDPA entity and the MAC protocol header has 3 bits dedicated to indicate the queue ID [2]. Therefore each mobile user can theoretically have up to 8 queues simultaneously. Each queue may be assigned a priority level depending on various conditions that may be exploited such as the application, service contract, or the propagation condition.

Figure 7.2 depicts the general architecture of the HSDPA. The packets arriving to the Node B from the core network are distributed into a maximum of 8 queues per user, according to the priority level. The queues of the same priority level are handled equally in the scheduler. The scheduler selects a set of users to transmit data on the next HS-PDSCH frame, and notifies to those users of the data presence by signaling on the HS-SCCH. A new data block transmitted is assigned an HARQ process, and stored in the Node B memory until the data block is correctly received by the mobile terminal, or the maximum number of retransmissions is reached. If the data block is still erroneous after the maximum number of retransmissions, the data recovery is left to the higher layer protocols such as the radio link control protocol (RLC) and TCP. The maximum number of parallel

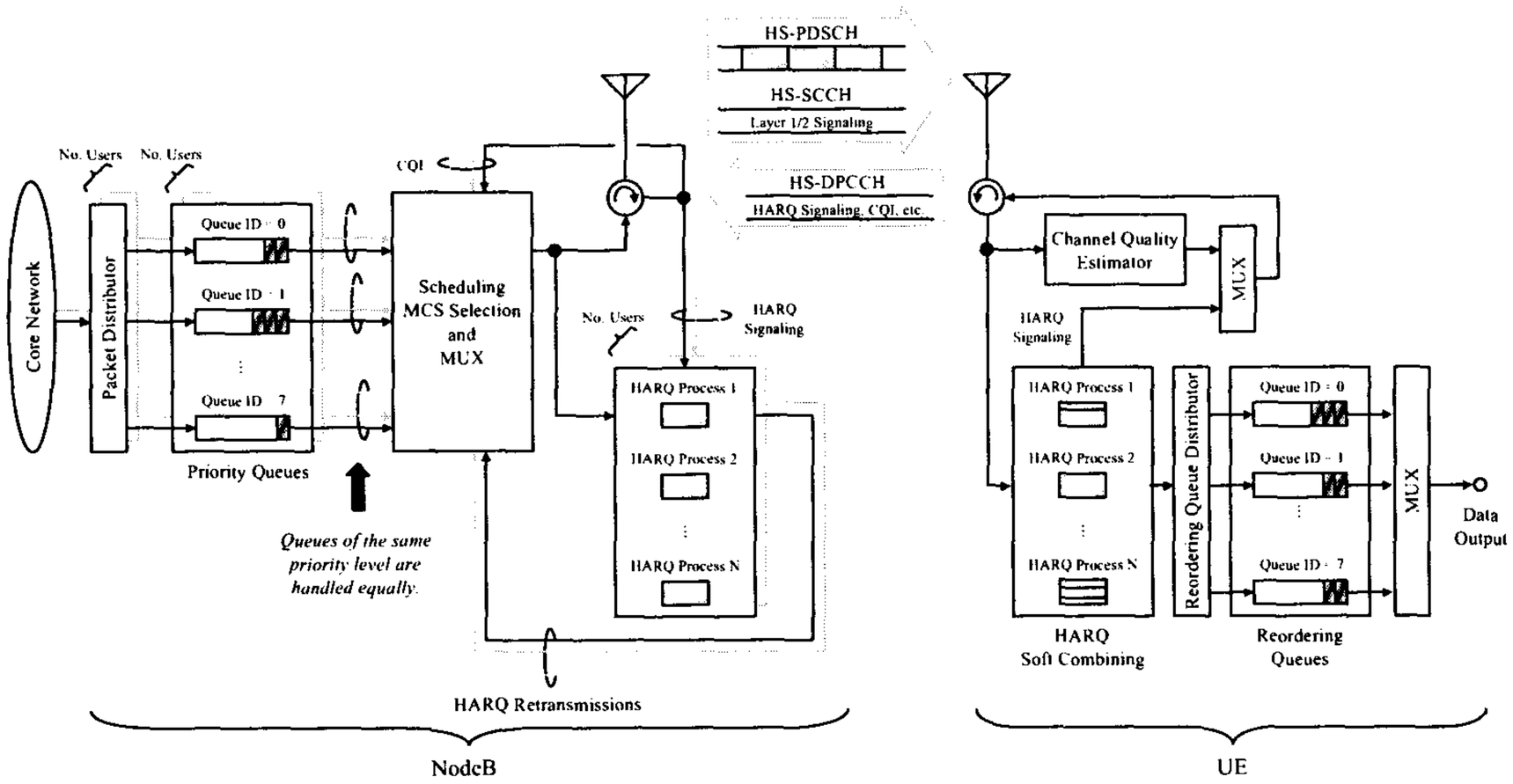

Figure 7.2: General architecture of HSDPA.

HARQ processes depends on the mobile terminal capability and the Node B configuration. Once an HARQ process becomes idle after a successful transmission, a new data block may be assigned to the HARQ process. Due to the N-SAW the sequential order of packets is not ensured at the receiver. Therefore, a reordering mechanism is needed in the receiver as in Fig. 7.2. The HARQ acknowledgement signaling and the CQI reporting is done through the uplink dedicated physical control channel (HS-DPCCH).

These priority queuing mechanism can be seen as a source for a number of novel ideas. Different queues per user can be assigned to different color of packets according to DiffServ packet drop precedence levels. In that sense IP QoS information can be explored by the link layer in order to increase the performance of conformant (in-profile) traffic. Also, a number of policies can be introduced; for example a retransmitted packet by higher layer protocols such as RLC and TCP may be given a higher priority. This should improve the packet delay performance and the overall quality of service.

Based on the above scenario, another interesting research direction would be to utilize IP based information, such as packet drop precedence, for handover procedures. As mentioned before, in the wireless access network the RNC can be considered as an edge DiffServ node. In that case, we can envision a synergy between the allocation of resources on the wireless link and resource

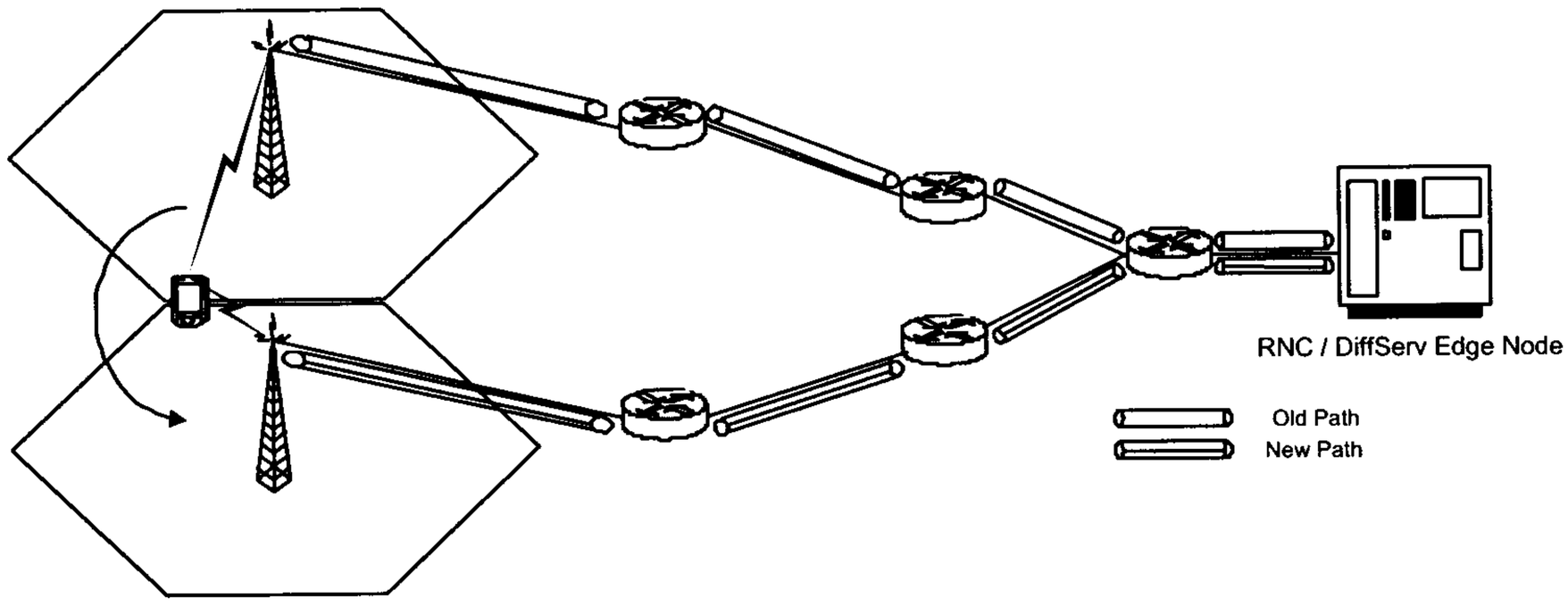

Figure 7.3: Joint path and wireless resource management in the Wireless Access Network.

allocation in the path from RNC to the Node B. As shown in figure 7.3 the RNC/DiffServ edge node is not only responsible for handling the handover request (i.e., allocating/releasing resources in the new/old cell) but also responsible for network resource allocation in the path between the RNC and Node B. In that sense, we can assume a more generalized framework where different schemes for prioritization of resource allocation in the case of handover depend not only on the last wireless hop but on the whole path in the wireless access network. Therefore, synergetic mechanisms between resource management on the last wireless hop and QoS routing and mobility management protocols [5] in the wireless access network can potentially improve the performance of the system.

7.3.2 Using Approximate Dynamic Programming for Power and Rate Adaptation

The drawback of the optimization algorithms discussed previously for power and rate adaptation is their inherent complexity. Except from the proposed sub-optimal greedy algorithm for joint power and rate adaptation that has linear complexity, solutions that based on well known numerical optimization methods (i.e., quasi-Newton) are not suitable for real time implementation because of their computational complexity. This complexity issue therefore render such algorithms infeasible for problems of practical scale. This issue call for alternative solutions that give insight into the structure of the stochastic optimization problems (with stochastic constraints), in order to allow derivation of optimal adaptive policies. In that respect, it can be shown that the problem of power and rate control

can be formulated as a *dynamic program*, i.e., in a mathematical framework where information and decisions evolve over a specific time horizon. The use of stochastic dynamic programming (DP) [7] can be used to find optimal policies for resource allocation to different mobile users.

7.4 Final Notes

Closing this last chapter, we should note that IP based resource management is currently in a rather embryonic stage and the architectural and algorithmic perspectives discussed in this thesis should be seen as a preliminary gesture towards a broader and deeper understanding of the interactions between QoS schemes in higher layers (RTP/TCP/IP) and air-interface specific resource allocation mechanisms. In order for different proposed cross-layer designs to be evaluated, there should be a common framework, a set of rules and methodological principles that provide the background assumptions of 'what' should be avoided and to 'what' degree information should be allowed to flow between layers.

Currently cross-layer designs can be seen as an extra-paradigm compared with the well established hegemonic paradigm of the traditional protocol stack. Maybe, in the future, the heterogeneity of wireless network technologies and the high degree of integration of these networks with the Internet question the capabilities and potentials of the current protocol stack and today's extra-paradigm becomes tomorrow's globally accepted paradigm. Moving beyond today's descriptive rather than judgmental analysis, maybe the biggest open research issue would be to provide a holistic view on the applicability of contemporary protocol stack design versus ones that are based on cross-layer architectural perspectives for future network architectures. This is, we believe, a crucial question with – still – an unknown answer, although in this thesis we tended to sympathize more the latter view.

7.5 List of Publications

1. V. Friderikos, L. Wang, M. Iwamura, A. H. Aghvami, DiffServ-aware Power and Rate Adaptation in DS/CDMA Networks, to appear in the Journal of Wireless Communications and

Mobile Computing, Special Issue on Radio Link and Transport Protocol Engineering for Future Generation Wireless Mobile Data Networks

2. V. Friderikos, L. Wang, A. H. Aghvami, Utilizing TCP information for Resource Management, under submission for Journal publication.

3. V. Friderikos, A. H. Aghvami, TCP-Friendly MPEG-4 Streaming Video in CDMA Networks via Power and Rate Control, to appear in International Journal of Wireless and Mobile Computing (IJWMC), special issue on Media streaming over Wireless and Mobile networks

4. V. Friderikos, A. Shah Jahan, H. Chaouchi, G. Pujolle, H. Aghvami, QoS Challenges in All-IP based Core and Synergetic Wireless Access Networks, IEC Annual Review of Communications, Volume 56, November 2003

5. V. Friderikos, L. Wang, A. H. Aghvami, TCP-aware Power and Rate Adaptation in DS/CDMA Networks, to appear in IEE Proceedings on Communications, 2004

6. V. Friderikos, A. Mihailovic, A. H. Aghvami, Analysis of Cross Issues Between QoS Routing and μ Protocols, IEE Proceedings on Communications, Vol. **151**, No. **3**, June 2004 (Special Issue on Internet Protocols, Technology and Applications)

7. Mikio Iwamura, Vasilis Friderikos, Lin Wang, and A. Hamid Aghvami, Color-aware Rate/Coverage Controlled DS/CDMA Downlink Transmission for DiffServ, to appear in IEE Proceedings on Communications, 2004

8. Lin Wang, Vasilis Friderikos, Mikio Iwamura, A.Hamid Aghvami, Misha Dohler, Colour-aware Link Adaptation for DiffServ over CDMA Systems, 13^{th} IST Mobile & Wireless Communications Summit 2004, June 27-30, 2004, Lyon, France

9. Vasilis Friderikos, Lin Wang, Mikio Iwamura, A.Hamid Aghvami, A Rate Adaptation Scheme for Out Of Profile Packets in a DiffServ enabled CDMA Network, 7th IEEE International Conference, HSNMC 2004, Toulouse, France, June 30- July 2, 2004, Proceedings Series : Lecture Notes in Computer Science , Vol. 3079, XVII, 2004

10. Mikio Iwamura, Vasilis Friderikos, Lin Wang, A. Hamid Aghvami, Biased Adaptive Modulation/Coding to Provide VoIP QoS over HSDPA, submitted in 14^{th} IST Mobile & Wireless Communications Summit 2005

11. Katerina P. Papadaki, Vasilis Friderikos, An Approximate Dynamic Programming Packet Transmission Scheme for Code Division Multiple Access (CDMA) Wireless Networks, in EURO XX, 20^{th} European Conference on Operational Research OR and the Management of Electronic Services, Rhodes, Greece, 4-7 July, 2004

12. A H Aghvami, V Friderikos, Future all IP based core and wireless access networks: The virtual router concept, Proceedings of WWRF, Beijing, China, April 7-9, 2003

13. V. Friderikos, H. Aghvami, Methods and Apparatus for use in Packet Switched Data Communications Networks, PCT Patent Application No. PCT/GB2003/005165, case: KC,017-PCT

14. V. Friderikos, H. Aghvami, Hop Based Queueing (HBQ): An Active Queue Management Technique for Multi Hop Wireless Networks, IEEE ICICS-PCM 2003, Singapore, Dec. 2003

15. Reshan Samarasinghe, Vasilis Friderikos, A.H. Aghvami, Analysis of Intersystem Handover: UMTS FDD & WLAN, London Communications Symposium, 8^{th} – 9^{th} September 2003

16. C.Pinart, C.Bader, C.Christophi, E.Tsiakkouri, I.Ganchev,V.Friderikos, C.Bohoris, L. Correia, L.Ferreira, ANWIRE mapping of user requirements for 4G mobile and wireless communication systems, IST Mobile and Wireless Communications Summit 2003. Aveiro (Portugal), June 15-18 2003.

17. M.O'Droma, I.Ganchev, G.Morabito, R.Narcisi, N.Passas, S.Paskalis, V.Friderikos, A.S.Jahan, E.Tsontsis, C.Bader, J.Rotrou, H.Chaouchi, Always Best Connected: Enabled 4G Wireless World, IST Mobile and Wireless Communications Summit 2003, Aveiro, Portugal, June 15-18 2003.

18. M. Siebert, H. Chaouchi, A. S Jahan, I. Demeure, I. Armuelles, L. M. Correia, J. Liu, M. O'Droma, V. Friderikos, W. Xing, N. Alonistioti, Towards an ANWIRE 4G Wireless System Integration Architecture, Workshop on Wireless, Mobile & Always Best Connected, Glasgow, 22^{nd} of April, 2003

19. Vasilis Friderikos et. al. ANWIRE Analysis of User Requirements for Future Heterogeneous Wireless Networks, Interantional Workshop on Wireless, Mobile & Always Best Connected, Glasgow, 22nd of April, 2003

20. H. Aghvami, V. Friderikos, Quality of Service Issues in 3G and Beyond, IEE Telecommunications Quality of Service (QoS), London, January 20-21 2003.

21. Vasilis Friderikos, A. Abella, A. Hamid Aghvami, Core-Centric Approach for QoS Support in Multi-Technology Pure-IP Mobile Networks, submitted in IEEE Network (Special Issue on Network Management of Multi-Service, Multimedia, IP-Based Networks)

22. Vasilis Friderikos, A. Hamid Aghvami, On the Joint Implications of Internet RTT, Traffic Mix and Wireless Links on TCP, IEEE SoftCom 2002

23. Vasilis Friderikos, A. Abella, A. Hamid Aghvami, Over-Provisioning versus Differentiated Services in Pure IP Mobile Networks, IEEE MWCN 2002, Stockholm 9-11 September 2002

24. Vasilis Friderikos, A. Hamid Aghvami, Dynamical System Approach Analysis of MPEG-4 Video Traffic, IEEE SoftCom 2001, October 09-12, 2001, Italy

25. Vasilis Friderikos, A. Hamid Aghvami, WAP Traffic Modelling, International Symposium on 3G Infrastructure and Services, 2-3 July 2001, Athens, Greece

26. Vasilis Friderikos, A. Hamid Aghvami, Internet Traffic Characterization, M-VCE Conference, November 6-7, 2001, Reading, U.K

Bibliography

[1] 3GPP, TS 25.308, High Speed Downlink Packet Access (HSDPA) overall description, *v6.0.0, Dec. 2003.*

[2] 3GPP, TS 25.321, Medium Access Control (MAC) protocol specification, *v6.0.0, Dec. 2003.*

[3] 3GPP, TS 25.213, Spreading and modulation (FDD), *v6.0.0, Dec. 2003.*

[4] Y. Ofuji, S. Abeta, and M. Sawahashi, Comparison of packet scheduling algorithms focusing on user throughput in high speed downlink packet access, *IEICE Trans. Commun., Vol. E86-B, No. 1, pp. 132-141, Jan. 2003.*

[5] Vasilis Friderikos, Andrej Mihailovic, Hamid Aghvami, Analysis of Cross Issues Between QoS Routing and μ-Mobility Protocols, *IEE Proceedings on Communications, Vol. **151**, No. **3**, June 2004*

[6] Kolding, Troels. Pedersen, Klaus. Wigard, Jeroen. Frederiksen, Frank. Mogensen, Preben, High Speed Downlink Packet Access: WCDMA Evolution, *IEEE Vehicular Technology Soceity (VTS) News, vol. 50, no. 1: 2003, pp. 4-10*

[7] Sheldon Ross, Introduction to Stochastic Dynamic Programming, *A volume in Probability and Mathematical Statistics, Academic Press, 1983*

[8] Yunnan Wu, Philip A. Chou, Qian Zhang, Senior Member, IEEE, Kamal Jain, Wenwu Zhu, and Sun-Yuan Kung, Network Planning in Wireless Ad Hoc Networks: A Cross-Layer Approach, *IEEE Journal on Selected Areas in Communications, vol. 23, no 1, January 2005*

Glossary and Acronyms

3GPP: 3rd Generation Partnership Project

3G: Third Generation

802.11b: IEEE Wireless LAN system

ABC: Always Best Connected

AF: Assured Forwarding

AMCS: Adaptive Modulation Coding Scheme

AP: Access Point

AQM: Active Queueing Management

ARQ: Automatic Repeat Request

CDMA: Code Division Multiple Access

CQI: Channel Quality Information

CIR: Committed Information Rate

cwnd: Congestion Window **Diffserv**: Differentiated Services

DS-CDMA: Direct Sequence CDMA

DT: Drop-Tail

EDGE: Enhanced Data-rates for GSM

EF: Expedited Forwarding

FDMA: Frequency Division Multiple Access

FIFO: First In First Out

FEC: Forward Error Control

IQR: Inter Quartile Range

MAC: Medium Access Control

GGSN: Gateway GSN

GOP: Group Of Pictures

GRP: Greedy Rate Packing

GPRS: General Packet Radio Service

GTP: GPRS Tunnelling Protocol

GSM: Global System for Mobile Communications

GSN: GPRS support node

HARQ: Hybrid ARQ

HBQ: Hop Based Queueing

HSDPA: 3GPP High Speed Downlink Packet Access

HTTP: Hypertext Transfer Protocol

IETF: Internet Engineering Task Force

IntServ: Integrated Services

ISP: Internet Service Provider

MANET: Mobile ad hoc Network

MH: Mobile Host

MIP: Mobile IP

MOP: Multi-objective Optimization Problem

OSPF: Open Shortest Path First

PAN: Personal Area Network

PDU: Protocol Data Unit

PER: Packet Error Rate

PHB: Per-Hop Behaviour

PIR: Peak Information Rate

QAM: Quadrature Amplitude Modulation

QoS: Quality of Service

RED: Random Early Detection

RIO: RED with In and Out

RLC: Radio Link Control

RNC: Radio Network Controller

RSVP: Resource Reservation Protocol

RTO: Retransmission Time-Out

RTP: IETF Real Time Protocol

RTT: Round trip time

SGSN: Serving GPRS Support Node

SIR: Signal to Interference Ratio

SLA: Service Level Agreement

SMTP: Simple Mail Transfer Protocol

SNMP: Simple Network Management Protocol

TFRC: TCP Friendly Rate Control

TCP: Transmission Control Protocol

TD-CDMA: TDD mode of operation for UTRA

TDD: Time Duplex Division

TDMA: Time Division/Domain Multiple Access

TSG: Technical Specification Group in 3GPP

UDP: User Datagram Protocol

UMTS: Universal Mobile Telecommunication System

UTRA: Universal Terrestrial Radio Access

UTRAN: Universal Terrestrial RAN

VoIP: Voice over IP

W-CDMA: Wideband Code Division Multiple

WLAN: Wireless LAN

WRR: Weight Round Robin

WWRF: Wireless World Research Forum

WWW: World Wide Web

ZigBee: PAN radio